



HAL
open science

Physiologie cardiaque et respiratoire : explorations, mesures et approches théoriques

Pascale Calabrese

► **To cite this version:**

Pascale Calabrese. Physiologie cardiaque et respiratoire : explorations, mesures et approches théoriques. Physiologie [q-bio.TO]. Université Grenoble Alpes, 2017. tel-01990874

HAL Id: tel-01990874

<https://theses.hal.science/tel-01990874>

Submitted on 23 Jan 2019

HAL is a multi-disciplinary open access archive for the deposit and dissemination of scientific research documents, whether they are published or not. The documents may come from teaching and research institutions in France or abroad, or from public or private research centers.

L'archive ouverte pluridisciplinaire **HAL**, est destinée au dépôt et à la diffusion de documents scientifiques de niveau recherche, publiés ou non, émanant des établissements d'enseignement et de recherche français ou étrangers, des laboratoires publics ou privés.

Physiologie cardiaque et respiratoire : explorations, mesures et approches théoriques

MEMOIRE

présenté et soutenu publiquement le 24 mai 2017 pour l'obtention de l'

Habilitation à Diriger des Recherches

de l'Université de Grenoble Alpes

par

Pascale Calabrese

Composition du jury :

Rapporteurs :

Véronique Bach
Nathalie Henrich-Bernardoni
Christian Straus

*PU, Université de Picardie Jules Verne
CR CNRS, Université Grenoble Alpes
PU-PH, Université Pierre et Marie Curie,
CHU Pitié Salpêtrière-APHP*

Examineurs :

François Boucher
Patrick Lévy
Frédéric Lofaso

*PU, Université Grenoble Alpes
PU-PH, Université Grenoble Alpes, CHUGA
PU-PH, Université de Versailles Saint-
Quentin-en-Yvelines, CHU Raymond
Poincaré-APHP*

Remerciements

Je tiens tout d'abord à adresser mes sincères remerciements à tous les membres du jury d'avoir accepté d'évaluer mon travail.

"Il n'y a pas de hasard, il n'y a que des rendez-vous" Paul Eluard

Ce manuscrit expose le fruit d'un travail en synergie avec les personnes que j'ai eu l'occasion de rencontrer dans mon parcours professionnel, un grand merci à elles.

"Lorsque les hommes travaillent ensemble, les montagnes se changent en or." Proverbe chinois

La Terre

Gila Benchetrit qui m'a accueillie dans l'équipe, accompagnée et toujours fait confiance. Le travail et les discussions dans son bureau sont autant de bons souvenirs. Pierre Baconnier, André Eberhard, Jean-Pierre Bachy qui ont participé à ce travail. Sans oublier Jacques Demongeot qui m'a ouvert les portes du laboratoire.

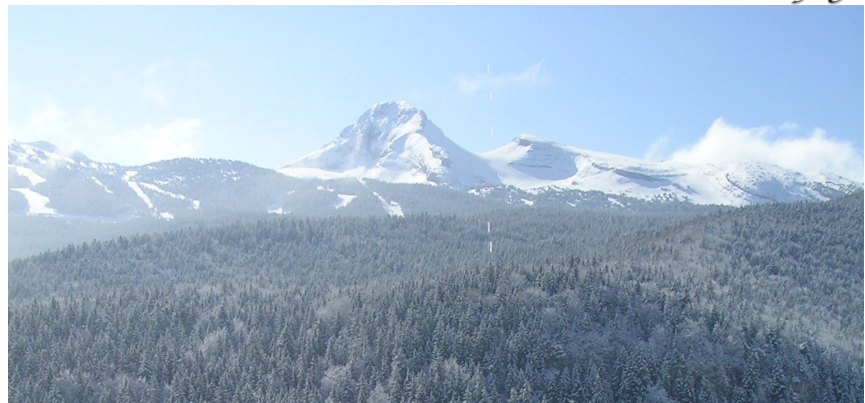
La forêt

Les stagiaires et thésards qui se sont investis et qui ont contribué à ce travail. Les membres du laboratoire et de l'équipe, tous ceux qui rendent la vie au laboratoire plus agréable au quotidien. L'équipe pédagogique de TIS avec un remerciement particulier à Emmanuel Promayon.

Le vent (au delà du bassin grenoblois)

Frédéric Lofaso pour son accueil et notre collaboration. Saad Saguem, Victor Vovc et Ion Moldovanu, pour les co-directions de thèses.

Mon refuge



Les copines "springdoardeuses" et nos "mémorables" pique-niques. Mes amis, ma famille, qui me ressourcent et m'équilibrent. Mon cœur et mes deux soleils, qui illuminent ma vie.

La source

Mon père,
Ma mère ...

... *"Tu n'es plus là où tu étais, mais tu es partout là où je suis."* Victor Hugo



Table des matières

PARTIE I CURRICULUM VITAE	6
I.1 PARCOURS	6
I.2 ENSEIGNEMENT	6
I.3 RESPONSABILITES	7
I.3.1 Scientifiques	7
I.3.2 Pédagogiques	7
I.4 EXPERTISES SCIENTIFIQUES	7
I.4.1 Rapporteur pour articles dans revues internationales.....	7
I.4.2 Rapporteur projet.....	8
I.5 COLLABORATIONS SCIENTIFIQUES.....	8
I.6 ENCADREMENT	8
I.6.1 Masters.....	8
I.6.2 Thèses	9
I.6.3 Stages et projets	9
I.7 CONTRATS	9
I.8 PUBLICATIONS.....	10
PARTIE II ACTIVITES DE RECHERCHE.....	15
II.1 PREAMBULE.....	15
II.2 MODE VENTILATOIRE : DIVERSITE ET “PERSONNALITE”	17
II.2.1 Introduction.....	17
II.2.1.1 <i>Les caractéristiques ventilatoires.....</i>	<i>17</i>
II.2.1.2 <i>Quantification de la forme des cycles ventilatoires (analyse harmonique).....</i>	<i>19</i>
II.2.1.3 <i>Comparaison multivariée de la forme des cycles ventilatoires (test de similarité).....</i>	<i>20</i>
II.2.2 La diversité des modes ventilatoires.....	20
II.2.2.1 <i>Chez les patients atteints de dystrophie myotonique (maladie de Steinert).....</i>	<i>20</i>
II.2.2.2 <i>Au cours de l'exercice imaginaire.....</i>	<i>29</i>
II.2.3 La “personnalité ventilatoire”	34
II.2.3.1 <i>Au cours de l'hyperventilation.....</i>	<i>34</i>
II.2.3.2 <i>Au cours de la ventilation assistée.....</i>	<i>41</i>
II.3 VARIABILITE DE LA FREQUENCE CARDIAQUE	47
II.3.1 Introduction.....	47
II.3.1.1 <i>La variabilité de la fréquence cardiaque.....</i>	<i>47</i>

II.3.1.2	<i>L'arythmie sinusale d'origine respiratoire.....</i>	47
II.3.1.3	<i>L'analyse du spectre de la fréquence cardiaque.....</i>	48
II.3.2	L'arythmie sinusale d'origine respiratoire.....	49
II.3.2.1	<i>Au cours de l'addition de résistance respiratoire.....</i>	49
II.3.2.2	<i>Au cours de différentes fréquences ventilatoires imposées.....</i>	54
II.4	MESURE PHYSIOLOGIQUE	60
II.4.1	Comparaison de la ventilation mesurée par pneumotachographie et pléthysmographie respiratoire à variation d'inductance.....	60
II.4.2	Méthode d'évaluation de la fonction respiratoire	66
II.4.2.1	<i>Différence de forme thorax-abdomen et évaluation des variations des résistances des voies aériennes.....</i>	66
II.4.2.2	<i>Les oscillations cardiogéniques et estimation de la mécanique de la paroi thoracique.....</i>	71
II.4.3	Méthode d'évaluation de la fonction cardiaque.....	71
II.4.3.1	<i>Analyse de l'arythmie sinusale d'origine respiratoire.....</i>	71
II.4.3.2	<i>Evaluation des variations du volume cardiaque à partir de mesure par pléthysmographie respiratoire à variation d'inductance.....</i>	76
II.5	APPROCHE THEORIQUE	78
II.5.1	Modèle simple de mécanique ventilatoire.....	78
II.5.2	Modèles non linéaires du générateur de rythme respiratoire.....	86
II.5.2.1	<i>Modèle déterministe chaotique.....</i>	86
II.5.2.2	<i>Oscillateur de Van Der Pol.....</i>	86
II.5.3	Modèle d'interaction cœur -respiration.....	88
II.5.4	Complexité.....	89
II.6	TRAVAUX EN COURS ET PERSPECTIVES	92
II.6.1	Déglutition et respiration	92
II.6.2	Interactions phonation-ventilation.....	94
II.6.3	Le syndrome d'hyperventilation	95
II.6.4	Asynchronisme thorax – abdomen : application.....	96
II.6.5	Diagnostic médical à partir d'une analyse des gaz respiratoires.....	96
II.7	REFERENCES	97

Table des figures :

Figure 1 : Thématiques et publications afférentes. Les publications indiquées en bleu sont insérées en entier dans le document	16
Figure 2 : Un cycle ventilatoire et ses caractéristiques : la durée totale T_{TOT} , les durées inspiratoire T_I et expiratoire T_E et le volume courant V_T	17
Figure 3 : Représentation de la forme d'un signal volume	17
Figure 4 : Débit ventilatoire instantané mesuré par pneumotachographie	18
Figure 5 : Représentation de l'analyse harmonique sur un cycle de débit : Les 4 premières harmoniques, le spectre de puissance de ce cycle, le débit d'origine et le débit reconstitué à partir des 4 premières harmoniques et la représentation de Fresnel associée.....	19
Figure 6 : Valeurs des volumes courant (V_T en litre, l) et des durées (T_{TOT} en seconde, sec) pour une série de cycles ventilatoires consécutifs en position assise (à gauche) et couchée (à droite) pour un patient.....	21
Figure 7 : Changement exprimé en pourcentage de la valeur de repos pour la fréquence cardiaque et la ventilation minute ($=V_T * f_R$, avec V_T : volume courant, f_R : fréquence ventilatoire) lors du visionnage de la course et durant l'imagination de celle-ci pour tous les sujets des 4 groupes : compétiteurs en aviron (1), sportifs (2), sédentaire (3), seniors (4).....	29
Figure 8 : Pour un sujet représentation des caractéristiques ventilatoires moyennes : volume courant (V_T), les durées inspiratoire et expiratoire (T_I , T_E), la représentation de Fresnel des 4 premières harmoniques obtenues d'une analyse cycle par cycle ventilatoire (débit) et le débit reconstitué correspondant, au cours de la ventilation spontanée (SP_1 et SP_2), d'une hyperventilation volontaire à la fréquence de la ventilation spontanée (HV_{SP}) et à 20/min (HV_{20}). Les valeurs moyennes de V_T , et de la fréquence ventilatoire (f_R) sont données pour chaque condition.....	34
Figure 9 : Illustration du phénomène d'arythmie sinusale d'origine respiratoire	48
Figure 10 : Spectre de la période cardiaque avec représentation des bandes de fréquences: basses fréquences (LF) de 0,04 et 0,15 Hz et hautes fréquences (HF) de 0,15 et 0,4 Hz.....	49
Figure 11 : Capteur et signaux de pléthysmographie respiratoire à variation d'inductance (PRI).....	61
Figure 12 : Représentation de volumes courants obtenus par intégration du signal débit mesuré par pneumotachographie (V_{PNT}) en fonction des volumes courants obtenu par le signal PRI (V_{PRI}) pour les 10 sujets dans toutes les 9 conditions : en position assise, couchée sur le dos et le côté au repos et avec l'addition de deux niveaux de résistances additionnelles.....	62
Figure 13 : Moyenne \pm erreur standard : de la distance (D) entre les signaux du thorax et l'abdomen calculée à partir de tous les cycles respiratoires sélectionnés (minimum 30) et de la résistance des voies aériennes (R_{aw} en kPa.l ¹ .sec)	67
Figure 14 : Volume mesuré par PRI (V_{PRI}) et électrocardiogramme (ECG). Sur le signal volume les flèches indiquent les "accidents" dus aux variations du volume provoqués par les battements cardiaques en correspondance avec l'ECG.....	76
Figure 15 : Représentation du modèle simple de mécanique ventilatoire. RC : compartiment thoracique (ressort) d'élasticité E_{RC} ; A : compartiment abdominal (ressort) d'élasticité E_A ; R : résistance du système respiratoire (amortisseur) de résistance visqueuse R. F_{mus} : force développée par les muscles respiratoires sur une barre sur laquelle les trois éléments sont fixés.	78
Figure 16 : Représentation des processus de simulation pour un type de déglutition en expiration (E). La figure de gauche représente la simulation de la déglutition au niveau du générateur de rythme respiratoire : le plus petit point (rouge, D) est le début de la déglutition, qui va se déplacer sur l'isochron du point d'arrêt (courbe en pointillée bleue) ; le plus gros point (violet, FD) représente la fin de la déglutition, à partir de ce point il y a un retour vers le cycle limite. La figure de droite représente les signaux de volume courant obtenus en sortie : pour le cycle avant la déglutition, pendant la déglutition (représentée par le point rouge, D) et les deux cycles suivants.....	88
Figure 17 : Signaux enregistrés au cours d'une déglutition. Signaux thoracique (THORAX) et abdominal (ABDOMEN) mesurés par pléthysmographie respiratoire à variation d'inductance (PRI), ECG : électrocardiogramme (bleu foncé), fréquence cardiaque (bleu claire), DEBIT_REC : Débit reconstitué à partir des signaux thoracique et abdominal.....	90
Figure 18 : Représentation de la valeur moyenne de la fréquence cardiaque, de l'écart type et du coefficient de variation avant et pendant chaque événement pour les 4 sujets.	90
Figure 19 : Pléthysmographe respiratoire à variation d'inductance (ventilation), électroglottographe (variations d'impédance au niveau de la glotte) et microphone (signal acoustique) placés sur un sujet.....	93
Figure 20 : Enregistrement sur un sujet sain des signaux électroglottographique (EGG), acoustique (micro) et de ventilation (thorax, abdomen et volume obtenus par pléthysmographie respiratoire à variation d'inductance) au cours d'évènements de déglutition et de parole.....	93

Partie I CURRICULUM VITAE

Pascale CALABRESE
Laboratoire TIMC-IMAG
38700 La Tronche
04 56 52 00 60

Pascale.Calabrese@univ-grenoble-alpes.fr

MAITRE DE CONFERENCES DE L'UNIVERSITE GRENOBLE ALPES

CNU 66 (Physiologie), Polytech Grenoble filière ingénieur "Technologies de l'Information pour la santé" (TIS), Laboratoire TIMC-IMAG, équipe PRETA (2002).

I.1 PARCOURS

- 2002- ... Maître de conférences de l'Université
- 2001-2002 ATER, TIS, Polytech Grenoble, Université Joseph Fourier
- 2000-2001 ATER, DEUG STAPS, Bourget du lac, Université de Savoie
- 1999-2000 Post-doctorat : Hôpital Raymond Poincaré, Garches (92) - Financement Institut Garches
- 1995-1998 Doctorat de Génie Biologique et Médical, Université Joseph Fourier
"Recherche d'une méthode de mesure non-invasive des résistances respiratoires. Effets ventilatoires et cardiaques de charges résistives "
Direction : Gila Benchetrit
Soutenue le 14/12/1998
- 1994-1995 DEA de Génie Biologique et Médical, Université Joseph Fourier
"Comparaison de données ventilatoires mesurées par deux méthodes différentes : 1) la pneumotachographie (mesure du débit ventilatoire à la bouche) et 2) la pléthysmographie par inductance respiratoire (mesure des variations de volume thoracique et abdominal)
- 1994 Maîtrise de Mathématiques Appliquées, IUP, Université Joseph Fourier

I.2 ENSEIGNEMENT

Physiologie (années 3 et 4 ingénieur Polytech Grenoble), génération de signaux physiologiques (année 3 Polytech Grenoble, Masters 1 et 2), initiation à la modélisation biomédicale (année 5 Polytech Grenoble), statistiques (DEUG STAPS), méthodes statistiques en épidémiologie (années 3 et 4 Polytech Grenoble, Masters 1 et 2, 2^{ème} année de médecine).

I.3 RESPONSABILITES

I.3.1 Scientifiques

- 2011-2012 Porteur projet de valorisation DECRO en pré- et maturation auprès de GRAVIT.
- 2009 Organisation du XXIX^{ième} séminaire de la Société Francophone de Biologie Théorique et coéditrice invitée pour la publication des actes de ce séminaire.
- 2008 Membre de la commission de sélection (poste MCF744 -Polytech Grenoble).
- 2006-... Plate-forme expérimentale sur volontaire sain de l'équipe PRETA (TIMC-IMAG).
- 2004-2006 Projet financé par le Programme Interdisciplinaire Complexité du Vivant et Action STIC-Santé (responsable scientifique)

I.3.2 Pédagogiques

- 2015-... Projets de fin d'étude de la filière ingénieur TIS (année 5), Polytech Grenoble (UJF)
- 2012-... Stages de la filière ingénieur TIS (année 4), Polytech Grenoble (UJF) et enseignement de physiologie sur les 3 années de TIS
- 2011-... UE "Mesures expérimentales et physiologie de l'effort" du Master 1 "Ingénierie pour la Santé et le Médicament" (UJF)
- 2007-... Plate-forme expérimentale en physiologie à Polytech Grenoble pour la filière TIS (UJF)
- 2005-2011 Année 4 de la filière ingénieur TIS, Polytech Grenoble (UJF)
- 2004-2009 UE "Mesure et Acquisition de Données Biocliniques" du Master 2 "Ingénierie pour la Santé et Médicament" (UJF)
- 2002-2007 Stages de la filière ingénieur TIS (4^{ième} année), Polytech Grenoble (UJF)

I.4 EXPERTISES SCIENTIFIQUES

I.4.1 Rapporteur pour articles dans revues internationales

- Institute of Electrical and Electronics Engineers (IEEE) Engineering in Medicine and Biology Society (EMBS)
- European Journal of applied physiology (EJAP)
- Computational and medical methods in medicine

I.4.2 Rapporteur projet

- Programme de Recherche Translationnelle en Santé (PRTS) 2013 de l'Agence Nationale de la Recherche (ANR)
- Programme Technologie pour la Santé et l'Autonomie (TECSAN) 2011 de l'ANR
- Thèse CIFRE pour l'Association Nationale de la Recherche et de la Technologie (ANRT) en 2010
- Programme pour le Medical Research Council 2010

I.5 COLLABORATIONS SCIENTIFIQUES

- Service de Physiologie et d'Explorations Fonctionnelles de l'Hôpital Raymond Poincaré à Garches (92).
- Université d'Etat de Médecine et "Nicolae Testemițanu", Département de physiologie humaine et biophysiques (Chisinau, République de Moldavie)
- Laboratoire de Biophysique Métabolique & Toxicologie Professionnelle et Environnementale Appliquée (Faculté de Médecine de Sousse, Tunisie)
- Laboratoire Grenoble Images Parole Signal Automatique (GIPSA-lab)
- Laboratoire de Physique Interdisciplinaire (LIPhy, Grenoble)

I.6 ENCADREMENT

I.6.1 Masters

- Alexandre BERDAH (2003) "*Mise en place d'une base de données de mesures expérimentales pour valider un modèle respiratoire.*" **M2** Ingénieries pour la Santé et le Médicament, Modèles et Instruments en Médecine et Biologie, abandon.
- Feras AL CHAMA (2004) "*Modélisation des interactions de la déglutition avec la respiration.*" **M2** Ingénieries pour la Santé et le Médicament, Modèles et Instruments en Médecine et Biologie
- Naïma MEZIOUD (2005) "*Modélisation de l'effet de la déglutition sur le cycle respiratoire.*" **M2** Ingénieries pour la Santé et le Médicament, Modèles et Instruments en Médecine et Biologie
- Frédéric BOONAERT (2014) "*Influence d'une manœuvre ostéopathique sur la variabilité de la fréquence cardiaque, une étude contrôlée.*" **M1** Ingénieries pour la Santé et le Médicament.
- Anthony COSTA (2014) "*Mise au point d'un protocole expérimental sur volontaires sains visant à différencier les phases de la respiration, de la parole et de la déglutition.*" **M1** Ingénieries pour la Santé et le Médicament.

I.6.2 Thèses

- Tudor BESLEAGA (19 octobre 2011) *“Effets ventilatoire et cardiaque de l'hyperventilation volontaire. Etude chez les volontaires sains et les patients souffrant de trouble panique.”* Cotutelle : TIMC-IMAG et Université d'Etat de Médecine “Nicolae Testemițanu”, Département de physiologie humaine et biophysiques (Chisinau, République de Moldavie), codirections V Vovc et I Moldovanu.
- Aïcha LAOUANI (15 décembre 2016) *“Nouvelle Technique d'évaluation, des variations de la résistance des voies respiratoires lors d'un test de réversibilité bronchique. Elaboration d'un modèle simple du système respiratoire pour interpréter des mesures non invasives de la ventilation”* Université de Monastir (Tunisie), Laboratoire de biophysique (faculté de Médecine de Sousse, Tunisie) en collaboration avec TIMC-IMAG, codirections : S Saguem et P Calabrese.

I.6.3 Stages et projets

- 3 stagiaires en Maîtrise des Sciences Biologique et Médicale (UJF-2000)
- 4 stagiaires en initiation à la recherche L3 STAPS (Univ Savoie-2001)
- Projet ingénieur Technologies d'Information pour la Santé 5^{ème} année, 4 élèves (UJF-2007)
- 1 stagiaire de DUT, Statistiques et Traitement Informatique des Données (UPMF-2009)
- Projet ingénieur Technologies d'Information pour la Santé 5^{ème} année, 4 élèves (UJF-2015)
- 1 stagiaire de DUT, Mesures Physiques (UGA-2016)

I.7 CONTRATS

- Responsable scientifique du projet “Interactions cardio-respiratoires: complexités nécessaires ou vestigiales ? Modèles et expériences” financé par le Programme Interdisciplinaire Complexité du Vivant & Action STIC-Santé-2 ans (2004-2005).
- Porteur du projet “Dispositif d'Exploration Cardiorespiratoire chez le Rongeur (DECRO)” pour le montage du dossier de demande de financement d'aide à l'innovation par Grenoble Alpes Valorisation Innovation Technologies (GRAVIT) en pré maturation et en maturation- 1 an (2011-2012)- demande acceptée en 2012
- Participation au projet “Déglutition et Respiration : Modélisation et e-Santé à domicile” (e-SwallHome) financé par l'ANR Technologies pour la Santé et l'Autonomie- 4 ans (2014- 2017).
- Participation au projet “Fast and sensitive breath analysis for medical diagnostics” financé par l'ANR du programme grands défis sociétaux, vie santé et bien être PRCE : Projets de recherche collaborative-entreprises-3 ans (2016-2018).

I.8 PUBLICATIONS

Les publications insérées en version intégrale dans le manuscrit, apparaissent en bleu.

ACL : *Articles dans des revues internationales ou nationales avec comité de lecture répertoriées.*

Calabrese P, Dinh TP, Eberhard A, Bachy JP, Benchetrit G (1998) *Effects of resistive loading on the pattern of breathing.* (1998) **Respir Physiol** 113 (2): 167-17

Dinh TP, Perrault H, Calabrese P, Eberhard A, Benchetrit G *New statistical method for detection and quantification of respiratory sinus arrhythmia* (1999) **IEEE-Inst Electrical Electronics Engineers Inc** 46 (9): 1161-1165

Calabrese P, Gryspeert N, Auriant I, Fromageot C, Raphael JC, Lofaso F, Benchetrit G *Postural breathing pattern changes in patients with myotonic dystrophy* (2000) **Respir Physiol** 122 (1): 1-13

Calabrese P, Perrault H, Dinh TP, Eberhard A, Benchetrit G *Cardiorespiratory interactions during resistive load breathing* (2000) **Am J Physiol-Regulatory Integrative and Comparative Physiology** 279 (6): R2208-R2213

Eberhard A, Calabrese P, Baconnier P, Benchetrit G *Comparison between the respiratory inductance plethysmography signal derivative and the airflow signal* (2001) **Adv Exp Med and Biol** 499: 489-494

Thibault S, Calabrese P, Benchetrit G, Baconnier P *Effects of resistive loading on breathing variability - Non linear analysis and modelling approaches* (2004) **Adv Exp Med and Biol** 551: 293-298

Bijaoui E, Anglade D, Calabrese P, Eberhard A, Baconnier P, Benchetrit G *Can Cardiogenic oscillations provide an estimate of chest wall mechanics?* (2004) **Adv Exp Med and Biol** 551: 251-257

Ben Lamine S, Calabrese P, Perrault H, Pham Dinh T, A. Eberhard E, Benchetrit G *Individual differences in respiratory sinus arrhythmia* (2004) **Am J Physiol-Heart and Circulatory Physiology** 286: H2305-H2313

Calabrese P, Messonnier L, Bijaoui E, Eberhard E, Benchetrit G *Cardioventilatory changes induced by mentally imaged rowing* (2004) **Europ J App Physiol** 91: 160-166

Scott A, Eberhard E, Ofir D, Benchetrit G, Pham Dinh T, Calabrese P, Lesiuk V, Perrault H *Enhanced cardiac vagal efferent activity does not explain training-induced bradycardia* (2004) **Auton Neurosc : Basic and Clinical** 112 : 60– 68

Fontecave Jallon J, Abdulhay E, Calabrese P, Baconnier P, Gumery PY *A model of mechanical interactions between heart and lungs* (2009) **Philos Transact A Math Phys Eng Sci** 367 (1908) : 4741-57

Emeriaud G, Baconnier P, Eberhard A, Debillon T, Calabrese P, Benchetrit G *Variability of end expiratory lung volume in premature infants* (2010) **Neonatology** 98:321–329

Calabrese P, Baconnier P, Laouani A, Fontecave Jallon J, Guméry PY, Eberhard A, Benchetrit G *A simple dynamic model of respiratory pump* (2010) **Acta Biotheor** 58(2-3) : 265-275

Calabrese P; Fontecave-Jallon J *Proceedings of the XXIXth Conference of the French-*

Speaking Society for Theoretical Biology Quantitative and Qualitative Approaches in Life Science: Formalisms, Models and Simulations in Biology and Health (2010) **Acta Biotheor** 58 (2-3) : 85-87

Fontecave-Jallon J, Gumery P-Y, Calabrese P, Briot R, Baconnier P A Wearable Technology Revisited for Cardio-Respiratory Functional Exploration: Stroke Volume Estimation From Respiratory Inductive Plethysmography (2013) **Inter J EHealth and Med Com** 4(1) : 12-22

Fontecave-Jallon J, Videlier B, Baconnier P, Tanguy S, Calabrese P, Gumery PY Detecting variations of blood volume shift due to heart beat from respiratory inductive plethysmography measurements in man (2013) **Physiol Measur** 34(9) : 1085-1101

Meric H*, Calabrese P*, Pradon D, Lejaille M, Lofaso F, Terzi N Physiological comparison of breathing patterns with neurally adjusted ventilatory assist (NAVA) and pressure-support ventilation to improve NAVA settings (2014) **Respir Physiol and Neurobiol** 195 : 11-18

*These authors contributed equally to the work

Besleaga T, Blum M, Briot R, Vovc V, Moldovanu I, Calabrese P Individuality of breathing during volitional moderate hyperventilation (2016) **Eur J Appl Physiol** 116:217–225

Laouani A, Rouatbi S, Saguem S, Calabrese P Thorax and abdomen motion analysis in patients with obstructive diseases (2016) **J Pulm Respir Med** 6: 313.

ACLN : Articles dans des revues nationales avec comité de lecture non répertoriées

Abdulhay E; Calabrese P; Baconnier P L'Estimation du Volume d'éjection Par La Thoracocardiographie est meilleure Quand la Glotte est fermée (2008) **Innov et Techno en Biol et Med-RBM** 29 : 297-301

ACTI : Communications avec actes dans un congrès international

Calabrese P, Ben Saïdane H, Eberhard A, Bachy JP, Levy P, Benchetrit G Thoraco-abdominal signal analysis during resistive loading and methacholine challenge (1997) **Eur Respir J** 10 (suppl. 25): 195s. (European Respiratory Society Annual Congress-Berlin, Présentation orale).

Benchetrit G, Azzouz M, Dinh TP, Eberhard A, Calabrese P, Perrault H Respiratory sinus arrhythmia is not enhanced in trained endurance athletes (1998) **Faseb J** 12 (5): 4011 Part 2 (Federation Amer Soc Exp Biol, Bethesda, USA)

Calabrese P, Eberhard A., Pham Dinh T, Bachy J.P, Benchetrit G Patterns of breathing during resistive loading (1998) **Am J Respir Crit Care Med** 157: A781. (American Thoracic Society, Chicago)

Calabrese P, Ben Saïdane H, Levy P, Benchetrit G Patterns of breathing during methacholine challenge (1999) **Am J Respir Crit Care Med** 159 (3) : A784-A784 (American Thoracic Society, New York)

Calabrese P, Ben Saïdane H, Levy P, Benchetrit G Patterns of breathing during methacholine challenge (1999) **Am J Respir Crit Care Med** 159: A784. (American Thoracic Society, San Diego)

Calabrese P, Perrault H, Pham-Dinh T, Eberhard A, Benchetrit G Respiratory sinus arrhythmia during respiratory resistive loading (1999) **Can J Appl Physiol** 24(5), 430 (Présentation orale).

Perrault H, Calabrese P, Pham-Dinh T, Eberhard A, Benchetrit G Heart rate variability and respiratory sinus arrhythmia is unchanged in highly trained endurance athletes (1999) **Can J Appl Physiol** 24(5), 472 (Présentation orale).

Calabrese P, Perrault H, Pham-Dinh T, Eberhard A, Benchetrit G *Respiratory sinus arrhythmia during respiratory resistive loading* (1999) **Can J Appl Physiol** 24(5), 430 (Présentation orale).

Perrault H, Calabrese P, Pham-Dinh T, Eberhard A, Benchetrit G *Heart rate variability and respiratory sinus arrhythmia is unchanged in highly trained endurance athletes* (1999) **Can J Appl Physiol** 24(5), 472 (Présentation orale).

Benchetrit G, Eberhard A, Calabrese P *Does the respiratory inductance plethysmography signal derivative provide a satisfactory approximation of the flow signal?* (2000) **Eur Respir J** (European Respiratory Society, Florence)

Calabrese P, Messonnier L, Bijaoui E, Eberhard A, Benchetrit G *Changes in breathing pattern induced by imagination of a rowing competition* (2002) **Eur Respir J** 20: Suppl. 38, 498s (European Respiratory Society, Stockholm)

Bijaoui E, Anglade D, Calabrese P, Eberhard A, Baconnier P, Benchetrit G *Can cardiogenic oscillations be used for assessing chest wall mechanics?* (2003) **Eur Respir J** 22: Suppl. 45, 189s (European Respiratory Society, Vienna)

Anglade D, Bijaoui E, Calabrese P, Eberhard A, Baconnier P, Benchetrit G *Can cardiogenic oscillations provide an estimate of chest wall mechanics?* (2004) **13h World Congress of Anaesthesiologists** (Paris)

Calabrese P, Sabil A, Benchetrit G, Baconnier P *Theoretical approach of thoraco-abdominal movements* (2004) **Eur Respir J** 24: Suppl. 48, 576s (European Respiratory Society, Glasgow)

Besleaga T, Calabrese P, Eberhard A, Benchetrit G, Vovc V, Baconnier P *Hyperventilation test recording by inductance plethysmography* (2005) **Eur Respir J** 26: Suppl. 49 (European Respiratory Society, Copenhagen)

Baconnier P, Mezioud N, Calabrese P *How to simulate the effect of swallowing on the respiratory rhythm generator?* (2006) **Eur Respir J** 28: 420s (European Respiratory Society, Munich)

Besleaga T, Calabrese P, Eberhard A, Trippenbach T, Benchetrit G, Vovc V, Baconnier P *Hyperventilation test at two different breathing rate: spontaneous and 20/min* (2006) **Eur Respir J** 28: 726s (European Respiratory Society, Munich)

Calabrese P, Besleaga T, Eberhard A, Vovc V, Baconnier P *Respiratory Inductance Plethysmography is suitable for voluntary hyperventilation test* (2007) **Annual inter conf of IEEE Eng in Med and Biol Society** p1055-1057

Calabrese P, Besleaga T, Dinh TP, Arnavielhe A, Eberhard A, Vovc V, Baconnier P *Individuality of breathing during voluntary hyperventilation* (2010) **Eur Respir J** 36 suppl.54: 412s (European Respiratory Society, Barcelona, Présentation orale)

Fontecave-Jallon J, Guméry PY, Calabrese P, Briot R, Baconnier P *A Wearable Technology Revisited for Cardio-Respiratory Functional Exploration: Stroke Volume Estimation From Respiratory Inductive Plethysmography* (2011) **pHealth**, Lyon

Videliér B, Fontecave-Jallon J, Calabrese P, Baconnier P, Guméry PY *Empirical Mode Decomposition of Respiratory Inductive Plethysmographic signals for stroke volume variations monitoring: respiratory protocol and comparison with impedance cardiography* (2012) **Annual inter conf of IEEE Engineering in Med and Biol Society**, San Diego

Laouani A, Calabrese P, Baconnier P and Saad S *Use of a Simple Respiratory Pump Model for Assessing Airway Resistance changes among Patients during the reversibility test* (2013) **Conférence Internationale de Bioinformatique et Biotechnologie**, Barcelone

Laouani A, Calabrese P, Rouatbi S and Saad S *Study for a non invasive Method of Respiratory Resistance Measurement among Patients with Airways obstructions* (2014) **Conférence Internationale de Biomécanique**, Venise

Laouani A, Rouatbi S, Calabrese P and Saad S *Airway Resistance evaluation by Respiratory inductive plethysmography in subjects with airway obstructions* (2015) **17th International conférence on médical image and Signal computing**, London

ACTN : *Communications avec actes dans un congrès national.*

Calabrese P *Effets de la posture et de la vigilance sur le mode ventilatoire des patients porteurs de la maladie de Steinert* (1999) **Actes des 12^{ème} Entretiens de l'Institut Garches**, Paris. (Présentation orale)

COM : *Communications orales sans actes dans un congrès international ou national.*

Al Chama F, Calabrese P, Benchetrit G, Baconnier P *Effets de la déglutition sur le rythme respiratoire* (2005) **Société Francophone de Biologie Théorique**, Saint-Flour

Fontecave J, Abdulhay E, Baconnier P, Calabrese P *Modèle d'interaction mécanique cœur-poumon* (2008) **Société Francophone de Biologie Théorique**, Saint-Flour

Calabrese P, Baconnier P, Brouta A *Un modèle fonctionnel simple pour l'interprétation des mesures non invasives de la ventilation* (2008) **Société Francophone de Biologie Théorique**, Saint-Flour

Fontecave J, Abdulhay E, Baconnier P, Calabrese P *Modélisation mathématique des échanges de gaz respiratoires dans l'organisme* (2009) **Société Francophone de Biologie Théorique**, Saint-Flour

AFF : *Communications par affiche dans un congrès international ou national.*

Calabrese P, Messonnier L, Benchetrit G *Variation of breathing during mental simulation of rowing competition* (2001) **PLügers Archiv Eur J Appl Physiol**, 442 (5), R92 (Société Française de Physiologie, abstract n°33)

Anglade D, Bijaoui E, Calabrese P, Eberhard A, Baconnier P, Benchetrit G *Peut-on estimer les variations du volume pulmonaire à partir des oscillations cardiogéniques ?* (2002) **Congrès de la SFAR** Paris

Anglade D, Bijaoui E, Calabrese P *Caractéristiques des respirateurs d'anesthésie en mode barométrique* (2002) **Congrès de la SFAR** Paris

Al Chama F, Calabrese P, Benchetrit G, Baconnier P *Effects of swallowing on central respiratory pattern generator* (2005) Société Française de Physiologie, Renne

Laouani A, Calabrese P, Eberhard A, Baconnier P *A simple dynamical model of respiratory pump* (2009) **Fund and Clinical Pharma** 23 : 6-6 abstract 31 (Congrès de Physiologie, Pharmacologie et Thérapeutique, Marseille)

Besleaga T, Calabrese P, Vovc V, Moldovanu I *Heart rate variability in voluntary hyperventilation at two frequencies* (2010) **High-tech, basic and applied research in**

physiology and medicine (International scientific-practical conference St Petersburg) 3 : 174-176 (International scientific-practical conference, St Petersburg)

Besleaga T, Calabrese P, Vovc V, Baconnier P, Moldovanu I *Effect of anxiety state on changes of breathing pattern during recovery after a voluntary hyperventilation test* (2011) **Fund and Clinical Pharma** 25 (1) : 64-64 abstract: 324 (Congrès de Physiologie, Pharmacologie et Thérapeutique, Grenoble)

Abdulhay E, Calabrese P, Fontecave-Jallon J, Gumery PY, Baconnier P *Respiratory inductive plethysmography for noninvasive cardio-respiratory monitoring* (2011) **Fund and Clinical Pharma** 25 (1) : 46-46 abstract: 230 (Congrès de Physiologie, Pharmacologie et Thérapeutique, Grenoble)

Heyer L, Calabrese P, Aitocine E, Gumery, PY, Trippenbach T, Baconnier P *Changes in the temporal relationship between onsets of alveolar activity and thoracic inspiratory muscles activity during auditory entrainment of the respiratory rhythm* (2011) **Fund and Clinical Pharma** 25 (1) : 74-75 abstract: 372 (Congrès de Physiologie, Pharmacologie et Thérapeutique, Grenoble)

Milano JR, Guméry PY, Gossard M, Fontecave-Jallon J, Heyer, L, Calabrese P, Trippenbach T, Baconnier P *Effet de l'entraînement du rythme respiratoire par un stimulus auditif sur la relation temporelle entre les débuts d'activité respiratoire des muscles des ailes du nez et du thorax* (2011) **Société Francophone de Biologie Théorique**, Autrans.

Fontecave-Jallon J, Calabrese P, Vettier B, Garbay C, Baconnier P *Sequential physiological analysis of daily-life recordings* (2012) **Fund and Clinical Pharma** 26 (1): 46 (Congrès de Physiologie, Pharmacologie et de Thérapeutique, Dijon)

Gossard M, Calabrese P, Heyer L, Milano JR, Guméry PY, Baconnier P. *Comparison between an automatic algorithm and experts for the detection of onsets of alveolar activity and thoracic inspiratory muscles* (2012) **Fund and Clinical Pharma** 26 (1) : 59 (Congrès de Physiologie, Pharmacologie et Thérapeutique, Dijon)

Direction d'ouvrage :

Calabrese P, Fontecave-Jallon J (Guest editors) *Proceedings of the XXIXth Conference of the French-speaking Society for Theoretical Biology (St-Flour, France, 14-17 June, 2009)* (2010) **Acta Biotheoretica**, 58 : 2-3

Thèse:

Calabrese P *Recherche d'une méthode de mesure non-invasive des résistances respiratoires. Effets ventilatoires et cardiaques de charges résistives* (14/12/1998) Génie Biologique et Médical, Université Joseph Fourier, Grenoble (<http://tel.archives-ouvertes.fr/tel-00968633>)

Partie II ACTIVITES DE RECHERCHE

II.1 PREAMBULE

Mon travail de recherche est essentiellement axé sur la **physiologie respiratoire** et **cardiaque**. A partir de données physiologiques enregistrés sur *des volontaires sains ou des patients*, j'ai cherché à:

- décrire ces deux fonctions physiologiques et leurs interactions dans certaines conditions (Figure 1 **Exploration**, § II.2 et II.3)
- mettre au point des nouveaux indices d'évaluation de données en physiologie respiratoire et cardiaque (Figure 1 **Mesure**, § II.4)
- formuler des approches théoriques pour la validation de modèles (Figure 1 **Approche théorique**, § II.5).

Les travaux de recherche en cours s'inscrivent dans la continuité des thématiques précédentes et seront présentés dans les perspectives (II.6).

L'ensemble des publications est présenté sur la Figure 1 pour chaque thématique précédente. Celles qui apparaissent en bleu, sont insérées en entier dans le document.

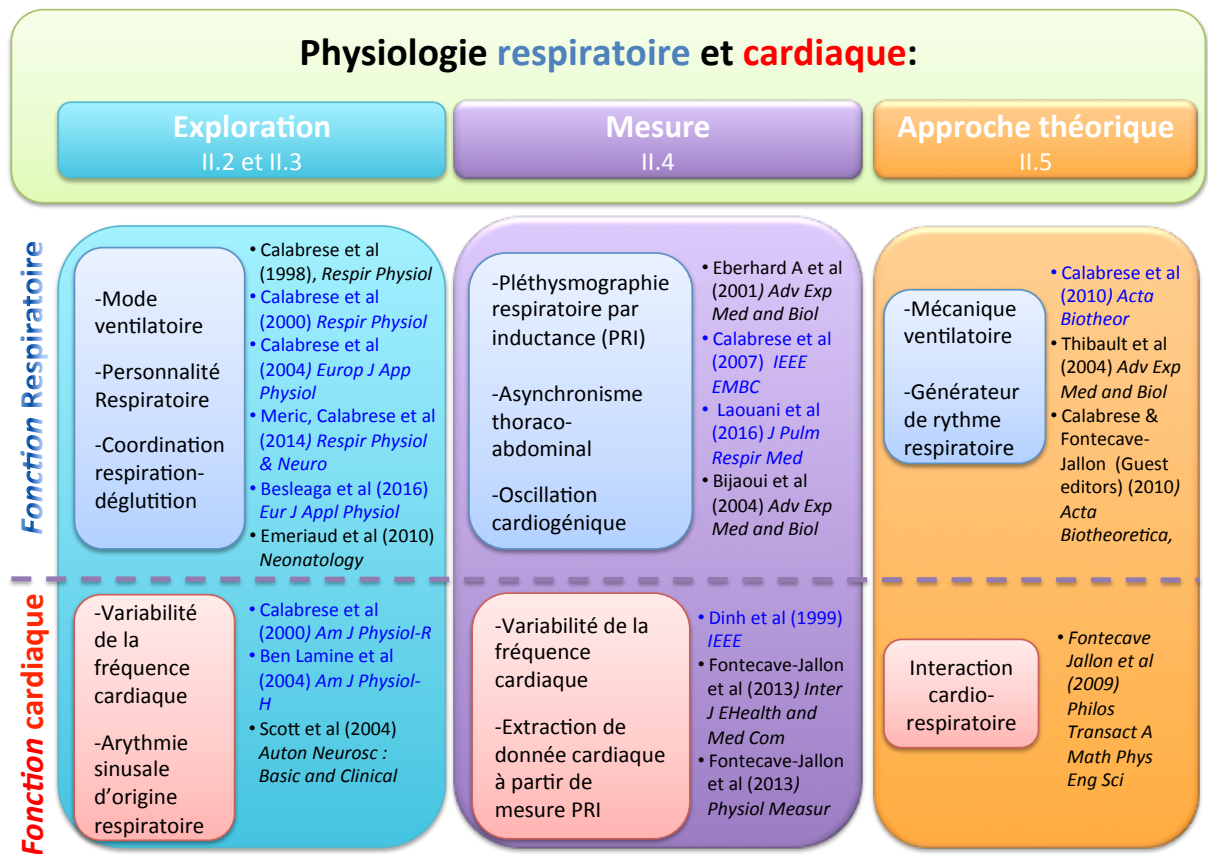


Figure 1 : Thématiques et publications afférentes. Les publications indiquées en bleu sont insérées en entier dans le document

Pour chacun des travaux de recherche, j'ai présenté dans un cadre bleu avec un code couleur: les conclusions, les *références des publications*, et quand il y a lieu les *collaborations scientifiques*, les *encadrements d'étudiants*, et les *contrats* associés.

II.2 MODE VENTILATOIRE : DIVERSITE ET “PERSONNALITE”

II.2.1 Introduction

II.2.1.1 Les caractéristiques ventilatoires

Chaque cycle ventilatoire (une inspiration et expiration) est caractérisé par sa durée T_{TOT} et son amplitude, le volume courant V_T , ainsi que les durées inspiratoire T_I et expiratoire T_E (Figure 2). La fréquence ventilatoire F_R exprimée en nombre de cycles par minute peut aussi être calculée $F_R = 60 / T_{TOT}$.

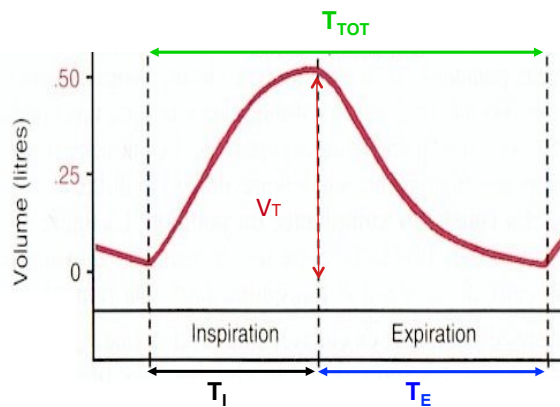


Figure 2 : Un cycle ventilatoire et ses caractéristiques : la durée totale T_{TOT} , les durées inspiratoire T_I et expiratoire T_E et le volume courant V_T .

La forme moyenne d'une courbe volume peut-être représentée en prenant ensemble les données T_I , T_E et V_T moyennes calculées à partir de valeurs obtenues pour chaque cycle ventilatoire (Figure 3).

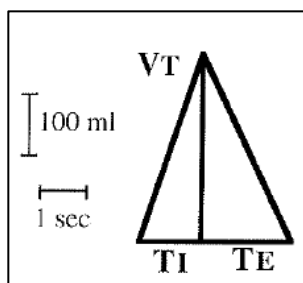


Figure 3 : Représentation de la forme d'un signal volume

La diversité des modes ventilatoires au repos a été rapportée dès le 19^{ième} siècle. La fréquence ventilatoire peut varier de 6 à 31 cycles par minute. Les durées des temps

inspiratoire et expiratoire présentent aussi une diversité ventilatoire, et des combinaisons différentes de T_I et T_E sont possibles quelle que soit la durée du cycle ventilatoire (T_I reste cependant toujours inférieur à T_E). Les volumes courant au repos peuvent prendre des valeurs allant de 442 à 1549 ml ([Dejours 1961](#)). L'individualité et la reproductibilité des modes ventilatoires au repos ont été rapportées au milieu du 20^{ème} siècle ([Proctor et Hardy, 1949](#); [Morrow et Vosten, 1953](#)). Le concept de "personnalité ventilatoire" a été introduit par Dejours et al (1961) : *"Un même débit ventilatoire total ou alvéolaire peut-être réalisé par une infinité de combinaisons du volume courant (V_T) et de la fréquence ventilatoire (F_R). Chaque sujet possède sa propre combinaison $F_R * V_T$ et, de plus, une forme des mouvements respiratoires qui lui est propre ; en réalité, tout sujet est doué d'une certaine personnalité ventilatoire."* Le travail de l'équipe PRETA a apporté une dimension supplémentaire au concept de "personnalité ventilatoire" en montrant l'existence pour chaque individu d'un mode ventilatoire et d'une forme de débit qui lui est propre. En effet, la forme du débit des cycles ventilatoires (débit enregistré à la bouche par pneumotachographie, Figure 4) présentait une diversité entre les différents sujets et une individualité pour chaque sujet.



Figure 4 : Débit ventilatoire instantané mesuré par pneumotachographie

Ce travail sur la forme des cycles ventilatoires a été possible en développant d'une part, des outils de quantification basés sur des méthodes d'analyse de signal (analyse harmonique) et d'autre part, en développant des méthodes statistiques de comparaison multivariée (test de similarité).

II.2.1.2 Quantification de la forme des cycles ventilatoires (analyse harmonique)

Afin de pouvoir les comparer, une méthode de quantification de la forme des cycles basée sur une analyse harmonique de chaque cycle de débit instantané a été mise au point au laboratoire ([Bachy et al, 1986](#)). La période de la fondamentale (T) est égale à la durée de chaque cycle. Les 32 harmoniques sont calculées et Bachy et al. (1986) ont montré que plus de 95 % de la puissance du signal est contenue dans la fondamentale et les trois premières harmoniques, la fondamentale contenant une grande part de ces 95%. La forme du cycle reconstitué à partir de la fondamentale et des trois harmoniques suivantes (qui ont respectivement pour période : $\frac{T}{2}$, $\frac{T}{3}$ et $\frac{T}{4}$) est donc très proche de la forme du signal initial (Figure 5). Chaque harmonique est caractérisée par un nombre complexe. Ainsi, la forme du cycle est représentée par quatre nombres complexes, ou huit nombres réels (coordonnées cartésiennes). Ces quatre (ou huit) nombres peuvent être représentés (Fresnel) dans le plan par quatre vecteurs.

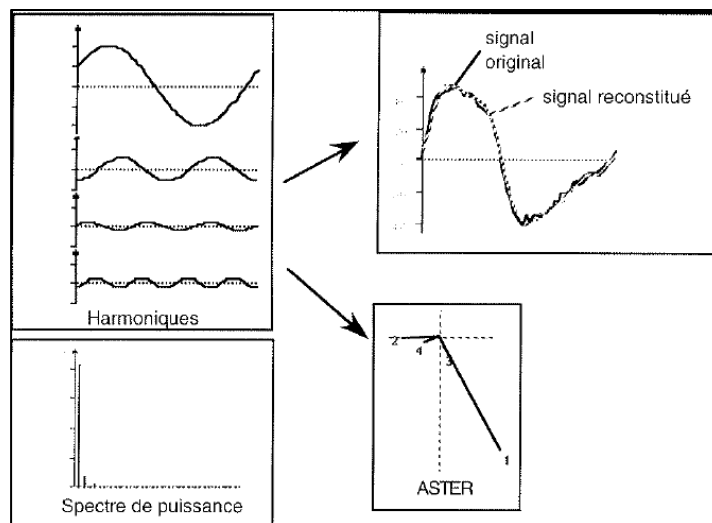


Figure 5 : Représentation de l'analyse harmonique sur un cycle de débit : Les 4 premières harmoniques, le spectre de puissance de ce cycle, le débit d'origine et le débit reconstitué à partir des 4 premières harmoniques et la représentation de Fresnel associée.

Cette analyse cycle par cycle permet d'obtenir, une quantification de la forme "moyenne" d'un cycle ventilatoire, en calculant la moyenne des coordonnées de l'analyse harmonique effectuée sur les cycles sélectionnés à partir de l'enregistrement du signal débit sur une durée déterminée.

II.2.1.3 Comparaison multivariée de la forme des cycles ventilatoires (test de similarité)

Un test statistique multivarié (test de similarité) a été mis au point dans l'équipe, afin de pouvoir comparer la forme des cycles ventilatoires soit en volume en prenant les trois données (T_i , T_E et V_T) soit en débit en prenant les huit coordonnées de l'analyse harmonique. Le principe de ce test est la comparaison des différences intra-individuelles avec les différences inter-individuelles dans deux conditions différentes, pour une variable ou un ensemble de variables. L'objectif de ce test est de montrer que dans deux situations différentes, chaque individu est "identifiable" parmi un ensemble d'individus. Un test significatif indique que les différences entre les formes des cycles ventilatoires d'un même individu enregistré dans deux conditions différentes sont moins grandes que les différences entre deux individus pris au hasard dans le même échantillon. Ainsi, les formes du volume d'une part, et du débit d'autre part, ont été comparées entre tous les individus d'un même échantillon dans deux situations. Cette méthode est détaillée par [Benchetrit et al \(1989\)](#) ainsi que dans ma thèse. Ces auteurs ont montré d'une part, un maintien de la forme des cycles ventilatoires (débit et volume) au repos pour chaque individu à quatre ans d'intervalle ([Benchetrit et al, 1989](#)) et d'autre part, la similarité de la forme de la ventilation de repos chez les jumeaux ([Shea et al, 1989](#)).

II.2.2 La diversité des modes ventilatoires

II.2.2.1 Chez les patients atteints de dystrophie myotonique (maladie de Steinert)

La diversité des modes ventilatoires a été étudiée chez des patients atteints de dystrophie myotonique (maladie de Steinert). En effet, ces patients souffrent de multiples déficiences et en ce qui concerne la fonction respiratoire, ces déficiences se manifestent aussi bien au niveau de la régulation que du mode ventilatoire. Les données ventilatoires ont été enregistrées par pneumotachographie et pléthysmographie respiratoire à variation d'inductance chez 9 patients myotoniques en position assise et couchée, yeux ouverts (pour éviter l'assoupissement).

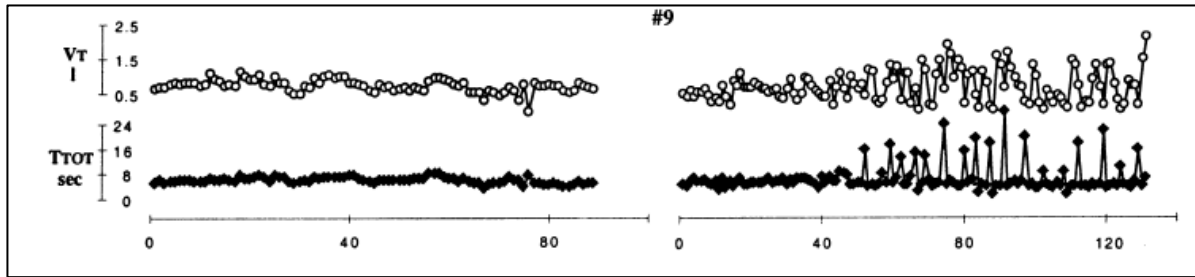


Figure 6 : Valeurs des volumes courant (V_T en litre, l) et des durées (T_{TOT} en seconde, sec) pour une série de cycles ventilatoires consécutifs en position assise (à gauche) et couchée (à droite) pour un patient.

Le principal résultat est l'apparition progressive d'une ventilation irrégulière en position couchée chez certains patients atteints de dystrophie myotonique (Figure 6).

La particularité de l'ajustement de la ventilation en relation avec la posture chez certain patient atteint de dystrophie myotonique est à prendre en compte lors de l'analyse des anomalies ventilatoires au cours du sommeil fréquemment observées chez ces patients.

Calabrese et al (2000) Postural breathing pattern changes in patients with myotonic dystrophy, Respir Physiol.

Post-doctorat, financé par l'Institut Garches, dans le Service de Réanimation Médicale (Pr Raphaël) à l'hôpital Raymond Poincaré (Hôpitaux Universitaires Paris Ile-de-France Ouest)-1999-2000



Postural breathing pattern changes in patients with myotonic dystrophy

Pascal Calabrese^a, Nicolas Gryspeert^a, Igor Auriant^b,
Claudine Fromageot^c, Jean-Claude Raphaël^b, Frederic Lofaso^c,
Gila Benchehri^{a,*}

^a Laboratoire de Physiologie Respiratoire Expérimentale, Théorique et Appliquée (PRETA-TM/C, UMR CNRS 5525),

Faculté de Médecine de Grenoble, Université Joseph Fourier, 38 700 La Tronche, France

^b Service de Réanimation Méthodique, Hôpital Raymond Poincaré, 92 280 Garches, France

^c Service de Physiologie et d'Explorations Fonctionnelles, Hôpital Raymond Poincaré, 92 280 Garches, France

Accepted 11 April 2000

Abstract

We recorded by pneumotachography the breathing in nine patients with myotonic dystrophy (MD), both seated and supine and with eyes open in both positions. Irregular breathing (coefficient of variation > 20% for VT and TROT) was observed in six of the patients; two of whom showed irregularity in both positions whilst the remaining four had irregular breathing only when supine. In addition, in this latter group, irregularities first appeared in VT and only after a few minutes in TROT. Whereas in the group exhibiting regular breathing in both seated and supine positions, irregularities were observed throughout the recording. However, no significant difference in any ventilatory variable was observed as between the two postures. Rib cage (RC) and abdomen (AB) motions were recorded by uncalibrated respiratory inductance plethysmography. Although for MD patients the mean values of the RC/AB ratio lay within the normal range the relative decrease in value as between seated (0.78 ± 0.52) and supine (0.31 ± 0.13) position was less than in healthy subjects. These observations suggest that MD may cause deficiencies in several mechanisms. Analyses of the respiratory pattern in each patient may provide information leading to the identification of the impaired respiratory mechanisms. © 2000 Elsevier Science B.V. All rights reserved.

Keywords: Disease; myotonic; dystrophy; Mammals; humans; Pattern of breathing; posture; myotonic; dystrophy

1. Introduction

Although a similar resting ventilation has been observed in patients with myotonic dystrophy (MD) to that in control subjects, high respiratory frequency and low tidal volume have been reported in the former (Bégin et al., 1982; Sersier et

2

al., 1982; Jammes et al., 1985; Bogard et al., 1992; Ververs et al., 1996). Myotonia of the respiratory muscles (Bégin et al., 1982; Rimmer et al., 1993), and altered afferent output from diseased muscles (Bégin et al., 1980; Sersier et al., 1982; Jammes et al., 1985) may offer an explanation for both tachypnea and the lower tidal volume in patients with MD.

Another feature of the breathing pattern in patients with MD is the occurrence of irregular breathing (Gilliam et al., 1964; Cocagna et al., 1975; Sersier et al., 1982). Such irregularities in breathing pattern have been described (Gilliam et al., 1964) as consisting of periods of irregular respiration occurring at more or less regular intervals and often separated by periods of apnea in the case of patients in a semi-recumbent position. For patients when awake, a significantly greater variability in tidal volume and respiratory cycle time was found than in control subjects (Bogard et al., 1992; Gibson et al., 1992; Veale et al., 1995; Ververs et al., 1996). In the view of several authors (Gilliam et al., 1964; Bogard et al., 1992; Ververs et al., 1996), this irregularity may be considered to result to a large extent, from influences during consciousness from the higher centres which are insufficiently corrected for by the chemical control mechanism. A behavioural influence also seemed to be present in patients with MD, since irregularity in breathing pattern, present in the wakeful state and during light sleep, decreased noticeably during slow-wave sleep (Gibson et al., 1992; Veale et al., 1995). It was suggested (Bogard et al., 1992) that the uncoordinated action of the expiratory and inspiratory intercostal muscles may provide a partial explanation of breathing irregularity in patients with MD. Another contributory factor would then be a deficiency in respiratory control related to disordered afferent information from the diseased muscles, since abnormalities in the muscle spindles of patients with MD have been documented (Swash and Fox, 1975) and there is evidence of impaired afferent activity from these muscles (Stranock and Newsom Davis, 1978).

The impairment of respiratory muscle function may also be studied by examining breathing patterns in different postures. Indeed, the movements associated with changes in posture, common in everyday life, call into play forces which alter the operating length of the respiratory muscles and induce changes in force distribution in the respiratory muscle and in the activity of various inspiratory muscles (Vealody et al., 1978).

The aim of the present study was to examine a possible deficiency in the mechanisms responsible for adjusting respiratory muscle activation to different body positions. Resting breathing in patients with MD was recorded by pneumotachography for both the seated and supine position, with eyes open in both postures. In addition, rib cage and abdominal motions in the supine and seated positions were recorded by inductance plethysmography, as patients with neuromuscular diseases have been reported to display in general abnormal thoracoabdominal patterns of breathing (Perez et al., 1996).

2. Methods

2.1. Patients

Nine patients (five male) with MD, seen at the hospital for a routine visit, participated in the study. According to muscular disability rating scale described by Bégin et al. (1997), these patients may be classified as III (moderate proximal weakness, ambulatory). Informed consent was obtained from all patients. The experimental protocol was examined and approved by the Institutional Ethics Review Board. Five patients had a passive pacemaker. Patient characteristics are summarized in Table 1. No patient exhibited severe respiratory deficiency but mild restrictive respiratory disorder was observed in three patients. Pulmonary function data, P_{50} , P_{aCO_2} and respiratory CO_2 response (Infrared analyser, Gould) are shown in Table 2. Predicted values for VC, FEV₁, and FEV₁/VC were those of the European Community (Quang et al., 1993) and for P_{limax} and P_{Fmax} those of Black and Hyatt (1969). A CO_2 rebreathing test was performed according to the method described by Reid (1967).

* Corresponding author. Tel.: +33-4-76637106; fax: +33-4-76637186.

E-mail address: gila.benchehri@img.fr (G. Benchehri).

2.2. Measurement and protocol

Airflow was measured with a pneumotachograph (Fleish head No. 1) and a differential pressure transducer (63PQ01D36, Micro Switch) mounted on a face mask. An uncalibrated respiratory inductive plethysmograph (RIP) was used to obtain rib cage (RC) and abdomen (AB) motion signals. The sensitivity and calibration factors were set at the same values for both channels (Respirace, model 150, Studley, Data).

Two series of 10-min recordings were performed corresponding to the seated and the supine position respectively. In each case patients were instructed to keep their eyes open during the entire recording period.

2.3. Data analysis

Data acquisition was performed with a recorder (TA11, Gould Electronic) on a PCMCIA card at a sampling rate of 200 Hz. A paper trace was also obtained. The PCMCIA card files were converted into compatible Macintosh microcomputer text files for further analysis. The flow signal was analyzed breath-by-breath in order to obtain tidal volume (VT) by integration of the flow signal, breath duration (Trot), and inspiratory (TI) and expiratory (TE) durations, for each breath. Minute ventilation, VT/TI and TI/Trot were calculated for each breath. Mean values of these variables were then calculated for each recording.

Table 1

Patients characteristics				
	Height (cm)	Weight (kg)	Age (years)	Sex
#1	164	73	38	F
#2	155	64	57	F
#3	182	83	36	M
#4	159	82	37	F
#5	162	82	36	F
#6	164	68	47	M
#7	173	92	33	M
#8	177	68	63	M
#9	167	77	48	M
Mean	167	77	48	
SD	9	10	12	

Table 2
Lung function tests and CO₂ sensitivity^a

	VC (%pred)		FEV ₁ (%pred)		FEV ₁ /VC (%pred)		P _I max (%pred)		P _E max (%pred)		PaO ₂ (kPa)	PaCO ₂ (kPa)	CO ₂ test
	Seated	Supine	Seated	Supine	Seated	Supine	Seated	Supine	Seated	Supine			
#1	85	83	93	90	109	108	86	70	86	76	12.05	6.35	
#2	86	87	72	74	84	85	62	62	53	42	11.40	4.90	1.00
#3	107	110	87	77	83	77	118	120	38	46			0.88
#4	71	64	65	56	91	87	59	46	39	33	10.50	5.40	0.80
#5	62	61	64	60	103	99	37	27	31	31	11.30	5.30	0.36
#6	83	88	70	74	84	84	73	73	44	40	8.03	6.18	1.81
#7	58	58	62	61	107	102	38	28	62	63	8.21	5.61	0.70
#8	85	81	67	62	79	77	44	33	32	27	13.10	5.52	1.40
#9	107	109	111	106	109	109	43	44	46	47			1.31

^a VC, vital capacity; FEV₁, forced expiratory volume in 1 sec; P_Imax and P_Emax, maximum static inspiratory and expiratory pressures; CO₂ test, slope of \dot{V}_1 versus PETCO₂ in seated position, l·min⁻¹ mmHg⁻¹. For VC, FEV₁, and FEV₁/VC predicted values were those of the European Community (Quanjer et al., 1993). For P_Imax and P_Emax predicted values were those of Black and Hyatt (1969). The CO₂ rebreathing test was performed according to the method described by Read (1967).

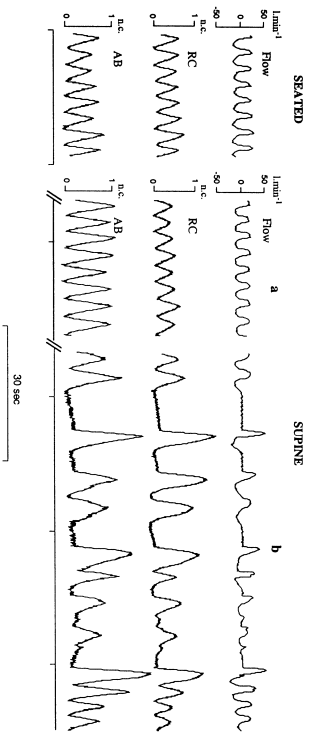


Fig. 1. An example of airflow, rib cage (RC) and abdomen (AB) motion signals recorded seated and supine at the beginning (a) and towards the end (b) in subject # 9.

case of four patients expiratory pauses were only observed in the supine position and occurred in the latter part of the recording a few minutes after the patients had lain down. An example of such recording is shown in Fig. 1. The two remaining patients exhibited expiratory pauses in both positions.

Expiratory pauses were associated with high values of V_T . Indeed, Table 3 shows greater variability in V_T , T_E and T_{TOT} . Irregular breathing was present only in the supine position in subjects # 1, 4, 6 and 9 but in both positions for subjects # 5 and 8. The remaining three patients showed less irregular breathing, i.e. the coefficients of variation of V_T and T_{TOT} were less than 20% in both supine and seated position. Series of breath duration (T_{TOT}) and tidal volume (V_T) are shown in Fig. 2, in both positions, for one representative patient of each group.

However, the pattern of irregular breathing in those patients with irregularities in both postures differed from that of those with irregularities only in the supine position. Indeed, in this latter group,

irregularities are first visible in V_T and only after a few minutes of being supine in T_{TOT} whereas in the former group (i.e. of irregular breathing both seated and supine), irregularities were observed throughout the recording.

The comparison of the respiratory variables T_{TOT} , T_I , T_E , V_T , V_I , V_T/T_I and T_I/T_{TOT} within subjects in the seated and supine position, is illustrated in Fig. 3, where mean values and standard deviations are shown for each subject. Identity lines were drawn to better illustrate the changes as between postures. Results show V_I , V_T and V_T/T_I to be lower in the supine position except in the case of subjects # 3 and 9 for V_I , subject # 1 for V_T and # 9 for V_T/T_I . As regards breathing time variables, T_{TOT} , T_I and T_E , and the T_I/T_{TOT} ratio values, no consistent trend was found to the changes.

Results of comparisons (paired *t*-test) of the mean values of the respiratory variables for all nine patients are reported in Table 3. No significant difference in any variable as between positions was observed.

Table 3
Respiratory variables for each subject seated and supine*

	T_{TOT} (sec)		T_I (sec)		T_E (sec)		V_T (l)		\dot{V}_I (l·min ⁻¹)		V_T/T_I (l·sec ⁻¹)		T_I/T_{TOT}	
	Seated	Supine	Seated	Supine	Seated	Supine	Seated	Supine	Seated	Supine	Seated	Supine	Seated	Supine
# 1	3.54	4.68	1.22	1.58	2.32	3.09	0.38	0.45	6.51	6.30	0.31	0.29	0.35	0.37
%	16.5	46.2	13.6	20.6	21.5	66.6	32.8	42.8	24.6	46.1	21.0	50.4	12.3	25.4
# 2	3.98	3.78	1.50	1.52	2.48	2.25	0.39	0.34	5.83	5.39	0.26	0.22	0.38	0.40
%	15.6	13.3	14.6	14.7	19.1	15.1	29.7	20.2	20.2	13.6	21.7	15.7	9.7	7.9
# 3	3.93	3.42	1.60	1.46	2.33	1.95	0.65	0.58	9.90	10.20	0.40	0.40	0.41	0.43
%	16.8	13.5	17.8	15.3	21.3	17.6	21.1	20.9	15.9	18.1	15.1	16.2	12.4	10.7
# 4	4.62	4.25	1.42	1.56	3.20	2.69	0.47	0.43	6.20	6.13	0.33	0.27	0.31	0.38
%	18.8	26.9	13.2	18.0	24.2	37.0	21.7	26.5	15.4	19.5	12.9	19.9	14.4	18.4
# 5	4.56	5.37	1.48	1.45	3.08	3.92	0.67	0.65	8.89	7.38	0.45	0.45	0.33	0.28
%	26.8	21.1	22.9	19.4	33.1	25.8	28.3	20.2	26.8	24.1	18.9	12.8	17.6	22.9
# 6	5.14	6.57	2.28	2.34	2.87	4.23	0.66	0.57	7.73	5.26	0.29	0.24	0.44	0.37
%	14.8	29.0	16.1	24.9	18.1	44.3	13.0	39.1	10.7	31.9	11.1	28.0	9.9	24.7
# 7	4.13	3.98	1.47	1.53	2.66	2.45	0.66	0.63	9.69	9.53	0.45	0.41	0.36	0.39
%	16.9	14.2	19.1	14.6	21.0	18.2	17.0	17.9	16.9	15.1	13.9	12.4	14.4	9.5
# 8	6.40	5.03	1.26	1.13	5.14	3.90	0.92	0.63	9.18	8.78	0.73	0.55	0.21	0.26
%	33.1	46.4	16.3	16.1	39.3	60.5	23.4	28.3	28.8	43.3	15.5	20.7	26.6	39.7
# 9	6.05	6.46	3.13	1.82	2.91	4.65	0.74	0.71	7.37	8.30	0.24	0.38	0.52	0.35
%	16.8	69.5	21.6	32.2	18.6	99.6	24.3	62.4	20.5	74.1	30.9	59.2	12.3	40.1
P	0.668		0.526		0.488		0.093		0.213		0.338		0.728	
Mean	4.70	4.84	1.71	1.60	3.00	3.24	0.61	0.55	7.92	7.48	0.39	0.36	0.37	0.36
%	19.6	31.1	17.2	19.5	24.0	42.7	23.5	30.9	20.0	31.7	17.9	26.1	14.4	22.1

* Mean values and coefficients of variation (%) of the respiratory variables for each subject seated and supine. T_{TOT} : breath duration; T_I and T_E : inspiratory and expiratory time; V_T : tidal volume; \dot{V}_I : minute ventilation; P: paired *t*-test results of comparisons of the mean values of the respiratory variables for all nine patients; Mean values and mean coefficients of variation calculated for all patients in both positions are represented on the bottom lines.

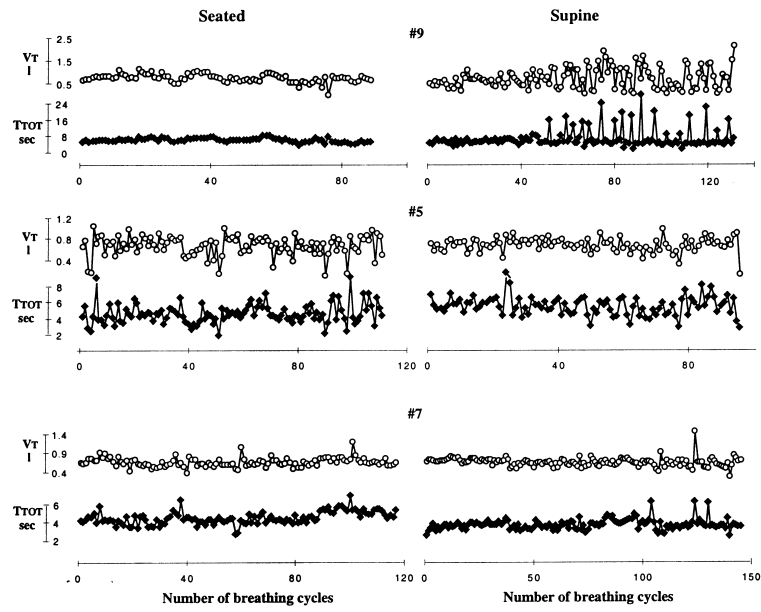
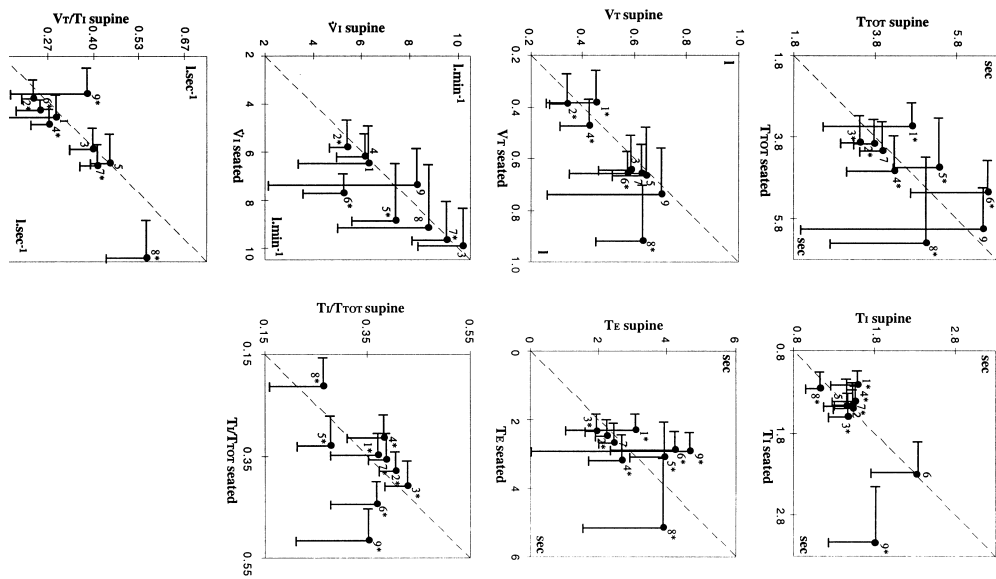


Fig. 2. Series of breath duration (TROT) and tidal volume (Vt) for three subjects. The top panel shows a subject in which irregular breathing appeared only in the supine position. The subject in the middle panel showed irregular breathing in both seated and supine positions while the subject in the bottom panel was considered to breathe regularly because their coefficient of variation was less than 20%.



3.2. Comparison of thoracoabdominal motion between seated and supine positions

Plots of mean RC versus mean AB for all subjects in both positions are represented in Fig. 4 with the same X and Y-axis scales. Fig. 4 shows that the RC versus AB plots are flattened ellipses, which indicate that there were no asynchrony between the rib cage and abdomen motions neither seated nor supine. For subject # 6, the RC versus AB plots crosses in both positions. This suggests that the RC and AB motion have different rate of changes.

The mean RC/AB ratio \pm standard deviation appears in the left-hand corner of each plot for the seated position and in the right-hand corner for the supine position. Significantly lower mean values of this ratio are found in the supine as compared to the seated position in all patients. The change in the RC/AB ratio as between seated and supine position seems to bear no relation to the breathing pattern variability. Indeed, as regards subjects # 2 and # 9 who exhibit the greatest change in the RC/AB ratio from seated to supine position, variability in T_{rot} is similar in both positions for subject # 2 whilst exhibiting a marked increase from seated to supine in subject # 9.

4. Discussion

In this study on nine wakeful patients with MD, breathing pattern analysis revealed irregularities for four patients in the supine position only whereas for two other patients irregular breathing was exhibited in both positions. Despite the irregular pattern observed in the supine position in these four patients, comparison of the mean values of the respiratory variables as between the seated and supine position revealed no significant difference.

Comparing breathing pattern in control subjects and patients with MD in seated and supine posi-

tion, a significant decrease in supine as compared to seated position was found only in V_T/T_I for patients but also for control subjects (Bégin et al., 1982). Although not significantly different, both V_T and V_T/T_I appeared to be lower in supine as compared to seated posture for most of the patients (Fig. 3) in the present study.

Irregularities in breathing pattern are clearly apparent when breath-by-breath values are plotted for the whole of the recording, as illustrated in Fig. 2. Irregular respiration in patients with MD has already been reported both in individual case studies (Cocagna et al., 1975) and in group studies (Serisier et al., 1982; Bogard et al., 1992; Gibson et al., 1992; Veale et al., 1995; Ververs et al., 1996) where a significantly more marked irregularity than in control subjects was observed. However, as in the present study, not all patients with MD manifest irregular breathing. In the earlier studies irregular breathing was reported in seven out of 19 myotonic patients with less marked irregularities in six others (Serisier et al., 1982), and in four out of seven patients when awake (Gibson et al., 1992; Veale et al., 1995). In the present study, it is noteworthy that the pattern of irregular breathing in those patients with irregularities in both positions was different from that of those with irregularities in the supine position only. Indeed, in the two patients with irregular breathing in both positions, irregularity was continuous (Fig. 2), whereas in the four patients with irregularities only when supine, periods of irregular breathing appeared after a few minutes in the supine position and occurred at more or less regular intervals.

It has been postulated that breathing irregularity results, to a large extent, from influences from the higher centers that are insufficiently corrected for by the chemical control mechanism (Ververs et al., 1996). Indeed, although statistically not significant, there was a tendency for patients with a normal ventilatory CO₂ response to breathe more regularly than patients with a lowered ventilatory CO₂ response (Bogard et al., 1992; Ververs et al., 1996).

Fig. 3. Comparison of respiratory pattern between the two postures in all subjects. Seated versus supine plots of mean \pm S.D. values of respiratory variables: Breath duration (T_{rot}), inspiratory time (T_I), expiratory time (T_E), tidal volume (V_T), minute ventilation (V_E), T_I/T_{rot} and V_T/T_I.

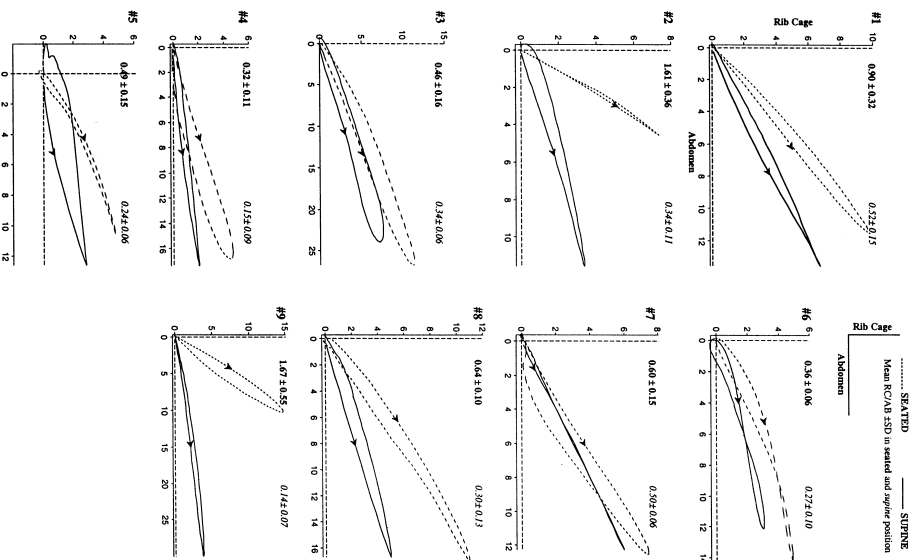


Fig. 4. Mean rib cage (RC) versus mean abdomen (AB) Fourier coefficients, calculated breath-by-breath, for the nine subjects in seated and supine positions. Mean values of the RC/AB ratio \pm S.D. for both positions are reported on each plot.

This hypothesis is also supported by Gilliam et al. (1964), who showed breathing irregularities in patients with MD to increase in cases of weakening of CO₂ sensitivity by an anesthetic agent (thiopentone). Although statistically not significant, an inverse relationship was found to exist between the ventilatory CO₂ sensitivity and the irregularity of respiratory cycle time and tidal volume (Bogard et al., 1992). Such mechanisms may explain irregularities such as those observed in patient #5, who exhibited irregular breathing in both positions associated with low CO₂ sensitivity. However, patient #8, with irregular breathing in both positions had a normal ventilatory CO₂ sensitivity response. Furthermore, we did not observe any correspondence between the value of Pa_{o2} and the irregularity of the breathing pattern.

The irregularities associated with the supine position may involve other mechanisms. Irregular breathing was found in patients sitting or lying undisturbed and it was not limited to periods of drowsiness (Serieter et al., 1982). Although drowsiness has often been reported in patients with myotonia (Kilburn et al., 1959; Plehmister and Small, 1961; Coccaagna et al., 1975), there is no possible question that our patients did not remain alert as they were instructed to keep their eyes open during the whole of the recordings. Thus, irregular breathing would not appear to be linked to drowsiness. Furthermore, the variability in breathing interval in patients with MD is only significantly higher during wakefulness and light sleep, than that in patients with nonmyotonic muscle disease and in normal subjects, all three groups showing similar variability during slow-wave sleep (Gibson et al., 1992; Veale et al., 1995).

Changes in posture involve the exertion of forces which alter the operating length of the respiratory muscles. In normal subjects there is adjustment of respiratory muscle activation such that any difference in respiratory characteristics between seated and supine position is remedied by the second breath following posture change. This ventilatory compensation during postural change is not obtained via vagal afferent information but rather through respiratory muscle receptors (Kin-

near et al., 1989). In this study irregular VTOT when supine occurs only after a few minutes whereas VT exhibits higher variability from the outset. One possible explanation could be that the mechanism adjusting ventilation when changing from seated to supine position does not operate as rapidly as in healthy subjects, leading to fluctuations in VT. The accumulation of deficits in this regulating mechanism may then be responsible of the occurrence of irregular breaths with expiratory pauses. On this hypothesis, impairment of the respiratory muscle receptors is assumed to trigger irregular breathing. Indeed, abnormalities in the muscle spindles of patients with MD are well recognized (Swash and Fox, 1975) and evidence of impaired afferent activity has been demonstrated (Stranock and Newson Davis, 1978). However, the weakness of the respiratory muscle can not be ruled out as a factor in irregular breathing. Weakness of respiratory muscles in patients with MD may be partly responsible for limiting ventilatory performance (Bégin et al., 1982) and for the pathogenesis of hypoventilation (Kilburn et al., 1959; Bégin et al., 1997). A large decrease in maximal mouth pressure in patients with MD as compared to that in normal subjects has been reported in several studies (Gilliam et al., 1964; Bégin et al., 1982; Serieter et al., 1982; Bogard et al., 1992). In addition, these studies reported a more marked impairment of P_{max} than of P_{max} consistent with the data in this study. This reduction is probably the result of weakness of the abdominal muscles which are the major expiratory muscles (Serieter et al., 1982).

Myotonia of the respiratory muscles could result in a decrease in compliance of the chest wall, which may in turn increase the work of breathing and threaten muscle fatigue resulting in a change of tidal volume and respiratory frequency in order to prevent this fatigue (Rimmer et al., 1993). Respiratory muscle weakness in patients with MD may induce abnormal motions of the rib cage and abdomen, similar to those observed in patients with neuromuscular diseases (Perez et al., 1996), these abnormalities being aggravated by the change from seated to supine position. Unlike Perez et al. (1996) we did not observe (Fig. 4) asynchrony between RC and AB motions. Indeed,

the RC versus AB plots in both positions are elliptic loops similar to those described by Verstraeten and Daniels (1995) in healthy subjects during quiet breathing.

The partition of VT into its thoracic and abdominal volume displacement did not differ as between patients with MD and control subjects, either in the seated or supine position (Bégin et al., 1982). A decrease of 74.4% in the RC/AB ratio has been reported (Velody et al., 1978) from seated to supine position, mean values being 0.90 seated and 0.23 supine. In another study (Sharp et al., 1975) an 82.7% decrease in the RC/AB ratio from seated to supine was found with however higher values of the RC/AB ratio in both positions (2.08 in seated and 0.36 in supine). Our results indicated a fall from 0.78 ± 0.52 in the seated position to 0.31 ± 0.13 in the supine, i.e. a decrease of 60.3% when changing from seated to supine position. Although the values of the RC/AB ratio were in the range of those already reported (Sharp et al., 1975; Velody et al., 1978), the percentage decrease appeared to be lower in patients with MD than in healthy subjects. However, it should be noticed (Fig. 4) that there is a great inter-individual difference in the values of the RC/AB ratio in the supine and seated position as well as in the percentage change in value between the positions (top left of plots). This would suggest that rather than using a single value of RC/AB, changes in this ratio monitored at regular time intervals would provide the basis of more meaningful data concerning respiratory muscle impairment.

In conclusion, this study on the breathing pattern of patients with MD corroborates previous observations that deficiencies may exist in several of the respiratory system mechanisms of these patients. Analyses of resting breathing pattern recorded by pneumotachography and inductance plethysmography may provide supplementary information to that obtained from lung function tests on the impaired ventilatory mechanism of each patient. Furthermore, this study suggests that it may be meaningful to compare seated and supine breathing pattern prior to sleep studies in these patients.

Acknowledgements

This study was supported by Institut Garches, Hôpital Raymond Poincaré, Garches, France.

References

- Bégin, P., Mathieu, J., Almiral, J., Grassino, A., 1997. Relationship between chronic hypercapnia and inspiratory muscle weakness in myotonic dystrophy. *Am. J. Respir. Crit. Care Med.* 156, 133–139.
- Bégin, R., Bureau, M.A., Lupien, L., Lemieux, B., 1980. Control and modulation of respiration in Steiner's myotonic dystrophy. *Am. Rev. Respir. Dis.* 121, 281–289.
- Bégin, R., Bureau, M.A., Lupien, L., Bernier, J.-P., Lemieux, B., 1982. Pathogenesis of respiratory insufficiency in myotonic dystrophy. The mechanical factors. *Am. Rev. Respir. Dis.* 125, 312–318.
- Black, L.F., Hyatt, R.E., 1969. Maximal respiratory pressures: normal values and relationship to age and sex. *Am. Rev. Respir. Dis.* 99, 696–702.
- Bogard, J.M., Van Der Meche, F.G.A., Hendriks, I., Verstraeten, C., 1992. Pulmonary function and resting breathing pattern in myotonic dystrophy. *J. Neurol. Neurosurg. Psychiatry* 55, 977–984.
- Gibson, J., Imartin, J.J., Veale, D., Walls, T.J., Serieter, D.E., 1992. Respiratory muscle function in neuromuscular disease. In: Jones, N.J., Kilburn, K.J. (Eds.), *Breathlessness: The Campbell Symposium*. Berlin/Heidelberg, Hamelin, G.W., pp. 109–120.
- Gilliam, P.K.S., Head, P.D., Kaufman, L., Lewis, B.G.B., 1964. Respiration in dystrophic myotonia. *Thorax* 19, 112–120.
- Jamnes, Y., Poeyet, J., Grimaud, C., Serrieter, G., 1985. Pulmonary function and electromyographic study of respiratory muscles in myotonic dystrophy. *Muscle Nerve* 8, 586–594.
- Kilburn, K.H., Eagen, J.T., Sliker, H.O., Heppner, A., 1959. Cardiorespiratory insufficiency in myotonic progressive muscular dystrophy. *N. Engl. J. Med.* 261, 1069–1096.
- Kramer, W., Hagenbottum, T., Shaw, D., Wallwork, J., Estenne, M., 1989. Ventilatory compensation for changes in posture after human heart-lung transplantation. *Respir. Physiol.* 77, 75–78.
- Perez, A., Madau, R., Vardon, G., Baros, A., Galligo, J., 1996. Thoracoabdominal pattern of breathing in neuromuscular disorders. *Chest* 110, 454–461.
- Plehmister, J.C., Small, J.M., 1961. Hypersomnia in dystrophic myotonia. *J. Neurol. Neurosurg. Psychiatry* 24, 173–175.
- Quarler, P., Framming, G., Coates, J., Pedersen, O., Pedin, R., Vermaut, J., 1993. Lung volumes and forced ventilation flows. Report working party. Standardization of lung

- function tests. European Community for Steel and Coal. *Eur. Respir. J.* 6 (suppl. 16): 5–40.
- Read D. 1967. A clinical method for assessing the ventilatory response to carbon dioxide. *Aust. Am. Med.* 16: 20–32.
- Rimmer, K.P., Golbar, S.D., Lee, M.A., Whitham, W.A. 1993. Myotonia of the respiratory muscles in myotonic dystrophy. *Am. Rev. Respir. Dis.* 148: 1018–1022.
- Sersier, D.E., Masuglia, F.L., Gibson, G.I. 1982. Respiratory muscle function and ventilatory control: II in patients with motor neurone disease. *II in patients with myotonic dystrophy.* *Q. J. Med.* 51: 205–226.
- Sharp, J.T., Goldberg, N.B., Druiz, W.S., Dhanon, J. 1975. Relative contribution of rib cage and abdomen to breathing in normal subjects. *J. Appl. Physiol.* 39: 608–618.
- Stranock, S.D., Newson Davis, J. 1978. Ultrastructure of the muscle spindle in dystrophia myotonica. II. The sensory and motor nerve terminals. *Neuropathol. Appl. Neurobiol.* 4: 407–418.
- Swash, M., Fox, K.P. 1975. Abnormal intercostal muscle fibres in myotonic dystrophy: a study using serial sections. *J. Neurol. Neurosurg. Psychiatry* 38: 91–99.
- Vedle, D., Cooper, B., Gilman, J.J., Walls, T.J., Griffith, C.J., Gibson, G.I. 1995. Breathing pattern awake and asleep in patients with myotonic dystrophy. *Eur. Respir. J.* 8: 815–818.
- Velchok, V.P., Nassery, M., Druiz, W.S., Sharp, J.T. 1978. Effects of body position change on thoracoabdominal motion. *J. Appl. Physiol.* 45: 581–589.
- Venckelken, J.A., Demedts, M.G. 1995. Normal thoraco-abdominal motions: influence of sex, age, posture, and breath size. *Am. J. Respir. Crit. Care Med.* 151: 399–405.
- Ververs, C.C.M., Van der Meek, F.G.A., Verbrak, A.F.M., Van der Sluis, H.C.M., Bogard, J.M. 1996. Breathing pattern awake and asleep in myotonic dystrophy. *Respiration* 63: 1–7.

II.2.2.2 Au cours de l'exercice imaginaire

L'augmentation de la ventilation et de la fréquence cardiaque au cours de l'exercice imaginaire ont été décrites chez des athlètes et des sédentaires avec des résultats divergents quant à la nécessité d'avoir une pratique préalable de l'exercice (Thornton et al, 2001 ; Wuyam et al, 1995). Pour vérifier cette hypothèse, nous avons enregistré la ventilation et l'électrocardiogramme (ECG) lors de l'imagination d'une compétition d'aviron. Après un enregistrement de repos, les sujets visionnent une course d'aviron d'environ 5 minutes. Ils doivent ensuite fermer les yeux, le film de la course démarre pour donner le départ de la course, le film est arrêté et le sujet doit alors s'imaginer exécuter l'exercice. Quatre groupes de sujets ont participé à l'étude : 1) 12 compétiteurs en aviron, 2) 12 sportifs (autre sport) appariés en âge, 3) 10 sédentaires appariés en âge et 4) 12 seniors (50 à 60 ans).

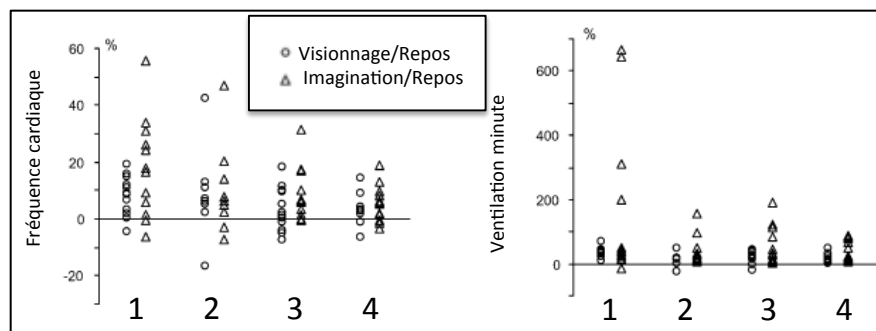


Figure 7 : Changement exprimé en pourcentage de la valeur de repos pour la fréquence cardiaque et la ventilation minute ($=V_T * f_R$, avec V_T : volume courant, f_R : fréquence ventilatoire) lors du visionnage de la course et durant l'imagination de celle-ci pour tous les sujets des 4 groupes : compétiteurs en aviron (1), sportifs (2), sédentaire (3), seniors (4).

Les résultats (Figure 7) ont montré une augmentation significative de la ventilation chez tous les sujets. La fréquence cardiaque était significativement augmentée chez 34 sujets répartis dans les 4 groupes. Trois compétiteurs en aviron ont augmenté considérablement leurs données cardio-ventilatoires, à tel point que l'enregistrement a dû être arrêté en raison d'une baisse considérable de CO_2 dans l'air expiré.

Ces résultats suggèrent que la pratique préalable de l'exercice n'est pas un prérequis pour observer une augmentation des données cardio-ventilatoires au cours de l'exercice imaginaire.

Calabrese et al (2004) Cardioventilatory changes induced by mentally imaged rowing. *Europ J App Physiol*

ATER Université de Savoie (DEUG STAPS, Bourget du lac)- 2000-2001

Psychale Calabrese · Laurent Messemnier · Eve Bijaoui André Eberhard · Ghis Brändert Cardioventilatory changes induced by mentally imaged rowing

Accepted: 1 July 2003 / Published online: 3 October 2003
© Springer-Verlag 2003

Abstract Mentally imaged but unexecuted physical activity has been reported to induce a cardiorespiratory change. In order to test whether the previous experience of the performed exercise was a prerequisite to observe these changes, ventilation and heart rate were recorded during mental imagination of a rowing race in four groups of volunteers: 12 competitive rowers, 10 non-rower athletes, 12 students (22–30 years old) and 12 senior subjects (50–60 years old). Recordings were performed at rest, during the viewing of a rowing race and during mental imagination of this race. Analysis of variance revealed significant condition effect for all cardiorespiratory variables. All subjects increased their breathing rate (mean increase: 16 breaths·min⁻¹ in rowers, 8 breaths·min⁻¹ in athletes, 8 breaths·min⁻¹ in students, and 6 breaths·min⁻¹ in seniors), 29 decreased their tidal volume (mean decrease: 100 ml in rowers, 102 ml in athletes, 120 ml in students and 26 ml in seniors) with an increase in the resulting ventilation in 38 subjects (mean increase: 14 l·min⁻¹ in rowers, 3.6 l·min⁻¹ in athletes, 2.8 l·min⁻¹ in students, 2.6 l·min⁻¹ in seniors). Heart rate was increased in 34 subjects (mean increase: 12 beats·min⁻¹ in rowers, 5 beats·min⁻¹ in athletes, 6 beats·min⁻¹ in students and 5 beats·min⁻¹ in seniors). The number of subjects who exhibited changes

was evenly distributed among the four groups. However, mean values of the changes were higher in rowers than in the three other groups, mainly due to three rowers who exhibited extremely large increases in cardioventilatory variables. Analysis of variance showed no significant group effect for heart rate and breathing rate. These results suggest that rowing experience may not be necessary for changes in heart rate and ventilation to be elicited by mentally imagining a rowing race.

Keywords Breathing pattern · Heart rate · Humans · Imagining exercise · Viewing exercise

Introduction

Mentally imaged but unexecuted physical activity has been reported to induce a cardiorespiratory response proportional to the amount of simulated exertion (Decey et al. 1991). This response did not appear to be due to peripheral factors since muscular metabolism – measured by NMR analysis – remained unchanged (Decey 1993). The hypothesis implicating voluntary control was ruled out (Decey et al. 1993) since automatic efference copies (voluntary control and also a voluntary increase in ventilation proportional to the amount of simulated exercise seem) unlikely. In addition, the ventilatory increase appeared to be specific to mentally imaged exercises, as Whipp et al. (1995) reported that the increases in ventilation were greater than the responses to a control task that consisted of fingering letters. More recently, Thornton et al. (2001) observed an increase in ventilation under hypnosis during imagination of cycling uphill and no change when imagining freewheeling downhill. However, these cardiorespiratory changes in response to imagined exercise were not observed in every subject. Decey et al. (1993) selected non-sedentary subjects on their ability for mental imagery. Wyman et al. (1995) reported in athletes only cardiorespiratory changes in response to imagination of previously performed treadmill exercise despite

the fact that there was no significant difference between the athlete and non-athlete groups in the subjective assessment of imagery ability. However, Thornton et al. (2001) reported that a cardiorespiratory response to imagined cycling uphill in healthy untrained expert-mentally naive subjects is only observed under hypnosis which, by isolating subjects from the environment, allows a more focused imagination than is possible when awake (Coe et al. 1980; Morgan et al. 1973). In contrast with the findings of Decey et al. (1991) and Wyman et al. (1995), the observations of Thornton et al. (2001) suggest that the cardioventilatory response to imagined exercise is independent of the nature or extent of the subjects' previous experience with regards to exercise and may be observed in any subject providing that optimal conditions for imagining, such as a state of hypnosis, exist.

The aim of this study was to examine the hypothesis that cardiorespiratory response to mentally imaged exercise is related to previous experience of this exercise. The exercise to be imagined was rowing, in which a particular rhythmic pattern of breathing – necessarily coupled to stroke rate – is adopted by the rowers. If the cardioventilatory response to imagined exercise reflects a learned response to exercise, it is reasonable to expect greater responses in experienced rowers due to a "memory" of the cardioventilatory response to actual rowing. The subjects were (1) competitive rowers, (2) non-rower athletes, (3) sedentary students (aged 22–30 years) and (4) sedentary senior subjects (aged 50–60 years). The seniors formed a separate group as a detrimental effect of age on the generation of mental images (Briggs et al. 1999; Bryner and Sculligan 2000; Ruz et al. 1999) has been reported. Only the competitive rowers had had the experience of the exercise to be mentally imaged and the other subjects' knowledge of rowing was only that obtained from watching a video of a race.

Methods

Subjects
Fifty-six healthy, naive subjects participated in the study. They were divided into four groups: (1) 12 rowers with experience of national level competition over several years – training for an average of 14.3 h per week; (2) 10 physical education students – the athlete

group – practising mostly team sports for an average of 10.3 h per week; (3) 12 post-graduate students with no specific physical training and practicing on average less than 4 h of sport per week; (4) 12 students with no experience of sport. The experimental protocol was examined and approved by the Institutional Ethics Review Board. Before giving their written consent, the subjects were informed of the protocol and the overall nature of the experiments that they were unaware of the aim of the study.

Experimental protocol

Prior to including the subject, the recording sequences were explained: (1) after a recording at rest with eyes closed; (2) a video of a rowing race would be shown and then (3) the subject would be asked to close his (her) eyes and to imagine him (her) self as an oarsman or oarswoman performing a rowing race.

The first recording, at rest with eyes closed, lasted 5–10 min and the second recording, performed while the subjects were watching a video of a rowing race, lasted 10 min. The video was shown for the entire recording period and immediately restarted so that the subjects heard the preparation for and the start of the race but with their eyes closed. The subjects were instructed to start their imagined race at the moment they heard the starting whistle. The video was shown throughout the recording. The video was of an Olympic 2000-m rowing race with four rowers without oarswoman. Male subjects watched a men's rowing race while female subjects watched a women's rowing race. The highest rowing frequency (approximately 49 strokes per minute for men, 44 for women) after which this frequency fell to a minimum in the middle of the race (37 strokes per minute for men, 33 for women) and then rose towards the end of the race (42 strokes per minute for men, 40 for women). The third recording lasted 6 min, i.e., the duration of the race. However, the experiment was stopped in those cases where imagining exercise induced hyperventilation leading to a fall in EtCO₂ values. At the end of the recordings all the subjects reported an attempt to imagine a rowing race, even though some subjects said that they had difficulty because they had never done any rowing.

Table 1 Characteristics of the subjects and weekly physical activity for each group. The number of women is given in parentheses; values for age and exercise are expressed as the mean \pm SD for all the subjects in each group

Group	Number of subjects	Age (years)		Weight (kg)		Height (m)		Exercise (hours per week)	
		Mean	SD	Mean	SD	Mean	SD	Mean	SD
Rowers	12 (4F)	23.8	4.1	70.9	7.5	1.80	0.08	14.25	3.47
Athletes	10 (1F)	22.2	5.2	72.4	7.9	1.79	0.06	10.33	3.08
Students	12 (4F)	26.5	4.2	72.0	12.0	1.75	0.09	1.92	2.19
Seniors	12 (8F)	54.3	3.0	72.8	13.4	1.66	0.09	3.09	5.22

Data analysis

Breathing pattern was analyzed breath-by-breath and rate tidal volume, respiratory rate, and end tidal CO₂. Breath-by-breath heart rate was calculated from the R-R interval of the electrocardiographic trace. Mean values and SD were calculated for each recording and for each group in each condition.

Analysis of variance (ANOVA) with repeated measures were used to analyze cardiorespiratory variables of the four groups of subjects during resting, watching, and imagining conditions. When overall differences were observed, Bonferroni-Dunn's multiple comparison procedure was used to study pairwise differences between groups and between conditions. In addition, for each subject, variables were compared between resting and watching conditions and between watching and imagining conditions. Significance was set at $p < 0.05$ for all tests.

Results

Changes in heart rate while watching the video and imagining the race

Analysis of variance (ANOVA) carried out on heart rate data in the four groups of subjects in three conditions revealed no group effect ($p=0.261$) but a significant condition effect ($p<0.001$). The Bonferroni-Dunn test showed a significant difference between all pair wise conditions. In Table 2 are reported the mean values and SD of the heart rate in the three conditions for each group. Student *t*-tests were performed on individual data; 35 subjects increased their heart rate significantly during watching the video and 34 while imagining. The number of subjects in each group who increased their heart rate significantly as compared to rest is evenly distributed among the four groups.

Changes in ventilatory variables while watching the video and imagining the race

Changes in breathing pattern induced by viewing or by imagining are observed as soon as the first breath while watching the video and while imagining the rowing race. The figures in Table 2 represent the number of subjects in each group who increased their heart rate significantly as compared to rest using paired *t*-tests ($p<0.05$).

Group (number)	Heart rate (min ⁻¹)	
	Rest	Viewing / Imagination
Rowers	67.8 (9.6)	72.9 (9.9) / 79.8 (8.0)
Athletes	70.0 (15.1)	70.9 (9.4) / 74.8 (12.5)
Students	77.3 (13.3)	79.0 (10.2) / 83.6 (13.2)
Seniors	74.1 (14.0)	75.8 (11.5) / 77.1 (11.1)
Mean	71.8 (12.7)	78.6 (13.8) / 81.6 (11.3)
46		35 ^a / 34

^aViewing was analyzed in nine athletes only

following the start of the video or of the race. This is illustrated in Fig. 1 where tidal volume, breathing rate, and FETCO₂ at rest, during viewing and during imagining are represented breath-by-breath for one subject. During the viewing, the decrease in tidal volume was associated with an increase in breathing rate resulting in a mild hypoventilation, as evidenced by a decrease in FETCO₂ from 5.5 to 5.2%. At the start of the video (dotted line), ventilatory variables were at the same level as at rest and hearing the preparatory instructions for the race initiated changes in breathing pattern. In this subject, during imagination, the slight decrease in tidal volume did not compensate for the large increase in breathing rate resulting in a decrease in FETCO₂ down to 3.5%. Similar changes in breathing rate and tidal volume are observed in all subjects, the decrease in FETCO₂ depending on the amount of hypoventilation. ANOVA carried out on breathing rate revealed no group effect ($p=0.534$) and a significant condition effect ($p<0.001$). The Bonferroni-Dunn test showed a significant difference between all pairwise conditions. For the tidal volume there was a significant group effect ($p<0.001$) as well as a significant condition effect ($p<0.001$). The Bonferroni-Dunn test showed a significant difference between the rowers and the students, between the rowers and the seniors and between the athletes and the seniors. As to the conditions, there was a significant increase between resting and viewings as well as between resting and imagining. ANOVA results on minute ventilation showed a significant group effect ($p<0.001$) and also a condition effect ($p<0.001$). Bonferroni-Dunn test revealed significant differences between the rowers and the students and also between the rowers and the seniors. As to the conditions, a significant difference was observed between resting and imagining on one hand and between viewing and imagining on the other hand.

In Table 3 are reported mean values and SD of breathing rate, tidal volume and minute ventilation in the three conditions for each group. Student's *t*-tests were performed to compare individual data between resting and viewing and also between resting and imagining. The figures in Table 3 represent the number of subjects in each group exhibiting significant changes as compared to rest for each variable. Altogether, during viewing as compared to rest, 40 subjects increased their breathing rate significantly, 29 decreased their tidal volume resulting in an increase in ventilation in 38 subjects. During imagination, 45 subjects increased significantly their breathing rate, 32 subjects decreased their tidal volume resulting in an increase in ventilation in 38 subjects.

These results are summarized in Fig. 2 where the percentages of changes in cardiorespiratory variables induced by viewing and by imagining are represented for all the subjects of the four groups. In nearly all subjects, breathing rate and minute ventilation were increased during these two conditions. A particularly large increase was observed in three rowers during imagination

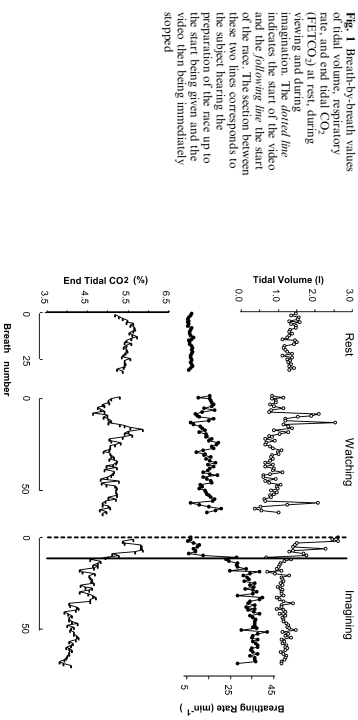


Fig. 1 Breath-by-breath values of tidal volume, respiratory rate, and end tidal CO₂ during resting, watching, and during imagination. The dotted line indicates the start of the video and the following line the start of the race. The section between the dotted line and the following line represents the preparation of the race up to the start being given and the video then being immediately stopped

which resulted in a large increase in minute ventilation. Tidal volume decreased in most subjects during viewing as well as during imagining condition, whereas, in most cases, an increase in heart rate was observed in both conditions.

Discussion

The main finding of the present study was that imagining a rowing race induced significant changes in cardiorespiratory variables in almost all subjects. The number of subjects who exhibited changes was evenly distributed among the four groups. Analysis of variance with repeated measures on the three conditions (resting, viewing and imagining) and the four groups (rowers, athletes, students and seniors) revealed a significant

increase in heart rate, breathing rate and minute ventilation and a decrease in tidal volume.

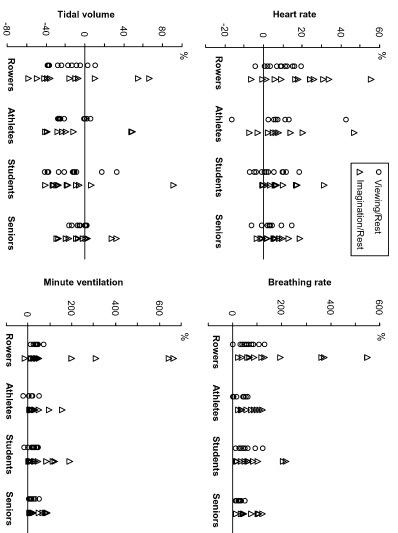
None of the subjects was aware of the aim of the experiment and the protocol was explained to them on the day of the experiment, just before the recording at rest. Their ability to perform mental imagery had not been previously tested, in contrast to the other studies (Decey et al. 1993; Wuyam et al. 1995). and, thus, selection was not made on this criterion. Rowing is not an exercise requiring mental imagery of the movements as in downhill skiing or high-diving. Therefore, one can assume that there was a comparable number of subjects with high or low ability to perform mental imagery in each group. Only rowers had practiced rowing, they had had experience of rowing races and performed a minimum of 10 h of training per week. They had never been coached in mental imagery before.

Table 3 Mean values (SD) of ventilatory variables for each group at rest, while watching the video and while imagining the rowing race. The figures in *italic* represent the number of subjects in each group who increased their heart rate significantly as compared to rest using paired *t*-tests ($p < 0.05$)

Group (number)	Breathing rate (min ⁻¹)		Tidal volume (l)		Minute ventilation (l·min ⁻¹)	
	Rest	Viewing / Imagination	Rest	Viewing / Imagination	Rest	Viewing / Imagination
Rowers	10.9 (3.2)	16.3 (3.5) / 26.9 (11.2)	918 (226)	739 (163) / 814 (388)	9.5 (1.8)	11.7 (2.1) / 23.5 (8.4)
Athletes	14.3 (2.7)	17.2 (2.8) / 22.2 (5.6)	766 (129)	656 (91) / 664 (190)	10.8 (2.1)	11.2 (1.5) / 14.4 (4.3)
Students	11.8 (3.4)	16.1 (3.6) / 20.3 (7.2)	684 (260)	542 (117) / 569 (248)	7.3 (1.4)	8.3 (1.1) / 11.1 (4.5)
Seniors	14.3 (2.1)	17.3 (2.4) / 23.6 (3.4)	494 (93)	465 (92) / 466 (147)	6.9 (0.8)	7.1 (1.1) / 9.0 (2.3)
Mean	12.7 (3.3)	16.7 (3.2) / 22.5 (8.0)	713 (250)	597 (164) / 627 (296)	8.5 (2.2)	9.7 (2.3) / 14.6 (11.5)
46		40 ^a / 45		29 ^a / 32		38 ^a / 38

^aViewing was analyzed in nine athletes only

Fig. 2 Changes expressed as a percentage of the resting value during viewing (○) and during imagination (△) of the four groups of all subjects of



Athletes were selected for their physical training in sports other than rowing, not requiring mental imagery of a specific movement, and they also had competition experience. The two groups of sedentary subjects formed the control group; they had no experience of rowing and, although some of them had regular physical activity, they had not taken part in competition. None of them was a rowing enthusiast. Thus the knowledge of rowing of these three groups of subjects was only that drawn from watching the video of the race. In that respect, subjects were asked to perform the imagination task in the first person – internal perspective. Indeed, Wang and Morgan (1992) reported that internal imagery resulted in an increase in ventilation and that the perceptual responses to internal imagery resemble actual exercise more than external imagery.

No subject were given to them during the imagination period because a "maintaining" effect of a rhythmic sound cannot be ruled out (Hass et al. 1986). This differs from the studies of Decety et al. (1993) who "played back to them through the earphones the noise of the oarwater, which had been taped during their own execution of actual leg exercise" and Wyman et al. (1995) who exposed the subjects to similar treadmill vibrations and sounds as during actual treadmill exercise. In our protocol, external stimulations were minimized to help subjects concentrate on imagining the case. In this, our protocol addresses the concern of Thornton et al. (2001), who hypothesized that unattended subjects in order to isolate them from the environment. Indeed, hypnosis allows a more focused imagination than is possible when awake (Coe et al. 1986; Morgan

et al. 1973) and has been reported to enhance imagery intensity and effectiveness in athletes (Lager 2000).

The increase in ventilation observed in rowers was on an average lower than that observed by Decety et al. (1993) in non-sedentary subjects and slightly higher than the increase obtained by Wyman et al. (1995) in highly trained athletes. We found an increase in breathing rate in the athletes of the same magnitude as in the two groups of sedentary subjects, all 24 of whom showed a significant increase in breathing rate, and 18 of the 24 likewise in heart rate. Others have not observed such responses in sedentary subjects, except Thornton et al. (2001) and this under hypnosis only.

The time course of the increase in ventilation during imagination observed in this study was also different from that reported by Decety et al. (1993) and Thornton et al. (2001). Indeed, these authors observed a progressive increase in the ventilatory variables, whereas as shown in Fig. 1, we observed the maximal values of heart rate and tidal volume within the five breaths following the start of the race and this was maintained throughout the recording.

Differences in the design of the study may account for these discrepancies, in particular (1) rowing as the exercise to be mentally imaged and (2) viewing prior to imagining the race. Several features of rowing are worth mentioning. First, the specificity of locomotor pattern during rowing; the arms do not move contra laterally with the legs but are forced through an unnatural motion in synchrony with the legs. In addition, thoracic and abdominal muscles are involved both in breathing and in propelling force generation, so that the period of the breath and the stroke are linked (Steinacker et al. 1993).

In addition, the majority of rowers exhibit entrainment of breathing at a frequency of a multiple of the stroke frequency (Mallier et al. 1991, 1994). The hypothesis that entrainment of breathing improves the effectiveness of rowing has even been examined (Maclemann et al. 1991; Steinacker et al. 1993; Szal and Schoene (1989) found that rowing causes hypoventilation with higher breathing rate and lower tidal volume than cycling. These results were observed in both oarswomen and age-matched untrained non-rower women. This suggests that the particular breathing pattern observed during rowing is not a result of training but is inherent to this specific activity. Lastly, rowing is a strenuous exercise with a high level of energy expenditure involving leg, arm and back muscles (Secher 1993). The rowing ergometer shows an oxygen uptake for a given workload higher than on the bicycle ergometer, for both the oarsmen and the control subjects (Boutkaert et al. 1983; Hagerman 1984). Thus, the viewing of the rowing race may evoke a strenuous exercise with a rhythmic component. Therefore, the observed increase in heart rate and ventilation may result from the perception of high energy-expenditure action with a rhythmic component. The importance of a rhythmic component has been suggested by Wyman et al. (1995).

In the present protocol, viewing was simply used to suggest the exercise to be mentally imaged. Although Fig. 1 shows that before the beginning of the imagination period, ventilation returned to its resting level, and that viewing in itself induced appreciable changes in heart rate and ventilation. Furthermore, these changes were, albeit to a lesser degree, in the same direction as during imagination, as can be seen in Fig. 1. Balduino et al. (1990) reported an increase in cardiac and respiratory rates during the viewing of film sequences, whatever their content, emotional or otherwise. An increase in breathing rate during observation of strenuous actions such as weightlifting or walking/running on a treadmill was observed by Pucellin and Jannarod (2000). The magnitude of increase was similar to that observed in our study. They also found that the respiratory rhythm increased linearly with the speed of the treadmill. They conclude that this latter finding demonstrates activation during the observation of strenuous actions of central mechanisms related to action performance. Similar conclusions have also been drawn from animal experiments where, in monkeys, neurons in the ventral prefrontal cortex exhibit similar responses at the sight of generation as at the execution of the same action (Culicsek et al. 1996). In human subjects, Fedida et al. (1995) observed an increase in the motor-evoked potentials from hand muscles during the observation of movements. The pattern of these motor-evoked potentials detected the pattern of muscle activity recorded when the subject executed the observed action. These results suggest the existence of an observation/execution matching system.

The amount of changes in all variables was less during viewing than imagining. This may be related to the observation of Gratton et al. (1996) who used PET scanning analysis to compare the observation and imagination of grasping. They found that the site in the supplementary motor area activated during observation, whilst almost coinciding with that during imagination, had a much weaker intensity of activation and extent. Thus the possibility that subjects "responded" to the imagination of the race because of their prior viewing cannot be excluded.

The results of the current study were not in agreement with the assumption that only competitive rowers – and possibly, to a lesser extent, athletes – would increase their ventilation and cardiac rate during the mental imagery of a rowing race. The cardiovascular variables changed similarly in all subjects except for the case of three rowers who exhibited much higher increases than the others. These three rowers were among those who had several years of experience at competitive level but other rowers with a lesser increase had similar competition experience. Nevertheless, their cardiovascular changes during imagination suggest that they mentally performed the race. The amount of increase is similar to that observed by Decety et al. (1993). These three rowers may represent the population that we expected to test for: they had the "memory" of a race and so were able to "relive" the race. For all other subjects, the observations should relate to imagination of an action perceived immediately before. This may explain the fact that, despite a great variability of the changes among the subjects, the amount of changes, at least for the breathing rate and the heart rate, is similar among the four groups. Even if the immediate increase in ventilation may be due to the neurogenic mechanism of anticipation (Krogh and Lindhard 1913), this mechanism cannot be responsible for the fact that ventilation remains at this level during the whole 5 min of the race. This suggests that because the imagination related to exercise, it was associated in the minds of the subjects with an increase in breathing rate, ventilation and heart rate. Whether mental imagination of an exercise could improve exercise performance needs further investigation.

Acknowledgment We are grateful to Alain Weeks, coach of the Rowing club of Grenoble, for his help in the completion of this study.

References

- Balduino B, Bistracchi MW, Trombini G, Polonchi D, Stegagno L (1990) Effects of an emotional negative stimulus on the cardiac, electrocardiographic, and respiratory responses. *Percept Mot Skills* 71:647-655
- Boutkaert J, Panzer JL, Vignas J (1983) Cardiorespiratory responses to mental imagery of ergometer exercise in oarsmen. *Europ J Appl Physiol* 51:51-59
- Briggs SD, Reiz N, Marks W (1999) Age-related deficits in generation and manipulation of mental images. I: The role of sensorimotor speed and working memory. *Psychol Aging* 14:427-435

- Byrger R, Sculligan JC (2000). Effects of aging on the generation of mental images. *Exp Aging Res* 26:337-351
- Coe W, St Jean R, Byrger J (1980). Hypnosis and the enhancement of mental images. *Percept Mot Behav* 72:207-214
- Decey J, Jeannerod M, Germain M, Paterne J (1991). Voluntary response during imagined movement is proportional to mental effort. *Behav Brain Res* 42:1-5
- Decey J, Jeannerod M, Durozard D, Bavelard G (1993). Central modulation of voluntary movement during the generation of mental images. *Percept Mot Behav* 64:549-559
- Fadiga L, Fogassi L, Pavet G, Rizzolatti G (1995). Motor facilitation during action observation: a magnetic stimulation study. *J Neurophysiol* 73:2608-2611
- Gallies V, Fadiga L, Fogassi L, Rizzolatti G (1996). Action representation in monkey. *Percept Mot Behav* 67:107-117
- Grillon ST, Aebih MA, Fadiga L, Rizzolatti G (1996). Localization of grasp representations in humans by positron emission tomography. 2. Observation compared with imagination. *Exp Brain Res* 112:103-111
- Hahn B, Benseid S, Xuan K (1986). Effects of perceived muscle force on motor output. *Int J Appl Physiol* 61:1185-1191
- Hagerman FC (1984). Applied physiology of rowing. *Sports Med* 1:303-326
- Krough A, Lindhardt J (1913). The regulation of respiration and circulation during the initial stages of muscular work. *J Physiol* 34:1-12
- Liegt DR (2000). Enhancing imagery through hypnosis: a performance aid for athletes. *Am J Clin Hypn* 43:149-157
- Madelman SE, Silvestri GA, Ward J, Malher DA (1991). Does entrained breathing improve the economy of rowing. *Med Sci Sports Exerc* 23:186-187
- Mahler DA, Decey J, Lantier T, Ward J (1991). Locomotor-respiratory coupling decoups in novice female rowers with training. *Med Sci Sports Exerc* 23:1362-1366
- Mahler DA, Shubart CR, Brew E, Stukel TA (1994). Ventilatory responses and entrainment of breathing during rowing. *Med Sci Sports Exerc* 23:619-624
- Martinez J, Decey J, Lantier T, D'Almeida R, Horowitz SM (1973). Perceptual and metabolic responses to standard bicycle ergometry following various hypnotic suggestions. *Int J Clin Exp Hypn* 21:86-101
- Pascalin C, Jeannerod M (2000). Changes in breathing observation during motor imagery. *Acta Psychol* 89:137-148
- Rae N, Briggs SD, Matherly A, Arnold JD (1999). Age-related deficits in generation and manipulation of mental images: II. The role of dorsolateral prefrontal cortex. *Psychol Aging* 14:436-444
- Scheer NH (1993). Physiological and biomechanical aspects of rowing: implications for training. *Sports Med* 15:24-42
- Schneider W, Shiffrin R (1977). Control of human information processing II. Perceptual learning, automatic attention and a general theory. *Psychol Rev* 84:127-90
- Sokal SE, Rohlf FJ (1995). *Biometry*. W. H. Freeman and Company, New York, NY, USA, 887 pp.
- Szal SE, Schoene RH (1989). Ventilatory response to rowing and cycling in elite rowers. *J Appl Physiol* 67:264-269
- Therrien M, Guz A, Murphy C, Sculligan R, Peden DJ, Lantier T, Ward J, Decey J, Sculligan B, Peden DJ (2001). Identification of higher brain centres that may encode the cardiorespiratory response to exercise in humans. *J Physiol (Lond)* 533:823-836
- Wang Y, Morgan WP (1992). The effect of imagery perspectives on cardiorespiratory responses to imagined exercise. *Behav Brain Res* 52:167-174
- Wagman B, Moosavi-SH, Decey J, Adams L, Lansing RW, Guz A (1995). Imagination of dynamic exercise produced ventilatory responses which more apparent in competitive sportsmen. *J Physiol (Lond)* 482:715-724

II.2.3 La “personnalité ventilatoire”

II.2.3.1 Au cours de l'hyperventilation

Dans le cadre d'un travail en collaboration avec l'Université de Chisinau (République de Moldavie) de la direction d'une thèse en cotutelle, nous avons étudié les modes ventilatoires et la personnalité ventilatoire chez les sujets sains (enregistrements réalisés à Grenoble) et chez les patients souffrant de trouble panique (enregistrements réalisés à Chisinau) dont un des symptômes est l'hyperventilation volontaire. L'objectif du travail effectué chez les sujets sains a été d'étudier les caractéristiques ventilatoires et rechercher la persistance de la personnalité ventilatoire au cours de l'hyperventilation volontaire. Nous avons enregistré la ventilation chez 18 sujets sains dans différentes conditions : au cours d'une ventilation spontanée (SP₁) puis d'une hyperventilation volontaire à la fréquence de la ventilation spontanée (HV_{SP}) d'une part, et au cours d'une ventilation spontanée (SP₂) puis d'une hyperventilation volontaire à une fréquence ventilatoire de 20 cycles /min (HV₂₀) d'autre part. La Figure 8 illustre pour un sujet les caractéristiques ventilatoires moyennes (T_I , T_E , V_T et f_R) dans ces différentes conditions ainsi que la quantification et la représentation du débit ventilatoire moyen (analyse harmonique cycle par cycle). La forme des débits semble similaire entre les deux conditions de repos et entre les deux conditions d'hyperventilation.

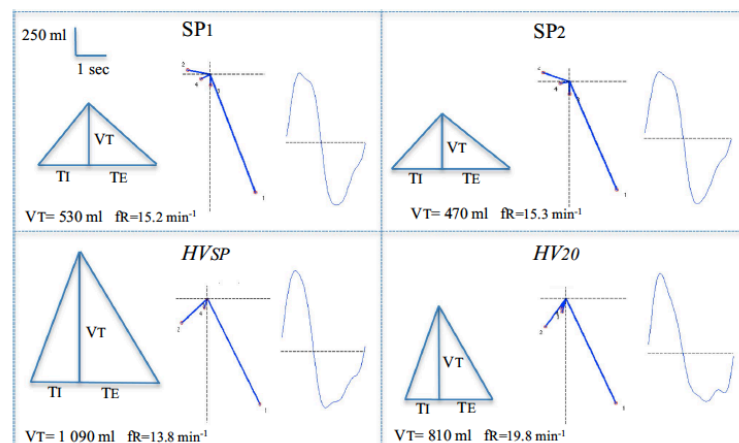


Figure 8 : Pour un sujet représentation des caractéristiques ventilatoires moyennes : volume courant (V_T), les durées inspiratoire et expiratoire (T_I , T_E), la représentation de Fresnel des 4 premières harmoniques obtenues d'une analyse cycle par cycle ventilatoire (débit) et le débit reconstitué correspondant, au cours de la ventilation spontanée (SP₁ et SP₂), d'une hyperventilation volontaire à la fréquence de la ventilation spontanée (HV_{SP}) et à 20/min (HV₂₀). Les valeurs moyennes de V_T , et de la fréquence ventilatoire (f_R) sont données pour chaque condition.

Le test de similarité appliqué à ces données a montré une similarité des formes des cycles ventilatoires entre HV_{SP} et HV₂₀.

Nos résultats montrent l'existence d'une individualité ventilatoire lors de l'hyperventilation volontaire chez les volontaires sains, quel que soit le mode de l'hyperventilation. Ceci suggère que la personnalité ventilatoire est une propriété inhérente à la fonction ventilatoire.

Besleaga et al (2016) Individuality of breathing during volitional moderate hyperventilation. Eur J Appl Physiol

Directeur de thèse de Tudor Besleaga (dérogation de l'EDISCE, UJF) en cotutelle avec l'Université d'Etat de Médecine "Nicolae Testemițanu", Département de physiologie humaine et biophysiques (Chisinau, République de Moldavie): "Effets ventilatoire et cardiaque de l'hyperventilation volontaire- Etude chez les volontaires sains et les patients souffrant de troubles paniques", soutenue le 19 octobre 2011 à Grenoble.



ORIGINAL ARTICLE

Individuality of breathing during volitional moderate hyperventilation

Tudor Belegaş¹ · Michael Blum² · Raphael Bräut¹ · Victor Vovč³ · Ion Moldavanu³ · Pascale Calabrese⁴

Received: 29 June 2015 / Accepted: 6 September 2015 / Published online: 23 September 2015
© Springer-Verlag Berlin Heidelberg 2015

Abstract

Purpose The aim of this study is to investigate the individuality of airflow shapes during volitional hyperventilation. **Methods** Ventilation was recorded on 18 healthy subjects following two protocols: (1) spontaneous breathing (SP) followed by a volitional hyperventilation at each subject's spontaneous (HV_{sp}) breathing rate; (2) spontaneous breathing (SP₂) followed by hyperventilation at 20/min (HV₂₀), HV_{sp} and HV₂₀ were performed at the same level of hypocapnia; and tidal CO₂ (F_{Ti}CO₂) was maintained at 1 % below the spontaneous level. At each breath, the tidal volume (V_T), the breath (T_{breath}), the inspiratory (T_I) and expiratory durations, the minute ventilation, V_E/T_I, T_I/T_{tot} and the airflow shape were quantified by harmonic analysis. Under different conditions of breathing, we test if the airflow profiles of the same individual are more similar than airflow profiles between individuals.

Results Minute ventilation was not significantly different between SP₂ (6.71 ± 1.64 l·min⁻¹) and SP₁ (6.57 ± 1.31 l·min⁻¹), nor between HV₂₀ (15.88 ± 4.92 l·min⁻¹) and HV_{sp} (15.87 ± 4.16 l·min⁻¹). Similar results were obtained for F_{Ti}CO₂ between SP₂ and SP₁.

Communicated by Susan Hopkins.

[✉] Pascale Calabrese

pascale.calabrese@img.fr

- 1 UFR-Génétique, ICRNS/UMC-IMAG UMR 5525/PRETA Team, 38041 Grenoble France
- 2 UFR-Génétique ICRNS/UMC-IMAG UMR 5525/BGCM Team, 38041 Grenoble France
- 3 Department of Human Physiology and Biophysics, State Medical and Pharmaceutical University "Nicolae Testemitanu", Chisinau, Republic of Moldova

(5.06 ± 0.54 %) and SP₂ (5.00 ± 0.51 %), and HV₂₀ (4.07 ± 0.51 %) and HV_{sp} (3.88 ± 0.42 %). Only T_I/T_{tot} remained unchanged in all four conditions. Airflow shapes were similar when comparing SP₂-SP₁, HV_{sp}-HV₂₀, and SP₂-HV_{sp} but not similar when comparing SP₂-HV₂₀.

Conclusions These results suggest the existence of an individuality of airflow shape during volitional hyperventilation. We conclude that volitional ventilation like automatic breathing follows inherent properties of the ventilatory system. Registered by Pascale Calabrese on ClinicalTrials.gov, # NCT01881945.

Keywords Breathing pattern · Individuality · Volitional hyperventilation · Healthy subjects

Abbreviations

End tidal CO₂ F_{Ti}CO₂
Voluntary hyperventilation at the spontaneous breathing rate HV_{sp}
Voluntary hyperventilation at a breathing rate of 20/min HV₂₀
Spontaneous breathing of protocol 1 SP₁
Spontaneous breathing of protocol 2 SP₂
Inspiratory breath duration T_I
Expiratory breath duration T_E
Breath duration (T_I + T_E) T_{tot}
Tidal volume V_T
Minute ventilation V_E × 60/T_{tot}

Introduction

The individuality of breathing pattern has been assessed over time in healthy adults from breath-by-breath analysis



of airflow shape (Benchert et al. 1989). This individuality was maintained during hypoxia (Eisele et al. 1992) and added resistive load (Calabrese et al. 1998). These results suggested that the individuality of breathing pattern is an inherent property of the respiratory system. A study testing the existence of a genetic component in the determination of the individuality of breathing was carried out on identical twins and showed significant similarities within twin pairs (Shea et al. 1989). However, the resting airflow shape appears to be preserved over a certain increase in ventilation beyond which it is modified for example during exercise (at 50 % of maximal O₂ consumption) (Eisele et al. 1992). This phenomenon is also observed when ventilation decreases when adding high levels of resistive load (Calabrese et al. 1998).

These findings suggest that the individual breathing pattern represents the shape of the respiratory pattern generator output for each subject with limited changes in ventilation around spontaneous breathing.

The aim of this study is to investigate the individuality of airflow profiles during volitional breathing. Volitional breathing, i.e. decision of taking a breath, voluntarily inspire and expire exists in human subjects and is not a regular way of breathing. If the individuality still exists in this condition, this would suggest that individuality is inherent to the respiratory system.

In a recent viewpoint Hsu et al. (2011) came to the conclusion that although the structures controlling breathing during volitional and spontaneous breathing are different, they both lead to the same outcome: eupneic breathing. In humans, volitional breathing suppresses the underlying automatic breathing and how this is achieved is still under debate. Volitional breathing rhythm may be initiated (at least partially) by cortical inputs relayed into medullary structures (McKay et al. 2003) or may bypass these structures and be triggered by acting on the phrenic motor nucleus (Corfield et al. 1998).

Whatever the interaction between cortical and medullary structures, the rhythm generated during volitional breathing can be considered as arising from a distinct pattern generator network (McKay et al. 2003). Besides, recent *in vivo* and *in vitro* studies suggest that respiratory rhythm generators may arise from multiple distinct networks whose outputs are similar (Mellon 2010).

Comparing the shape of individual breathing pattern during volitional and spontaneous breathing may bring insight on the differences or similarities of patterns generated by two different networks and consequently on the determinants of the individuality of breathing pattern.

For this purpose, spontaneous and volitional breathing was recorded in 18 healthy subjects. The volitional breathing was ascertained by inducing a moderate level of hyperventilation at (1) spontaneous breathing rate, and (2) a

breathing rate of 20/min. The airflow shape was quantified by breath and comparisons were performed between spontaneous and volitional hyperventilation.

Materials and methods

Subjects

Eighteen healthy volunteers recruited from the university staff, ten men and eight women (mean ± SD height: 171.1 ± 8.5 cm; weight: 69.9 ± 12.0 kg) between 21 and 65 years of age (mean 34.0 ± 13.4 years) participated in the study. After a description of the experimental design and protocol, each subject signed an informed consent form. The experimental protocol was examined and approved by the Institutional Ethics Review Board of the CHU Grenoble, and the study was registered on ClinicalTrials.gov (# NCT01881945).

Experimental protocol

Volunteers were comfortably laid in semi-supine position—comfortable position—in a quiet room and were asked to relax and to breathe freely. They wore a facemask equipped with a flowmeter (Fresh head No. 1) and differential pressure transducer (163PC01D36, Micro Switch). Prior to recordings, leaks around the mask were checked for with an infrared CO₂ analyzer (Engstrom, Ethz/Eliza MC). End tidal CO₂ (F_{Ti}CO₂) was subsequently measured continuously using the same apparatus providing breath-by-breath F_{Ti}CO₂ (Fig. 1). Volunteers were asked to keep their eyes open during the whole recording period.

The infrared CO₂ analyzer displays the mean value of the breathing rate and F_{Ti}CO₂ measured over a period of 30 s. The mean breathing rate and F_{Ti}CO₂ at rest were calculated and used for the voluntary hyperventilation periods of both protocols.

Volunteers followed protocols 1 and 2. During protocol 1, spontaneous breathing (SP) was recorded during 3 min followed by 3 min of hyperventilation HV_{sp} at the spontaneous breathing rate but with a larger volume. During the complete voluntary hyperventilation process, the subject was guided to change the tidal volume to maintain F_{Ti}CO₂ 1 % below the spontaneous level and to have a stable and consistent hypocapnia.

In protocol 2, the 3-min spontaneous breathing (SP) was followed by 3 min of hyperventilation at a breathing rate of 20/min (HV₂₀) and again, the subject was guided to change the tidal volume to achieve a 1 % decrease in F_{Ti}CO₂.

In both protocols, the breathing rate was imposed by an auditory cue indicating the beginning of inspiration.



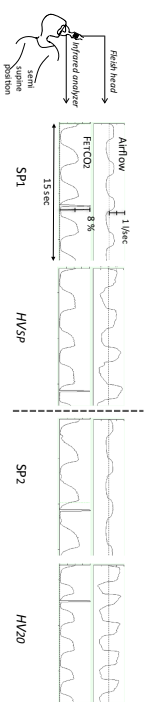


Fig. 1 Experimental device and data recordings. Healthy subjects were in semi-supine position. Airflow (measured by a flowmeter; Fleisch head No. 1 mounted on a facemask) and the fraction of CO₂ (measured by an infrared CO₂ analyzer) were recorded during two

A minimum of 10 min separated the two protocols, to let the subject recover its initial level of ventilation. Preliminary tests showed a full recovery after 5 min.

Analysis

A breath-by-breath analysis was performed over the whole period for each recording (SP₁, HV_{SP}, SP₂, and HV₂₀). The breaths, which included swallowing or a sigh, were discarded from the analysis.

The shape of the airflow was quantified for each remaining breath using harmonic analysis applying normalized Fast Fourier Transform to airflow signal to take account of variation in breath duration. This method has been previously described (Bachly et al. 1986) and it was demonstrated that the first four harmonics contain at least 95 % of the power of the original signal. Each harmonic is characterized by a phase and an amplitude, which can be represented by a vector (Fresnel representation). The shape of the airflow was quantified by the eight cartesian coordinates of these four vectors. In addition to the normalization in breath duration (harmonic analysis), a normalization in the amplitude was performed by dividing each of the 8 coordinates by the square root of the sum of the square of all 8 coordinates. The mean value of each coordinate was then calculated for all breaths at each recording, providing a mean flow shape. In addition, an airflow profile can be reconstructed from the mean 8 coordinates.

Figure 2 shows the ventilatory characteristics of one subject, the vector representation of the airflow shape and the reconstructed airflow profile under the four conditions of recording.

In addition, the following data were derived for each breath: tidal volume (V_T) by integration of the flow signal, breath duration (T_{breath}) and inspiratory (T_I) and expiratory (T_E) durations. Minute ventilation (V_T × 60/T_{breath}), V_I/T_I and T_I/T_{breath} were also calculated for each breath.

Mean values of the ventilatory characteristics, F_{ET}CO₂ and airflow shape were also calculated from retained breaths.

protocols: at spontaneous breathing (SP₁), volitional hypoventilation at each subject's spontaneous breathing rate (HV_{SP}), and at spontaneous breathing (SP₂), volitional hypoventilation at 20/min (HV₂₀)

To compare ventilatory variables between and within the protocol 1 and protocol 2 (SP₁ versus HV_{SP}, SP₂ versus HV₂₀, SP₁ versus SP₂, and HV_{SP} versus HV₂₀), a Wilcoxon paired test was applied.

For the multivariate (eight variables) airflow profile, we test if two profiles coming from the same individual are more related than expected by chance. There may be differences within an individual under different conditions but each individual has a certain airflow profile that can be recognized among airflow profiles of other individuals. The null hypothesis of the test is that the sum of differences within individuals is not different from the sum of differences between pairs of individuals sampled randomly; the alternative hypothesis is that the sum of differences within individuals is significantly less than that between random pairs of individuals. (This test has been described in details by Bencherit et al. (1989) and Shea et al. (1989) and has been used to show the similarity in the airflow profile within an individual under two different conditions (Shea et al. 1990; Bessie et al. 1992; Calabrese et al. 1998; Bencherit 2000; Mercier et al. 2014).

This analysis was then applied to test whether the spontaneous breathing frequency (HV_{SP}) results in an increase in ventilation from 6.71 ± 1.64 to 15.88 ± 4.92 l·min⁻¹ (+9.17 l·min⁻¹) inducing a decrease in F_{ET}CO₂ from 5.06 ± 0.54 to 4.07 ± 0.51 % (-1.02 %). Concerning spontaneous breathing (SP₂), hypoventilation at a breathing rate of 20/min (HV₂₀) results in a change in ventilation from 6.57 ± 1.31 to 15.87 ± 4.16 l·min⁻¹ (+9.30 l·min⁻¹) with a decrease in F_{ET}CO₂ from 5.00 ± 0.51 to 3.88 ± 0.42 % (-1.12 %).

Table 2 shows respiratory characteristics of all subjects in both protocols 1 and 2. The results of the Wilcoxon paired test applied to these variables show that as expected, T_{breath}, T_I and T_E are not significantly different between SP₁ and HV_{SP}, whereas they are significantly different between SP₂ and HV₂₀. In both protocols, V_I and V_I/T_I are significantly different from spontaneous to hypoventilation, but T_I/T_{breath} is not significantly different between SP₁ and HV_{SP}. Similar comparisons can be taken between SP₂ and HV₂₀. Time variables (T_{breath}, T_I, T_E) and V_T are significantly

Results

Analysis of the ventilatory data

The mean minute ventilation and F_{ET}CO₂ of each recording for all subjects are given in Table 1. Changes in minute ventilation and F_{ET}CO₂ are not significantly different between SP₁ and SP₂, and HV_{SP} and HV₂₀.

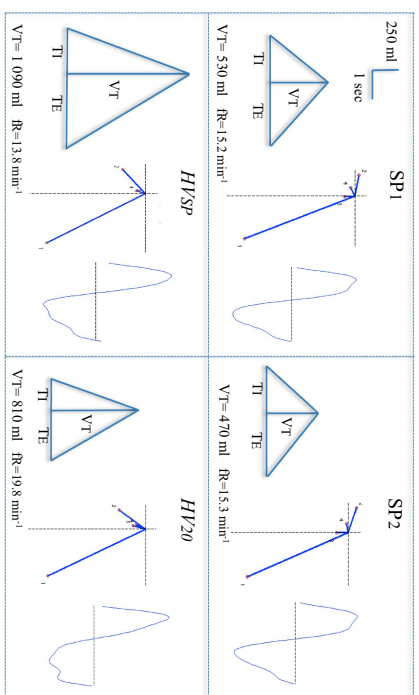


Fig. 2 For the subject EE, mean ventilatory characteristics: tidal volume (V_T), inspiratory (T_I) and expiratory (T_E) durations; the vectorial representation of the first four harmonics of a harmonic analysis of the airflow shape; and the corresponding reconstructed airflow profile are represented in the four conditions of recording (at spontaneous

breathing (SP₁), hypoventilation at subject's spontaneous breathing rate (HV_{SP}), volitional hypoventilation at 20/min (HV₂₀), and breathing rate (R) are given in each condition

Similarity of airflow profile within individuals

The reconstructed airflow profiles for all subjects under the four conditions at stake are represented in Fig. 3.

The similarity test performed between the two spontaneous breathing periods (SP₁ versus SP₂) shows that differences within individuals are significantly less than those between individuals randomly sampled ($p < 0.001$). Identical results are obtained when comparing airflow profile at HV_{SP} and HV₂₀ ($p < 0.001$).

When comparing SP₁ and HV_{SP} we find that differences within individuals are significantly less than those between individuals ($p = 0.005$). By contrast, differences within individuals are not significantly less than those between individuals, when comparing SP₂ and HV₂₀ ($p = 0.593$). We also applied the similarity test on SP₁ versus HV₂₀ ($p = 0.085$) and SP₂ versus HV_{SP} ($p = 0.057$).



Table 1 Mean values \pm standard deviations (18 healthy subjects) of minute ventilation (V_E), V_E at spontaneous breathing ($V_{E,sp}$), at voluntary hyperventilation at each subject's spontaneous breathing rate ($V_{E,sp}$), at spontaneous breathing (SP_2) and voluntary hyperventilation at 20/min (HV_{20})

Subject	$V_E \times 60/T_{TOT}$ (l min ⁻¹)				F_{I,CO_2} (%)			
	SP_1	HV_{sp}	SP_2	HV_{20}	SP_1	HV_{sp}	SP_2	HV_{20}
LA	4.90	13.27	5.75	10.85	4.47	3.14	4.62	3.24
CK	7.16	20.12	7.27	20.18	6.15	4.48	6.17	4.27
EE	8.01	15.07	7.22	16.03	4.24	3.27	4.48	3.75
FL	5.40	11.93	5.31	18.54	4.90	4.16	4.65	3.31
FC	6.71	20.23	7.09	17.34	4.59	3.81	4.41	3.47
GB	4.94	11.79	5.18	10.32	4.38	3.63	4.43	3.57
HA	5.27	14.98	5.24	12.47	5.14	3.91	5.22	4.13
JC	5.14	8.78	4.78	10.22	5.50	4.80	5.48	4.45
SJ	5.71	13.06	6.71	18.13	4.90	4.64	4.71	4.11
KM	6.55	16.48	6.28	17.97	4.60	3.61	4.54	3.42
ZN	7.69	19.73	7.18	17.33	5.04	3.97	4.93	3.81
TT	6.35	13.11	6.51	18.16	5.29	4.47	5.11	4.01
TG	6.44	14.96	5.55	10.54	5.56	4.44	5.48	4.28
TB	9.61	24.96	8.32	23.69	5.30	3.98	5.05	3.84
DD	5.40	9.71	5.11	12.94	6.11	5.16	6.02	4.16
NH	10.87	26.31	9.74	22.21	5.16	3.68	4.98	3.75
FJ	6.81	19.03	7.06	16.47	4.67	3.78	4.87	3.64
AB	7.82	12.25	7.90	11.85	5.02	4.09	4.93	4.10
Mean	6.71	15.88	6.57	15.87	5.06	4.07	5.00	3.88
SD	1.64	4.92	1.31	4.16	0.54	0.51	0.51	0.42

Significant differences (Wilcoxon paired test; $p < 0.05$) for: * SP_1 versus HV_{sp} ; # SP_2 versus HV_{20}

Discussion
The main observation of this study is that there exists an individuality in airflow profile among human subjects during volitional breathing as well as during spontaneous breathing. In addition, when comparing the airflow profile during volitional hyperventilation at spontaneous breathing and at a breathing rate of 20/min, there is a similarity in the flow profile, despite differences in V_T and T_{TOT} .

In our study, volitional ventilation was ensured by inducing a mild hyperventilation (1) at spontaneous breathing rate (HV_{sp}) and 2) at an increased respiratory rate (HV_{20}) maintaining F_{I,CO_2} 1% below the spontaneous level in both conditions for all subjects. In this way, somatic symptoms and discomfort induced by hypocapnia were minimized (Hornsveld et al. 1995) and allowed stable hypocapnia and a consistent decrease in F_{I,CO_2} . The resulting increase in ventilation was of the same order of magnitude in the two protocols, 9.17 l min⁻¹ in protocol 1 and 9.30 l min⁻¹ in protocol 2, respectively, ensuring a moderate volitional hyperventilation. A similar increase in ventilation was induced by Mckay et al. (2003) to study the neural correlates of voluntary breathing in humans.

To investigate the individuality of breathing pattern during moderate hyperventilation, airflow profile is compared under different conditions. Indeed, comparing the ventilatory characteristics (V_T , T_E , T_I) either one by one or all together as done in other studies (Benvenuti et al. 1989; Shest et al. 1989), was not relevant, as breathing depth and rate were voluntarily changed. Airflow profile containing valuable information was suggested by Proctor and Hardy as early as 1949, and Gray and Godwin (1951) proposed that "Transformation of the tracings to a completely non-dimensional form should be the first step in analyzing the significance of their shape". The harmonic analysis we used is indeed one such method of quantification of the airflow shape. In addition, normalization of both the duration and the amplitude allows focusing solely on the airflow shape.

The multivariate statistical test compares, under two different conditions, the differences between two recordings within individuals with the differences observed between random pairs of recordings. Thus, it provides a result on the group rather than on each individual. Therefore, even if there are changes in an individual, there are more similarities within individuals than between individuals when comparing SP_1 and HV_{sp} or SP_2 and HV_{20} . A detailed interpretation of the similarity test is given in Benvenuti (2000).



Table 2 Mean values \pm standard deviations (18 healthy subjects) of ventilatory characteristics: breath (T_{TOT}), inspiratory (T_I) and expiratory (T_E) durations, tidal volume (V_T), V_T/T_I and T_I/T_{TOT} at spontaneous breathing (SP_1), voluntary hyperventilation at each subject's spontaneous breathing rate (HV_{sp}), at spontaneous breathing (SP_2) and voluntary hyperventilation at 20/min (HV_{20})

Subject	T_{TOT} (s)				T_I (s)				T_E (s)				V_T (l)				T_I/T_{TOT}				V_T/T_I (l.s ⁻¹)			
	SP_1	HV_{sp}	SP_2	HV_{20}	SP_1	HV_{sp}	SP_2	HV_{20}	SP_1	HV_{sp}	SP_2	HV_{20}	SP_1	HV_{sp}	SP_2	HV_{20}	SP_1	HV_{sp}	SP_2	HV_{20}	SP_1	HV_{sp}	SP_2	HV_{20}
LA	3.75	2.98	2.79	3.64	1.19	1.41	1.16	1.44	2.56	1.57	1.64	2.20	0.29	0.65	0.27	0.62	0.34	0.47	0.42	0.42	0.24	0.47	0.23	0.43
CK	4.47	4.59	4.44	2.91	2.08	2.01	1.94	1.38	2.40	2.58	2.50	1.54	0.53	1.54	0.54	0.98	0.46	0.44	0.44	0.47	0.26	0.76	0.28	0.71
EE	3.94	4.35	3.91	3.03	1.70	1.63	1.72	1.19	2.24	2.72	2.19	1.83	0.53	1.09	0.47	0.81	0.43	0.38	0.34	0.39	0.31	0.67	0.27	0.68
FL	6.67	5.48	6.72	3.00	1.91	1.93	2.02	1.30	4.76	3.55	4.70	1.70	0.48	1.09	0.51	0.93	0.35	0.35	0.34	0.43	0.25	0.57	0.25	0.71
FC	4.76	4.89	4.27	3.12	1.99	1.76	1.76	1.40	2.77	3.14	2.50	1.72	0.53	1.65	0.50	0.90	0.42	0.36	0.41	0.45	0.27	0.94	0.29	0.65
GB	7.15	6.93	6.89	2.92	2.37	2.02	2.20	1.08	4.78	4.91	4.69	1.84	0.58	1.36	0.58	0.50	0.33	0.29	0.32	0.37	0.25	0.69	0.27	0.47
HA	7.08	6.66	6.02	3.00	2.85	2.84	2.38	1.19	4.24	3.82	3.65	1.81	0.62	1.66	0.53	0.62	0.40	0.43	0.39	0.40	0.22	0.59	0.22	0.53
JC	5.97	5.83	5.62	3.09	2.47	1.89	2.49	0.98	3.50	3.94	3.13	2.11	0.51	0.85	0.45	0.55	0.41	0.32	0.44	0.32	0.21	0.46	0.18	0.57
SJ	5.40	5.00	3.88	2.99	2.47	2.41	1.62	1.47	2.94	2.59	2.26	1.52	0.53	1.09	0.43	0.90	0.45	0.48	0.41	0.49	0.21	0.45	0.27	0.61
KM	3.19	3.27	2.94	2.97	1.35	0.90	1.25	1.01	1.85	2.37	1.69	1.96	0.35	0.90	0.31	0.89	0.42	0.28	0.43	0.34	0.26	1.01	0.25	0.88
ZN	3.56	3.77	3.58	3.03	1.39	1.78	1.37	1.40	2.17	1.98	2.21	1.63	0.45	1.23	0.42	0.87	0.39	0.47	0.38	0.46	0.33	0.70	0.31	0.62
TT	4.66	4.47	4.49	3.02	1.80	1.75	1.81	1.16	2.86	2.71	2.68	1.87	0.49	0.98	0.49	0.91	0.39	0.39	0.40	0.38	0.27	0.56	0.27	0.79
TG	4.95	5.24	5.50	3.11	1.97	2.41	2.19	1.41	2.98	2.82	3.31	1.71	0.53	1.30	0.50	0.55	0.40	0.46	0.40	0.45	0.27	0.54	0.23	0.39
TB	4.00	3.87	3.82	3.03	1.61	1.40	1.52	1.10	2.39	2.47	2.31	1.93	0.64	1.61	0.53	1.20	0.41	0.36	0.40	0.36	0.40	1.16	0.35	1.09
DD	6.85	7.53	5.95	2.95	2.87	3.52	2.31	1.43	3.98	4.01	3.64	1.52	0.61	1.22	0.50	0.64	0.42	0.47	0.39	0.49	0.22	0.35	0.22	0.44
NH	2.53	2.50	2.77	3.00	1.05	1.09	1.13	1.43	1.47	1.42	1.63	1.57	0.46	1.10	0.45	1.11	0.42	0.43	0.41	0.48	0.43	1.01	0.40	0.78
FJ	3.89	4.01	3.65	3.00	1.73	1.64	1.62	1.11	2.16	2.36	2.03	1.89	0.44	1.27	0.43	0.82	0.44	0.41	0.44	0.37	0.26	0.78	0.27	0.75
AB	2.91	2.91	2.94	3.00	1.32	1.54	1.31	1.67	1.59	1.36	1.63	1.33	0.38	0.59	0.39	0.59	0.45	0.53	0.44	0.56	0.29	0.39	0.30	0.36
Mean	4.76	4.68	4.46	3.05	1.89	1.89	1.77	1.29	2.87	2.80	2.69	1.76	0.50	1.18	0.46	0.80	0.41	0.41	0.41	0.42	0.27	0.67	0.27	0.64
SD	1.47	1.42	1.35	0.16	0.54	0.62	0.43	0.19	1.01	0.96	0.97	0.22	0.09	0.32	0.08	0.20	0.04	0.07	0.03	0.06	0.06	0.23	0.05	0.19

Significant differences (Wilcoxon paired test $p < 0.05$) for: * SP_1 versus HV_{sp} ; # SP_2 versus HV_{20} ; # HV_{sp} versus HV_{20}



Although ventilation increases by the same order of magnitude in the two protocols, there were differences in the ventilatory data during the voluntary hyperventilation period: in HY_{50} the imposed respiratory rate is the spontaneous one and changes concern mainly the tidal volume, whereas in HY_{20} both respiratory rate and tidal volume are changed in almost all subjects (Table 1). In our study, we fixed the level of hypocapnia and imposed respiratory rate and depth to maintain this level; thus only T_E and T_E could vary. $T_I/T_{I\text{Tot}}$ remained unchanged in all four conditions, despite a decrease in $T_{I\text{Tot}}$ during volitional breathing at a rate of 20/min. Unchanged $T_I/T_{I\text{Tot}}$ was also observed by Calhese et al. (1998) when adding resistive load, which led to an increase in $T_{I\text{Tot}}$. These authors suggested that the unchanged $T_I/T_{I\text{Tot}}$ at different levels of added load might represent an optimal value for each subject. In our study, the fact that $T_I/T_{I\text{Tot}}$ was the same during volitional breathing as that during spontaneous breathing (at least in this increased ventilation range) suggests that both automatic and volitional systems lead to the same optimal value of $T_I/T_{I\text{Tot}}$. According to Houshi (2011), even though the structures controlling breathing during volitional and spontaneous breathing are different, they both lead to the same outcome: maintaining blood gas homeostasis.

Figure 3 represents all airflow profiles under the four conditions of recording. There are differences in airflow profile between individuals during spontaneous breathing and during volitional breathing as well.

For each subject, the airflow profile at SP_1 and SP_2 appears similar as well as the airflow profile at HY_{50} and HY_{20} . The results of the similarity test confirm these observations. The similarity between SP_1 and SP_2 is in agreement with all previous findings on the individuality of breathing pattern. The similarity between the two conditions of volitional ventilation suggests that there exists an individuality of breathing airflow shape during volitional moderate hyperventilation. The question then arises as to know if this airflow is the same at rest and during hyperventilation. The similarity test provides no clear response to answer to this question. Indeed, the comparison of spontaneous breathing and voluntary hyperventilation airflow profiles shows that only SP_1 and HY_{50} have less differences within than between individuals ($\rho = 0.005$). These results appear paradoxical. However, two points deserve consideration. First, statistical tests do not imply transitivity. Second, in both protocols leading to moderate hyperventilation, the breathing rate and depth are volitionally imposed to maintain the same level of hypocapnia during HY_{50} and HY_{20} . However, $T_{I\text{Tot}}$ and V_T were changed in almost all subjects in HY_{20} , whereas only changes in V_T were obtained in HY_{50} . Thus, there may be a greater intensity of volitional control during HY_{20} . These results may

be explained in two ways: either a threshold of ventilation that changes the individual's resting airflow shape is attained during hyperventilation at 20 breaths per minute, but not during hyperventilation at resting frequency, or the duration of the breath has a significant effect on respiratory individuality. As the increase of ventilation is not very high and similar in the two protocols, we think that the second hypothesis may be the most realistic.

Our assumption from these results would be that there exists an individuality of flow profile during volitional hyperventilation and this flow profile is different from the spontaneous flow profile.

The airflow profile observed during volitional hyperventilation may result either from hyperventilation itself or from the volitional character of the ventilation. The fact that during hyperventilation induced by exercise, the individuality of airflow shape is different from the resting one, suggests that hyperventilation per se can induce another individuality of breathing. Following this assumption, volitionally generated hyperventilation may also lead to individuality of breathing pattern. Furthermore, Houshi and Bell (2009) concluded that non-mediatory respiratory structures involved in volitional breathing can develop the respiratory control processes "in a manner that 'mimics' functions normally associated with medullary brain stem structures". This demonstrates the presence of profound degeneracy, defined by Edelman and Cady (2001) as "the ability of elements that are structurally different to perform the same function or yield the same output". If the airflow shape may be considered as a ventilatory output, the similarity between airflow shapes generated automatically or volitionally may suggest degeneracy in pattern generation.

Degours et al. (1961) claimed that "each subject has his own combination of respiratory rate and tidal volume and also his own shape of ventilatory movements" and thus, he first introduced the concept of "Personnalité Respiratoire". Further studies showed the existence of breathing pattern individuality in various conditions. The possible determinants of this individuality were exhaustively envisaged by Sheu and Garz (1992).

Our results suggest that if volitional and spontaneous breathing originates from two separate systems, then ventilatory rhythm generating systems are not a determinant of the airflow shape individuality. Although the individuality of airflow profile may be modified in various conditions, it remains an inherent property of the ventilatory system.

In conclusion, during moderate volitional hyperventilation, unchanged $T_I/T_{I\text{Tot}}$ combined with the existence of airflow shape individuality, although different from spontaneous flow shape, suggests that volitional ventilation follows inherent properties of the ventilatory system.

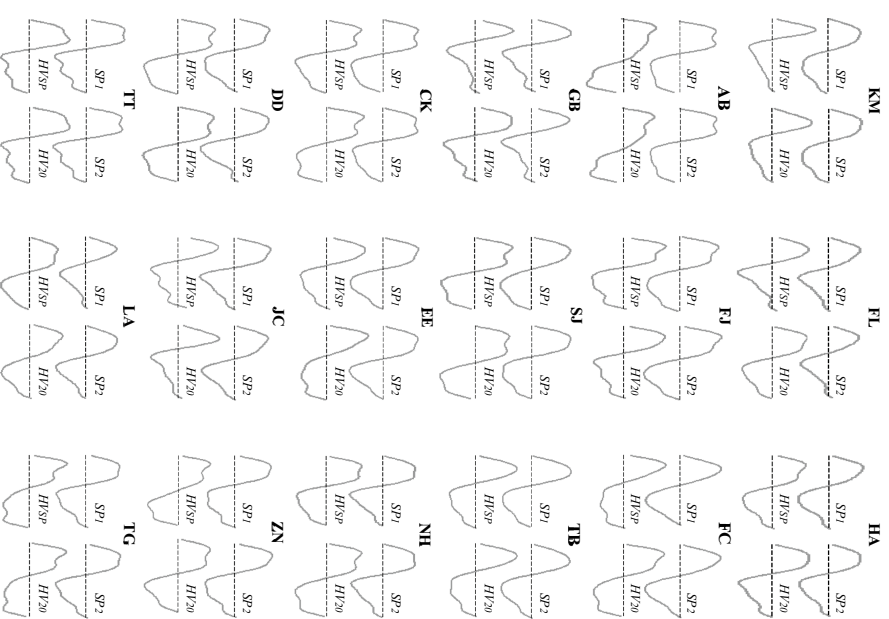


Fig. 3 Reconstructed airflow profiles from the first four harmonics of a harmonic analysis of the airflow shape are represented for all subjects in the four conditions (a) spontaneous breathing (SP_1), voluntary hyperventilation at each subject's spontaneous breathing rate (HY_{50}), (b) hyperventilation at 20 breaths per minute (HY_{20})

Compliance with ethical standards

Conflict of interest The authors declare that they have no conflict of interest.

Ethical approval All procedures performed in this study involving human participants were carried out in accordance with the ethical standards of the institutional research committee and with the 1964 Helsinki declaration and its later amendments or comparable ethical standards.

Informed consent Informed consent was obtained from all individual participants included in the study.

References

- Elekium GM, Gally JA (2001) Degeneracy and complexity in biological systems. *Proc Natl Acad Sci* 98:13763–13768
- Elske JH, Wuyam B, Sissonoy G, Bernadoni J, Bittel JH, Bencherif G (1992) Individual differences in breathing patterns during hypoxia and exercise. *J Appl Physiol* 72:246–253
- Gay JS, Gordin FS (1951) Respiration. *Annu Rev Physiol* 13:217–232
- Hawaz P (2011) Initiating inspiration outside the medulla does produce eupneic breathing. *J Appl Physiol* 110:854–856
- Hawaz P, Bell HJ (2009) Control of breathing and voluntary respiratory rhythm in humans. *J Appl Physiol* 106:904–910
- Hornscheid H, Garsen B, Van Spiegel P (1995) Voluntary hyperventilation: the influence of the respiratory rhythm on the development of symptoms. *Bull Psychol* 40:299–312
- Mackay LC, Evans KC, Fendowsak RS, Corfield DR (2003) Neural correlates of voluntary breathing in humans. *J Appl Physiol* 95:1170–1178
- Melton NM (2010) Degeneracy as a substrate for respiratory regulation. *Respir Physiol Neurobiol* 172:1–7
- Mere H, Calabrese P, Pradon D, Legalle M, Lofaso F, Terzi N (2014) Physiological comparison of breathing patterns with acutely induced voluntary apnea (VNA) and pressure-support ventilated voluntary VNA settings. *Respir Physiol Neurobiol* 195:11–18
- Proctor DF, Hardy JB (1949) Studies of respiratory airflow. I. Significance of the normal pneumothorax. *Bull Johns Hopkins Hosp* 85:253–280
- Shea SA, Guz A (1992) Personalized ventilator-Au overview. *Respir Physiol* 87:275–291
- Shea SA, Bencherif G, Pham-Dinh T, Hamilton RD, Guz A (1989) Breathing patterns of identical twins. *Respir Physiol* 75:211–222
- Shea SA, Horner RL, Bencherif G, Guz A (1990) The persistence of a respiratory personality in stage IV of sleep in man. *Respir Physiol* 80:33–44
- Bachy JP, Eberhard A, Baccomer P, Bencherif G (1986) A program for cycle-by-cycle analysis of biological rhythms. Application to respiratory rhythm. *Comput Methods Program Biomed* 25:1–10
- Bencherif G (2000) Breathing patterns in humans: diversity and individuality. *Respir Physiol* 123:123–129
- Bencherif G, Shea SA, Pham-Dinh T, Bodocco S, Baccomer P, Guz A (1989) Individuality of breathing patterns in adults assessed over the time. *Respir Physiol* 75:199–210
- Calabrese P, Dinh TP, Eberhard A, Bachy JP, Bencherif G (1998) Effects of resistive loading on the pattern of breathing. *Respir Physiol Neurobiol* 10:169–179
- Corfield DR, Apple LC, Guz A (1998) Does the motor cortical control of the sleep breathing pattern depend on respiratory centres in man? *Respir Physiol* 114:109–117
- Degens P, Bachel-Lambouise Y, Monzen P, Renard J (1961) Etude de la diversité des régimes ventilatoires chez l'Homme. *J Physiol* 53:320–321

II.2.3.2 Au cours de la ventilation assistée

Les modes ventilatoires et la personnalité ventilatoire au cours de la ventilation assistée ont ensuite été étudiés. La ventilation assistée n'est ni naturelle ni physiologique, puisque l'on impose une entrée d'air dans les poumons ce qui entraîne une augmentation de la pression au cours de l'inspiration, alors qu'en ventilation spontanée, l'action des muscles inspiratoires entraîne une expansion de la cage thoracique et une diminution de la pression alvéolaire. De nombreux modes d'assistance ventilatoire existent, la finalité étant de permettre de répondre aux besoins ventilatoires du patient tout en ajustant son effort ventilatoire. Le mode de ventilation mécanique *Neurally Adjusted Ventilatory Assist* (NAVA) délivre une pression proportionnelle à l'activité neuronale de la commande centrale respiratoire du patient (via une mesure de l'activité électrique du diaphragme). L'aide inspiratoire (AI), très utilisée, nécessite un paramétrage du ventilateur identique pour tous les cycles ventilatoires ce qui, dans certains cas, ne présente pas une assistance optimale pour le patient. Nous avons évalué l'effet de différents niveaux de pression pour chaque mode de ventilation mécanique NAVA et AI, sur le mode ventilatoire, la personnalité ventilatoire et la normocapnie du sujet. La mesure des mouvements de la cage thoracique par pléthysmographie optoélectronique a aussi permis de compléter ce travail en étudiant la répartition des mouvements des compartiments thoracique et abdominal au cours de la ventilation assistée en comparaison avec la ventilation spontanée. En collaboration avec le Pr Frédéric Lofaso (investigateur principal), j'ai rédigé le protocole "Etude comparée du mode ventilatoire au cours de la ventilation mécanique NAVA" qui a permis l'inclusion et l'enregistrement de 10 volontaires sains à l'hôpital Raymond Poincaré (acceptation par le Comité de Protection des Personnes "Ile-de-France XI" en avril 2012). Les enregistrements sur les volontaires sains ont été effectués dans différentes conditions : au cours de la ventilation spontanée, et au cours de trois niveaux de ventilation mécanique pour chaque mode (AI et NAVA) correspondant à des valeurs des pressions inspiratoires maximum de 5, 8, et 10 cmH₂O. L'activité électrique diaphragmatique diminue significativement avec le niveau d'assistance pour les deux modes d'assistance AI et NAVA. V_T augmente et la pression partielle transcutanée de CO₂ (PtCO₂) diminue avec l'augmentation des niveaux d'assistance pour AI seulement (aucun changement n'est cependant observé pour la NAVA). La synchronisation sujet-ventilateur est meilleure avec la NAVA qu'avec l'AI. Pour les deux modes NAVA et AI,

les mouvements du compartiment abdominal diminuent tandis que les mouvements du compartiment thoracique augmentent. La personnalité ventilatoire n'est pas maintenue au cours de la ventilation mécanique à chaque niveau d'assistance quel que soit le mode (AI ou NAVA).

Cette étude chez les volontaires sains montre que :

1- La personnalité ventilatoire n'est pas maintenue au cours de la ventilation mécanique pour les deux modes d'assistance ventilatoire : Aide Inspiratoire (AI) ou *Neurally Adjusted Ventilatory Assist* (NAVA).

2- Le mode NAVA semble "plus physiologique" que l'AI : meilleure synchronisation avec l'effort inspiratoire et maintien du volume courant et de la pression partielle transcutanée de CO₂.

Meric, Calabrese et al (2014) Physiological comparison of breathing patterns with neurally adjusted ventilatory assist (NAVA) and pressure-support ventilation to improve NAVA settings. Respir Physiol & Neurobiology.

Délégation CNRS : Service de Physiologie et d'Explorations Fonctionnelles, Hôpital Raymond Poincaré (Garches 92)-2011-2012.



Physiological comparison of breathing patterns with neurally adjusted ventilatory assist (NAVA) and pressure-support ventilation to improve NAVA settings

Henri Meric^{a,b,h,i}, Pascale Calabrese^{c,d}, Didier Pradon^{a,b,h}, Michèle Legaille^{a,b,h}, Frédéric Lofaso^{a,b,h}, Nicolas Terzi^{c,d,g,h,i,*}

^a Centre d'Investigation Clinique – Innovations Technologiques, Services de Physiologie – Expérimentation Fonctionnelle, Hôpital Raymond Poincaré, AP-HP, France
^b EA 4497, Université de Versailles-Saint-Quentin en Yvelines, 92380 Garches, France
^c UFR-Cariologie, UFR-ORL, CHU de Nancy, 54035 SCSPIREXIN, France, Grenoble F-38041, France
^d Centre de Recherche en Neurosciences, Université de Strasbourg, France
^e Normandie Université, France
^f UNICEN, COMETE, 14032 Caen, France
^g Inserm, U 1075 COMETE, 14032 Caen, France
^h CHU de Creteil, Département de Pneumologie, F-93000 Creteil, France

ARTICLE INFO

Article history:

Accepted 30 January 2014

Keywords:
 Breathing control
 Mechanical ventilation
 Neurally adjusted ventilatory assist
 Open-source pneumography

ABSTRACT

Neurally adjusted ventilatory assist (NAVA) assists spontaneous breathing in proportion to diaphragmatic electrical activity (Eadi). Here, we evaluate the effects of various levels of NAVA and PSV on the breathing pattern and, thereby, on PaCO₂ homeostasis in 10 healthy volunteers. For each ventilation mode, four levels of support (delivered pressure 0.1c, baseline, 5, 8, and 10 cmH₂O) were tested in random order. The mean respiratory pressure (P_{rs}) and tidal volume (V_T) were measured during the last 2 min of ventilation distribution with PSV and NAVA. Eadi decreased with increasing level of assist (P = 0.0004, respectively). Tidal volume (V_T) increased and P_{rs} decreased with increased levels of PSV (P = 0.004 and P = 0.0004, respectively) while no change was observed with NAVA. Subject-ventilator synchronization was better with NAVA than with PSV. NAVA and PSV similarly decreased the abdominal contribution to V_T. No airflow profile similarities were observed between baseline and mechanical ventilation. Diaphragmatic activity can decrease during NAVA without any change in V_T and P_{rs}. This suggests that NAVA adjustment is not a simple function of P_{rs} and V_T.
 Registered by Frédéric Lofaso and Nicolas Terzi at ClinicalTrials.gov, #NCT01514873.
 © 2014 Elsevier B.V. All rights reserved.

1. Introduction

Breathing is a complex process (Younes, 1981) designed to maintain arterial partial pressure of oxygen (PaO₂) levels in a narrow range. In recent years, diaphragmatic innervation during controlled mechanical ventilation was shown to cause ventilator-induced diaphragmatic dysfunction (VIDD) (Jaber et al., 2011; Vassilakopoulos and Petrof, 2004). These data have led to the increased use of assist modes. Among these, pressure-support ventilation (PSV) is widely used, most notably during the weaning phase (Esteban et al., 2008). Several studies have shown that

* Corresponding author. Tel.: +33 231 664 716; fax: +33 231 664 916.
 E-mail addresses: terzi@chu-nancy.fr (N. Terzi).

These authors contributed equally to the work.
 1569-9048/\$ – see front matter © 2014 Elsevier B.V. All rights reserved.
<http://dx.doi.org/10.1016/j.resp.2014.01.021>

volunteers decrease their inspiratory activity under PSV but do not maintain normal CO₂ homeostasis when PSV exceeds the demand of breathing (Lofaso et al., 2007). Tidal volume (V_T), Geopneustics (2007) and pressure support (PS) (Lofaso et al., 2007) modes that deliver a level of assistance proportional either to the patient's inspiratory muscle effort, in proportional assist ventilation (PAV), or to the diaphragmatic electrical activity (Eadi), in neurally adjusted ventilatory assist (NAVA) (Navajas and Costa, 2003; Sinderby et al., 1999). Clinical studies in critically ill patients have confirmed many of the expected short-term physiological benefits of NAVA, including better patient-ventilator synchronization and a decreased risk of overinflation (Terzi et al., 2012). However, although increasing the level of assistance during PSV's well known to increase V_T and to reduce hypoapnea in healthy subjects (Geopneustics et al., 1997; Ström et al., 1994), there is concern about the effects of increasing NAVA support on V_T and PaCO₂.

The main objective of our study was to evaluate the effects of varying levels of NAVA and PSV on breathing patterns and, thereby, on PaCO₂ homeostasis. In healthy volunteers, effective NAVA or PSV levels necessarily result in overassistance.

2. Methods

2.1. Study population

We studied 10 healthy volunteers. The appropriate ethics committee (Hôpital A. Paré, Paris, France) approved the study, which was registered on ClinicalTrials.gov (#NCT01514873). All volunteers provided their written informed consent before study inclusion.

2.2. Study procedures

The volunteers were in the supine position, wore a noseclip, and breathed via a mouthpiece avoiding leaks. They received non-invasive ventilation using a ventilator able to deliver both PSV and NAVA (Servo[®], Maquet Critical Care, Solna, Sweden). The specific non-invasive (NIV) mode was not used.

As previously described (Sinderby et al., 2007), the electrical activity of the diaphragm (Eadi) was recorded using a commercialized nasogastric Eadi-catheter (8 French diameter, 125 cm long, Maquet Critical Care, Solna, Sweden), with an electrode array on its distal segment. Correct Eadi catheter positioning was checked using the “Eadi catheter positioning” ventilator function.

2.2.1. Experimental setup

To compare breathing patterns assessed under the different conditions using the same measurement devices, airway pressure (Paw) and airflow were measured using a differential pressure transducer (Validyne, Northridge, CA) and a Fleisch #1 pneumotachometer (Lausanne, Switzerland), both connected to the mouthpiece.

Transcutaneous partial pressure of carbon dioxide (PtcO₂) and oxygen saturation (SpO₂) were monitored noninvasively using an earclip and a Sentr-A6 monitor (Therwil, Switzerland).

Pressure, flow, PtcO₂, and SpO₂ signals were digitized at a sampling rate of 100Hz and recorded directly on a personal computer equipped with the WP 130 data-acquisition system (Dspace Systems, San Diego, CA, USA).

Eadi, monitored by the ventilator, were recorded through an 85232 interface at a sampling rate of 1001Hz, using the dedicated software (Nova Tracker V2.0, Maquet Critical Care), and Eadi was analyzed using customized software. Thoracic and abdominal volume changes were monitored using optoelectronic plethysmography (OEP) with 52 markers attached to the patient's thorax, as described by Cah et al. (1996). A CX1 condensation system (Chamwood Dynamics Ltd, Rothley, UK) was used to monitor and record marker movements during the experiment. Accuracy of OEP volume measurement was checked by comparing vital capacity values estimated by OEP and by spirometry. The difference was always less than 10% of the spirometry value.

Synchronization of the three computer recordings was obtained by triggering the OEP and Eadi recordings with the start of the flow and pressure contours and of the inspiratory and expiratory times of each cycle was checked.

2.2.2. Experimental protocol

Data were recorded first during spontaneous breathing (SB) then with non-invasive ventilation (PSV and NAVA). Inspiratory

pressure support was set to obtain peak inspiratory pressure of 10 cmH₂O (PEEP of 5 cmH₂O, P_{rs} of 15 cmH₂O, P_{rs} to PEEP ratio of 3) and airflow of 10 L/min. After 2 min to allow breathing stabilization, we used the “NAVA Preview” ventilator function to estimate the NAVA level that would achieve the same inspiratory pressures (NAVAS, NAVAS8, and MAVA10, respectively). Positive end-expiratory pressure (PEEP) was set at zero and inspired oxygen fraction (F_iO₂) at 21%, and these settings were kept constant throughout the study. Flow and Eadi triggers had each been adjusted previously by the physicians to be as sensitive as possible without auto-triggering. Eadi and flow triggers were kept constant throughout the trial for each patient and were set at 0.8 μV (0.8–0.8) and 0.5 L/min (0.5–0.5), respectively. During PSV, the expiratory ramp was set at 25% of the maximal inspiratory flow and the inspiratory ramp at 100Hz. PSV and NAVA were tested in random order, in 10 min cycles. Each mode was tested for 8 min or more to allow the volunteer at least time to attain the steady state. Only the last 2 min were used for the analysis.

2.3. Data analysis

Mean values of the 2 last minutes of each condition were used for the analysis. Only Eadi was analyzed manually. By an expert who was blinded to flow and pressure signals, which were analyzed automatically for computation of the usual breathing pattern parameters. Respiratory frequency (f_R) and expiratory tidal volume converted to BTPS conditions (V_T) were determined from the flow signal.

The Eadi signal was used to determine (1) the patient's neural inspiratory time, defined as the time from the beginning of the Eadi signal increase to the Eadi signal peak; (2) inspiratory diaphragmatic activity, defined as the area from the onset of the rise to the peak of the Eadi signal (represented by the striped area in Fig. 1); (3) the ventilator inspiratory trigger delay (ITD), defined as the time from the beginning of the inspiratory effort (detected by the Eadi signal to the onset of ventilator pressurization); and (4) the insufflation in excess (I_{ex}), defined as the difference between the end of the patient's inspiratory effort, i.e., the Eadi signal peak, and the end of ventilator pressurization (Fig. 1).

OEP allowed us to assess lung volume distribution between the thorax and abdomen (Cah et al., 1996). We were thus able to determine the relative contribution of PSV/NAVA to the increase in volume to that seen during SB. We expected to find this effect of NAVA because diaphragmatic activity persists throughout insufflation with NAVA but does not always persist during PSV, which can maintain pressurization without any further diaphragmatic contraction once the insufflation is triggered.

2.4. Breathing pattern comparison

For each recording, airflow shape was quantified by eight variables having no physiological significance. The first four harmonics (described by a phase and an amplitude) of a serial Fourier analysis applied to a breath contain at least 95% of the power of the original signal and are sufficient to quantify airflow signal shape. Analytical expressions of the first four harmonics of a breath is termed ASTER and the airflow shape of a breath is quantified by the eight Cartesian coordinates of these four vectors (8 values). For statistical comparisons of ASTERs to take into account only airflow shape, each ASTER was normalized (for amplitude) by dividing each coordinate by the square root of the sum of the square of all eight recordings. The mean ASTER value was also calculated for each recording.

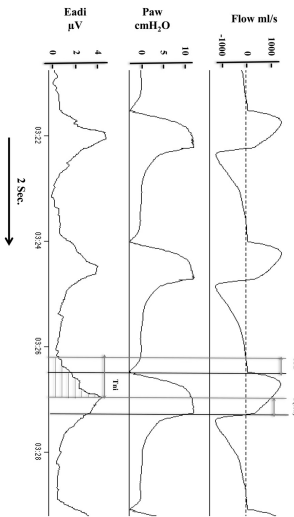


Fig. 1. Flow, airway pressure (Paw), and electrical activity of the diaphragm (Edi) signals for one subject during pressure-support ventilation at level 8 (PS/8). The figure shows the patients' normal inspiratory rate (T10), ventilation inspiratory trigger delay (T10), and inspiration in excess (T1ex). Inspiratory diaphragmatic activity, defined as the area from the onset of the rise to the peak of the flow signal, is represented by the shaded area.

2.5. Statistical analysis

The data were described as median ± interquartile range (25–75th percentiles). As data distribution was not normal, Friedman's test was used to separately evaluate the effects of PSV and NAVA on Edi, \dot{V}_E , and delta P_{ao}, expressed as the differences from baseline, i.e. spontaneous breathing without assistance in inspiration, which therefore could be considered as the level 0 of both PSV and NAVA. Thus, we performed Friedman's test to evaluate the differences among four PSV or NAVA levels (delivered pressure 0, i.e. baseline, 5, 8, and 10 cmH₂O). When the Friedman's test was significant a two by two comparison was performed using the Wilcoxon test. Neural inspiratory time, T1D, T1ex, and regional distribution of \dot{V}_E expressed as combination of the abdomen to \dot{V}_E were compared between PSV or NAVA using the Wilcoxon test. The level of tests was performed for all values, independently from the level of tests.

A specific analysis (Benech et al., 1989; Calhoun et al., 1988; Elsie et al., 1992; Shea et al., 1987)

This was designed to compare interindividual differences to interindividual within-group differences between two conditions (e.g. spontaneous breathing and a level of assisted ventilation). The null hypothesis was that the sum of interindividual differences was not different from the sum of differences between pairs of individuals taken randomly; the alternative hypothesis was that the sum of interindividual differences was significantly less than the sum of differences between pairs

of individuals taken randomly. This test provides information on interindividual differences in the global characteristics of the respiratory system, but not on the specific characteristics. For example, we tested whether airflow shape differences between SB and a specific level of an assisted ventilation mode (e.g. PSV5) were the same in a given individual relative to differences in two conditions (e.g. SB and PSV5) between all individuals in the same group. We repeated this analysis between pairwise combinations of all conditions: SB vs. PSV8, SB vs. PSV10, SB vs. NAVA5, SB vs. NAVA8, SB vs. NAVA10, PSV5 vs. NAVA5, PSV8 vs. NAVA8 and finally, PSV10 vs. NAVA10. P values lower than 0.05 were considered significant. Statistical tests were run using the Statview 5 package (SAS Institute, Grenoble, France).

3. Results

3.1. Study population

We enrolled 10 consecutive healthy volunteers with normal findings from a physical examination and pulmonary function tests. Table 1 reports the characteristics of 10 volunteers. One of the volunteers was unable to tolerate the gastroesophageal catheter. During NAVA, gains were 1.25 (0.95–1.6) cmH₂O/LV, 2 (1.4–2.6) cmH₂O/LV, and 2.6 (2–2.9) cmH₂O/LV, to match PSV settings of 5, 8, and 10 cmH₂O.

Table 1
Characteristics of the 10 healthy volunteers.

#	Age (y)	Height (cm)	Weight (kg)	Sex	VC (litre) (%)	MIP (cmH ₂ O)	MEP (cmH ₂ O)
1	54	183	92	M	106	142	177
2	23	180	87	M	107	141	108
3	25	183	81	M	91	124	153
4	27	171	71	F	108	116	113
5	24	166	65	F	108	81	ND
6	22	156	57	F	ND	152	ND
7	37	190	100	M	116	152	221
8	49	173	62	M	111	113	112
9	26	172	62	M	111	113	112
10	58	177	58	F	83	47	70

Abbreviations: F, female; M, male; VC, vital capacity; % of predicted value; MIP, maximal inspiratory pressure; MEP, maximal expiratory pressure; ND, not done. #6 was unable to tolerate the gastroesophageal catheter.

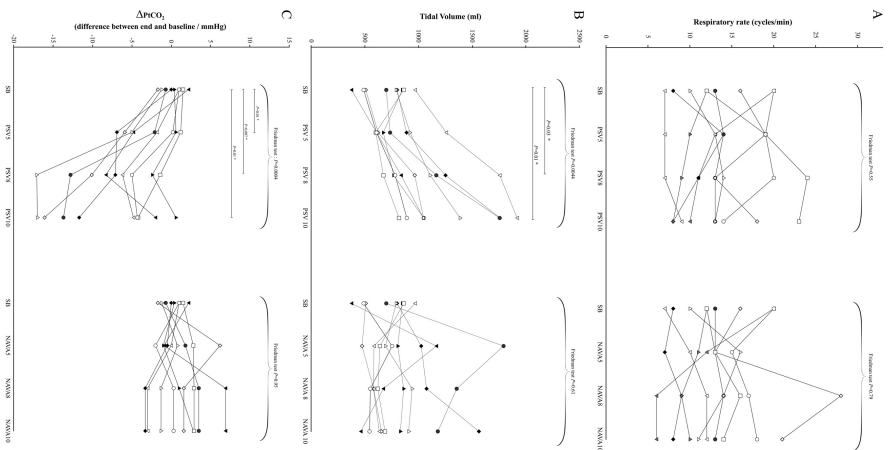


Fig. 2. Comparison of respiratory rate (panel A), individual data for tidal volume (panel B), and ΔP_{ao2} as the difference between end and baseline (panel C), according to the support level in cmH₂O. The numbers indicate the number of subjects who tolerated the support level in cmH₂O.

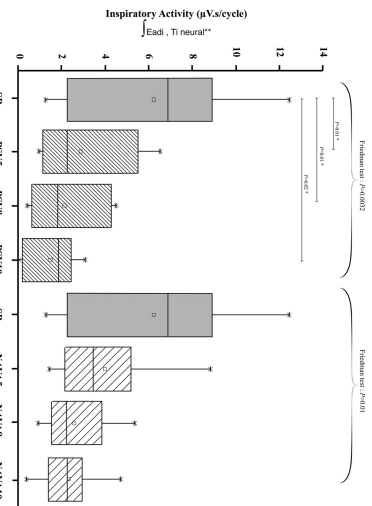


Fig. 3. Effect of mechanical ventilation on inspiratory activity defined as the electrical activity of the diaphragm. SB, spontaneous breathing; PSV, pressure-support ventilation; and NAVA, neurally adjusted ventilatory assist. Wilcoxon test; * $p < 0.05$; ** $p < 0.01$; *** $p < 0.001$.

3.2. Effect of mechanical ventilation on breathing pattern

As shown in Fig. 2A, no significant change in f_i occurred with either PSV ($P = 0.55$; 0.238) or NAVA ($P = 0.12$; 0.238) (Fig. 2A). However, f_i was significantly higher during PSV 8 and PSV 10 compared to SB ($P = 0.03$ and $P = 0.01$ respectively; Wilcoxon test). Delta P_{ao} (difference between end and baseline) decreased significantly with increasing levels of support during PSV ($P = 0.0004$; Friedman test) but showed no change with the level of support during NAVA ($P = 0.95$; Friedman test) (Fig. 2C). Delta P_{aCO_2} decreased significantly during PSV 5, PSV 8 and PSV 10 compared to SB ($P = 0.01$; $P = 0.007$ and $P = 0.01$ respectively; Wilcoxon test).

Individual airflow shapes during SB were not maintained during assisted ventilation. Patients were >0.5 l for comparisons of SB vs. PSV 5; SB vs. PSV 8; SB vs. PSV 10; SB vs. NAVA 5; SB vs. NAVA 8; and SB vs. NAVA 10.

vs. NAVA 10. Moreover, when comparing PSV vs. NAVA at the same level of support, the airflow shapes were not maintained with PSV 8 vs. NAVA 8 and PSV 10 vs. NAVA 10.

3.3. Effect of mechanical ventilation on inspiratory activity

During both PSV and NAVA, electrical inspiratory activity decreased as the support level increased (P values 0.0072 and 0.01 during PSV and NAVA respectively; Friedman test) (Fig. 5).

3.4. Patient-ventilator synchronization

Inspiratory trigger delay was always longer with PSV than with NAVA ($P = 0.01$; Wilcoxon test). Transition in excess and mean IAVA ($P = 0.01$; Wilcoxon test) were also longer with PSV than with NAVA ($P = 0.01$; Wilcoxon test) ($P > 0.23$ respectively; Wilcoxon test) (Table 2).

Table 2
Subject-ventilator interaction.

MODE	PSV 5	PSV 8	PSV 10	NAVA 5	NAVA 8	NAVA 10
TD	160.1 ± 47.5 (142–190)	190.1 ± 40 (175–215)*	160.1 ± 40 (146–190)*	70.1 ± 10 (70–80)	80.20 ± 7 (70–90)*	80.20 ± 7 (70–90)*
Ti (ml)	205 ± 80 (140–300)	190 ± 110 (140–300)	230 ± 70 (130–300)	200 ± 120 (130–300)	180 ± 80 (100–300)	210 ± 70 (130–300)
Ti neural	1.46 ± 0.15 (1.26–1.87)	1.40 ± 0.10 (1.20–1.70)	1.30 ± 0.10 (1.00–1.90)	1.30 ± 0.10 (1.00–1.70)	1.00 ± 0.10 (0.90–1.30)	1.10 ± 0.10 (1.00–1.40)
Ti/Ti _{total}	0.42 ± 0.05 (0.38–0.44)	0.40 ± 0.09 (0.32–0.42)	0.43 ± 0.08 (0.38–0.46)	0.46 ± 0.04 (0.42–0.48)	0.41 ± 0.04 (0.39–0.46)	0.43 ± 0.04 (0.41–0.46)

The data are described as median ± interquartile range (25–75th percentiles). TD, tidal volume; Ti, inspiratory volume; Ti neural, time of inspiration measured on EMG signal; Ti/Ti_{total}, time of inspiration to total breath duration measured on flow signal.

* $P < 0.05$; NAVA 5 vs. PSV 5.
* $P < 0.05$; NAVA 8 vs. PSV 8.
* $P < 0.05$; NAVA 10 vs. PSV 10.
Values without asterisk indicate that there is no statistical difference between the values observed in PSV and NAVA.

3.5. Lung volume distribution

V_T as assessed by orofunctional plethysmography during SB correlated closely with V_T measured by pneumothorax ($r^2 = 0.954$). The Bland-Altman plot showed that the mean difference was 14 ml (95%CI, –62 ml to +76 ml), and the limits of agreement were 92 ml (95%CI, –62 ml to +246 ml) and –64 ml (95%CI, –62 ml). Thorax V_T increased with the support level during NAVA and PSV ($P = 0.019$ and 0.021 respectively; Friedman test). Abdominal V_T decreased as the support level increased during PSV and NAVA ($P = 0.021$ and 0.019 respectively; Friedman test). Regional ventilation distribution was not significantly different between PSV and NAVA.

4. Discussion

In our study, healthy volunteers receiving different levels of NAVA maintained their baseline minute ventilation and carbon dioxide homeostasis by decreasing their inspiratory activity. In contrast, PSV induced hypoventilation with hypocapnia. In addition, synchronization of the assist with the beginning of the inspiratory effort was better with NAVA than with PSV.

The main objective of the respiratory control system is to maintain P_{aO_2} at a near-constant level via an array of compensatory adjustments (Cherneck and Alviso, 1981).

Devices have been developed to allow investigation of the effects of unloading (Trone and Ward, 1986; Younes et al., 1987). By unloading the respiratory system, one can determine whether the normal abnormal respiratory pattern is altered. The normal pattern (Chalder and Younes, 1989) and Trone et al. (1987) were the first to use assisted mechanical ventilation to achieve partial resistive unloading of the respiratory system. They demonstrated that the inspiratory resistive load was an important determinant of the pattern of respiratory motor output. Thus, inspiratory resistive unloading caused significant shortening and shape changes of the pressure generated by the inspiratory muscles.

Also for evaluating the effects of resistive and elastic unloading, Younes et al. were the first to develop a ventilator prototype in which the assist used the principles of equations of motion to ensure (Pooner, 1992). Subsequently, an intensive care ventilator (PVC; Gordon, 1991) was developed to automatically unload the respiratory system. The PVC was designed to provide the assist with constant unloading fractions of the approximate values of respiratory system resistance and elastance (Gondal et al., 2009). In a study of normal volunteers during assist-volume control, PSV and PAV with the assist level set at the highest comfortable value, P_{aO_2} remained close to its set point during PAV, preventing the occurrence of respiratory alkalosis (Mironska et al., 1989). However, during PAV this ventilator provides support only once it detects an inspiratory flow initiated by the patient. A substantial time lag can occur between such detection and inspiratory muscle effort initiation in patients with dynamic hyperinflation. Finally, as with PSV (Nava et al., 1995), loss of patient-ventilator synchrony was observed with PVC. Moreover, problems on changes in mechanical properties can induce unwanted phenomena (Schnitzler et al., 1997).

The latest improvement in methods of inspiratory muscle unloading is the development of NAVA, in which the assist is proportional to Padi (Tseti et al., 2012). NAVA artificially increases the conversion of phrenic nerve impulses to inspiratory driving pressure and, therefore, to V_T , and the feedback loops (including the chemical feedback loop) that control the phrenic nerves may be the only remaining determinants of V_T and V_E .

Expert for subject-ventilator interaction parameters and ventilator settings

NAVA and PSV were not compared directly (Friedman's test evaluated PSV and NAVA independently) because the airway pressure profile over time differed between these two modes. PSV delivers a pressure level that is constant and determined by the prescriber, instead of being proportional to feedback loop activity. Therefore, pressure support can rapidly exceed the patient's needs, resulting in excessively high V_T values (Azarian et al., 1993). In this situation, f_i adjustment may fail to prevent hypocapnia (Schied et al., 1994). In contrast, as previously described (Schnitzler et al., 2007), NAVA decreased the inspiratory activity, which, according to the closed loop process, in turn modified the shape of pressure assistance without significantly changing V_T or f_i . In keeping with these mechanisms, normocapnia was maintained during NAVA in our study. These results suggest that NAVA is a more effective ventilator than PSV for the control of the respiratory system. Thus, the breathing pattern observed with NAVA is the result of a complex multifactorial physiological process involving the subjects' chemical and neural components, which were not specifically and separately evaluated in our study.

In our study, whereas the expiratory trigger was comparable with NAVA and PSV, the NAVA inspiratory trigger outperformed the PSV inspiratory trigger. In keeping with previous clinical studies (Tseti et al., 2010) demonstrating better patient-ventilator synchronization with NAVA than with PSV, with NAVA, Eadi triggers the assist when the subject makes an inspiratory effort, even during expiration with intrinsic PEEP (Fiquelaud et al., 2011), and a decrease in Eadi terminates the assist.

Using an objective system, we showed that both NAVA and PSV were able to unload the respiratory system. However, the muscle activity with increasing levels of support suggests that the downward course of the diaphragm may decrease with increasing support levels in healthy individuals. In contrast, motion of the upper and lower thoracic compartments increased significantly with increasing support levels during both NAVA and PSV, in agreement with an earlier study (Alberti et al., 2000). This finding may be attributable to the lung inflation induced by mechanical ventilation. The differences in chest-wall motion between spontaneous breathing and assisted mechanical ventilation may explain the breathing pattern differences observed between these two conditions. Indeed, using a previously validated method to analyze the breathing pattern, we found no significant changes in breathing pattern when the assist was increased during PSV or NAVA.

Our study has several limitations. First, we cannot exclude an influence of cortical inputs on the recorded breathing patterns. However, none of the subjects reported any discomfort during any of the conditions, suggesting that the breathing patterns were normally influenced by the cortical inputs, which are usually active during wakefulness. Second, the difference in effects of PSV vs. NAVA on P_{aO_2} is among our most striking findings. Arterial P_{aO_2} measurement would have been scientifically preferable but ethically unacceptable in our healthy volunteers. Previous studies have demonstrated that P_{aO_2} is very close to P_{aCO_2} and that P_{aO_2} changes are representative of P_{aCO_2} changes (Schnitzler et al., 1997). However, we did not investigate global inspiratory activity in the volunteers. However, the diaphragm is the main inspiratory muscle and diaphragmatic activity can therefore be considered representative of inspiratory activity (Mogroni et al., 1969). Finally, the absence of esophageal and gastric pressure traces might appear as an obstacle to independent determination of the neural inspiratory time. Nevertheless, previous work establishes that neural inspiratory time is

better estimated using diaphragmatic electromyography than using esophageal and gastric pressure (Parramattam, Joffe et al., 2009).

4.1. Clinical implications

In clinical practice, determining the optimal NAVA level remains challenging, and several methods have been suggested. Contrary to PSV, NAVA generates V_T levels that can remain consistent independently from the support level once the patient's ventilation needs are satisfied (Brander et al., 2009). One study evaluated breathing pattern analysis during a titration procedure as a means of determining the best NAVA support level (Brander et al., 2009). Titration consisted in increasing the NAVA level from about 3 cmH₂O in 1-l H₂O/AU steps every 3 min/AU refers to Arbitrary Unit and is the tidal signal intensity in V_T). The response in terms of V_T and airway pressure (P_{aw}) was biphasic. During the first phase, V_T and P_{aw} increased until the target V_T was reached. In the second phase, P_{aw} and airway muscle effort) and Eadi decreased, further increases in the NAVA level (second phase) did not significantly change V_T but continued to decrease the esophageal pressure–time product and Eadi. Thus, the first phase may indicate an insufficient NAVA level to support the patient's needs, the second phase may correspond to the lowest support level that satisfies the patient's needs. Thus, the optimal (or adequate) NAVA level may be equal to or greater than this inflection point. However, our finding that CO₂ homeostasis is preserved during overassistance with NAVA indicates that NAVA settings cannot rely solely on a V_T or P_{aw} target. Other targets seem needed. One study used Eadi as the target (Gore et al., 2011). This value was determined daily at the target V_T and at the target P_{aw} during the titration procedure of 7 cmH₂O and no PEEP. This method proved feasible and well tolerated until excubation but was time consuming. An alternative might consist in adapting the support level to the patient's respiratory discomfort once the V_T plateau is attained with NAVA (Schmidt et al., 2011). However, further studies are needed to confirm this possibility.

Azami, K., Adenso, F., Zanek, E., Lotun, H., Mahr, C., Sahay, D., Hatz, A., 1993. Resuscitation with positive end-expiratory pressure in patients with acute respiratory failure. *Chest* 103, 522–528.

Bailey, P., Richardson, A., Brummer, P., Bencherif, G., 1986. A program for cycle-by-cycle control of volume in patients with respiratory failure. *Comput. Methods and Programs in Biomedicine* 23, 297–307.

Bencherif, G., Sheeh, S.A., Dinj, P., Bledsoe, S., Brummer, P., Gao, A., 1980. Individualized ventilator settings in adults: a retrospective study. *Respiration* 47, 191–202.

Brander, L., George, H., Beck, J., Benett, J., Hutchins, S.J., Sledge, A.S., Sindenby, C., 2007. Titration and programming of neurally adjusted ventilatory assist in patients with severe acute respiratory failure. *Crit. Care* 11, R30.

Cah, S.L., Koyon, C.M., Ferguson, G., Gerweil, W., Alvent, A., Madhok, T., 2007. Evidence-based analysis. *Journal of Applied Physiology* 97, 2859–2869.

Calverley, P., Dinj, P., Bernard, A., Binley, J.P., Bencherif, G., 1998. Effects of respiratory load on the pattern of breathing. *Respiration* 65, 574–580.

Chatterjee, K., 1997. *Respiratory Physiology: Principles and Practice*. In: Murray and Tenet, Marcel Dekker, New York.

Brander, P., 2007. The design, use, and results of Transcutaneous carbon dioxide sensors: current and future directions. *Acute Care Medicine* 105, 548–552.

Bleth, J.H., Wygan, B., Sawoney, C., Hernandez, J., Briel, J.H., Bencherif, G., 1992. *Methodology of ventilatory systems: 44398*. In: *Journal of Applied Physiology* 73, 248–255.

Ettema, A., Ferguson, N.D., Meade, M.O., Froneo-Vwart, A., Perezgonzalez, C., Broedl, L., Rajmohan, R., Kuan, N., Hernandez, J., Vones, V., Gonzalez, M., Elizalde, J., Ngfin, F., Marinis, D., Montaner, A., Alvarez, A., 2008. Evaluation of mechanical ventilation in response to clinical research. *American Journal of Respiratory and Critical Care Medicine* 178, 1009–1017.

Gallegos, C.C., Yonnes, M., 1989. Effect of pressure assist on ventilation and respiratory mechanics in heavy exercise. *Journal of Applied Physiology* 66, 823–827.

Garcia, R., Temple, E., Goffel, L., Aplienne, S., Terzi, N., 2011. Accuracy of a transcutaneous carbon dioxide pressure monitoring device in emergency room patients with acute respiratory failure. *Bioscience Research* 3, 248–255.

Geppert, M., 1997. Respiratory response to CO₂ during pressure-support ventilation in conscious normal humans. *American Journal of Respiratory and Critical Care Medicine* 155, 1010–1016.

Jaber, S., Chatterjee, K., Wang, H., Chammone, G., Benett, J.P., Abuel, C., Rougier, H., Conouable, P., Kocshin, Ramonanos, C., Sebaste, M., Simonski, T., Scheer-Norman, V., Meber, A., Gajjala, A., Moore, D., Mercier, J., Leckamp, A., 2010. Intra-arterial mechanical ventilation in humans. *American Journal of Respiratory and Critical Care Medicine* 181, 364–371.

Koucký, M., Martinek, J., Kapusta, R., Kocour, V., 2006. The effect of pressure–proportional assist ventilation with load-adjustable gain factors on tidal volume and respiratory mechanics in normal humans. *European Journal of Applied Physiology* 96, 670–676.

Ma, S.C., 2006. *Respiratory Support: Principles and Practice*. Elsevier, Amsterdam.

Martinez, G.A., 2007. Pressure support. *Bioscience Research* 2, 692–698.

Mattos, J., 1995. Effect of pressure support on respiratory mechanics. *European Journal of Applied Physiology* 71, 417–420.

Meade, M.O., 2007. Evidence-based analysis. *Journal of Applied Physiology* 97, 2859–2869.

Mogkoni, F., Sabine, F., Santambrogio, G., 1989. Contribution of the diaphragm and the other respiratory muscles to different levels of tidal volume and static lung volume. *Respiration* 56, 517–524.

Nava, E., 2002. *Neurally Adjusted Ventilatory Assist: A New Approach to Respiratory and Intra-arterial Pressure Support*. *Critical Care Medicine* 30, 1871–1879.

Nava, E., 2007. *Neurally Adjusted Ventilatory Assist: A New Approach to Respiratory and Intra-arterial Pressure Support*. *Critical Care Medicine* 35, 151–158.

Parasuraman, S., Joffe, A., Teoh, M., 2000. Assessment of neural respiratory theory in patients with severe acute respiratory failure. *Respiration* 67, 434–439.

Riquelme, L., Vigano, A., Bialak, E., Roeder, J., Sothmann, T., Latzer, P., 2006. Patient-ventilator interaction. *Intensive Care Medicine* 11, 265–271.

Roon, C.S., Ward, S.A., 1985. A device to provide respiratory-mechanical unloading. *Chest* 87, 494–498.

Roon, C.S., Ward, S.A., Whinn, B.L., 1987. Influence of inspiratory assistance on ventilatory control during moderate exercise. *Journal of Applied Physiology* 62, 1571–1580.

Roon, C.S., Goss, S., Meach, L., Martin, S., Pace, T., Brena, A., Giddell, R., 1997. Effects of proportional assist ventilation on respiratory muscle effort in patients with chronic obstructive pulmonary disease and acute respiratory failure. *Am. J. Respir. Crit. Care Med.* 155, 1495–1501.

Rooze, H., Lardinois, A., Ferrer, V., Germain, A., Donnic, A., Comte, F., Janet, C., Ouattara, A., 2011. Daily titration of neurally adjusted ventilatory assist using the diaphragmatic electromyography. *Critical Care Medicine* 37, 1087–1094.

Schmid, M., 2007. *Neurally Adjusted Ventilatory Assist: A New Approach to Respiratory and Intra-arterial Pressure Support*. *Critical Care Medicine* 35, 151–158.

Schmid, M., 2007. *Neurally Adjusted Ventilatory Assist: A New Approach to Respiratory and Intra-arterial Pressure Support*. *Critical Care Medicine* 35, 151–158.

Schmid, M., 2007. *Neurally Adjusted Ventilatory Assist: A New Approach to Respiratory and Intra-arterial Pressure Support*. *Critical Care Medicine* 35, 151–158.

Sources of support

This study was supported by the Association of French Red Cross of Handicaps (ADBP).

Author contributions

NT, PC, and FI conceived the original protocol then initiated and conducted the study, PC, HM, and ML recorded the data, NT analyzed the data and drafted the manuscript, HM, PC, DP, ML, and FI helped to conduct the study and to draft the final manuscript, NT and FI participated in the coordination of the study, All authors read and approved the final manuscript.

References

Alvent, A., Dinj, P., Benett, P., Ghimbla, D., Pedini, A., Carlineni, L., 2009. On-demand, pressure–proportional neurally adjusted ventilatory assist. *Journal of Intensive Care Medicine* 24, 1546–1552.

Schmid, M., Spinelli, A., Peber, R., Arnold, J., Sironi, S., Mosler, P., 2011. Spontaneous breathing during pressure support ventilation in critically ill patients. *Critical Care Medicine* 39, 2039–2045.

Sheeh, S.A., Walter, J., Murphy, K., Gao, A., 1987. Evidence for individuality of breathing patterns in patients with acute respiratory failure. *Respiration* 44, 191–196.

Sheeh, S.A., Walter, J., Murphy, K., Gao, A., 1987. Evidence for individuality of breathing patterns in patients with acute respiratory failure. *Respiration* 44, 191–196.

Sledge, A.S., 2007. Intra-arterial pressure support in neurally adjusted ventilatory assist. *Respiration* 74, 248–255.

Sledge, A.S., Bencherif, G., Beck, J., Sledge, Y., Commons, N., Kiberg, S., Gerweil, W., Linderholm, L., 1996. Neural control of mechanical ventilation in respiratory failure. *Respiration* 63, 1424–1428.

Sledge, A.S., Bencherif, G., Beck, J., Sledge, Y., Commons, N., Kiberg, S., Gerweil, W., Linderholm, L., 1996. Neural control of mechanical ventilation in respiratory failure. *Respiration* 63, 1424–1428.

Sledge, A.S., Bencherif, G., Beck, J., Sledge, Y., Commons, N., Kiberg, S., Gerweil, W., Linderholm, L., 1996. Neural control of mechanical ventilation in respiratory failure. *Respiration* 63, 1424–1428.

Sledge, A.S., Bencherif, G., Beck, J., Sledge, Y., Commons, N., Kiberg, S., Gerweil, W., Linderholm, L., 1996. Neural control of mechanical ventilation in respiratory failure. *Respiration* 63, 1424–1428.

Sledge, A.S., Bencherif, G., Beck, J., Sledge, Y., Commons, N., Kiberg, S., Gerweil, W., Linderholm, L., 1996. Neural control of mechanical ventilation in respiratory failure. *Respiration* 63, 1424–1428.

Sledge, A.S., Bencherif, G., Beck, J., Sledge, Y., Commons, N., Kiberg, S., Gerweil, W., Linderholm, L., 1996. Neural control of mechanical ventilation in respiratory failure. *Respiration* 63, 1424–1428.

Sledge, A.S., Bencherif, G., Beck, J., Sledge, Y., Commons, N., Kiberg, S., Gerweil, W., Linderholm, L., 1996. Neural control of mechanical ventilation in respiratory failure. *Respiration* 63, 1424–1428.

Sledge, A.S., Bencherif, G., Beck, J., Sledge, Y., Commons, N., Kiberg, S., Gerweil, W., Linderholm, L., 1996. Neural control of mechanical ventilation in respiratory failure. *Respiration* 63, 1424–1428.

Terzi, N., Benett, J., Gerweil, W., Bencherif, G., Bencherif, G., Bencherif, G., Bencherif, G., 1992. Proportional assist ventilation, a new approach to ventilatory support in patients with acute respiratory distress syndrome: a prospective study. *Critical Care Medicine* 20, 1830–1836.

Terzi, N., Benett, J., Gerweil, W., Bencherif, G., Bencherif, G., Bencherif, G., Bencherif, G., 1992. Proportional assist ventilation, a new approach to ventilatory support in patients with acute respiratory distress syndrome: a prospective study. *Critical Care Medicine* 20, 1830–1836.

Terzi, N., Benett, J., Gerweil, W., Bencherif, G., Bencherif, G., Bencherif, G., Bencherif, G., 1992. Proportional assist ventilation, a new approach to ventilatory support in patients with acute respiratory distress syndrome: a prospective study. *Critical Care Medicine* 20, 1830–1836.

Terzi, N., Benett, J., Gerweil, W., Bencherif, G., Bencherif, G., Bencherif, G., Bencherif, G., 1992. Proportional assist ventilation, a new approach to ventilatory support in patients with acute respiratory distress syndrome: a prospective study. *Critical Care Medicine* 20, 1830–1836.

Terzi, N., Benett, J., Gerweil, W., Bencherif, G., Bencherif, G., Bencherif, G., Bencherif, G., 1992. Proportional assist ventilation, a new approach to ventilatory support in patients with acute respiratory distress syndrome: a prospective study. *Critical Care Medicine* 20, 1830–1836.

Terzi, N., Benett, J., Gerweil, W., Bencherif, G., Bencherif, G., Bencherif, G., Bencherif, G., 1992. Proportional assist ventilation, a new approach to ventilatory support in patients with acute respiratory distress syndrome: a prospective study. *Critical Care Medicine* 20, 1830–1836.

Terzi, N., Benett, J., Gerweil, W., Bencherif, G., Bencherif, G., Bencherif, G., Bencherif, G., 1992. Proportional assist ventilation, a new approach to ventilatory support in patients with acute respiratory distress syndrome: a prospective study. *Critical Care Medicine* 20, 1830–1836.

Terzi, N., Benett, J., Gerweil, W., Bencherif, G., Bencherif, G., Bencherif, G., Bencherif, G., 1992. Proportional assist ventilation, a new approach to ventilatory support in patients with acute respiratory distress syndrome: a prospective study. *Critical Care Medicine* 20, 1830–1836.

Terzi, N., Benett, J., Gerweil, W., Bencherif, G., Bencherif, G., Bencherif, G., Bencherif, G., 1992. Proportional assist ventilation, a new approach to ventilatory support in patients with acute respiratory distress syndrome: a prospective study. *Critical Care Medicine* 20, 1830–1836.

This study was supported by the Association of French Red Cross of Handicaps (ADBP).

Author contributions

NT, PC, and FI conceived the original protocol then initiated and conducted the study, PC, HM, and ML recorded the data, NT analyzed the data and drafted the manuscript, HM, PC, DP, ML, and FI helped to conduct the study and to draft the final manuscript, NT and FI participated in the coordination of the study, All authors read and approved the final manuscript.

References

Alvent, A., Dinj, P., Benett, P., Ghimbla, D., Pedini, A., Carlineni, L., 2009. On-demand, pressure–proportional neurally adjusted ventilatory assist. *Journal of Intensive Care Medicine* 24, 1546–1552.

II.3 VARIABILITE DE LA FREQUENCE CARDIAQUE

II.3.1 Introduction

II.3.1.1 *La variabilité de la fréquence cardiaque*

La variabilité de la fréquence cardiaque (VFC) est la variabilité de la fréquence cycle par cycle cardiaque, obtenue à partir des intervalles R-R. Cette variabilité est le reflet de l'influence du système nerveux autonome (SNA) sur la fréquence cardiaque. Ainsi, la VFC reflète l'équilibre entre les influences sympathique (cardio-accélératrice) et parasympathique (cardio-inhibitrice) sur le rythme du nœud sinusal. L'analyse du spectre de la fréquence cardiaque a contribué à mieux comprendre la régulation par le système nerveux autonome, et la signification de ses différentes composantes grâce à l'administration de bloqueurs sympathique et parasympathique ([Akselrod et al, 1981](#) et [1985](#)).

Depuis, la VFC a été largement utilisée comme un indicateur du niveau du SNA dans certains états physiologiques: stress, fatigue (travail, sport) ou pathologiques comme l'hypertension artérielle, le diabète, le syndrome d'apnée du sommeil, etc. Elle est également utilisée comme indicateur du niveau d'analgésie ([Pomfrett et al, 1993](#)) ou de la douleur.

II.3.1.2 *L'arythmie sinusale d'origine respiratoire*

L'arythmie Sinusale d'origine Respiratoire (ASR) représente les variations du rythme cardiaque au cours du cycle respiratoire. L'ASR est la variabilité du rythme cardiaque en synchronisation avec le rythme respiratoire, et contribue en partie à la VCF (Cf analyse spectrale II.3.1.3). L'interaction entre rythme cardiaque et respiration a été constatée en [1847 \(Ludwig\)](#). Ce n'est cependant qu'au début du 20^{ème} siècle que le phénomène est analysé plus précisément ([Anrep et al, 1936](#); [Heymans, 1929](#)): pendant l'inspiration, la fréquence cardiaque augmente et, pendant l'expiration, la fréquence cardiaque diminue. Ce phénomène est illustré sur la Figure 9 qui représente l'enregistrement chez un volontaire sain d'un électrocardiogramme (ECG), d'un débit ventilatoire mesuré à la bouche et de la fréquence cardiaque calculée à partir de l'ECG.

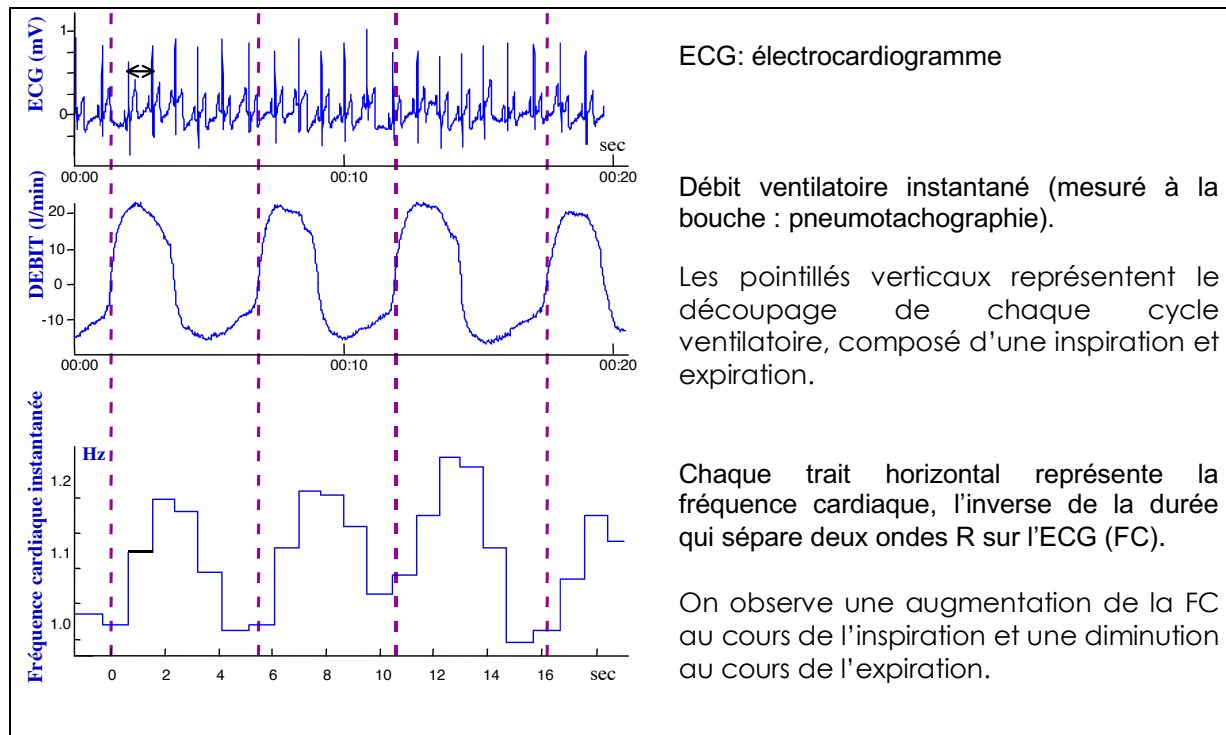


Figure 9 : Illustration du phénomène d'arythmie sinusale d'origine respiratoire

L'arythmie cardiaque d'origine respiratoire est souvent considérée comme un indicateur de l'activité vagale cardiaque. La signification physiologique de l'ASR n'a pas été complètement élucidée. On fait l'hypothèse que l'ARS optimise l'échange des gaz dans la circulation pulmonaire, améliore la relation entre la perfusion pulmonaire et la ventilation dans le cadre du cycle respiratoire.

II.3.1.3 L'analyse du spectre de la fréquence cardiaque

L'étude de VFC peut se faire par une analyse dans le domaine temporel ou dans le domaine fréquentiel. Le domaine fréquentiel est largement utilisé et consiste en l'analyse du spectre de puissance de la fréquence cardiaque ou de la période cardiaque (Figure 10). Les puissances spectrales sont mesurées dans des bandes de fréquences suivantes et ont été plus ou moins identifiées comme ayant une signification physiologique :

- *puissance totale* (total frequency power : Ptot) de 0 à 0,4Hz : reflet global de la VFC
- *ultra basses fréquences* (ultralow frequency power : ULF) de 0 et 0,0033 Hz et très basses fréquences (very low frequency power : VLF) de 0,0033 et 0,04 Hz: non encore complètement identifiées, thermorégulation, catécholamines, angiotensine II

- basses fréquences (Low Frequency power : LF) de 0,04 et 0,15 Hz : reflètent l'influence sympathique (accélération du rythme cardiaque), et à un moindre degré parasympathique (ralentissement du rythme cardiaque), modulée par les barorécepteurs
- hautes fréquences (High Frequency power : HF) de 0,15 et 0,4 Hz : correspondent à la modulation du tonus vagal normalement en lien avec la respiration (part de l'arythmie cardiaque d'origine respiratoire quand la fréquence ventilatoire est comprise dans cet intervalle de fréquence)

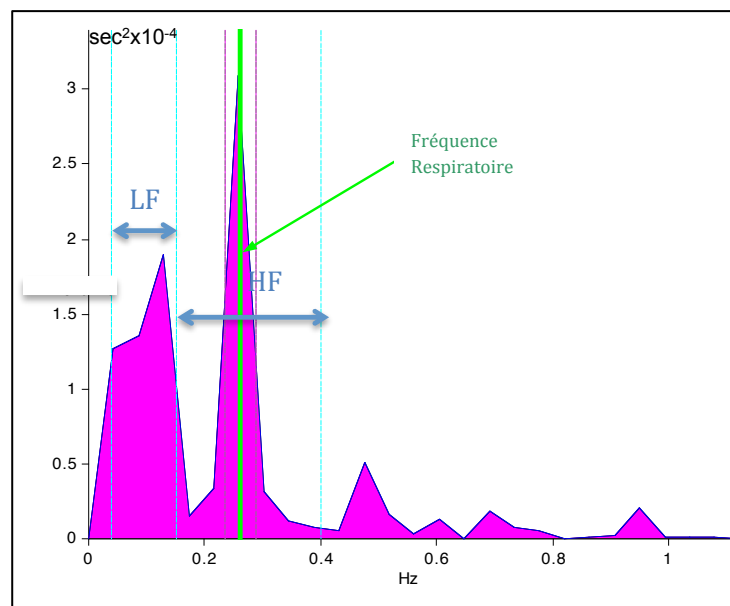


Figure 10 : Spectre de la période cardiaque avec représentation des bandes de fréquences: basses fréquences (LF) de 0,04 et 0,15 Hz et hautes fréquences (HF) de 0,15 et 0,4 Hz

II.3.2 L'arythmie sinusale d'origine respiratoire

II.3.2.1 Au cours de l'addition de résistance respiratoire

L'addition des résistances à la bouche entraîne une augmentation de la pression négative intra-thoracique et une stimulation des barorécepteurs intra-thoraciques. Nous avons étudié les changements de VFC et ASR induits par l'addition de résistances respiratoires à la bouche (stimulus du système cardio-ventilatoire) chez sept volontaires sains pour quatre niveaux de résistance additionnelle. Les résultats montrent une augmentation des caractéristiques de VFC et ASR avec la diminution de la fréquence respiratoire induite par l'addition des résistances.

Afin de préciser l'origine des variations obtenues, diminution de fréquence respiratoire ou addition de résistance, nous avons comparé les caractéristiques de VFC et ASR à deux valeurs de fréquences ventilatoires, chacune obtenue soit en additionnant une résistance, soit en imposant la fréquence. Les caractéristiques de VFC et ASR sont identiques à une fréquence ventilatoire donnée.

Ces résultats soulignent l'importance du mode ventilatoire dans les variations de la variabilité de la fréquence cardiaque (VFC) et l'arythmie sinusale d'origine respiratoire (ASR). L'utilisation des variations de VFC et ASR comme index du système nerveux autonome serait plus pertinente si les variations de la fréquence respiratoire étaient prises en considération.

Calabrese et al. (2000) Cardiorespiratory interactions during resistive load breathing. Am J Physiol-Regulatory Integrative and Comparative Physiology

Cardiorespiratory interactions during resistive load breathing

PASCALÉ GALABRESE,¹ HELENE PERRAULT,² TUAN PHAM DINH,³
ANDRÉ EBERTHARD,³ AND GIILA BENOCHET¹

¹Laboratoire de Physiologie Respiratoire Expérimentale, Théorie et Appliquée,
Université Joseph Fourier, 38700 La Tronche, France; ²Département de Physical Education,
McGill University, Montreal, H3W 1S4, and ³Laboratoire de Modélisation et Calcul,
Université Joseph Fourier, BP 533X, 38041 Cedex, Grenoble, France

Received 1 March 2000; accepted in final form 7 August 2000

Cardiorespiratory interactions during resistive load breathing. *Am J Physiol Regulatory Integrative Comp Physiol* 279: R2208–R2213, 2000.—The addition to the respiratory system of a resistive load results in breathing pattern changes that are characterized by 1) an increase in the amplitude of the cardiorespiratory interaction, and to examine the extent of the changes in heart rate variability (HRV) and respiratory sinus arrhythmia (RSA) in relation to the breathing pattern changes, HRV and RSA were studied in seven healthy subjects where four resistive loads were applied in a random order during the breath and 8-min recordings made in each condition. The HRV spectral power components were analyzed in the RSA band. The breathing pattern, the amplitude and phase were computed from the simultaneous instantaneous heart rate within each breath. Adding resistive loads resulted in 1) increasing respiratory period, 2) undulating heart rate, and 3) increasing HRV and changing RSA characteristics. HRV and RSA characteristics are linearly correlated to the respiratory period. These modifications appear to be linked to load-induced changes in the respiratory period in each individual, because HRV and RSA characteristics were not affected by the resistive load either by loading or by imposed frequency breathing. The present results are discussed with regard to the importance of the breathing cycle duration in these cardiorespiratory interactions, suggesting that these interactions may depend on the time necessary for activation and dissipation of neurotransmitters involved in RSA.

Key words: heart rate variability; respiratory sinus arrhythmia; human subject; individuality of ventilatory pattern

EVIDENCE OF THE INFLUENCE of baroreceptor stimulation on respiratory sinus arrhythmia (RSA) was documented in 1936 by Anrep et al. (2), who measured inspiratory and expiratory R-R intervals in anesthetized dogs during pressure increase produced by infusions of epinephrine. They observed that 1) at low arterial pressures there were no differences in inspira-

tory and expiratory R-R interval and no sinus arrhythmia, 2) at higher pressures the inspiratory R-R interval remained constant, whereas the expiratory R-R interval increased and sinus arrhythmia developed, and 3) at the highest pressures similar results as in the first point were again observed. These results were taken to suggest a modulatory role of the arterial baroreflex in the generation of sinus arrhythmia. Some forty years later, Eckberg and Orsham (9) further characterized the modulatory role of arterial baroreflex in the RSA phenomenon in humans using briefly applied neck suction during both the inspiratory and expiratory phases of respiration to explore the relationship between breathing phase and the responsiveness of vagal cardiac motoneurons to baroreceptor stimulation. Results showed that moderate (30 mmHg) neck suction applied during expiration induced greater R-R interval prolongation than when applied during inspiration, indicating that vagal motoneurons become reactivated but cardiac output remains unchanged (60 mmHg) because of sustained breathing inspiration and expiration. Thus inspiration reduces the sinus node responses to moderate, but not intense, baroreflex stimulation. In agreement with observations using carotid sinus nerve stimulation in animals (7, 14, 15), these results suggest that inspiration interferes with the ability of baroreceptors to stimulate vagal motoneurons but that this influence is limited inasmuch as intense baroreceptor stimuli can overcome the inspiratory inhibition of vagal firing.

Breathing under resistive loading increases negative intrathoracic pressure, the pressure gradient across the aortic wall and aortic dimension (16), as well as the aortic baroreceptor firing (1). The addition of a resistive load can thus be considered as increasing within-respiratory cycle arterial baroreceptor stimulation (4, 18). It is well known, however, that under resistive loading, the breathing pattern is changed resulting in an increase in respiratory period and tidal volume (V_T), the

Address reprint requests and other correspondence: G. Benochet, IPR, PFR/TA, UMR CNRS 5525, Faculté de Médecine de Grenoble, Université Joseph Fourier, 38700 La Tronche, France (E-mail: galabrese@leimg.fr).

R2208

0361-6190/00 \$5.00 Copyright © 2000 the American Physiological Society

http://www.ajp-rregu.org

The costs of publication of this article were defrayed in part by the payment of page charges. This article must therefore be hereby marked "advertisement" in accordance with 18 U.S.C. Section 1734 solely to indicate this fact.

CARDIORESPIRATORY INTERACTIONS IN RESISTIVE LOAD BREATHING

R2209

magnitude of these depending on the load (6, 19). The influence of the respiratory pattern on heart rate variability (HRV) and RSA has been clearly demonstrated in the study of Galabrese et al. (10). The changes in HRV and RSA during the respiratory period and V_T (11), and in marked influence of the breathing parameters on both the low-frequency and respiratory frequency components of the R-R power spectra has been reported (5). On the other hand, load-compensating mechanisms exhibit a great interindividual variability (3, 6) as do other factors producing changes in RSA (11). To take account of these potentially interacting parameters, fixed-phase resistive breathing was used (4) where no within- or between-individual variations in breathing pattern were allowed in response to the addition of loads, and it was concluded that the absolute magnitude of RSA was increased by breathing against resistances, whereas the extent of transfer through the arterial baroreflex was reduced. It is therefore possible that factors other than the arterial baroreflex made an important contribution to the modification of the RSA response under resistive breathing.

The hypothesis in this study was that the changes in HRV induced by the resistive loading may be explained by the negative intrathoracic pressure and/or by the changes in the breathing pattern. This may be tested by adding resistive loads to induce changes in HRV and in breathing pattern. If the changes in HRV appear to parallel the changes in the breathing pattern, the role of the breathing pattern may be evaluated by comparing HRV at a given breathing rate, obtained either by resistive loading or by frequency-imposed breathing. This was done in the present study by comparing the breathing pattern induced by HRV, load by breathing factors by using both spectral and breath-by-breath R-R interval analyses to quantify the RSA changes at four different resistive loads assessed throughout the entire breathing cycle.

METHODS

Subjects. Seven healthy volunteers recruited from among the laboratory staff and graduate students (means \pm SD height: 168.4 \pm 11.0 cm, weight: 65.9 \pm 13.0 kg) between 19 and 59 yr of age (mean 31.7 \pm 15.0 yr) participated in the present study. All subjects gave their informed consent. The experimental protocol was examined and approved by the Institutional Ethics Review Board.

Experimental protocol. Subjects were comfortably seated and wore a face mask on which was mounted a flowmeter (fresh head no. 1) and a differential pressure transducer (163PFO1D36, Micro Switch). Mouth pressure was measured with another differential pressure transducer (142PFO1D1, Micro Switch) inserted in the mouth. The subjects were asked to breathe using an infrared CO₂ analyzer (Datascan Elite/Elizir/MC). End-tidal CO₂ (PETCO₂) was measured continuously using the same apparatus, and an electrocardiographic trace (ECG) was obtained for the whole recording period.

A series of 8-min recordings were obtained, with no resistive load (R_0) or in the presence of one of four levels of resistive load (R_1, \dots, R_4), applied throughout the entire

breathing cycle in random order. Resistive loading was ensured by connecting a tube containing increasing thicknesses of scoring pads to the end of the face mask and flowmeter setup. The apparatus dead space including the flowmeter and resistance-applying unit remained under 40 ml. For each recording, the value of the resistance was calculated using a mouth pressure-flow plot on a breath-by-breath basis (amplitude of the pressure divided by the flow) (12). The mean resistance was 3.25 \pm 0.16 kPa (R_1), 6.24 \pm 0.20 kPa (R_2), 9.25 \pm 0.16 kPa (R_3), and 12.51 \pm 0.63 cmH₂O (R_4). Data acquisition was started within a few minutes of addition of resistance.

HRV data analysis. The acquisition of the data was performed on a Macintosh microcomputer equipped with an analog-to-digital interface card. Sampling rate was 256 Hz. The R-R interval, respiratory period (T_{RP}) and V_T and were analyzed for HRV and RSA. The data were stored and reformatted of all recordings (involving an average of 50 breaths/recording). The ECG signal was processed, and the R-R interval series were extracted and displayed on the computer screen to verify that the signal exhibited no noticeable trend and to show possible errors. Means \pm SD of the R-R intervals were calculated for each recording. R-R intervals were interpolated linearly at 0.25-s intervals to obtain equidistant time series of R-R intervals. The frequency power spectrum was recorded (length of at least 1,024 sample data points). A fast Fourier Transform procedure was applied to obtain the low (LF: 0.04–0.15 Hz) and high-frequency (HF: 0.15–0.40 Hz) spectral power components. For each recording, a restricted respiratory frequency power component identified as the respiratory centered frequency (RCFP) component was also calculated, using the frequency range corresponding to 210% of the respiratory rate averaged over the entire recording (17).

A more specific analysis of RSA was performed using a breath-by-breath HRV analysis (17). To quantify the extent of within-respiratory cycle RSA, a sinusoid is calculated, fitting to the changes in instantaneous heart rate within the respiratory cycle (Fig. 1). Its amplitude, which may be considered as the maximum heart rate within each breath, is expressed as a percentage of the maximum heart rate. The percentage of this maximum is expressed either as a fraction of breath duration, (phase) or in seconds (delay). Average amplitude, phase, and delay values over several breaths are then calculated for each recording.

Statistical analysis. Values are expressed as means \pm SD. Mean comparison of R-R interval, respiratory period, and R-R interval spectral frequency components in response to the four resistive loads was performed using a one-way ANOVA. The coefficient of variation of R-R interval and respiratory period were compared using Kruskal-Wallis test.

RESULTS

Effect of respiratory resistive loading on HRV and RSA. Applying resistive loads throughout the entire breath results in lengthening of respiratory period and increases in V_T with, however, no noticeable changes in PETCO₂. Table 1 shows mean values and mean coefficients of variation of both T_{RP} and R-R interval calculated over the seven subjects. The mean respiratory period can be seen to increase with increasing load while variability remains unchanged. In contrast, the mean R-R interval remains unchanged with increasing load, whereas the variability observed at the highest

Downloaded from ajp-rregu.physiology.org on February 24, 2012

Downloaded from ajp-rregu.physiology.org on February 24, 2012

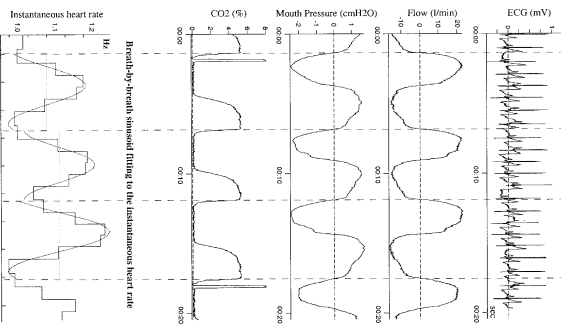


Fig. 1. Example of breathing with a resistive load of 5.48 cmH₂O⁻¹s and the sinusoid fitted to breath-by-breath changes in instantaneous heart rate, ECG, electrocardiogram.

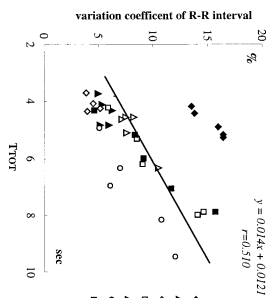


Fig. 2. Coefficient of variation of R-R interval versus respiratory period (T^{TOT}) for all 7 subjects for no resistive load and the four levels of resistive loads.

However, the increase in LF compared with that in HF at R_2 and R_3 may be explained by the low corresponding breathing frequencies that are in the LF rather than the HF domain. At low breathing rates (≤ 0.15 Hz), the changes in the RCF spectral component are a better reflection of changes in respiratory-related R-R variability than those in the HF component.

Figure 2 represents HRV expressed as the coefficient of variation of R-R interval plotted versus T^{TOT} for all loads in all subjects. The coefficient of linear correlation calculated over these data is significantly different from zero ($r = 0.510$, $P < 0.01$).

RSA amplitude, phase, and delay versus T^{TOT} for all subjects and for the five conditions are represented in Fig. 3. Each point is a mean value for each recording of amplitude, phase, and delay calculated from the sinusoid fitted to the changes in the instantaneous heart rate within each breath. Both amplitude ($r = 0.479$, $P < 0.01$) and phase ($r = -0.705$, $P < 0.0001$) are linearly correlated to T^{TOT} , and therefore the delay- T^{TOT} regression is quadratic ($r = 0.695$, $P < 0.0001$). It may be noted that according to this parabolic fit, the maximum value of the delay is reached for a T^{TOT} of 7.52 s.

Table 1. HRV during resistive loading: respiratory period, R-R interval, and spectral analysis of R-R interval series

	T^{TOT} , s		R-R interval, s		Total Power, 10^{-6} s ²	Spectral Components, 10^{-6} s ²		
	Mean	Mean variation coefficient	Mean	Mean variation coefficient		LF	HF	RF
R_0	4.26	0.10	0.844	0.06	1.70 ± 2.04	0.38 ± 0.38	0.87 ± 1.45	0.22 ± 0.86
R_1	5.29	0.12	0.847	0.08	2.22 ± 3.18	0.25 ± 0.88	1.06 ± 1.56	0.91 ± 1.56
R_2	6.89	0.11	0.845	0.10	4.16 ± 3.35	1.89 ± 1.96	1.86 ± 2.72	1.48 ± 1.85
R_3	6.88	0.12	0.846	0.13	5.82 ± 3.03	3.15 ± 2.32	1.85 ± 2.14	2.58 ± 1.38
P values	<0.001	0.994	0.653	0.044	<0.001	<0.001	0.622	<0.001

R_0 : control; R_1 , R_2 , R_3 : increasing resistive loads; T^{TOT} : respiratory period; Total power, total power of the R-R interval series spectrum; LF: low-frequency component (0.04–0.15 Hz); HF: high-frequency component (0.15–0.40 Hz); RF: respiratory-related frequency spectrum; LF power, HF power, HF variability, P values are the results of an ANOVA performed on each variable except for mean and standard deviation, which were compared by using a Kruskal-Wallis nonparametric test because they are not normally distributed.

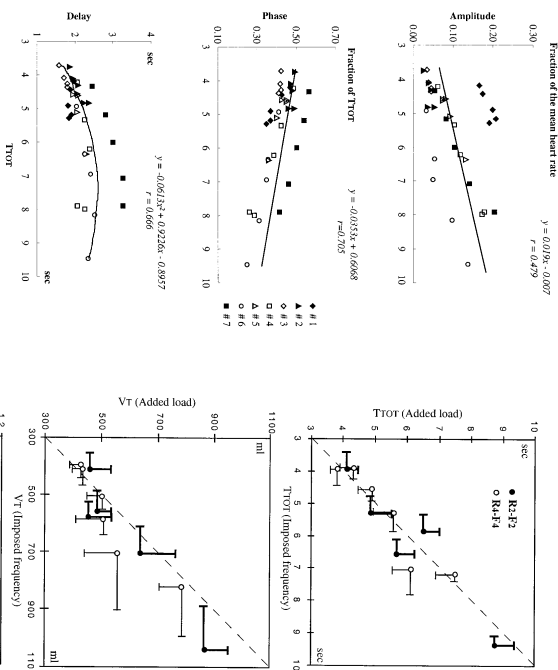


Fig. 3. Amplitude (top), phase (middle), and delay (bottom) versus T^{TOT} plotted for all 7 subjects. Amplitude, phase, and delay are calculated breath by breath from the sinusoid fitted to the instantaneous heart rate. The amplitude is expressed as a fraction of mean heart rate, phase as a fraction of T^{TOT} , and delay in seconds.

Comparison of HRV and RSA for a given breathing rate with and without resistive loading. To examine whether changes in HRV and RSA during loaded breathing can be attributed to the accompanying fall in breathing frequency, further recordings were performed on another group of participants. The first of two sets of 8-min airflow and ECG recordings was obtained with a breathing resistance, whereas the second was obtained with the subject breathing at an imposed rate namely fixed at a frequency equivalent to that observed during the loaded breathing condition. Two levels of resistance were applied: $R_2 = 4.95$ and $R_4 = 12.23$ cmH₂O⁻¹s. The corresponding imposed respiratory rates were provided by an auditory cue during the individual breathing conditions. The ECGs were checked and first heart rate was given to increase or decrease T^{TOT} such that the T^{TOT} was 1 second constant. Means ± SD of T^{TOT} , R-R interval, and VT

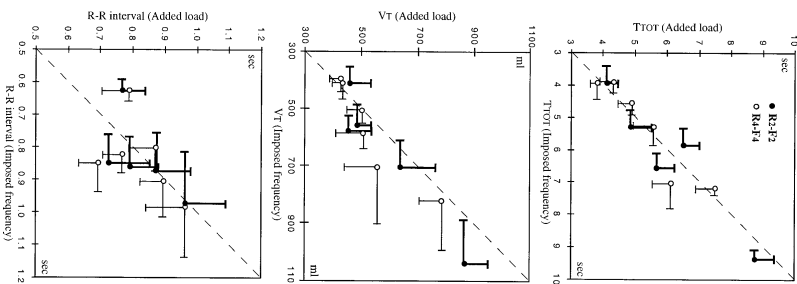


Fig. 4. Mean ± SD of R-R interval (bottom), tidal volume (V_T , middle), and T^{TOT} (top) at resistive load (R_2 and R_4) on x-axis and corresponding imposed frequency (F_2 and F_4) on y-axis. Identity lines are drawn for each graph. Comparison between loaded and imposed breathing frequency conditions were achieved by using paired t test ($P = 0.895$ for R_2 , $P = 0.468$ for R_4 , and V_T , $P = 0.217$ for T^{TOT}).

obtained for resistive loading R_2 and R_3 and the equivalent imposed breathing frequencies f_2 and f_3 are shown in Fig. 4 for each subject. Residual pressure P_{res} is compared with the pressure difference as defined in the text. Table 2 shows results of the spectral and breath-by-breath HRV analysis performed on these data. Comparisons revealed no significant differences either in any of the HRV spectral components (paired t -test) or in the amplitude or phase (paired Wilcoxon-test).

DISCUSSION

Results of the present study show that adding resistive loads throughout the entire breathing cycle resulted in an increase in HRV and RSA with the mean R-R interval remaining unchanged.

The increase in HRV and RSA appears to be linearly correlated to the increase in respiratory period in response to resistive loading. An important additional observation here is that there were no significant differences between HRV and RSA for a given subject breathing at an equivalent frequency obtained by resistive loading or imposed breathing frequency.

The observed increase in RSA could probably be accounted for by either increases in intrathoracic pressure and the ensuing stimulation of baroreceptors or changes in the respiratory pattern following resistive loading. Changes in intrathoracic pressure can produce both oscillations in arterial blood pressure, which are sensed by carotid sinus and aortic baroreceptors, and fluctuations in cardiac filling sensed by cardiac baroreceptors. Indeed, by using graded levels of phenylephrine and nitroglyceride infusions in human subjects to respectively increase and decrease arterial pressure (10), RSA was found to be slight at low levels of baroreceptor stimulation but to increase asymptotically with higher levels.

According to Seals et al. (18), adding a resistive load to the respiratory part of the respiratory cycle would $\sim 1/3$ greatly increase the heart rate during the entire cycle. Such changes are likely given that volume during voluntary inspiration, producing a significant decrease in systemic arterial pressure and (2) markedly increase central respiratory motor output. These authors observed that the major effect of applying increased in-

spiratory resistance (of 20 cmH₂O⁻¹s⁻¹) was to cause the arterial blood pressure to fall significantly during early inspiration. In our experiments, resistive loads were added throughout the entire cycle leading to a decrease in mean arterial pressure which reached the level of about 6 cmH₂O for the highest added resistance R_3 (12.51 cmH₂O⁻¹s⁻¹), compared with under 1 cmH₂O for R_1 (0.76 cmH₂O⁻¹s⁻¹). It may be argued that, in the present study, the resistive load applied was insufficient to alter baroreceptor input to cardiac motoneurons, because a similar RSA amplitude (as well as HF and RCP power components) was observed for both loaded and nonloaded breathing at an equivalent breathing frequency. An alternative explanation might, in agreement with other findings (4), be that the marked within-respiratory cycle arterial blood pressure oscillations are not the predominant factor involved in the changes in RSA. There is strong evidence (8) that respiration modulates autonomic outflow by interfering with the ability of baroreceptor inputs to influence the activity of autonomic motoneurons. It has been reported that the effect of lung inflation itself can suppress or mask baroreceptor influences in the intact human (10, 18). Changes in sympathetic and/or vagal outflow during quiet breathing may thus be due to respiration itself rather than to arterial pressure changes accompanying respiration.

Changes in respiratory pattern are well known to influence RSA. Whereas the average R-R interval remains unchanged over a wide range of breathing frequencies, an increase in RSA is observed with increasing respiratory period and/or V_T (9, 13) even where these latter increases are passive (11). In agreement with these previous observations our results show that HRV and RSA increase with the longer respiratory period induced by resistive loading, whereas the mean R-R interval (data not shown) remains unchanged (Table 1). The use of f_{TOT} by the subject for each factor had a significant influence on the results for spectral and amplitude influences to be dispensed, resulting in a lower residual vagal tone and thus a greater heart rate response, hence leading to an unchanged mean R-R interval associated with a shorter T_{TOT} (the effects of cholinergic

other hand, with shorter T_{TOT} the effects of cholinergic

Table 2. Spectral and breath-by-breath analysis of HRV and RSA at given breathing rates with and without resistive loading

	Total Power, 10^{-6}		Spectral Components, 10^{-6}		Amplitude	Phase
	LF	HF	RCP	HRV		
R_1	2.94 ± 1.37	0.95 ± 0.68	1.06 ± 0.57	0.71 ± 0.37	0.09 ± 0.02	0.44 ± 0.02
R_2	3.90 ± 2.71	0.78 ± 0.66	1.30 ± 0.99	0.88 ± 0.53	0.10 ± 0.02	0.46 ± 0.05
R_3	4.57 ± 3.19	1.82 ± 0.53	1.75 ± 0.62	1.76 ± 0.37	0.13 ± 0.02	0.40 ± 0.05
F_1	4.67 ± 3.08	0.96 ± 0.73	2.37 ± 1.72	1.99 ± 1.78	0.12 ± 0.03	0.42 ± 0.09
P	0.814	0.186	0.485	0.893	0.026	0.225

R_1 , R_2 , and R_3 are the added loads and F_1 , and F_2 are the corresponding imposed respiratory rates. Mean values were calculated over 6 subjects for R_1 , F_1 , and 5 subjects for R_2 , F_2 . Amplitude and Phase are expressed, respectively, as a fraction of mean heart rate for each breath and a fraction of respiratory cycle duration. Comparisons between loaded and imposed breathing frequency conditions were achieved by using paired t -test for R-R interval, respiratory period, tidal volume, and R-R interval spectral frequency components and by paired Wilcoxon test for amplitude and phase. No significant difference was found between the 2 conditions for any variable.

influences released during expiration may persist, limiting the extent of the residual vagal release and ensuing increase in R-R heart rate. Reading again to an unchanged HRV and RSA.

In conclusion, this study on the effect of resistive load breathing on cardiorespiratory interactions shows that these interactions and particularly the changes in RSA are strongly dependent on the changes in the breathing pattern resulting from ventilatory load-compensatory mechanisms.

Perspectives

Fluctuations of R-R intervals or heart rates are used widely as indices of the level of autonomic traffic to the heart. If these fluctuations are to be taken as valid noninvasive indexes of autonomic neural traffic, they then should reflect such traffic faithfully and should not be influenced importantly by respiratory and autonomic interactions unrelated to net neural outflow. Given the major influence of breathing pattern on HRV, one possible strategy may be to quantify the effect of breathing pattern changes and possibly to "subtract" this effect.

In our study, there was a linear relationship between HRV and T_{TOT} and also between RSA characteristics and T_{TOT} . On the other hand, there were no significant differences in HRV and RSA characteristics between control and loaded conditions at the same breathing frequency. These results are also in favor of the important influence of the breathing pattern in HRV. They also suggest that an individual or a generic HRV- T_{TOT} or RSA characteristic- T_{TOT} may be established, which can be used as an estimation of the T_{TOT} effect. Changes in T_{TOT} may be obtained either by imposed breathing frequency, or by resistive loading, which involves ventilatory compensating mechanisms.

We gratefully acknowledge the technical assistance of Angélique Brown.

REFERENCES

1. Angel-James JE. The effects of changes in extrathoracic, intrathoracic, pressure on aortic arch baroreceptors. *J Physiol (Lond)* 218: 89-100, 1971.

2. Arroyo CV, Poonan W, and Roubin R. Respiratory variations of the heart rate. I. The reflex modulation of respiratory variability. *Proc Roy Soc (Lond Ser B)* 119: 299, 1936.
3. Axon K, Spitzer Haus S, Haus P, Gaudino D, and Haus A. Ventilatory adjustments during sustained mechanical loading in man. *J Appl Physiol* 75: 2310-2317, 1983.
4. Blauer AP and Hargison HL. Cardiorespiratory interactions during fixed-resistive breathing. *J Appl Physiol* 80: 1818-1826, 1986.
5. Brown TG, Heighway LA, Koh J, and Eschberg DL. Important role of the respiratory system in the control of heart rate. Largely ignored. *J Appl Physiol* 75: 2310-2317, 1983.
6. Calabrese P, Pines D, Eberhard A, Pardy JP, and Bonaventura G. Effects of resistive loading on the pattern of central inspiration. *Respiratory Physiology and Biomechanics*. In: *Peripheral Arterial Chemoreceptors and Respiratory-Cardiovascular Integration*. Oxford: Clarendon, 1987, p. 244-268.
7. Dohy D, and Pines D. Respiratory sinus arrhythmia and other human cardiovascular neural periodicities. In: *Regulation of Breathing* (2nd ed.), edited by Dempsey JA and Pack AI. New York: Dekker, 1995, p. 669-740.
8. Eschberg DL, and Oshin CR. Respiratory and baroreceptor interactions in man. *Acta Physiol Scand* 133: 221-231, 1985.
9. Eschberg DL, Rea RF, and Anderson OK. Baroreflex modulation of sympathetic activity and sympathetic neurotransmitters in humans. *Acta Physiol Scand* 133: 221-231, 1985.
10. Grossman P, and Kohn M. Respiratory sinus arrhythmia: causal relations. *Psychophysiology* 30: 488-495, 1989.
11. Hargison HL, and Pines D. Respiratory sinus arrhythmia: modulation of respiratory sinus arrhythmia by breathing pattern. *Psychophysiology* 30: 488-495, 1989.
12. Hargison HL, Pines D, and Pines D. Respiratory sinus arrhythmia in humans: how breathing pattern modulates heart rate. *Am J Physiol Heart Circ Physiol* 241: H620-H629, 1981.
13. Hirsch JA, and Bishop B. Respiratory sinus arrhythmia in humans: how breathing pattern modulates heart rate. *Am J Physiol Heart Circ Physiol* 241: H620-H629, 1981.
14. Koopman HP, Lux HD, and Wagner PA. Untersuchungen zur Atemregulation bei der Nervenstimulation. *Zentralblatt für Bakteriologie, Supplementum* 1981, p. 133-134.
15. Koopman HP, Wagner PA, and Lux HD. Über die Zusammenhänge zwischen zentraler Erregbarkeit, reflektorischem Tonus und Atemrhythmus bei der Nervenstimulation. *Zentralblatt für Bakteriologie, Supplementum* 1981, p. 133-134.
16. Peters J, Kindred MK, and Bobbiano JJ. Transient analysis of cardiopulmonary interactions. I. Diastolic events. *J Appl Physiol* 64: 1506-1517, 1988.
17. Pines D, and Pines D. Cardiorespiratory interactions in humans: how breathing pattern modulates heart rate. *Am J Physiol Heart Circ Physiol* 241: H620-H629, 1981.
18. Seals DR, Swartzon O, Joyner MJ, Ivers C, Copeland JC, and Pines D. The effects of resistive loading on the respiratory system in humans: how breathing pattern modulates heart rate. *Am J Physiol Heart Circ Physiol* 241: H620-H629, 1981.
19. Zoccolman FW, Haddi FG, and Hall WE. Effects of graded resistive loads on tracheal airflow in man. *J Appl Physiol* 10: 386-392, 1957.

II.3.2.2 Au cours de différentes fréquences ventilatoires imposées

Il a été observé des différences inter-individuelles non seulement sur les caractéristiques de ASR mais aussi sur l'amplitude de leurs variations. Afin de préciser le rôle de la fréquence ventilatoire spontanée (individualité ventilatoire) dans ces variations de ASR, nous avons étudiées chez 12 volontaires sains les caractéristiques de ASR lors de ventilation à fréquence imposée. Les valeurs de fréquences imposées étaient de part et d'autre de celle de la fréquence spontanée (FR_s) de chaque individu (FR_s -6, FR_s -3, FR_s +3, FR_s +6 cycles/min). Les résultats montrent que plus la fréquence ventilatoire spontanée est basse, moins l'amplitude de ASR augmente avec la diminution de la fréquence ventilatoire imposée.

Les variations des caractéristiques de l'arythmie sinusale d'origine respiratoire induites par les changements de fréquence ventilatoire peuvent partiellement être expliquées par la fréquence ventilatoire spontanée de chaque individu.

Ben Lamine et al. (2004) Individual differences in respiratory sinus arrhythmia. Am J Physiol-Heart and Circulatory Physiology

Nous avons aussi recherché si la diminution de la fréquence cardiaque de repos consécutive à l'entraînement était due à une diminution du tonus vagal. Chez 20 athlètes et 12 sujets témoins appariés en âge, l'ECG, la respiration et la pression artérielle ont été enregistrés à la fréquence ventilatoire spontanée ainsi qu'aux fréquences ventilatoire spontanées \pm 4 cycles par minute. Les caractéristiques de VFC et ASR ont été analysées. Les résultats montrent que seule la fréquence cardiaque de repos est significativement plus basse chez les athlètes.

Ces résultats suggèrent que le tonus vagal objectivé par l'arythmie sinusale d'origine respiratoire n'est pas modifié par l'entraînement.

Scott et al (2004) Enhanced cardiac vagal efferent activity does not explain training-induced bradycardia. Auton Neurosc : Basic and Clinical

Individual differences in respiratory sinus arrhythmia

Santa Ben Lamine,¹ Pascale Calabrese,¹ Hélène Perrault,²
Tuan Phan Dinh,³ André Eberhard,² and Gila Bendavid^{1*}

¹Laboratoire de Physiologie Respiratoire Expérimentale, Théorique et Appliquée, Université Joseph Fourier, 38700
La Tronche, France; ²Département de Physiologie Humaine, McGill University, Montreal, Quebec, Canada H3W 1S6; and
³Laboratoire de Modélisation et Calcul, Université Joseph Fourier, 58041 Grenoble, France

Submitted 10 July 2003; accepted in final form 26 January 2004

In addition to this "multidimensional" aspect to parasympathetic cardiac control, the between-individual differences in RSA increase the difficulty of RSA interpretation. In the latest committee report on heart rate (HR) variability (HRV), method, and interpretation (3), this between-individual aspect is mentioned several times leading to the conclusion that "caution needs to be exercised in interpreting RSA, especially for between-subject comparisons." For example, the relationship between RSA amplitude and pharmacologically defined vagal tone when investigated for a number of subjects appears to be less close than that found within a given subject (15, 20). The increase in RSA amplitude with increasing breathing period also varies among individuals (4, 17).

Given the importance of the respiratory modulation of human autonomic rhythms and the propensity of breathing in generating respiratory frequency rhythms (1), the incidence of these spontaneous breathing rate is worth clarifying because there exists an individuality of the breathing pattern (2, 11). In fact, the breathing period in a normal physiological condition is 11.2–16 s. We designed an experimental breathing period analysis. To quantify RSA, we used a breath-by-breath analysis where a sinusoid is fitted to the instantaneous HR for each breath (23). The amplitude and the phase (or delay) of this sinusoid constitute the characteristics of RSA for that breath, and mean values are calculated for each breathing period. We thus quantified RSA in healthy subjects at various breathing rates.

Our hypothesis was that the rate of increase in RSA amplitude with respiratory period might be similar in all subjects, provided a comparable range of breathing rates is examined. We defined this comparable range by starting from the individual spontaneous respiratory frequency of each subject and by choosing breathing rates surrounding this spontaneous breathing rate. Our results show that, even under these conditions, a difference in the rate of increase in RSA amplitude with the breathing period existed between individuals. Similarly, difference between individuals was found in the parameters of the parabola fitted to the delay-breathing period relationship. However, these differences (the rate of increase in RSA on one hand and the curvature of RSA on the other hand) were correlated with the spontaneous breathing period and not with the mean R-R interval.

These results suggest that in all individuals there are changes in RSA characteristics with total respiratory period (TRTP), but there are differences between individuals in the features of

INDIVIDUALITY OF RESPIRATORY SINUS ARRHYTHMIA

these changes. These differences appear to be related to the spontaneous breathing period of the subjects. In addition, this protocol gives the possibility of performing a transfer function analysis of the RSA control system (22). Indeed, the pole of the normalized RSA (amplitude of RSA) had a volume (V_T) versus TRTP provides the gain of the system at each TRTP for each individual.

METHODS

Twelve healthy volunteers between 18 and 28 yr of age, seven of whom were men, participated in the study (means \pm SD: height, 173.5 \pm 7.8 cm; weight, 64.7 \pm 10.4 kg; age, mean 22.9 \pm 3.1 yr). Informed consent was obtained from all subjects. The experimental protocol was examined and approved by the Institutional Ethics Review Board.

Experimental Protocol

Subjects were comfortably seated and wore a face mask on which a flowmeter (Fresh head no. 1) and a differential pressure transducer (63P001D)56, Micro Switch) were mounted. Leaks from around the mask were checked for before the recording was initiated using an infrared CO₂ analyzer (Engstrom Elizabeth MC). End-tidal CO₂ (P_{ET}-CO₂) was measured continuously using the same apparatus, and an electrocardiographic trace (ECG) was obtained covering the whole of the recording period. For each subject, six series of 5–10 spontaneous breathing and the following five with randomly sorted sequences: at an imposed frequency fixed at the mean spontaneous respiratory frequency and at the mean spontaneous respiratory frequency \pm 3 and \pm 6 and \pm 3 and \pm 6 breaths/min. For subject with a low spontaneous respiratory frequency, the \pm 3 and \pm 6 breaths/min recordings were replaced by \pm 2 and \pm 4 breaths/min. The highest breathing rate observed among our subjects was 17 breaths/min, so that the highest breathing rate was 19 breaths/min. The lowest breathing rate observed was 7 breaths/min, whereas the lowest breathing rate observed was 7 breaths/min with recordings accordingly performed at 3, 5, 7, 9, and 11 breaths/min.

To impose the breathing rate, an auditory cue was used, which signaled only for the inspiration to begin. Hence, the inspiratory I_{to}-expiration time ratio, as well as the V_T was chosen by the subject. However, if P_{ET}-CO₂ departed more than 20–40% from the target, the subject was asked to breathe at a different rate. In fact, in most cases, during imposed frequency breathing, subjects are inclined to hypoventilate and thus before the recording was started, they were asked to decrease the V_T.

Data Acquisition

The acquisition of the data was carried out on a Macintosh microcomputer equipped with an analog-digital interface card. The sampling rate was 256 Hz. To calculate TRTP and V_T, and to study HRV and RSA, a breath-by-breath analysis of all recordings was performed. The ECG signal was processed, and the R-R interval series were identified. The V_T was calculated from the tidal volume signal obtained on a nonrecording trial and to show, in possible error, means and SD of the R-R intervals were calculated for each recording. R-R intervals were interpreted linearly at 0.25-s intervals to obtain equidistant time samples, and spectral analysis was performed using a recording length of at least 1,024 sample data points.

Data Analysis

A Fourier transform procedure was applied to obtain the low-frequency (LF; 0.04–0.15 Hz) and high-frequency (HF; 0.15–0.40 Hz) components. For each recording, a residual respiratory frequency component identified as the respiratory centered frequency component identified as the respiratory centered frequency component corresponding to \pm 10% of the expiration flow averaged over the entire recording (23). The power corresponding to the different frequency ranges was expressed as a percentage of the total spectral power minus that corresponding to the very LF (0–0.04 Hz).

A more specific analysis of RSA was performed using a breath-by-breath HRV analysis (23). To quantify the extent of within-respiratory cycle HRV, a sinusoid was fitted to the changes in instantaneous HRV. In parallel, the amplitude of the sinusoid, in its maximum value of the sinusoid, was expressed as a percentage of the mean cardiac frequency calculated over that breath. This maximum value is used as a measure of RSA amplitude. The time lagging between the beginning of the breath and the occurrence of this maximum value is expressed either in terms of the fraction of breath duration (phase) at which it occurs or in seconds (delay = phase \times TRTP). Average amplitude, phase, and delay values over several breaths were then used to calculate the mean RSA amplitude (mean breath \times average RSA amplitude) (RSA amplitude divided by the corresponding V_T) was calculated.

Statistical Analyses

Values are expressed as means \pm SD. Mean values of the various variables between spontaneous and imposed breathing at the same rate were compared using a paired *t*-test, whereas SDs were compared using a Wilcoxon paired test.

To compare HRs between different recordings for a given subject, mean R-R intervals at different imposed breathing frequencies were compared using ANOVA. Linear regressions and regression lines were calculated for each subject from amplitude against breathing period plots using all the values available for this subject (230–300 breaths). To test the hypothesis of a parallel regression line for all subjects, a linear regression line was also calculated using all the values of all subjects. The differences in slope between this common line slope and the individual slopes were calculated, and the sum of the weighted differences was computed using a χ^2 -test with 11 degrees of freedom as the number of subjects. A χ^2 -test was also used to test the hypothesis that the fit was calculated for each subject on delay vs. breathing period plots. Also, one parabolic shape was adjusted using all available values of all subjects. As in the case of the regression lines, to test the hypothesis of the existence of a common parabola, the sum of the weighted differences between the curvature parameter of the common parabolic shape and those of the individual parabolas were calculated again using a χ^2 -test.

For all tests, significance was set at $P < 0.05$.

RESULTS

The values of TRTP and R-R interval during spontaneous breathing are given in Table 1.

RSA for Spontaneous and Imposed Breathing at the Same Frequency

Figure 1 shows an example of two recordings on one subject when breathing spontaneously (left) and when breathing at an imposed frequency equal to the spontaneous breathing rate (right). Figure 1 also shows the instantaneous HR, delimited breath by breath, and the corresponding spectral analysis for the whole recording.

Comparison of the TRTP, V_T, R-R interval, and RSA analyses for spontaneous and imposed breathing at the same rate for all 12 subjects is illustrated in Figs. 2 and 3. The P values of the tests corresponding to the different variables for mean values and SD are given in the legend to the figures. In Fig. 2A

RESPIRATORY SINUS ARRHYTHMIA (RSA) is often considered to be a valid index of vagal control justified by the highly linear relationship between f vagal efferent activity and the magnitude of RSA in spontaneously breathing anesthetized dogs (18) and 2) the R-R interval and RSA amplitude during progressive childhood blockade for a given subject (19, 24). These relationships are related to the cardiac vagal outflow and to the cardiac vagal tone, respectively. RSA is also affected by other aspects of autonomic cardiac control such as the parasympathetic baroreflex (9, 11) and it has recently been shown that the cardiac sympathetic outflow may also modulate RSA (25).

*Address for reprint requests and other correspondence: G. Bendavid, Laboratoire PRTS-TMCC, Faculté de Médecine, 38700 La Tronche, France. (E-mail: gila.bendavid@univ-jf.fr).

0363-6138/04/3310-H2305\$15.00 Copyright © 2004 the American Physiological Society

H2305

Table 1. Parameters of amplitude = $f(T_{TOT})$ and delay = $f(T_{TOT})$ relationships

Subject No.	Spontaneous Breathing		Imposed Breathing		Parabola fitting Delay = $f(T_{TOT})$	
	T_{TOT} , s	R-R interval, s	Amplitude slope = $f(T_{TOT})$	Curvature	T_{TOT} , s	Delay, s
1	3.3	0.799	0.041	-0.119	5.2	1.8
2	7.4	0.818	0.013	-0.027	8.7	2.5
3	5.3	0.617	0.022	-0.036	9.1	3.2
4	6.9	0.766	0.019	-0.048	8.4	3.5
5	7.2	0.789	0.017	-0.041	8.5	3.2
6	5.6	0.823	0.010	-0.041	8.5	2.9
7	4.1	0.886	0.015	-0.037	9.7	3.0
8	3.8	0.733	0.017	-0.048	8.5	3.2
9	4.1	0.733	0.017	-0.048	8.5	3.2
10	8.3	0.829	0.007	-0.017	13.2	3.7
11	6.5	0.923	0.009	-0.034	11.6	3.5
12	4.2	0.918	0.029	-0.030	8.5	2.9

The curvature (2a) of a parabola, $ax^2 + bx + c$ is often used to characterize this parabola because it is independent of the origin. T_{TOT} , total respiratory period.

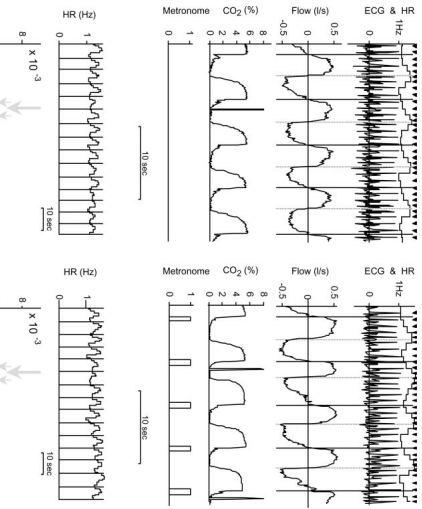


Fig. 1. Comparison of total respiratory period (T_{TOT}), spontaneous and imposed breathing at the same frequency. The plot represents mean values and SDs for imposed frequency against spontaneous breathing for all 12 subjects. The mean values and SDs went to T_{TOT} , mean values ($P = 0.947$) and SDs ($P = 0.154$) were not significantly different. For V_T , the mean value was significantly higher during imposed breathing ($P = 0.001$), whereas SDs were not different, neither the mean values ($P = 0.376$) nor the SDs ($P = 0.268$) differed significantly between the two conditions.

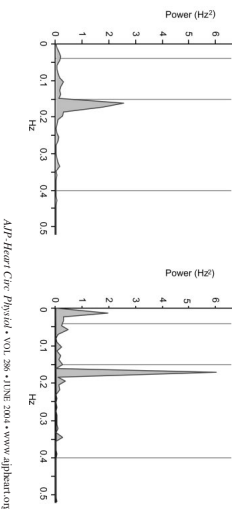
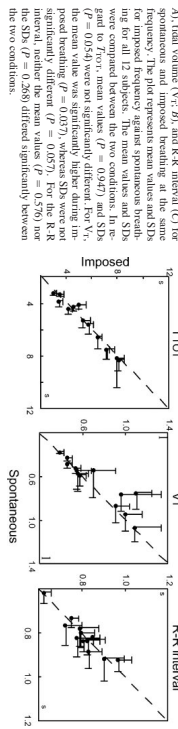


Fig. 3. Comparison of HR variability (A) power spectrum, amplitude (B) and delay (C) for spontaneous and imposed breathing at the same frequency. The mean values and SDs went to T_{TOT} , mean values ($P = 0.947$) and SDs ($P = 0.154$) were not significantly different. For V_T , the mean value was significantly higher during imposed breathing ($P = 0.001$), whereas SDs were not different, neither the mean values ($P = 0.376$) nor the SDs ($P = 0.268$) differed significantly between the two conditions.

Fig. 2. Comparison of total respiratory period (T_{TOT}), spontaneous and imposed breathing at the same frequency. The plot represents mean values and SDs for imposed frequency against spontaneous breathing for all 12 subjects. The mean values and SDs went to T_{TOT} , mean values ($P = 0.947$) and SDs ($P = 0.154$) were not significantly different. For V_T , the mean value was significantly higher during imposed breathing ($P = 0.001$), whereas SDs were not different, neither the mean values ($P = 0.376$) nor the SDs ($P = 0.268$) differed significantly between the two conditions.



is plotted the mean imposed breathing period against the spontaneous period for all subjects. Although there was no significant difference between the two conditions as to the mean value, the imposed breathing appears to be more regular, as shown by a smaller SD. The V_T (Fig. 2B) was slightly, but significantly, higher during imposed breathing with, however, no difference in SD with regard to the two conditions. Nor was any significant difference found in the T_I and T_I -to- T_{TOT} ratio with $P = 0.082$ and $P = 0.133$, respectively. Comparison of the R-R interval (Fig. 2C) with regard to the two conditions showed no difference either in mean value or SD.

The power of the spectral components of the R-R interval signal was also compared for the two conditions: there was no significant difference in either the LF ($P = 0.422$) or HF component (Fig. 3A), whereas the RCF component was significantly higher for the imposed frequency condition due to more regular breathing in this condition. R- R_{SA} amplitude and delay were also compared between the two conditions (Fig. 3, B and C), and there was no significant difference with regard to either mean values or SDs.

Spectral analysis. Figure 4 shows the RCF and HF components of all the imposed breathing frequency recordings for the 12 subjects. As expected, the HF component falls for respiratory periods longer than 0.78 s (0.13 Hz), whereas the RCF component exhibits a plateau at 80% of the total power and T_{TOT} mean is close to values of T_{TOT} of the test condition.

R- R_{SA} amplitude and delay. For each subject, the coefficient of linear correlation between R- R_{SA} amplitude and T_{TOT} was calculated on all breaths recorded for that subject. All 12 correlation coefficients differed significantly from zero, and their values ranged from 0.91 to 0.99. Individual regression lines were also calculated for each subject. These regression lines are shown in Fig. 5, and individual values of the slopes are given in Table 1. The hypothesis of a common slope applying for all subjects was then tested using a χ^2 -test. The value of the test was $\chi^2 = 698$, and thus the hypothesis was rejected ($P < 0.001$).

To investigate the relationship between these individual regression lines and the subject characteristics, individual slopes were plotted versus mean R-R interval (Fig. 6, r_{slope}) and also mean T_{TOT} (Fig. 6, l_{slope}) calculated from the recording at spontaneous breathing. It can be seen that, whereas no correlation was observed with R-R interval ($r = 0.135$, not significant), the linear correlation with spontaneous T_{TOT} was significantly different from zero ($r = 0.648$, $P < 0.03$). The slope of the latter regression line is negative, indicating that the higher the spontaneous T_{TOT} the lower the rate of increase of R- R_{SA} amplitude with respiratory period. R- R_{SA} delay. The delay increased with T_{TOT} up to a certain value and then decreased. For each subject, a parabolic fit was found. The coefficients of multiple correlation were significantly different from zero for all subjects, and their value varied from 0.93 to 0.99 among subjects. These parabolas are shown in Fig. 7. However, the parabola appeared to differ between individuals as can be seen in Table 1, where the curvature and the coordinates of the maximum of individual parabolas are shown. The curvature (2a) of a parabola ($ax^2 + bx + c$) is often used to characterize this parabola because it is independent of the origin. χ^2 -test was used to test the hypothesis of a parabola common to all subjects. The value of the test was $\chi^2 = 93.5$, $P < 0.01$, and thus the hypothesis for all the parabolas curvature was rejected. As above, we investigated the relationship between these parabolas and the individual characteristics. We plotted the curvature versus mean R-R interval (Fig. 8, r_{curve}) and mean

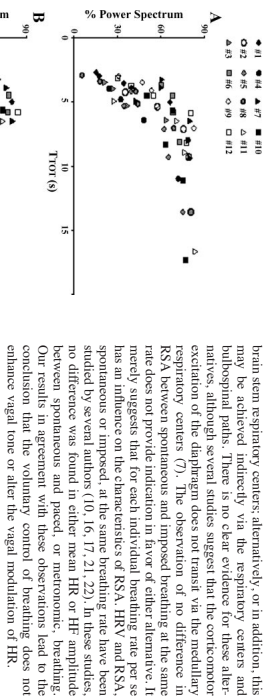


Fig. 4. The power at RCF (A) and HF (B) for all the recordings and for all subjects. The power is expressed as a percentage of the total power minus that at T10 (V12 < 0.26 Hz).

*T*_{10T} (Fig. 8, left) calculated from spontaneous breathing. Only the correlation coefficient ($r = 0.660$, $P < 0.03$) between curvature and spontaneous *T*_{10T} was significantly different from zero, indicating that greater curvature is associated with longer spontaneous *T*_{10T}.

RSA transfer function analysis. The normalized RSA amplitude (RSA amplitude-*b*-V₁ ratio) was plotted versus *T*_{10T} for each subject. Correlation coefficients were calculated for each subject. All coefficients were significantly different from zero, and individual linear regression lines were calculated (Fig. 9).

DISCUSSION

The main findings of this study were that (1) there exist differences between individuals in that RSA characteristics change with *T*_{10T} and (2) these differences may be, at least partly, explained by the differences in the spontaneous breathing period between subjects. Furthermore, interindividual differences in the HR modulation system are suggested by the results of a transfer function analysis performed on these data.

Spontaneous Versus Imposed Breathing

Before studying RSA corresponding to different imposed breathing periods, we felt that the RSA for spontaneous and imposed breathing at the same rate should be compared to ascertain that the respiratory period was the main explicative factor and thus to justify the study being carried out with imposed breathing rates.

In humans, voluntary breathing arises from a corticomedullar excitation of the diaphragm, which may act directly on the phrenic motor nucleus via the cervicothoracic tract, bypassing

brain stem respiratory centers; alternatively, or in addition, this may be achieved indirectly via the respiratory centers and bulbospinal paths. There is no clear evidence for these alternatives, although several studies suggest that the corticomedullar excitation of the diaphragm does not transit via the medullary respiratory centers (7). The observation of no difference in RSA between spontaneous and imposed breathing at the same rate does not provide indication in favor of either pathway. It merely suggests that for each individual breathing rate per se has an influence on the characteristics of RSA, HRV and RSA spontaneous or imposed, at the same breathing rate have been studied by several authors (10, 16, 17, 21, 22). In these studies, no difference was found in either mean HR or HF amplitude between spontaneous and paced, or metronomic, breathing. Our results in agreement with these observations lead to the conclusion that the voluntary control of breathing does not enhance vagal tone or alter the vagal modulation of HR.

Experimental Protocol

We chose to impose breathing frequencies starting off from the spontaneous breathing rate of each subject. This was done because of the great variability in resting breathing rate among subjects (8) and also because this breathing rate appears to be an individual characteristic (2). Thus the recordings were not performed over the same range of breathing frequency for all 12 subjects, and also the width of the frequency range varied with the individual subject. This can be seen clearly in Fig. 5, where the extremities of a regression line show the extreme values of respiratory period obtained for the subject concerned. These differences may be considered as a bias in the experimentation, but on the other hand it should be pointed out that a frequency of 12 breaths/min represents an increase in breathing rate for some subjects and a decrease for others, and this may influence the regulatory mechanisms brought into play. In this study, for each subject, starting from a breathing rate corresponding to the spontaneous rate two higher and two lower rates were imposed, thus surrounding the spontaneous rate.

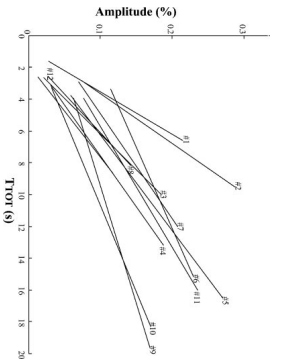


Fig. 5. Amplitude-*T*_{10T} regression lines for all subjects. The regression lines were obtained over all the breaths recorded for each subject. For each parabola, the extremities correspond to the lowest and highest values recorded for that subject.

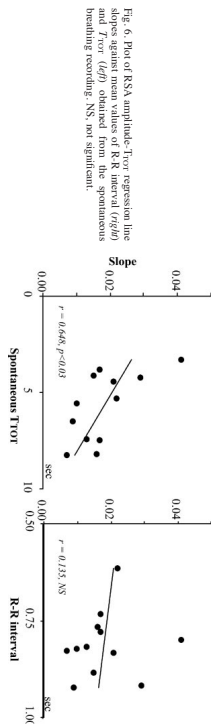


Fig. 6. Plot of RSA amplitude-*T*_{10T} regression line slopes against mean values of RR interval (left) and *T*_{10T} (left) obtained from the spontaneous breathing recording. NS, not significant.

R-R Interval, Mean Value and Spectrum for Different Breathing Period

Changing the respiratory period did not change the HR. This observation is in accordance with several authors (1, 4, 17), and, as suggested by Brown et al. (4), different within-subject breathing frequencies and depths distribute vagal firing within the respiratory cycle but do not alter the level of vagal outflow. Kollin and Mizes (20) found that the mean heart period changed in response to slow breathing and that the nature of the change (increase, decrease, or no change) varied with the individual. Differences in the experimental protocol and in the range of periods explored in each subject may explain this.

The percentages of the power spectrum occurring in the HF band and RCF bands of the instantaneous cardiac rate signal are shown in Fig. 4. It can be seen that, as expected, the power in the HF band is greater than power in the RCF band up to the period (6.7 s) corresponding to 0.15 Hz and that beyond this there is a noticeable difference between the two plots: the values of HF fall, whereas a plateau is reached for RCF, which appears to be at ~80% of the total power spectrum. It should

be noted that if the HF band is not suitable as a means of describing the power corresponding to breathing at low breathing rates, the RCF band has the disadvantage of varying in width with breathing rate.

Nevertheless, as the total surface of the power spectrum represents the variance of the analyzed signal, the percentage of the power in a given band (here, RCF) may be considered to be the variance associated with this frequency range. Thus the fact that the power in the RCF band reaches a plateau suggests that the extent of the HRV dependent on breathing rate does not exceed 80% of the total variability.

RSA Amplitude

All subjects exhibited an increase in RSA amplitude with increasing respiratory period at least in the explored range of periods. This observation is in accordance with the findings of Hirsch and Bishop (17), who estimated RSA amplitude as the difference between the fastest and highest instantaneous HRs in each subject and also those of other authors who used spectral analysis (10).

Our initial hypothesis, which was that parallel regression lines could be found, representing the RSA amplitude-versus-breathing period relationship for all subjects, was rejected by the statistical test, which indicated interindividual differences in this relationship. Similar results have been reported by Hirsch and Bishop (17), who plotted RSA amplitude versus breathing rate for each subject on a log-log scale. They found a constant RSA for low breathing rates, below 3–7 breaths/min, and then a decreasing relationship, the slope of which was expressed in decibels per decade and which defined the system roll-off. The origin of the decreasing relationship (LF intercept) varied among subjects, as did the roll-off, i.e., the slope of the log RSA-log breathing frequency plot.

In the same way as for the roll-off, the slope of RSA amplitude-breathing period relationship exhibited interindividual differences and this slope was not related to an individual's HR but correlated to their spontaneous breathing period. This slope, which represents the rate of change of RSA amplitude with *T*_{10T}, may be considered to be a measure of the responsiveness of the HR modulation mechanism to changes in respiratory period. The significant negative correlation with the spontaneous *T*_{10T} suggests that subjects with a low spontaneous breathing period (high rate) will be more responsive; i.e., their RSA amplitude will increase more with increasing period than for subjects with long breathing periods.

Downloaded from ahajournals.physiology.org on November 25, 2010

Downloaded from ahajournals.physiology.org on November 25, 2010

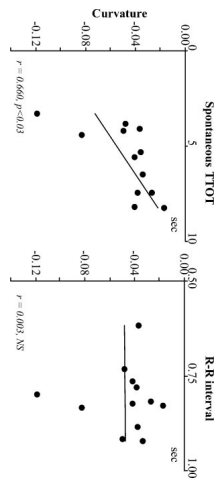


Fig. 8. Plot of curvature of the parabola against the mean values of R-R interval and T_{tot} obtained from (2). (a) of a parabola ($ax^2 + bx + c$) is often used to characterize this parabola because it is independent of the origin.

This responsiveness is somewhat different from the one defined by Kotlaj and Misztal (20). They defined an individual RSA responsiveness expressed as the ratio $\Delta HP/\Delta RSA$, where ΔHP is the change in heart period with increasing respiratory period. Because three types of ΔHP were found (individuals with increasing (A), decreasing (Z), and unchanged (AZ) ΔHP), the slope of the ΔHP -RSA plot was respectively positive, negative, or close to zero. This ratio was found to be correlated to parasympathetic control (PC), defined as the change in heart period after complete parasympathetic blockade by the administration of atropine. Although there was a continuum of distribution of subjects along the ΔHP -RSA, against-PC regression line, the A type was mainly distributed on the left-hand side of the graph (i.e., high responsiveness associated with low PC) and the Z type was mainly distributed at the right-hand end of the regression line. Kotlaj and Misztal concluded that the interindividual differences in RSA have their origin mainly in the differences in PC, although they found that introducing respiratory characteristics (T_{tot} and V7) improved the degree of RSA-PC correlation.

The delay is the time elapsing in each breath between the onset of inspiration and the reaching of the maximal value of

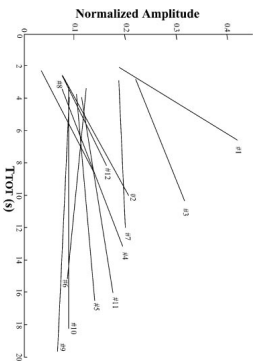


Fig. 9. Normalized amplitude T_{tot} regression lines for all subjects. The regression lines were obtained over all the breaths recorded for each subject. The extremities of each regression line correspond to the lowest and highest values recorded for that subject.

ALP Heart Circ Physiol • VOL. 286 • JUNE 2004 • www.ahpheart.org

Downloaded from ahpheart.physiology.org on November 25, 2010

is the breathing rate. Thus the breathing rate changes may be considered as an input to the HR modulation system, the output of which is RSA. As any change in the breathing rate is associated with changes in V_T to compare the gain of the HR modulation system within and between subjects, the amplitude of RSA of each breath has to be normalized, i.e., divided by its V_T .

Figure 9 shows that the change in the gain of the system varies among individuals, in some subjects (subjects 7, 9, and 10) there were little changes, in contrast to some others (subjects 1, 3, and 2). Furthermore, over a fixed respiratory period range, there are between-individual differences in the gain of the system. This indicates that these differences are not due to the size of the amount of the input but rather to the change in the gain of the system.

Thus if one subject's line is "higher" than another subject's line, intersets with another subject's line, then the former subject has greater gain over a particular range of respiratory period and lesser gain over the remaining respiratory range.

Transfer function analyses have been used in physiological (25) and pathological (13) conditions where the gain of the system was quantified and considered as being a measure of the autonomic tone.

Individuality of RSA?

These results, in addition to several other observations (4, 15, 20) on interindividual differences in RSA changes, suggest that there may exist an individuality of RSA. However, the existence of individuality implies not only differences between individuals but also reproducibility for a given subject. Little data are available on the reproducibility of RSA at a given period. Grossman et al. (14) and Grossman and Kotlaj (15) showed that behavioral tasks known to influence cardiac vagal tone produce closely corresponding within-subject changes in mean R-R interval and RSA when the respiratory parameters are controlled. The comparison of spontaneous and metronomic breathing as in this study and several other studies suggests that there was no difference in RSA amplitude between these two conditions even in head-up tilt and low body negative pressure situations, as reported by Pavloukian et al. (22). For respiratory periods other than spontaneous, the RSA amplitude corresponding to an increased respiratory period induced by the addition of resistive load was similar to the RSA amplitude for the same imposed respiratory period (5).

In conclusion, in addition to the differences in RSA between individuals, there exist interindividual differences in the RSA control system response to changes in T_{tot} (dependent on 1) the spontaneous breathing period and 2) on the strength of autonomic tone.

Therefore, these results suggest that, in addition to the influence of respiratory characteristics on the gaining of sympathetic and vagal modulations responsiveness, the individual breathing rate may play a role in the build-up of the PC of HR.

ACKNOWLEDGMENTS

The authors thank the subjects who participated in this study. We are also grateful to Peter Benczer and Abdelcheli Solhi for valuable discussion on this manuscript and to Angélique Brunot for technical assistance.

ALP Heart Circ Physiol • VOL. 286 • JUNE 2004 • www.ahpheart.org

Downloaded from ahpheart.physiology.org on November 25, 2010

REFERENCES

1. Bader L, Cooke WH, Hong JB, Grossman AA, Kanesh TA, Tamman K, and Eckberg DL. Respiratory modulation of human sinus arrhythmia. *Am J Physiol Regul Integr Physiol* 200; R2075-R2088, 2001.
2. Benditt G, Shea S, Puan Dinh T, Boudon S, Baccouer P, and Guz A. Individuality of breathing pattern in adults assessed over time. *Respir Physiol Neurobiol* 199; 210-217, 1998.
3. Benditt G, Boudon S, Puan Dinh T, Baccouer P, Guzman P, Karfman PC, Malik M, Nageppa RK, Porges SW, Sant DJ, Stone JH, and Van Der Molan MW. Heart rate variability: origins, methods and interpretive cautions. *Psychophysiology* 34; 623-648, 1997.
4. Brown TE, Bregstad LA, Koh J, and Eckberg DL. Important influence of cardiorespiratory interactions during restful breathing. *Am J Physiol Regul Integr Physiol* 299; R2208-R2213, 2005.
5. Calhoun SE, Porges SW, and Eckberg DL. Human central autonomic integration. *J Physiol* 517; 617-628, 1999.
6. Guzman P, Porges SW, and Eckberg DL. Human response to upright tilt: a window on central autonomic integration. *J Physiol* 517; 617-628, 1999.
7. Corfield DR, Murphy K, and Guz A. Does the motor control of breathing depend on the brain stem respiratory centres in man? *Respir Physiol Neurobiol* 199; 210-217, 1998.
8. Dejours P, Bouchel-Johnson Y, Monodin P, and Raymond J. Fluidic diversity des réflexes ventilatoires chez l'homme. *J Physiol* 53; 320-321, 1961.
9. Eckberg DL. Human sinus arrhythmia as an index of vagal cardiac control. *Am J Physiol* 237; H1075-H1080, 1979.
10. Eckberg DL, Neebci C, and Wadlin BV. Respiratory modulation of musc sympathetic and cardiac outflow in man. *J Physiol* 365; 181-196, 1984.
11. Eckberg DL and Oshun CB. Respiratory and baroreceptor reflexes. *J Appl Physiol* 72; 2446-2453, 1992.
12. Esclé JH, Wuyson B, Smerony G, Berrardet J, Hird JH, and Benditt G. The individuality of breathing patterns during hypoxia and exercise. *J Appl Physiol* 72; 2446-2453, 1992.
13. Brennan K, Cohen RJ, and Sant JP. Transfer function analysis of respiratory sinus arrhythmia. *Am J Physiol* 262; H1075-H1080, 1992.
14. Grossman P, Kamenaker J, and Wieling W. Prediction of tonic cardiac control using respiratory sinus arrhythmia: the need for respiratory control. *Psychophysiology* 28; 202-218, 1991.
15. Guzman P, and Eckberg DL. Within- and between-individual relations: vagal tone, and respiration, within- and between-individual relations. *Psychophysiology* 30; 488-495, 1993.
16. Hayano J, Maki S, Sasaki M, Okada A, Takano K, and Fujimori T. Effect of respiratory interval on vagal modulation of heart rate. *Am J Physiol Regul Integr Physiol* 286; H2022-H2027, 2004.
17. Hirsch JA and Bishop K. Respiratory sinus arrhythmia in humans: how breathing pattern modulates heart rate. *Am J Physiol Heart Circ Physiol* 241; H620-H629, 1981.
18. Kassam PG and Jin R. Respiratory sinus arrhythmia: a noninvasive measure of parasympathetic status. *Am J Physiol* 276; H979-H985, 1973.
19. Kassam PG, Lipson D, and Brander P. Opposing central and peripheral effects of atropine on parasympathetic cardiac control. *Am J Physiol Heart Circ Physiol* 252; H146-H151, 1997.
20. Kuo AD, Eckberg DL, and Eckberg DL. Human sinus arrhythmia is a limited measure of cardiac parasympathetic control in man. *J Physiol* 424; 529-542, 1990.
21. Pavloukian KR, Evans AJ, Bruce EA, Eckberg DL, and Kampy CF. Voluntary control of breathing does not alter vagal modulation of heart rate. *Am J Physiol* 262; H1075-H1080, 1992.
22. Pavloukian K, Evans J, Bruce E, and Kampy C. Heart rate variability during sympathetic excitatory challenges: comparison between spontaneous and metronomic breathing. *Respir Physiol Neurobiol* 94; 336-350, 2001.
23. Poon J, Poon T, Perrault H, Calhoun S, Demaria A, and Benditt G. Human sinus arrhythmia. *IEEE Trans Biomed Eng* 46; 1161-1165, 1999.
24. Rebecqwska M, Eckberg DL, and Eberl T. Muscarinic challenge receptors modulate vagal cardiac responses in man. *Auton Nerv Syst* 7; 271-276, 1983.

ALP Heart Circ Physiol • VOL. 286 • JUNE 2004 • www.ahpheart.org

INDIVIDUALITY OF RESPIRATORY SINUS ARRHYTHMIA

H2313

25. **Said P, Berger RD, Chen MH, and Cohen RJ.** Transfer function of the respiratory sinus arrhythmia response to a respiratory sinus arrhythmia stimulus. *Physiol Heart Circ Physiol* 206: H153-H161, 1989.
26. **Shaw S, Horner R, Bendischi G, and Guz A.** Persistence of a respiratory "personality" into stage IV sleep in man. *Keio Physiol* 80: 33-44, 1980.
27. **Shaw S, Walker J, Mapple K, and Guz A.** Evidence for individuality of the respiratory sinus arrhythmia response to a respiratory sinus arrhythmia stimulus. *Physiol Heart Circ Physiol* 48: 533-544, 1987.
28. **Taylor JA, Myers CV, Halliwell JR, Sedit H, and Eckberg DL.** Sympathetic restraint of respiratory sinus arrhythmia: implications for vagal cardiac tone assessment in humans. *Am J Physiol Heart Circ Physiol* 280: H2804-H2811, 2001.

Downloaded from ajpheart.physiology.org on November 25, 2010

II.4 MESURE PHYSIOLOGIQUE

La signification et la pertinence de la mesure physiologique constituent une part importante de mes travaux de recherche.

Le recueil de données expérimentales sur des volontaires sains ou des patients, leurs analyses et leurs interprétations ont constitué les bases de mes travaux de recherche quel qu'en soit l'axe : exploration, mesure ou approche théorique.

Le recueil de données nécessite une autorisation de lieu de recherche biomédicale délivré par l'Agence Régionale de Santé d'une part, et un avis favorable d'un Comité de Protection des Personnes pour chaque protocole d'étude, d'autre part.

Dans ce cadre, j'ai pris en charge depuis 2005, au sein de l'équipe PRETA, la responsabilité de la réalisation d'un plateau technique pour pratiquer des enregistrements sur volontaires sains à partir de mesures non invasives. J'ai entièrement rédigé le dossier de demande d'autorisation de lieu de recherche biomédicale pour la salle d'enregistrement de notre laboratoire. Cette autorisation a été obtenue pour la première fois en 2008. J'ai aussi rédigé et soumis un protocole sur volontaires sains intitulé « Validation d'outils d'étude de la respiration et de ses interactions avec la circulation et la déglutition », qui a été accepté pour trois ans par le Comité de Protection des Personnes "Sud Est V" (CHU de Grenoble) en mai 2008, pour lequel, j'ai demandé un renouvellement accepté jusqu'en juin 2013. L'autorisation de lieu de recherche ainsi qu'un protocole ont ensuite été reconduits par l'équipe et je suis actuellement coresponsable (depuis 2013) de ce plateau technique et veille à la mise en application du protocole en étroite collaboration avec le médecin investigateur. J'ai aussi participé au projet qui consiste à promouvoir cette plate-forme au sein de l'Université, et ainsi permettre le partage de notre matériel et de notre savoir-faire avec des chercheurs d'autres équipes.

II.4.1 Comparaison de la ventilation mesurée par pneumotachographie et pléthysmographie respiratoire à variation d'inductance

La pléthysmographie respiratoire à variation d'inductance (PRI) est une méthode de mesure non-invasive mesurant des variations de sections de surface du thorax

(PRI_{THO}) et de l'abdomen (PRI_{ABD}) ([Martinot-Lagarde et al, 1988](#)) qui repose sur les lois de la magnétostatique. En effet, Les variations de courant induit par un champ magnétique généré à l'intérieur des spires d'une bobine entourant les compartiments du thorax et de l'abdomen, permettent de déduire les variations de surfaces de sections de ces compartiments (courant induit dépendant de l'aire incluse dans la bobine). Les spires sont constituées de fils conducteurs isolés, cousus en zig-zag sur un gilet en tissu extensible (Figure 11).

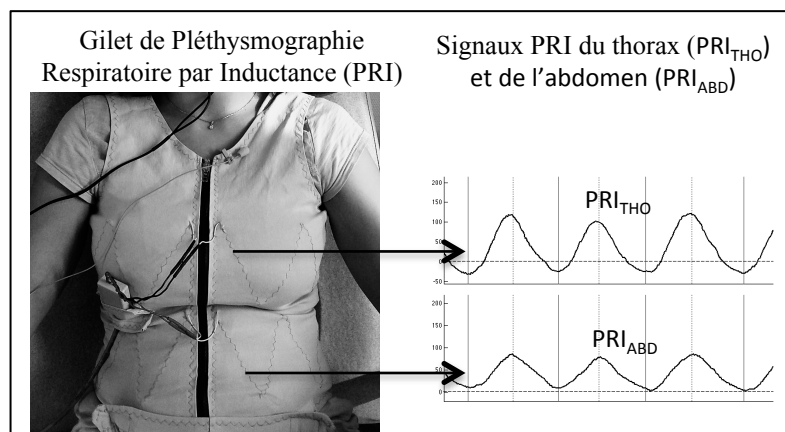


Figure 11 : Capteur et signaux de pléthysmographie respiratoire à variation d'inductance (PRI)

Le volume (V_{PRI}), estimation du volume courant, est obtenu par la combinaison linéaire pondérée des signaux du thorax (PRI_{THO}) et de l'abdomen (PRI_{ABD}) mesurés par PRI : $V_{PRI} = \tau PRI_{THO} + \alpha PRI_{ABD}$. La détermination des coefficients de pondération τ et α constitue la calibration du système de mesure PRI. De nombreuses méthodes de calibration existent, pour notre étude nous avons utilisé les valeurs $\tau = 2$ et $\alpha = 1$ ([Banzett et al, 1995](#)). Le débit ventilatoire obtenu par PRI (D_{PRI}) peut aussi être calculé en dérivant puis en filtrant (filtre passe-bas) ce volume V_{PRI} .

Afin de vérifier la validité des données ventilatoires obtenues par PRI, la respiration a été enregistrée simultanément par PRI et pneumotachographie chez dix volontaires sains au repos et au cours d'addition de deux niveaux de résistances à la bouche, en position assise, couchée sur le dos et sur le côté. Les volumes courants obtenus par les deux méthodes (V_{PRI}) et par intégration du signal débit mesuré par pneumotachographie (V_{PNT}) sont très proches pour des volumes inférieurs à un litre. Au dessus de cette valeur, la mesure par PRI semble sous estimer les volumes (Figure 12).

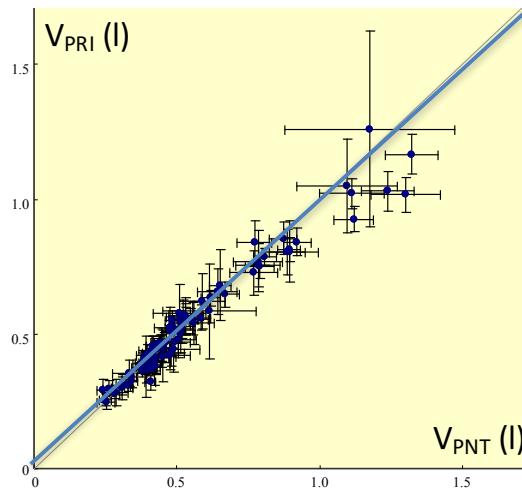


Figure 12 : Représentation de volumes courants obtenus par intégration du signal débit mesuré par pneumotachographie (V_{PNT}) en fonction des volumes courants obtenu par le signal PRI (V_{PRI}) pour les 10 sujets dans toutes les 9 conditions : en position assise, couchée sur le dos et le côté au repos et avec l'addition de deux niveaux de résistances additionnelles.

Ce qui peut s'expliquer par le fait que pour des volumes courants élevés, les variations de sections de surfaces du thorax et de l'abdomen ne sont pas les seules composantes des variations de volume.

Nous avons calculé la qualité de l'ajustement entre les signaux de débit ventilatoire obtenus par pneumotachographie (D_{PNT}) et par dérivation du volume PRI (D_{PRI}). Elle est la plus élevée en ventilation spontanée, reste supérieure à 90% pour la plus faible des résistances additionnelles ($\approx 5 \text{ cmH}_2\text{O.s.l}^{-1}$) et est nettement plus faible pour la deuxième résistance ($\approx 14 \text{ cmH}_2\text{O.s.l}^{-1}$).

Ce qui peut suggérer que lors de l'addition de résistance, les variations des compartiments du thorax et de l'abdomen peuvent être de formes différentes entraînant des écarts entre les formes débits D_{PNT} et D_{PRI} .

En conclusion, les données respiratoires acquises par pléthysmographie respiratoire à variation d'inductance (PRI), peuvent être utilisées pour l'évaluation de la ventilation, la limitation étant le niveau du volume courant (inférieur à un litre). Quant à la forme des signaux de débit ventilatoire obtenu par PRI et par pneumotachographie, la qualité de l'ajustement est satisfaisante dans les conditions de repos et diminue avec le niveau croissant des résistances additionnelles.

Eberhard A et al (2001). Comparison between the respiratory inductance plethysmography signal derivative and the airflow signal. Adv Exp Med and Biol

Afin d'étendre les conditions de validité de la mesure PRI pour l'évaluation de la ventilation (notamment pour des $VT > 1$ litre), nous avons modifié le traitement des signaux PRI. En effet, précédemment le signal de débit D_{PNT} a été obtenu après dérivation de V_{PRI} puis filtrage avec le même filtre passe bas quel que soit le sujet ou la condition. Dans ce travail, nous avons étudié l'utilisation d'un filtre adapté à chaque individu (filtre individuel) dans une condition donnée et la possibilité de l'appliquer pour le même individu dans une autre condition. La respiration a donc été enregistré par pneumotachographie et PRI chez douze volontaires sains au cours de la ventilation de repos et de deux protocoles d'hyperventilation volontaire : 1) à la fréquence ventilatoire de repos et 2) à une fréquence ventilatoire de 20 cycles/min.

Un filtre adapté individuel a donc été calculé en se basant sur les signaux mesurés par PRI et pneumotachographie (fonction de transfert) en respiration de repos. Ce filtre a ensuite été appliqué sur les signaux obtenus en hyperventilation volontaire puis lors de la phase de récupération. Un filtre individuel a aussi été calculé à partir des signaux enregistrés au cours des autres conditions (hyperventilation volontaire et récupération). Dans plus 90% des cas, la qualité de l'ajustement entre D_{PNT} et D_{PRI} en appliquant un filtre individuel calculé avec les enregistrements au repos était supérieure à 90%. Elle n'est pas meilleure lorsque l'on applique un filtre individuel calculé avec les enregistrements de la condition (hyperventilation volontaire et récupération).

L'application d'un filtre individuel permet d'étendre le domaine de validité des mesures de la ventilation par pléthysmographie respiratoire à variation d'inductance (PRI). Le filtre individuel calculé à partir des signaux PRI et de pneumotachographie de repos peut-être appliquée à différentes conditions de ventilation (hyperventilations volontaires et récupérations) pour un sujet donné.

Calabrese et al (2007) Respiratory Inductance Plethysmography is suitable for voluntary hyperventilation test" Annual inter conf of IEEE Eng in Med and Biol Society

Respiratory Inductance Plethysmography is suitable for voluntary hyperventilation test.

Pascal Calabrese, Tudor Beselaga, André Eberhard, Victor Vovc and Pierre Baccomier.

Abstract.— The aim of this work was to evaluate the goodness of fit of the airway signal measured by pneumotachography (PNT) and the airway signal measured by respiratory inductance plethysmography (RIP) in order to be applied to the study of voluntary hyperventilation, and recovery. RIP derivative signal was filtered with an adjusted filter based on each subject airflow signal (pneumotachography). For each subject and for each condition (rest, voluntary hyperventilation, and recovery) comparisons were performed between the airflow signal and the RIP derivative signal filtered with an adjusted filter obtained either on rest signal or on the studied part of the signal (voluntary hyperventilation or recovery). Results show that the goodness of fit of the filtered RIP derivative signal is higher than the goodness of fit of the unfiltered RIP derivative signal (122 on 132). (2) not improved by applying an adjusted filter obtained on the studied part of the signal. These results suggest that RIP could be used for studying breathing during voluntary hyperventilation and recovery using adjusted filters obtained from comparison to airflow signal at rest.

1. INTRODUCTION

RESPIRATORY inductance plethysmography (RIP) is a noninvasive method for measurement of breathing providing rib cage and abdomen cross sectional area changes. The linear combination between rib cage and abdomen cross sectional area changes allows to estimate breathing volume changes. There are very few comparisons between airflow and RIP derivative signal in physiological conditions. Eberhard et al. [1] have compared airflow and RIP derivative signal in three different postures (seated, lateral and dorsal supine) and also in control and in two resistive loaded conditions. The fit of RIP derivative to the airflow signal remained well in control condition and at a resistance of ~ 5 cm H₂O/s but lesser at a resistance of ~ 14 cm H₂O/s. The RIP derivative signal was smoothed by using the same low-pass filter for all subjects and all conditions.

Voluntary hyperventilation test have been proposed to test predisposition to the hyperventilation syndrome [2] which is used to describe patient with the somatic symptoms of both hypocapnia and anxiety [3]. RIP allows recording of breathing without using mask (needed for

pneumotachography) and thus subjects may not be aware that their breathing is recorded. The aim of the present work was to evaluate the consistency between airflow (pneumotachography) and RIP derivative during voluntary hyperventilation, and recovery. Airflow and RIP signals were both recorded in healthy subjects during rest, voluntary hyperventilation, and recovery. The RIP derivative signal was processed by a filter calculated with airflow (pneumotachography) taken as the reference signal, for each subject in each of all circumstances. Comparison of the goodness of fit of the filtered RIP derivative to the airflow signal in different conditions was performed in order to determine if the adjusted filter obtained on rest recording could be applied to the other conditions and thus allows to go without the mask during voluntary hyperventilation and recovery.

II. MATERIALS AND METHODS

A. Materials and experimental protocol

We studied twelve healthy volunteers between 24 and 65 years of age. Five of whom were men. All study participants provided informed consent. The study was approved by the relevant ethics committee (CHU Grenoble). Breathing was recorded simultaneously with a flowmeter (Fleish head no 1) and a differential inductance (163PC01D36, Micro Switch) placed on a face mask and with a RIA (Viasorp, RBL). Leaks from around the mask were checked for before the recording was initiated using an infrared CO₂ analyser (Engström, Elizaldiza MC, End-tidal CO₂ fraction (F_{ET}CO₂) was measured continuously using the same apparatus. Subjects were in semi-supine position. Two series of recordings were performed successively: (1) at rest (three minutes, Rest1), during voluntary hyperventilation at each subject's spontaneous breathing rate (three minutes, HV1), during recovery (ten minutes, Rec1), and (2) successively at rest (three minutes, Rest2), during voluntary hyperventilation at 20 breaths/min (three minutes, HV2), during recovery (ten minutes, Rec2). Subjects were encouraged to increase tidal volume in order to descend F_{ET}CO₂ to 3.5%. To impose the breathing rate, an auditory cue was used, which signaled only for the inspiration to begin.

B. Methods

All signals were digitized at a rate of 1000Hz. For each recording, we obtained a minimum of 25 breaths at rest up to 150 for the recovery period. The 15 most regular (duration) consecutive breaths of the airflow signal were chosen and formed the reference part. A least squares method was used

over this part of signal to obtain a RIP volume signal (V_{RIP}) by combination of rib cage (RCA_{RIP}) and abdominal (ABD_{RIP}) signals compared to the integrated flow signal (V_{PNT}):

$$V_{RIP} = \alpha \cdot RCA_{RIP} + \beta \cdot ABD_{RIP}, \quad (1)$$

where $\alpha = 2$ was imposed [4]. The derivative of V_{RIP} (F_{RIP}) was then calculated by using centered divided differences:

$$F_{RIP} = (V_{RIP}(t+\Delta t) - V_{RIP}(t-\Delta t)) / 2\Delta t \quad (2)$$

A transfer function was calculated over the reference part between RIP derivative and airflow signal to take out an adjusted filter. Then the adjusted filter calculated on the reference part of signals was applied on the entire recording. The goodness of fit of the filtered RIP derivative to the airflow signals (concordance ρ) was calculated on the entire recording:

$$\rho = 1 - \frac{\sum_{i=1}^N (F_{RIP}(t_i) - F_{PNT}(t_i))^2}{\sum_{i=1}^N (F_{PNT}(t_i) - \overline{F_{PNT}})^2} \quad (3)$$

where F_{RIP} and F_{PNT} are respectively the airflow and the filtered RIP derivative signals at each instant and F_{PNT} is the mean value of F_{PNT} over the whole recording. For one subject the concordance was calculated between the standard airflow signal and RIP derivative signal filtered with an adjusted filter based either on reference signals (Rest1) or on HV1, Rec1, Rest2, HV2 and Rec2 signals. For each subject 11 concordances were then obtained applying an adjusted filter calculated on different conditions: concordance of "rest filter" applied to Rest1 signal (Rest1/Rest1), to HV1 (HV1/Rest1) and all other conditions (total 6 concordances) and concordances of adjusted filters calculated on their own conditions (HV1/HV1, Rec1/Rec1, ..., total 5 concordances).

III. RESULTS

Fig. 1 shows airflow signal (pneumotachography) and RIP derivative signal for HV1 obtained with adjusted filter calculated (a) on Rest1 (concordance = 97.03%), and (b) on HV1 (concordance = 97.88%) for subject #5.

Fig. 2 and Fig. 3 show concordances expressed in percentage for each subject and each conditions. The goodness of fit was (1) higher than 90% at almost all comparisons (122 on 132), (2) not improved by applying a filter adjusted on the studied condition except for subject #4 for which concordance increase from 29.12% to 85.18% when filters are calculated on Rest1, and on HV1 (Fig. 3, b).

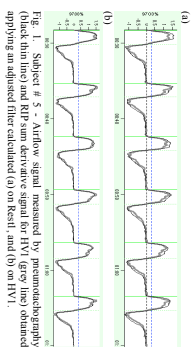


Fig. 1. Subject # 5 - Airflow signal measured by pneumotachography (PNT) and the airway signal measured by respiratory inductance plethysmography (RIP) in order to be applied to the study of voluntary hyperventilation, and recovery. The figure shows three subplots (a), (b) and (c) for subject #5.

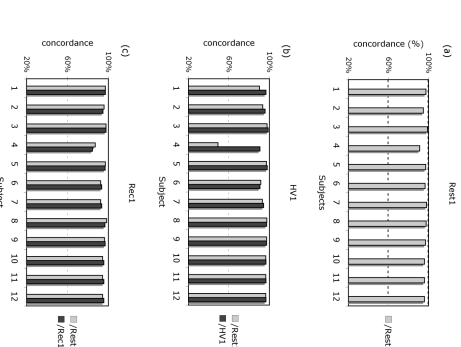


Fig. 2. Concordance goodness of fit of the RIP derivative to the standard airflow signal for HV1 obtained with adjusted filter calculated (a) on Rest1, (b) on HV1, and (c) on Rest1. The figure shows three bar charts (a), (b) and (c) for 12 subjects. In all cases, concordance is high, generally above 90%.

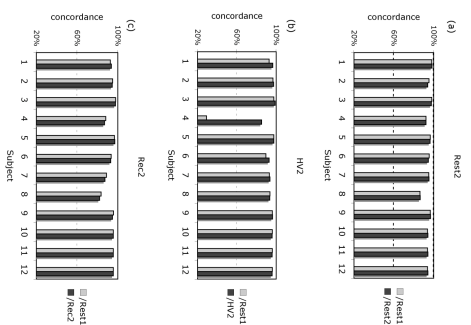


Fig. 3. Concordance, goodness of fit of the RIP sum derivative to the standard airflow signal, expressed in percentage for each subject and each condition: (a) at rest (Rest2), (b) during voluntary hyperventilation at 20 breath/min (HV2), and (c) during recovery (Rest2). For Rest2 adjusted filters calculated respectively on Rest1 (grey square, Rest1) and on Rest2 (black square, Rest2) adjusted filters. For HV2 adjusted filters calculated respectively on Rest1 (grey square, Rest1) and HV2 (black square, HV2) were applied, for Rest2 adjusted filters calculated respectively on Rest1 (grey square, Rest1) and on Rest2 (black square, Rest2) were applied.

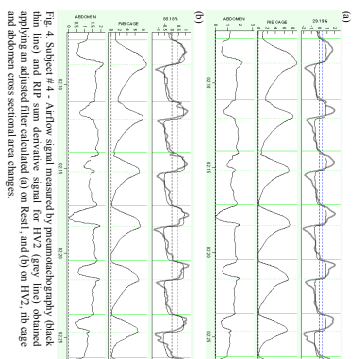


Fig. 4. Subject #4 - Airflow signal measured by pneumotachography (black thin line) and RIP sum derivative signal for HV2 (grey line) obtained applying an adjusted filter calculated (a) on Rest1, and (b) on HV2, (b) cage and abdomen cross sectional area changes.

IV. DISCUSSION

The superimposed airflow and RIP derivative signals (Fig. 1) and concordance values presented (Fig. 2 and 3) show that the fit of RIP derivative to the airflow signal is well and not improved by applying a filter adjusted on the studied condition, except for subject #4 (Fig.3.b). Fig.4 shows airflow signal (pneumatotachography) and RIP sum derivative signal for HV2 obtained applying an adjusted filter calculated (a) on Rest1 (concordance = 29.19%), and (b) on HV1 (concordance = 85.18%) for subject #4. The unusual (plateaued) shape of abdominal signal may explain the differences obtained by the two methods for this subject.

These results indicate that RIP could be used for studying breathing during voluntary hyperventilation and recovery without a mask, provided that airflow signal was recorded at rest during a short period (about 15 breaths). A limiting condition seems to be that rib cage and abdomen signals show no disturbance. This work suggests that respiratory signals recorded at rest contain a pertinent information usable for respiratory signals recorded in other conditions (voluntary hyperventilation and recovery).

REFERENCES

- [1] A. Eberhard, P. Calabrese, P. Bascioni, G. Bensch, "Comparison between the respiratory inductance plethysmography signal derivative and the respiratory inductance plethysmography signal derivative," *Journal of Applied Physiology*, vol. 91, pp. 1165-1170, 2001.
- [2] H.J. Barendt, and E.M. Bramer, *Hyperventilation syndrome*, 2000.
- [3] In P.J. Vinken and G. W. Bruyn, eds., *Handbook of Clinical Neurology*, Vol.38. Neurological Manifestations of System Disease, Part I. Amsterdam, North Holland Publ., 1979, pp. 309-360.
- [4] M. J. Griffin, "The relationship between hyperventilation and anxiety associated with anxiety states: the hyperventilation syndrome," *Cell Stress and Related Topics*, vol. 1, pp. 17-22, 1997.
- [5] R.B. Barzani, S.T. Mahan, D.M. Cairner, A. Bolognera and S.H. Loring, "A simple and reliable method to enhance respiratory inductance plethysmography signals during hyperventilation," *Journal of Applied Physiology*, Vol. 75, pp. 2169-2176, 1995.

II.4.2 Méthode d'évaluation de la fonction respiratoire

II.4.2.1 Différence de forme thorax-abdomen et évaluation des variations des résistances des voies aériennes

Au cours de la respiration de repos, les mouvements du thorax et de l'abdomen ne sont pas tout à fait synchrones et il a été observé que les "décalages" entre les variations de mouvements de ces deux compartiments sont faibles chez les sujets sains et plus importants chez des patients atteints d'obstruction bronchique ([Sharp et al, 1977](#) ; [Ringel et al, 1983](#)). [Agostoni et Mognoni \(1966\)](#) et [Konno et Mead \(1967\)](#) ont été les premiers à effectuer des mesures sur chaque compartiment. Depuis, de nombreuses méthodes ont été explorées pour mesurer les mouvements du thorax et de l'abdomen. Dans un bilan, [Seddon \(2015\)](#) a conclut que la pléthysmographie respiratoire à variation d'inductance (PRI) est la méthode la plus utilisée chez les adultes et particulièrement chez les enfants, pour l'évaluation de l'asynchronisme thoraco-abdominal ([Allen et al, 1990, 1991](#) ; [Sivan et al, 1990](#) ; [Davis et al, 1993](#) ; [Hammer et al, 1995](#) et [2009](#) ; [Selbie et al, 1997](#) ; [Reber et al, 2001](#) ; [Mayer et al, 2003](#) ; [Upton et al 2012](#) ; [Chien et al, 2013](#)).

Au cours de ma thèse, j'ai pu montrer une corrélation significative entre la différence (quantifié par une distance) entre les mouvements du thorax et l'abdomen mesurés par PRI et les valeurs de résistances ajoutées au niveau de la bouche chez des volontaires sains. L'évaluation de l'asynchronisme thoraco-abdominal pourrait ainsi constituer une méthode non-invasive d'évaluation de la sévérité de l'obstruction.

Ce travail a été poursuivi et approfondi dans le cadre d'une thèse (Université de Monastir) que j'ai codirigée en collaboration avec le laboratoire de biophysique de la faculté de Médecine de Sousse (Tunisie). Chez 44 patients suivis pour une obstruction bronchique modérée au CHU de Sousse (service d'exploration fonctionnelle respiratoire), deux explorations fonctionnelles respiratoires avec mesure des résistances respiratoires obtenues par pléthysmographie corporelle, ont été réalisées avant et après la prise d'un bronchodilatateur. Les signaux du thorax et l'abdomen ont été enregistrés dans ces deux conditions par PRI. Des volontaires sains appariés en âge, taille et poids avec le groupe obstructif ont suivi un test d'exploration fonctionnelle avec mesure des résistances respiratoires obtenues par pléthysmographie corporelle et les signaux thoracique et abdominal ont été enregistrés au repos par PRI.

Les valeurs de résistance respiratoire et de distance entre les signaux du thorax et de l'abdomen sont significativement moins élevées chez le groupe de sujets sains que chez le groupe de patients obstructifs aussi bien avant qu'après la prise de bronchodilatateur. Chez les patients, la résistance et la distance diminuent significativement après bronchodilatation (Figure 13).

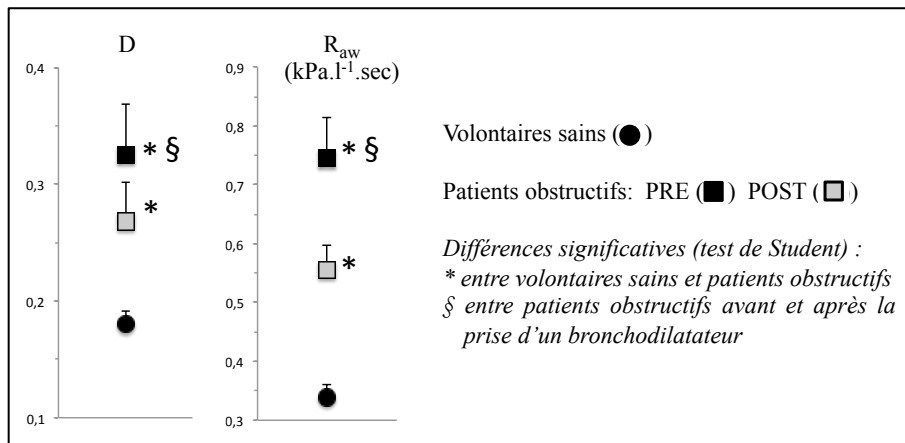


Figure 13 : Moyenne ± erreur standard : de la distance (D) entre les signaux du thorax et l'abdomen calculée à partir de tous les cycles respiratoires sélectionnés (minimum 30) et de la résistance des voies aériennes (R_{aw} en kPa.l⁻¹.sec)

De plus, la distance et la résistance sont significativement et positivement corrélées chez les patients aussi bien avant qu'après la prise du bronchodilatateur.

Ces résultats suggèrent que la distance calculée à partir des signaux de pléthysmographie respiratoire à variation d'inductance peut être utilisée pour une évaluation des variations de la bronchoconstriction.

Laouani et al (2016) Thorax and Abdomen Motion Analysis in Patients with Obstructive Diseases J Pulm Respir Med

Codirection de thèse de l'Université de Carthage (Tunisie) d'Aïcha Laouani, au Laboratoire de Biophysique Métabolique & Toxicologie Professionnelle et Environnementale Appliquée (Faculté de Médecine de Sousse, Tunisie): "Nouvelle Technique d'évaluation, des variations de la résistance des voies respiratoires lors d'un test de réversibilité bronchique. Elaboration d'un modèle simple du système respiratoire pour interpréter des mesures non invasive de la ventilation", soutenue le 15 décembre 2016 à Sousse.



Research Article

Open Access

Thorax and Abdomen Motion Analysis in Patients with Obstructive Diseases

Authors: Achta Louani, Sonia Rouah, Saad Saguem, and Pascale Calbrete

Abstract: We evaluated changes in bronchoconstriction by a new approach based on respiratory inductive plethysmography (RIP) signal analysis.

Methods: Thoracic and abdominal motions were recorded (5 min) by uncalibrated RIP in 44 adult subjects with a diagnosis of moderate bronchial obstruction (Obstructive group) and 50 healthy adult controls (Healthy group).

Results: D and R were higher in the Obstructive group than in the Healthy group in both PRE and POST conditions.

Conclusion: D, as calculated from signals recorded by RIP, appears to be a useful non-invasive parameter for continuous monitoring of changes in bronchoconstriction.

Keywords: Respiratory inductive plethysmography; Airway resistance; Bronchoconstriction; Thorax motions; Abdomen motions

Introduction: The most common method to detect the presence and severity of airflow limitation associated with obstructive lung disease is spirometry, considered as the gold standard pulmonary function testing.

Although airway resistance (Rw) is seldom used to identify airway obstruction in clinical practice [2], its measurement becomes the only possibility of detecting airway obstruction in patients who cannot cooperate or perform reliable spirometry.

Respiratory Inductive Plethysmography (RIP) is another method that has the advantage over other techniques of being non-invasive. RIP allows recording of thorax and abdomen breathing movements using two sensors inserted in elastic bands surrounding thoracic and abdominal compartments.

Corresponding author: Achta Louani, Laboratory of Biophysics, Faculty of Medicine of Sousse, Sousse, Tunisia. Tel: +216 98560071; Fax: +216 73 28864; Email: achta.louani@univ-sousse.tn

Chattalon: Louani A, Rouah S, Saguem S, Calbrete P (2016) Thorax and Abdomen Motion Analysis in Patients with Obstructive Diseases. J Palm Respir Med 6: 313. doi:10.4172/2161-055X.1000313

for patients with airway obstruction disease. D was compared to Rms measured by body plethysmography both before and after bronchodilator administration.

Materials and Methods

Subjects

This cross-sectional analytic study was conducted in the Department of Physiology and Experiments in Habib Richard Hospital of Sousse (Tunisia) in accordance with the Declaration of Helsinki. The local Ethics Committee of the Hospital approved the study protocol.

The study was carried out on 44 (20 women) adult subjects with a diagnosis of moderate bronchial obstruction, as defined by comparison to reference values established by a local study [11]. This Obstructive group was compared to a Healthy group of 50 (25 women) healthy adult controls. Male and female subjects data were not reported separately.

All subjects were more than 18 years of age. The group with known airway obstruction contained subjects with a ratio of forced expiratory volume at the first second/forced vital capacity below the lower normal limit according to the American Thoracic Society guidelines [2]. The subjects with obstructive defects were clinically stable and did not show any signs of worsening symptoms or a need for increased medication or emergency care. The obstructive subjects had not required hospitalization within the previous weeks. The healthy controls included 18 young subjects (age less than 18 years, cigarette smoking alcohol abuse, renal failure, heart and coronary disease and current desmopressin therapy) for reduction or administration of an allergic reaction. Subjects having received beta agonists, oral or inhaled glucocorticoids, anti-histamines, anticholinergics, calcium, magnesium and beta-blockers during the previous 72 hours were also excluded. The healthy controls were volunteers non-smokers, over 20 years of age without a history of allergy and free from asthma, allergies, pulmonary tuberculosis or recent respiratory tract infection. The controls had normal pulmonary function tests and were free from any respiratory problems.

Imperfect performance of respiratory maneuvers was applied as an exclusion criterion in both study groups.

Body plethysmography

Pulmonary function measurements were performed with a body plethysmograph (ZAN 500 Body II, Messergers-Göhl, Germany) by applying International recommendations. The breathing method used in the present study to record total airway resistance. The following data were measured or calculated: airway resistance (Rw in BPL, lsec), forced vital capacity (FVC, l), forced expiratory volume in one second (FEV1) and the FEV1/FVC ratio.

Respiratory inductive plethysmography (RIP)

Thorax (THO) and abdomen (AB) breathing movements were recorded by RIP (Viasport[®], RM, France). The THO and AB signals were digitized at a sampling rate of 40 Hz. Breaths were delimited using the algorithm developed by Bachy et al. [12] on a flow signal and applied to the RIP signal as the derivative of the filtered signal obtained

from linear combination of both THO and ABD signals. Breaths involving swallowing, sigh, THO or AB signal drift were discarded from the analysis. A breath-by-breath analysis was then performed to calculate distance between THO and AB signals. Each THO and AB cycle included the same number (n) of samples (same digitized sampling rate and duration). For each breath, the THO and AB signal amplitude was normalized to obtain a zero average and a standard deviation of one. The distance between normalized THO and ABD signals (D) and abdomen (AB) signals (R) were calculated in samples according to the equation: D = (Rms - R) / Rms. The sensors of RIP incorporated in a wearable jacket (Viasport[®]) at the thoracic and abdominal compartment level (CA), thus recorded THO and ABD signals and delimited breaths on the RIP signal (B) and calculation of Dms (C).

For each recording, the mean distance (D) was calculated over all selected (minimum 30) breaths.

Experimental protocol

All subjects (Healthy and Obstructive) underwent body plethysmography measurement followed by a 15-minute RIP recording at spontaneous breathing. Each patient then inhaled at 20 sec intervals four successive doses of 100 mg of short-acting beta2-sympathomimetic after a gentle and incomplete expiration and held the breath for 5-10 sec. Each patient again underwent body plethysmography measurements and RIP recording. The RIP signal was recorded at a standard protocol used in pulmonary function testing [2]. Thus, two conditions are to be taken into consideration in this Obstructive group: PRE (before bronchodilation) and POST (after bronchodilation).

Data analysis

All data have been expressed as the mean ± SEM (Standard Error of the Mean). Student's t-test was used to compare the mean data between Healthy and Obstructive groups. Student's paired t-test was used to compare data within the Obstructive group before and after bronchodilation.

In the Obstructive group, Pearson correlation coefficient was used to evaluate the linear relationship between D and Rms, as well as between D and spirometric data and between Rms and spirometric data in PRE and POST conditions. A binomial test was used to check the number of cases where bronchodilation entailed a decrease in D and Rms.

Significance was set at the 0.05 level.

Results

Figure 2 shows mean ± SEM values of D, R, and spirometric data (FEV1, FVC, FEV1/FVC) for both Healthy and Obstructive groups in PRE and POST conditions. It can be seen that D and Rms values are lower in the Healthy group than in the Obstructive group in both PRE and POST conditions, whereas FEV1, FVC, and FEV1/FVC are higher in the Healthy group than in the Obstructive group in both PRE and POST conditions. Comparing Student's t-test and spirometric data on one hand, and Healthy and Obstructive POST on the other hand showed significant variations in all data (p<0.05), except FVC, which exhibited no significant difference between Healthy and Obstructive POST.

As expected in the Obstructive group, bronchodilation entailed a decrease in D and Rms, while spirometric data increased. Comparison (Student's paired t-test) between Obstructive PRE and Obstructive POST showed significant difference in all data (p<0.05).

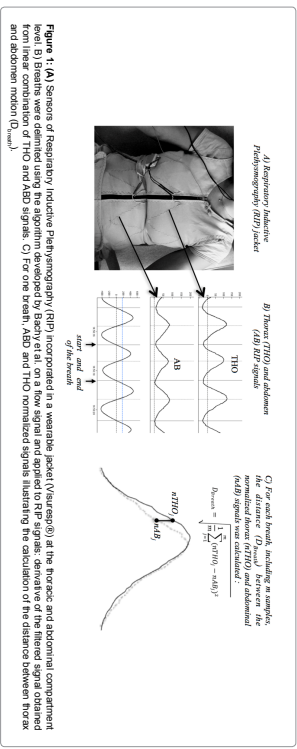


Figure 1: (A) Sensors of Respiratory Inductive Plethysmography (RIP) incorporated in a wearable jacket (Viduesu®) at the thoracic and abdominal compartment level. (B) Signals were obtained using the algorithm developed by Babbitt et al. on raw signals and applied to RIP signals. (C) Derivation of the linear signal obtained from the RIP signals (D) and (D₀) signals. (D) and (D₀) normalized signals illustrating the calculation of the distance between thorax and abdomen motion (D_{max}).

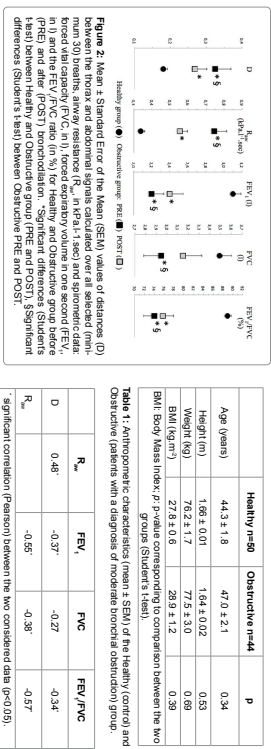


Figure 2: Mean ± Standard Error of the Mean (SEM) values of distances (D) between the thorax and abdominal signals calculated over all selected (minimum 30) breaths. (Healthy resistance (R_{th}) in Pa.s; (sao) and sponnetic data in 0) and the FEV₁/FVC ratio (in %) for Healthy and Obstructive group before (PRE) and after (POST) bronchodilation. *Significant differences (Student's t-test) between Healthy and Obstructive group (PRE and POST). Significant differences (Student's t-test) between Obstructive PRE and POST.

Using a Bionomial test, it was found that it was a significant number of subjects showing a decrease in D (28 subjects over 44, p=0.024) and R_{th} (32 subjects over 44, p=0.001) values after bronchodilation. It must be underlined at this point that these subjects did not systematically exhibit a simultaneous decrease in both D and R_{th} values.

We did however calculate correlation coefficients between D and R_{th}, as well as between D and sponnetic data and between R_{th} and sponnetic data, in PRE (Table 2) and POST (Table 3) conditions within the Obstructive group. A positive correlation exists between D and R_{th}, both in PRE and POST conditions, but the correlations between D and sponnetic data were negative and significant for all variables, except for FVC in Obstructive PRE condition. R_{th} was significantly and negatively correlated with all sponnetic data in both conditions.

Discussion

The main result of this study is that the distance D calculated between thorax and abdomen normalized signals, as recorded by respiratory inductive plethysmography may provide information on bronchoconstriction. Indeed, 1) D was significantly higher in the Obstructive group in both PRE and POST conditions than in the Healthy group and 2) in the Obstructive group, D and R_{th} were

	Healthy n=50	Obstructive n=44	p
Age (years)	44.3 ± 1.8	47.0 ± 2.1	0.34
Height (m)	1.66 ± 0.01	1.64 ± 0.02	0.55
Weight (kg)	76.2 ± 1.7	77.5 ± 3.0	0.69
BMI (kg/m ²)	27.8 ± 0.6	28.9 ± 1.2	0.38

	R _{th}	FEV ₁	PVC	FEV ₁ /PVC
D	0.48*	-0.37*	-0.27	-0.34
R _{th}	-0.55*	-0.38*	-0.37	-0.57

	R _{th}	FEV ₁	PVC	FEV ₁ /PVC
D	0.39*	-0.44*	-0.38	-0.35
R _{th}	-0.49*	-0.37	-0.43	-0.43

Healthy and Obstructive groups showed no significant difference in anthropometric data (age, height, weight and BMI). The sponnetic data, R_{th} and D were significantly different between Healthy and Obstructive groups in PRE condition, and there still was a significant difference between Healthy and Obstructive groups in POST condition, except for FVC.

Although splanometry is considered as the gold standard to detect airflow limitation in obstructive diseases, recent articles resisted the contribution of this test, such as the body resistance measured by respiratory inductive plethysmography [9]. Interest for separate thoracic and abdominal motions during breathing was introduced in the 1960s. Indeed, Agostoni and Moadini initiated the measure of chest wall deformation [13], and Komo and Mead evaluated the separate volume of the two compartments [14]. Since then, a large variety of methods have been employed for measuring thorax and abdomen motions, as reviewed by Seddon [9]. Since the 1990s, RIP has been the most common method in both adults and children, particularly for evaluating thoraco-abdominal asynchrony [5,6,15,23]. Thoracic and abdominal motions have been analyzed to quantitatively evaluate thoraco-abdominal asynchrony (TAA) defined by Prisk et al. [8] as the non-contract motion of the cage and abdomen during breathing. Several methods have been used to quantify TAA with or without calibrating RIP. On one hand, the values calculated using uncalibrated RIP can be either phase angle (Lissajous figure), X-Y plots of thorax versus abdomen [5,16-18,23], or percent time paradoxical to tidal volume during inspiration, expiration or total breath [24] and phase relation during total breath (percentage of total breath) [24] and where thorax and abdomen are asynchronously moving [20,22]. On the other hand, the values calculated with calibrated RIP can be either asynchrony index [23], inhaled breathing index (maximal compartment amplitude sum of maximal excursion of thorax and abdomen) as proportion of tidal volume [7] or 70 cage contribution to tidal volume (maximal excursion of thorax as a percentage of tidal volume) [26].

In our study, distances between the thoracic and abdominal normalized signals serve to evaluate differences in these two compartments motion. This was calculated breath-by-breath on the minutes recordings. Thus, the mean value (D) may be considered as calculated over a steady-state and we assumed that it provides a satisfactory evaluation of motion difference between thoracic and abdominal compartments induced by bronchoconstriction. However, concerning R_{th} data they result from a single measurement. This may account for the observed discrepancies between D and R_{th}, such as the fact that following a bronchodilation, more people showed a decrease in R_{th} (rather than a decrease in D). Indeed, the shift for R_{th} was higher in the Obstructive group than in the Healthy group (both conditions). D and R_{th} were significantly correlated and they also correlated with splanometric data. Indicates that D as well as R_{th} may assess bronchoconstriction.

These results suggest that beside classical methods [1,2] used to evaluate bronchoconstriction, inductive plethysmography provides relevant information on bronchoconstriction with several notable advantages. Indeed, RIP is a non-invasive method to record thoracic and abdominal motion without requiring quiet breathing. Thus, since no subject cooperation or specific training is required, measurements can be performed in a wide range of patients (children, elderly, bedridden, etc.) [27,28]. In the present study, the use of the chest and abdomen in a fixed position (Figure 1A) allowing data compression continuous recordings. Prior calibration in various postures [30] may then be applied in longitudinal measurements of respiratory function by RIP [22]. RIP monitoring can then be envisaged to assess changes in bronchoconstriction induced by therapeutics, environmental variations or various conditions such as sleep.

Conclusion
The breath-by-breath distance between thorax and abdomen normalized signals recorded by respiratory inductive plethysmography and averaged over a 5-min period provide a new method of RIP use for bronchoconstriction changes evaluation.

Conflict of Interests
The authors declare that there is no conflict of interests regarding the publication of this paper.

21. Chen Y, Kuan SY, Huang YC, Yu CL, Yang PC (2013) Asynchronous thoraco-abdominal motion in patients with obstructed or normal ventilation in patients with COPD. *Respir Care* 58: 520-526.

22. Mauer CH, Clapano RG, Sr, Lavezi AF, McDonough JM, Alton JL (2005) Respiratory inductance plethysmography in healthy 3- to 5-year-old children. *Chest* 124: 1812-1819.

23. Reiser A, Böhler SA, Hammer J, Frei FJ (2001) Effect of airway opening manoeuvres on thoraco-abdominal asynchrony in anesthetized children. *Eur Respir J* 17: 1238-1243.

24. Benamer M, Giddiman MD, Eccley C, Sautler C (1993) Ventilation and thoracoabdominal synchrony during halothane anaesthesia in infants. *J Appl Physiol* (1992) 74: 189-194.

25. Warren RH, Anderson SH (1994) Chest wall motion in neonates utilizing respiratory inductive plethysmography. *J Biomech* 14: 191-195.

26. Herkerson MB, Cain AA, Voth ME, Stark AR (1990) Changes in the thoracoabdominal motion cage to tidal breathing during sleep. *Am Rev Respir Dis* 141: 922-925.

27. Gonzalez H, Hailer B, Wilson H, Sauer MA (1984) Accuracy of respiratory inductive plethysmograph over wide range of air cage and abdominal compartmental contributions to tidal volume in normal subjects and in patients with chronic obstructive pulmonary disease. *Am Rev Respir Dis* 130: 171-174.

28. Derhard A, Calabrese P, Baccorin P, Berchtold G (2001) Comparison between the respiratory inductance plethysmography signal derivative and the airflow signal. *Acta Esp Med Sci* 194: 493-497.

29. Calabrese P, Baraboga T, Derhard A, Vuc J, Baccorin P (2007) Respiratory inductive plethysmography signal derivative as a measure of tidal volume. *Conf Proc IEEE Eng Med Biol Soc* 2007: 1065-1067. "Hypercalcaemia 1841".

30. Sauer MA, Wilson H, Baraboga T, Fainman D, Sauer M, et al. (1989) Calibration of respiratory inductive plethysmograph during natural breathing. *J Appl Physiol* 66: 410-420.

OMICS International: Publication Benefits & Features

- Unique features:**
- International digital archive of articles through multiple disciplines and indexing
 - Showing recent research output in a timely and updated manner
 - Special issues on the current trends of scientific research
- Special Features:**
- 700 Open Access Journals
 - 5000+ editorial team
 - Quality and quick editorial, review and publication processing
 - Indexing at Multiple (ISI/Scopus, EBSCO, Medline, Copernicus and Google Scholar etc)
 - Author, Reviewer and Editor reward with online Scientific Credits
 - Better discount for subsequent articles
- Submit your manuscript at: www.omicsonline.org/submit/

II.4.2.2 Les oscillations cardiogéniques et estimation de la mécanique de la paroi thoracique

Les battements cardiaques produisent des déformations mécaniques des poumons qui engendrent des petites fluctuations sur la pression et le débit des voies aériennes. Il est possible d'observer ces fluctuations, nommées oscillations cardiogéniques, sur le signal respiratoire notamment au cours d'apnée. Les oscillations cardiogéniques sont aussi observables sur les signaux du thorax et de l'abdomen mesurés par PRI. Nous avons tenté d'utiliser l'amplitude de ces oscillations enregistrées sur les signaux PRI et sur la pression mesurée à la bouche pour identifier une donnée en lien avec les propriétés mécaniques de la paroi thoracique. Des enregistrements ont été effectués chez des sujets sains en position couchée sous ventilation mécanique à différents niveaux de pression de fin d'expiration et dans deux conditions : bras le long du corps et bras levés. Nous avons mesuré les variations de volume PRI (ΔV_{co}) simultanément avec les variations de pression (ΔP_{co}) au cours d'une oscillation cardiogénique. Le rapport $C_{co} = \Delta V_{co} / \Delta P_{co}$ est la compliance cardiogénique et peut-être considéré comme un indicateur de la compliance thoracique. Ce rapport est indépendant du niveau de pression de fin d'expiration. En revanche, ce rapport diminue lorsque les bras sont levés.

L'analyse des oscillations cardiogéniques pourrait fournir une méthode non invasive d'évaluation des variations de la compliance thoracique chez des sujets sous ventilation mécanique.

Bijaoui et al (2004) Can Cardiogenic oscillations provide an estimate of chest wall mechanics? Adv Exp Med and Biol

II.4.3 Méthode d'évaluation de la fonction cardiaque

II.4.3.1 Analyse de l'arythmie sinusale d'origine respiratoire

De nombreuses méthodes d'analyse, dans le domaine fréquentiel et temporel, ont été développées pour estimer l'arythmie sinusale d'origine respiratoire (ASR). J'ai participé à l'élaboration d'une méthode statistique originale de l'analyse de l'ASR basée sur une étude cycle par cycle ventilatoire. La méthode proposée permet d'avoir :

- 1) une représentation de l'ASR soit cycle par cycle ventilatoire, soit sur un ensemble de cycles ventilatoires,
- 2) un test statistique pour détecter la présence de l'ASR sur une courte durée (par exemple cinq cycles ventilatoires),
- 3) l'amplitude et la phase de l'ASR dans chaque cycle ventilatoire en ajustant une sinusoïde sur la fréquence cardiaque cycle par cycle dans un cycle ventilatoire.

Cette méthode présente l'avantage de permettre une détection spécifique de l'ASR et sa quantification.

New statistical method for detection and quantification of respiratory sinus arrhythmia Dinh et al. (1999) IEEE-Inst Electrical Electronics Engineers

Nous avons utilisé cette méthode dans plusieurs travaux développés dans le paragraphe II.3.2 ayant fait l'objet de trois publications :

Calabrese et al. (2000) Cardiorespiratory interactions during resistive load breathing. Am J Physiol-Regulatory Integrative and Comparative Physiology

Ben Lamine et al. (2004) Individual differences in respiratory sinus arrhythmia. Am J Physiol-Heart and Circulatory Physiology

Scott et al (2004) Enhanced cardiac vagal efferent activity does not explain training-induced bradycardia. Auton Neurosc : Basic and Clinical

Communications

New Statistical Method for Detection and Quantification of Respiratory Sinus Arrhythmia

Tuan Pham Dinh, Hélène Pernati, Pascal Calhèse,
André Eschard, and Gila Bencherif*

Abstract—A statistical method with the advantages of 1) enabling the detection of the presence of respiratory sinus arrhythmia (RSA) in a 2-min recording window, and 2) providing breath-by-breath RSA amplitude and phase obtained from the fitting of a sinusoid to the instantaneous relative heart rate is presented.

Index Terms—Heart rate variability, respiration, respiratory sinus arrhythmia (RSA), spectral analysis, statistical method.

1. INTRODUCTION

Centrally modulated cardiac, vagal, and sympathetic efferent activities associated with respiration are a major component of heart rate variability, referred to as "respiratory sinus arrhythmia" (RSA). Several methods exist to qualitatively and quantitatively assess RSA [1], [2] since it is a recognized marker of cardiac autonomic function integrity. Standard power spectral density analysis of the tachogram has been extensively used to provide an index of sympathetic-vagal balance expressed as the ratio of low frequency (LF) and high frequency (HF) power components [3]. Although extension of the HF bandwidth to include the observed breathing frequency will ensure its positioning within the considered HF band, this will not isolate the respiratory-related component.

Mathematical methods have also addressed this issue by proposing a respiratory-based approach for the assessment of heart rate variability including breath-by-breath analysis of RSA [1], [4]–[6]. Investigation of RSA in clinical settings however may require rapid assessment of one course of RSA changes, such as resulting from drug administration, changes in breathing patterns or mechanical ventilation, or even from the onset of a clinical event. This requires a distribution or worded analysis [2]. However, few methods provide real-time information of heart rate or respiratory sinus arrhythmia variability [5].

We propose a new statistical method to provide quasi-real-time information on RSA based on a breath-by-breath fractional cardiac

cycle count. The proposed procedure provides 1) a graphical representation of RSA, either breath-by-breath or globally for a population of breaths (box plot), 2) a test for detecting the presence of RSA on a short time window (i.e.: five breaths), and 3) an index of the intensity and phase of RSA associated with each breath.

We applied this technique to data obtained from 16 healthy volunteers (mean age 23 \pm 5 yrs) and compared results with those obtained using standard spectral analysis of heart rate variability. Imposed breathing being commonly used in spectral analysis of heart rate variability to ensure bandwidth of the respiratory frequency within the standard HF bandwidth and to minimize spectral power dispersion, we examined RSA both during spontaneous and imposed breathing conditions. Because the extent of RSA is dependent upon respiratory frequency [2], we selected to impose a breathing rate equal to the spontaneous breathing frequency.

II. DATA ACQUISITION AND ANALYSIS

Two 5-min recordings of airflow (French Head no. 1 mounted on a face mask) and ECG were obtained in each subject. The first recording was obtained after a 2-min acclimatization period with subjects breathing quietly at their spontaneous breathing rate. The second recording was obtained while subjects were asked to follow a breathing rate given by an auditory cue, at the breathing rate corresponding to each subject's spontaneous rhythm.

Acquisition of data was performed on a Macintosh microcomputer equipped with an analog-digital interface card. Sampling rate was 256 Hz. Heart rate, mean RR interval and the standard deviation of the RR intervals or RR intervals were linearly interpolated at 0.2-s intervals. Heart rate values or RR intervals were then interpolated at 0.2-s intervals using a spline approximation of at least 1024 sample points. A fast Fourier transform procedure was applied to obtain spectral power component: LF (0.04–0.15 Hz), HF (0.15–0.40 Hz) and a restricted respiratory frequency power component identified as the respiratory component frequency (RCF) was also calculated using the frequency range corresponding to $\pm 10\%$ of the respiratory rate averaged over the entire recording. Definition of an RCF band using limits of ± 0.02 Hz [7] or assessment of spectral power at the influence of RSA, We [8] have previously been used to isolate the influence of RSA. We selected to delimit the respiratory band in keeping with the generally accepted margin of biological variability.

III. NEW STATISTICAL METHOD

A. Fractional Cycle Count and Instantaneous Heart Rate

The basis of our method is the fractional count of cycles. Let t_0, t_1, \dots, t_n be the sequence of heartbeats instants. We considered the i th cycle $[t_{i-1}, t_i]$ as the interval between two consecutive heartbeats. The window $[t_{i-1}, t_i]$ is counted the number of cycles within the window, the cycle $[t_{i-1}, t_i]$ is counted as one if $T_i \leq t_i - t_{i-1} < t_i - t_{i-1}$, as $(t_i - t_{i-1}) / (t_i - t_{i-1})$ if $T_i \leq t_i - t_{i-1} < t_i - t_{i-1}$, as $(T_i - t_{i-1}) / (t_i - t_{i-1})$ if $T_i > t_i - t_{i-1}$ and as $(T_i - t_{i-1}) / (t_i - t_{i-1}) - 1$ if $T_i > t_i - t_{i-1}$. In this figure the total cardiac count in the window is 8.4364, but if heartbeats were counted, one would get eight. The advantage of a

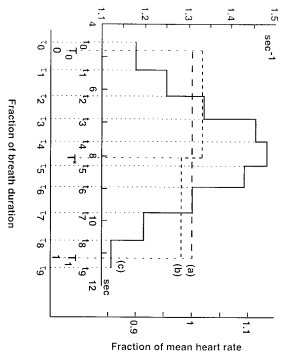


Fig. 1. Fractional cardiac cycle count. T_i , T_i^* and T_i indicate the heartbeats instants, t_{i-1} and t_i are the instants of the i th heartbeats. T_i^* , \dots , T_i are the fitting in fraction of breath duration. (a) mean heart rate over the window, (b) mean heart rate over half windows, and (c) instantaneous heart rate.

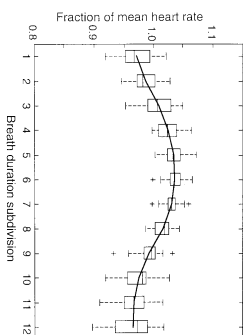


Fig. 2. Box plot of mean relative heart rate for each breath. Each box plot is from a sample of real data from Fig. 3. The median, first, and third quartiles as well as the minimum, maximum, and outlying values (\pm) are plotted over the reality of respiratory cycles are represented at each breath subdivision. The relative heart rate is plotted over the relative heart rate during the respiratory cycle.

cardiac cycle count over a heartbeat count becomes apparent if we consider the two half-windows $[T_i, T_i^*]$ and $[T_i^*, T_i]$. The number of beats for each is four, whereas the cycle count yield 4.2977 and 4.1387, respectively.

Having defined the cycle count within a window, we define the mean heart rate as the ratio of this count to the total window length. The mean heart rate in the half windows $[T_i, T_i^*]$ and $[T_i^*, T_i]$ are similarly defined. In Fig. 1 these rates are traced as a dashed horizontal line (Fig. 1(a)) and a step-like line (Fig. 1(b)). By shrinking the analysis window to a point, we obtain the *instantaneous* heart rate. It is represented by the solid, step-like line in Fig. 1(c). This representation shows clearly that the heart beats fastest around the middle and slowest around the end of the window.

Figure 1(c) also makes this line and above the zero reference axis denoted as T_i and T_i^* as the relative heart rate. The relative heart rate is defined by any window boundaries similarly is equal to the cycle count within the window. We could in fact use this equality to define the cycle count.

B. Relative Heart Rate and RSA

In studying RSA, one must take into account the possibility of a gradual drift in heart rate through the course of the experiment. The relative heart rate is defined as the ratio of the heart rate to the mean rate over a given window, implicitly standardizing the data, suppressing low-frequency variations and thus can be an alternative to detrending procedures. In order to study RSA we chose one breath-span as a window. Relative heart rate data from each breath can also be pooled for between-recording comparisons. To this end it is preferable to normalize breath duration to one, by expressing time within each breath as a fraction of total breath duration.

A simple way to get a picture of within-respiratory cycle variability is to subdivide the breath into subdivisions of equal length and look at the relative mean heart rate in each subdivision. The number of subdivisions should provide a tradeoff between better resolution and less statistical variability. If a large number of breaths are available, one could consider the subdivision and average the relative heart rates associated with each subdivision. A useful statistical tool for

displaying a population graphically is the box plot [9]. This plots the median, the first and third quartiles, the minimum and maximum and some of the outlier points, if any, of the population. An example of box plots is shown in Fig. 2. On the other hand, if one is only interested in detecting the presence of RSA, one may subdivide the window into two halves and compare the relative mean heart rate in each half. In Section III-C, a test for arrhythmia based on this idea will be detailed.

C. Testing for Arrhythmia: The Wilcoxon Signed Rank Test

The idea of the test is to look for a systematic pattern in relative heart rate variations within a breath. To be specific, let $r(t)$, $r \in [0, 1]$ be the relative instantaneous heart rate in a normalized breath (thus r denotes the time as a fraction of the breath duration). This is a piecewise constant function with jumps at heartbeat times. We consider a contrast defined as a function $\{r(t), r \in [0, 1]\}$ with zero integral. Then we define the statistic $T = \int_0^1 r(t)^2 / (r(t) - \bar{r})^2 dt$. By construction $T = 0$ if $r(t)$ is constant. If the pattern of heart rate variation is random from one breath to the next, then one would expect T to be negative or positive with equal probability. If T were positive more often than negative, then this would be an indication of some systematic pattern in the pattern of cardiac rhythm and that of the contrast.

To test for RSA we could use the Student test for the hypothesis that the expected value of T is zero against the alternative that it is positive. However, the distribution of T is not normal. The test involves the Central Limit Theorem. Since, neither assumption can necessarily be met, a nonparametric test is preferable. No particular assumption is required except that the statistics T corresponding to different breaths are independent. It is quite plausible that the heartbeat periods in one breath are independent from those in another. Even if there may be some dependence because some cardiac cycles stretch over two consecutive breaths, one can expect that it is fairly slight. In this nonparametric setup we test the null hypothesis $H_0: T \leq 0$ against the alternative that $H_1: T > 0$. The Wilcoxon signed rank test is a statistical test for the null hypothesis $H_0: T \leq 0$ against the alternative that $H_1: T > 0$. Let T_1, \dots, T_m be obtained from m breaths and R_i be the rank of $|T_i|$, $i = 1, \dots, m$. The Wilcoxon signed rank test rejects the null hypothesis if the rank sum

Manuscript received November 18, 1998; revised March 22, 1999. Asterisk indicates corresponding author.

This work was supported in part by the Laboratoire de Médecination et de Cardiologie, Université Joseph Fourier, 38041 Cedex, Grenoble, France. H. Pernati was with Laboratoire de Psychologie Respiratoire Expérimentale, Théorique et Appliquée (PRETA-TIMC), UMR CNRS 5252, Centre de Recherche de Grenoble, Université Joseph Fourier, 38000 Grenoble, France. S. Bencherif is with the Laboratoire de Psychologie Respiratoire Expérimentale, Théorique et Appliquée (PRETA-TIMC), UMR CNRS 5252, Centre de Recherche de Grenoble, Université Joseph Fourier, 38000 Grenoble, France. P. Calhèse is with the Laboratoire de Psychologie Respiratoire Expérimentale, Théorique et Appliquée (PRETA-TIMC), UMR CNRS 5252, Centre de Recherche de Grenoble, Université Joseph Fourier, 38000 Grenoble, France. *G. Bencherif is with the Laboratoire de Psychologie Respiratoire Expérimentale, Théorique et Appliquée (PRETA-TIMC), UMR CNRS 5252, Centre de Recherche de Grenoble, Université Joseph Fourier, 38000 Grenoble, France. E-mail: gilab@lepr.ujf-grenoble.fr.

Publisher Item Identifier S 0018-9294/99/091610-X.

0018-9294/99/09161000 © 1999 IEEE

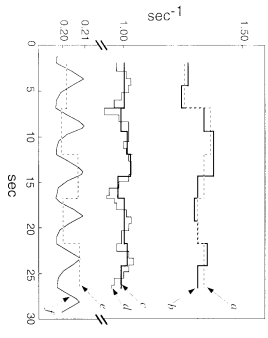


Fig. 3. Processing of a sample of data taken over 30 s. Graphical representation of (a) mean heart rate per breath, (b) mean heart rate per half-breath, (c) respiratory frequency, and (d) volume expressed in arbitrary units.

$S = \sum_{i=1}^n r_i < T_i$ over the set of indexes i for which T_i is negative does not exceed some critical threshold, determined to meet a desired statistical significance level. This test can be computed through a convolutional algorithm, at least for small values of n . Note that this test is not applied to the original sample r_i and T_i (see Fig. 10), which also provides tables of significance levels. Note that since the threshold is necessarily an integer, not all these levels can be selected.

Since we are interested in quasi-real-time detection of arrhythmias, we consider small values of m and we choose $m = 5$ since this leads to a significance level close to the customary 5% for the threshold one. The exact level is 6.25%, which can be computed straightforwardly.

1) Test Based on Half-Respiratory Cycle Mean Heart Rate Comparisons (Test A): This test uses the simple contrast which equals one in the first half of the window and -1 in the other half. The test statistic T is simply the difference between the relative mean heart rate in the first and the second half of the breath. Thus, the test would detect RSA if it results in that the heart beats faster in the first than in the second half of the breath. Fig. 3 shows processing of a sample of data taken over a 30-s recording. An application of test A on a 30-s sample of the data presented in Fig. 3 is shown in Fig. 4(b).

2) Test Using the Heart Rate and Respiratory Volume Signals (Test B): The aspect of test A is its simplicity and that the only extra information it needs is the overall duration. But it is based on the relative mean heart rate, not on the absolute heart rate. This is not the case in the first half and a decrease in the second half of the breath. However, in our experience, it appears in some instances that the inspiration/duration/heart duration is such that the maximum heart rate occurs around the middle of the breath so that the mean heart rate in the two halves are roughly the same. Test B avoids this difficulty by exploiting the extra information provided by the respiratory volume. It is based on the contrast $c(T) = V(T) - \int_0^T V(\tau) d\tau$ where $V(T)$ is the volume signal at normalized time expressed as a fraction of total breath duration. In our experiments, since we consider the volume only at heartbeat time t_i , we take the volume between these beats as at the heart of the preceding beat. Thus our $V(\tau)$ lags somewhat behind the real volume signal but since the heart rate also lags behind the latter, this constant amount) to the relative instantaneous heart rate within the respiratory cycle. The "average" $\int_0^T V(\tau) d\tau$ then becomes $V(t_0)(T-t_0) + \dots + V(t_{n-1})(t_n - t_{n-1}) + \Delta t \sum_{i=1}^n V_i$ where $\Delta t = (t_n - t_0)/n$ and $V_i = V(t_i)$.

3) Test Using the Heart Rate and Respiratory Volume Signals (Test C): This test uses the simple contrast which equals one in the first half of the window and -1 in the other half. The test statistic T is simply the difference between the relative mean heart rate in the first and the second half of the breath. Thus, the test would detect RSA if it results in that the heart beats faster in the first than in the second half of the breath. Fig. 3 shows processing of a sample of data taken over a 30-s recording. An application of test A on a 30-s sample of the data presented in Fig. 3 is shown in Fig. 4(b).

4) Test Using the Heart Rate and Respiratory Volume Signals (Test D): This test uses the simple contrast which equals one in the first half of the window and -1 in the other half. The test statistic T is simply the difference between the relative mean heart rate in the first and the second half of the breath. Thus, the test would detect RSA if it results in that the heart beats faster in the first than in the second half of the breath. Fig. 3 shows processing of a sample of data taken over a 30-s recording. An application of test A on a 30-s sample of the data presented in Fig. 3 is shown in Fig. 4(b).

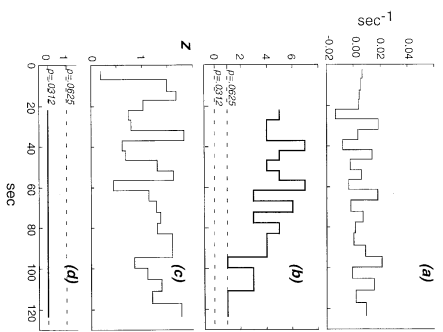


Fig. 4. Two test-statistics of RSA plotted against time. (a) Differences in mean heart rate in two half-breaths, (b) the corresponding Wilcoxon signed-rank statistic, (c) the sum of ranks of negative differences over two consecutive breaths, and (d) the test statistic based on the volume signal. The lower and upper dotted lines indicate the significance probabilities of the test statistic: 3.125% and 6.25%, respectively.

$t_0 = \Delta t \cdot i_0 + 1$ and $t_i = \Delta t \cdot i_i + 1$ denote the heartbeat times within the breath. a_i and b_i are the fractions of the first and last cardiac cycle within i and $n = i_0 + 1 + \dots + i_i + 1$ is the fractional cardiac cycle count. Under the null hypothesis of no RSA, the resulting statistics T associated with successive breaths are still independent, hence the Wilcoxon test remains valid. Note that these statistics can be regarded as the correlations between the instantaneous heart rate and the volume signal, up to a constant factor, computed at different breaths. They may be used to assess the dependence between the two signals. For accurate assessment one should apply the Fisher's z transformation [11] to the correlation coefficient to obtain a statistic with a distribution closer to the Gaussian and a standard deviation which is constant over the whole set of breaths. The parameters of the fitting curve are then estimated (see Section 4 for the details) by the method of least squares. Fig. 4(d) shows the application of this test to the data presented in Fig. 3.

D. Amplitude and Phase of RSA Based on Sinusoidal Fitting to the Relative Heart Rate

To obtain a quantitative description of the heart rate variations within each breath, we attempted to fit a sinusoid (shaded by a constant amount) to the relative instantaneous heart rate within the respiratory cycle. A shaded sinusoid is represented by $c \cos(2\pi f t + \text{phase}) + c$, where a , b , and c are coefficients and the variable t

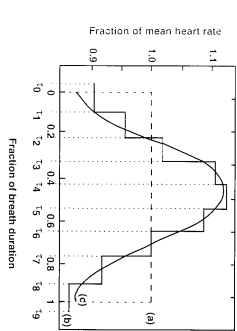


Fig. 5. Sinusoidal fitting to the relative heart rate. (a) Relative mean heart rate over the window, (b) relative instantaneous heart rate, and (c) the sinusoid fit. The deviation of the relative instantaneous heart rate from the mean heart rate.

denotes the normalized time within the breath. The above coefficients will be adjusted such as to provide the best possible fit of the sinusoid to the observed relative instantaneous heart rate curve $\{r_i(t_i), t_i \in [0, 1]\}$, but since the latter is a piecewise constant curve with jumps at the heartbeat times, we first replace the sinusoid by an equivalent piecewise constant curve $\{r_i(t_i), t_i \in [0, 1]\}$ (with the same jump times as the original curve). The sinusoid is then fitted by the method of least squares and two consecutive heartbeats are equal to those under the minimizing $\int_0^1 (r_i(t_i) - c \cos(2\pi f t + \text{phase}))^2 dt$. Details on this minimization (which does not require integrations) are omitted (but can be obtained from the author by request) to save space. The parameter c is found to be always equal to one which is to be expected, since $r_i(t_i)$ is a relative rate.

It is of interest to rewrite the fitted curve as $1 + A \cos(2\pi f t + \phi)$ where $A = \sqrt{a^2 + b^2}$, which can then be used as an index of the intensity of RSA, and $\phi = \arctan(b/a)/(2\pi)$, which indicates the point at which the maximum heart rate value is reached within each breath. They can be averaged over different populations of breaths and standard statistical tests can be performed to test for differences between these populations.

To assess the goodness of our fit, we compare the relative instantaneous heart rate $r_i(t_i)$ (not with the fitted curve but with the equivalent piecewise constant curve, $\delta(t_i)$, described as above. We then test for the non-response of the relative error (SSE), and the sum of squares of errors (SSE), similar to those in analysis of variance: $SST = \sum_{i=1}^n (r_i(t_i) - c)^2$, $SSR = \sum_{i=1}^n (\delta(t_i) - c)^2$, and $SSE = \sum_{i=1}^n (r_i(t_i) - \delta(t_i))^2$. The first sum of squares equals the sum of the linear AIC can be computed as sums and not integrals.

The sinusoidal curve possesses three degrees of freedom, corresponding to the three coefficients a , b , and c . Hence, the "effective" degree of freedom for SSE may be taken as the fractional cardiac cycles count in the breath minus three. The square root of the ratio of SSE to this number can thus be taken as an estimation of the standard deviation of the error. This can be useful in assessing the true magnitude of RSA. However, we would refrain from performing an F test based on the above SSR and SSE since the Gaussian model conditions of the analysis of variance are not fulfilled and the "sample size" is often too small. The time evolution of amplitude and phase of RSA computed from the data of Fig. 3 is shown in Fig. 6. An estimate to the error based on the SSE is also presented.

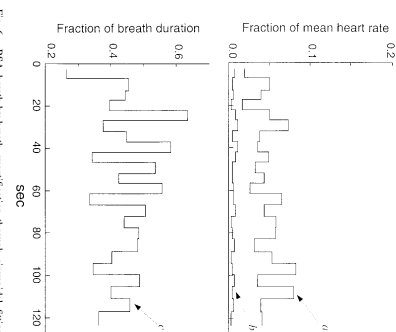


Fig. 6. RSA breath-by-breath quantification through sinusoidal fitting (as explained in Fig. 5). (a) Amplitude of the sinusoid fitted to the deviation of the relative instantaneous heart rate from the mean heart rate expressed in fraction of the mean heart rate, (b) phase of the sinusoid, (c) estimate of standard deviation of the fraction of the mean heart rate, and (d) phase of the same fitted sinusoid, in fraction of breath duration.

IV. RESULTS AND DISCUSSION

A. Testing for Respiratory Sinus Arrhythmia

Results indicate that a RSA is significantly detected in approximately 40% of recording duration using test A. In test B based on both time events and volume signal, not only the resulting event but also the associated volume signal can be detected. As soon as exactly 83% of recording duration by test B thus indicating a higher sensitivity compared to test A. This is in agreement with the accepted view that lung volume is an important determinant of RSA [12] but does not express a causal relationship between lung volume and cardiac cycle duration.

In practice, when only breathing rate is available, test A based on time events only can be used. A similar test has been proposed by Pontieri *et al.* [5] using a circular statistical analysis applied to ECG and ventilation followed by Rayleigh's test for randomness.

B. Quantifying Respiratory Sinus Arrhythmia

Variations in the magnitude of RSA have been shown to reflect modulations in parasympathetic tone to the sinus node [2] and have been widely used as an indicator of impaired autonomic regulation of the heart rate [13]. The newly proposed method enables quantification of the respiratory-related heart rate variability or RSA since it is based on a respiratory cycle window. Examination of cardiac cycle length variability over a respiratory cycle window enables determination of "fractional heart rate count over each given window." The analysis of RR interval length indexes the degree of the RR intervals from their sequence number disregarding the information

pertinent to timing of occurrence in the series. Several studies have examined the relationship between RSA and heart rate variability. RSA [2], [3], [13] and heart rate variability [14] were measured and related. The correlation between RSA and heart rate variability was found to be significant. The relationship between RSA and heart rate variability was found to be significant. The relationship between RSA and heart rate variability was found to be significant.

In the box plot representation, a fine subdivision of the breath is made into 12 subdivisions in Fig. 4 and relative heart rates pooled for a large number of breaths are represented in these subdivisions. This representation shows an overall picture of RSA for a given recording providing information on heart rate variations in each window, timing of the highest heart rate within the breath and the amplitude of the heart rate change.

In our analysis, relative heart rate during a breath was found to be reasonably well fitted by a sinusoidal curve, as can be seen in Fig. 6(b). The sinusoidal curve fitting error which was generally found to be less than 10%. This sinusoidal curve fitting error was used as an index of RSA intensity for the breath and the phase as the time of occurrence of the highest cardiac rate in that breath. RSA amplitude expressed as fraction of mean heart rate ranged between 0.086 and 0.196 and mean RSA amplitude was not found to be significantly different between spontaneous or imposed breathing conditions (0.086 \pm 0.053 versus 0.094 \pm 0.048). Mean indices of RSA phase expressed as fraction of respiratory cycle duration) were similar under both conditions, values being 0.437 \pm 0.076 for the spontaneous and 0.437 \pm 0.093 for the imposed breathing condition. These observations indicate these indices to be insensitive to the scatter in breathing frequency as they are issued from a breath-by-breath based analysis.

Results indicate a positive linear correlation between the RSA amplitude and breath duration, in both spontaneous ($r = 0.55$) and imposed breathing conditions ($r = 0.72$) which is in keeping with the generally assumed relationship between breathing frequency and the amount of RSA [2].

C. Spontaneous Versus Imposed Breathing

Mean heart rate as well as the standard deviation of the mean heart rate were unchanged by the imposed breathing. In the present spectral analysis, a RCF band was introduced to better define the respiratory related heart rate variability. The spectral power of the RCF component was found to be greater under the imposed than the spontaneous breathing condition (0.0053 versus 0.0049) which is a significant difference ($p < 0.05$) as determined by the F -test. This difference was not observed for the mean HF power component (0.0026 versus 0.0019 e^2 , respectively). From a methodological standpoint the present results indicate that the selection of a bandwidth centered around $\pm 10\%$ of the respiratory frequency only allows to capture the heart rate variability associated with respiration and is thus a better marker of RSA than the HF band.

RSA characteristics assessed by the statistical method were not affected by the imposed breathing condition as reflected by the similar proportion of RSA detection (Test B: 83.71% \pm 28% versus 79.72% \pm 37.5%), RSA amplitudes (0.086% \pm 0.053% versus 0.094% \pm 0.048%), and phases (0.43% \pm 0.08% versus 0.43% \pm 0.09%). These observations may be taken to suggest that RSA is influenced more by the breathing frequency per se than the voluntary modulation of respiratory drive.

V. CONCLUSION

In this paper, we have presented a comprehensive statistical method for the assessment of heart rate variability of a respiratory origin. Results from the present study indicate this method to be a valuable tool allowing for quasi-real-time monitoring of RSA which does not require the pattern of breathing to be controlled. Despite the large number of degrees of freedom, the curve is found to fit well to the heart rate variations within a breath and the method allows to pinpoint this method presents the advantage of allowing for a selective detection and quantification of the respiratory component of heart rate variability.

REFERENCES

- [1] P. Grossman, J. Van Ruck, and C. Whipple, "A comparison of three quantification methods for estimation of respiratory sinus arrhythmia," *Psychophysiol.*, vol. 27, pp. 702-713, 1990.
- [2] D. Eckhart, "Respiratory sinus arrhythmia and other human cardiacs," *York Medical Dictator*, 15, pp. 669-740, 1995.
- [3] J. Alami and O. Schmitt, "Basic technology of voluntary cardiorespiratory synchronization in electrocardiology," *IEEE Trans. Biomed. Eng.*, vol. BME-27, pp. 289-293, July 1974.
- [4] M. Zappalà, J. J. Coenen, and J. N. Snelton, "Respiratory response curve analysis of heart rate variability," *IEEE Trans. Biomed. Eng.*, vol. 44, pp. 321-325, Apr. 1997.
- [5] C. Fontana, J. J. Coenen, and T. Healy, "Respiratory sinus arrhythmia: An analysis of the relationship between respiratory and heart rate variability," *Psychophysiol.*, vol. 33, pp. 100-104, 1997.
- [6] J. Friedman, M. Perrot, R. Cohen, and J. Snel, "Respiratory sinus arrhythmia: Time domain characterization using autoregressive moving average analysis," *Amer. J. Physiol.*, vol. 268, pp. H223-H228, 1995.
- [7] C. Hagenwiler, J. Bannier, M. Ad, and A. Proy, "Modulation of respiratory sinus arrhythmia by breathing pattern," *Clin. Sci.*, suppl. 91, pp. 40-42, 1996.
- [8] J. Hayano, Y. Sakakima, A. Yamada, M. Yamada, S. Makai, T. Fujiwara, K. Yokoyama, Y. Watanabe, and K. Takano, "Accuracy of analysis," *Amer. J. Cardiol.*, vol. 67, pp. 199-204, 1991.
- [9] J. T. Fildes, *Empirical Data Analysis*. Reading: MA: Addison-Wesley, 1977.
- [10] E. Lehmann and H. D. Ahrens, *Neurophysiologie, Statistische Methoden*. Berlin: Springer-Verlag, 1975.
- [11] G. Snedecor and W. Cochran, *Statistical Methods*, 7th Edition, Ames, IA: Iowa State Univ. Press, 1980.
- [12] M. de Borge, PhD, "Interactions between respiration and circulation," in *Respiratory Physiology: A Practical Approach*, ed. J. R. Stradford, C. B. Parrish, Bethesda, MD: Amer. Physiol. Soc., sect. 3, ch. 16, pt. 2, vol. II, pp. 559-594, 1986.
- [13] P. Knaouf and F. Ah, "Respiratory sinus arrhythmia: Noninvasive measure of prehypertensive cardiac control," *J. Appl. Physiol.*, vol. 39, pp. 801-805, 1975.

II.4.3.2 Evaluation des variations du volume cardiaque à partir de mesure par pléthysmographie respiratoire à variation d'inductance

Les signaux PRI de variations de section thoracique et abdominal au cours de la respiration, exhibent souvent de petits "accidents" (Figure 14) qui sont dus aux variations du volume provoqués par les battements cardiaques.

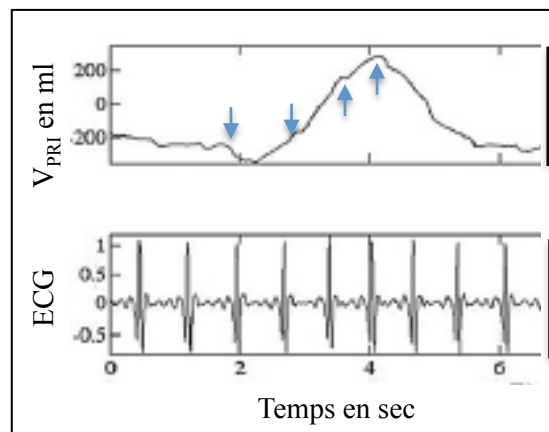


Figure 14 : Volume mesuré par PRI (V_{PRI}) et électrocardiogramme (ECG). Sur le signal volume les flèches indiquent les "accidents" dus aux variations du volume provoqués par les battements cardiaques en correspondance avec l'ECG.

Nous avons cherché à extraire cette information cardiaque en utilisant des méthodes temps-échelle de traitement du signal. Nous avons comparé les variations de volume dues aux battements cardiaques extraites du signal PRI avec les variations de volume d'éjection systolique mesurées par un cardiographe d'impédance sur 15 volontaires sains. Les enregistrements ont été effectués en position assise et couchée, au repos et au cours d'une manœuvre respiratoire (maintenir une pression en soufflant dans un manomètre à eau) qui a pour effet de diminuer le volume d'éjection systolique. Bien que la méthode PRI sous estime légèrement les variations de volume cardiaque, les résultats montrent que la méthode PRI détecte les variations de volume cardiaque engendrées par la manœuvre, et qu'il existe une corrélation significative et positive entre les volumes cardiaques évalués par la méthode PRI et mesurés par le cardiographe d'impédance.

Ces résultats suggèrent que la pléthysmographie respiratoire à variation d'inductance peut être utilisée pour détecter des variations de volume cardiaque chez les volontaires sains.

Fontecave-Jallon et al (2013) A Wearable Technology Revisited for Cardio-Respiratory Functional Exploration: Stroke Volume Estimation From Respiratory Inductive Plethysmography. Inter J EHealth and Med Com

Fontecave-Jallon et al (2013). Detecting variations of blood volume shift due to heart beat from respiratory inductive plethysmography measurements in man. Physiol Measu

Montage du dossier de demande de financement d'aide à l'innovation par Grenoble Alpes Valorisation Innovation Technologies (GRAVIT) en pré maturation et en maturation "Dispositif d'Exploration Cardiorespiratoire chez le Rongeur (DECRO)" -2011-2012 (acceptation en 2012)

II.5 APPROCHE THEORIQUE

Des modèles ont été utilisés dans l'objectif d'interpréter les données expérimentales mais aussi de formuler des hypothèses sur le fonctionnement 1/ de la mécanique ventilatoire et 2/ du générateur du rythme respiratoire.

II.5.1 Modèle simple de mécanique ventilatoire

Afin d'étudier les interactions entre les forces produites par les mouvements de la paroi thoracique lors de la ventilation, nous avons proposé un modèle basé sur le système de levier de [Hillman and Finucane \(1987\)](#) et introduit des propriétés dynamiques du système respiratoire. Les éléments passifs (thorax et abdomen) sont considérés comme étant des compartiments élastiques reliés à l'air libre par un tube résistif représentant les voies aériennes. La force développée par les muscles respiratoires (F_{mus}) agit sur les deux compartiments thoracique (RC) et abdominal (A). Ces deux compartiments sont représentés par deux ressorts caractérisés par leurs élasticités respectives E_A et E_{RC} . La résistance du système respiratoire est représenté par un amortisseur caractérisé par sa résistance visqueuse R . Chacun des trois éléments est fixé à une barre rigide non horizontale sur laquelle la force F_{mus} agit sur les éléments E_A , E_{RC} et R (Figure 15).

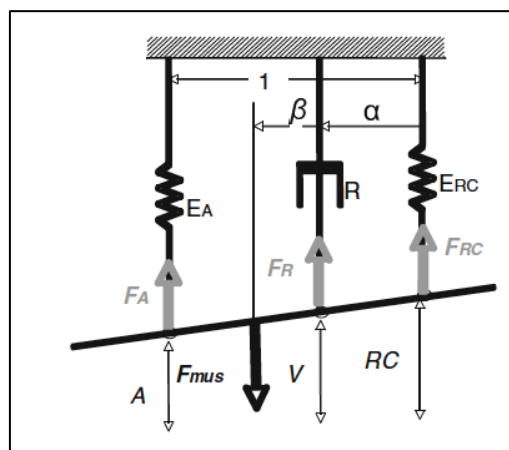


Figure 15 : Représentation du modèle simple de mécanique ventilatoire. RC : compartiment thoracique (ressort) d'élasticité E_{RC} ; A : compartiment abdominal (ressort) d'élasticité E_A ; R : résistance du système respiratoire (amortisseur) de résistance visqueuse R . F_{mus} : force développée par les muscles respiratoires sur une barre sur laquelle les trois éléments sont fixés.

Les paramètres du modèle ont été identifiés en utilisant les données enregistrées sur 11 volontaires sains dans cinq conditions : au repos et au cours de l'addition de quatre différents niveaux de résistance. Une analyse cycle par cycle montre que, pour un nombre important de cycles, le débit simulé par notre modèle s'ajuste avec celui mesuré par pneumotachographie avec un coefficient de détermination $\geq 0,70$ et ce, quel que soit le sujet ou la condition.

La comparaison des signaux débits ventilatoires, obtenus expérimentalement et par simulation, montre une bonne concordance. Ce modèle peut être utile pour interpréter les variations des caractéristiques des compartiments thoracique et abdominal au cours de la ventilation.

Calabrese et al (2010) A simple dynamic model of respiratory pump. Acta Biotheor.

Organisation du XXIX^{ième} séminaire de la Société Francophone de Biologie Théorique et coéditrice invitée pour la publication des actes de ce séminaire :

Calabrese P, Fontecave-Jallon J (Guest editors) (2010) Proceedings of the XXIXth Conference of the French-speaking Society for Theoretical Biology (St-Flour, France, 14-17 June, 2009) Acta Biotheor.

A Simple Dynamic Model of Respiratory Pump

Pascal Calabrese · Pierre Bacomnier · Aicha Laouani ·
Julie Fontecave-Jallon · Pierre-Yves Gannery ·
André Eberhard · Ghia Bencherit

Received: 1 June 2010 / Accepted: 28 June 2010 / Published online: 23 July 2010
© Springer Science+Business Media B.V. 2010

Abstract To study the interaction of forces that produce chest wall motion, we propose a model based on the lever system of Hillman and Finncane (J Appl Physiol 63(3):951–961, 1987) and introduce some dynamic properties of the respiratory system. The passive elements (rib cage and abdomen) are considered as elastic compartments linked to the open air via a resistive tube, an image of airways. The respiratory muscles (active) force is applied to both compartments. Parameters of the model are identified in using experimental data of airflow signal measured by pneumotachography and rib cage and abdomen signals measured by respiratory inductive plethysmography on eleven healthy volunteers in five conditions: at rest and with four level of added loads. A breath by breath analysis showed, whatever the individual and the condition are, that there are several breaths on which the airflow simulated by our model is well fitted to the airflow measured by pneumotachography as estimated by a determination coefficient $R^2 \geq 0.70$. This very simple model may well represent the behaviour of the chest wall and thus may be useful to interpret the relative motion of rib cage and abdomen during quiet breathing.

Keywords Respiratory pump model · Respiratory inductive plethysmography · Pneumotachography · rib cage · Abdomen

1 Introduction

The interaction of forces that produce chest wall motion is complex and not completely understood. This interaction has been studied for several years

P. Calabrese (✉) · P. Bacomnier · A. Laouani · J. Fontecave-Jallon ·
P.-Y. Gannery · A. Eberhard · G. Bencherit
Laboratoire TIMC-IMAG, UMR 5525, Pavillon Taillefer Faculté de médecine de Grenoble,
Université Joseph Fourier–Grenoble 1, CNRS, 38700 La Tronche, France
e-mail: Pascal.Calabrese@imag.fr

 Springer

(Agostoni and Mogroni 1966; Gilbert et al. 1981; Goldman and Mead 1973; Konno and Mead 1967; Sharp et al. 1975; Wade 1954).

Mathematical models are used to understand these interactions and the mechanics of respiratory system better. Hillman and Finncane (1987) have produced a simple model of the respiratory pump that “appears to be appropriate for most breathing maneuvers and allows predictions to be made of the effect on chest wall of changes in applied forces”. An advantage of this model compared with previous models (Macklem et al. 1979; Primitano 1982) and analyses (Loring and Mead 1982; Macklem et al. 1983; Mead et al. 1985) is that it provides a simple conceptual aid to understand how the motion of the chest wall observed at the body surface varies with changes in the active (muscle) and passive forces acting on it. The model is a lever system, represented by an imaginary bar on which forces act at four fixed sites. Although this model did not take into account the dynamic component of the system, it appears valid for different respiratory maneuvers and has the advantage of being simple and easy to use compared with other more complicated models of chest wall. One of these models (Macklem et al. 1983; Ward et al. 1992) divided the rib cage into two compartments, one that apposed to the lung and one that apposed to the diaphragm. Ricci et al. (2002) proposed a two-compartment model of the inspiratory pump, which used a realistic modelisation, distinguishing an active, an elastic and a viscous component. Their model parameters identification derived from actual measurement obtained by magnetic resonance imaging in normal humans.

We developed a simple dynamical model of respiratory pump based on the lever system of Hillman and Finncane (1987). We used experimental data provided by (1) respiratory inductive plethysmography (RIP), a noninvasive method of measurement of the rib cage and abdomen cross sectional area changes, which allows to estimate by a linear combination breathing volume changes (Konno and Mead 1967) and (2) pneumotachography, to calculate model parameters at rest and at four levels of added resistive load.

The fit between the airflow simulated by our model and the airflow measured by pneumotachography was estimated by the determination coefficient.

2 Methods

2.1 Description of the Model

Our model is based on the lever system proposed by Hillman and Finncane (1987) and introduces some dynamic properties of the respiratory system. Roughly, the respiratory system can be divided into the rib cage and abdominal elements, considered as passive, and the active respiratory muscles. The passive elements are considered to be elastic compartments linked to the open air via a resistive tube, an image of airways. The respiratory muscles force is applied to both compartments.

This simplified representation of the respiratory system is modeled in the following way (Fig. 1). The passive elastic rib cage and abdominal compartments are represented by two springs characterized by their elasticity (respectively E_{rc} and E_{a}). The resistances of respiratory system are represented by a dashpot

 Springer

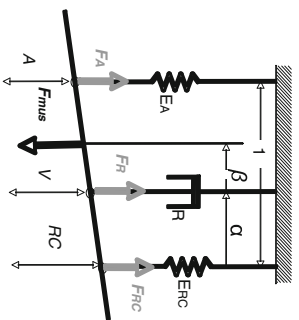


Fig. 1 Mechanistic representation of the respiratory pump

(characterized by its viscous resistance R). All three elements are attached to a rigid roof. The respiratory muscles force (F_{mus}) is applied to this system through a stiff bar without inertia sliding on the bottom ends of the springs and the piston.

Cross sectional area changes of abdomen (respectively rib cage) are represented by changes of the vertical position of the bottom end of the springs and the dashpot of any point of the bar is a linear combination of A and RC . The dashpot is attached to the bar at the point where this linear combination corresponds to the one used for the estimation of breathing volume changes from rib cage and abdomen cross sectional area changes provided by respiratory inductive plethysmography (RIP) measurement. Then, the vertical displacement of the bottom end of the dashpot represents volume changes (V).

In reaction to the respiratory muscles force (F_{mus}), three forces are opposed: two elastic tension forces of the springs (F_{rc} and F_{λ}) and the viscous resistance force (F_R) of the dashpot. Some simplification allows to minimize the number of parameters. The simplifications that have been taken into account are: the displacements are parallel and vertical, and the horizontal distance between abdominal and rib cage elements is normalized ($=1$). There are two geometric parameters (1) α the horizontal distance between the dashpot and the "rib cage" spring with $0 < \alpha < 1$ and (2) β the horizontal distance between the dashpot and the application point of F_{mus} , with $\alpha - 1 < \beta < \alpha$, and three mechanical parameters, namely rib cage (E_{rc}) and abdominal (E_{λ}) elasticity and respiratory resistance (R).

2.2 Equations of the Model

By construction of the geometric properties of the model, vertical displacement of the bottom end of the dashpot is a linear combination of vertical displacements of the bottom end of abdominal (respectively rib cage) spring A (respectively RC) (Eq. 1).

$$V = \alpha A + (1 - \alpha)RC \quad (1)$$

The viscous resistance force (F_R) is in the opposite direction to the direction of displacement of the lower end of the dashpot, and is the product of the simulated flow (dV/dt) and the viscous resistance of the dashpot (R) (Eq. 2).

$$F_R = -R \frac{dV}{dt} \quad (2)$$

The elastic tension forces of the springs (F_{rc} and F_{λ}) are in the opposite direction of the deformation of the spring, and also the product of the elastances (E_{rc} and E_{λ}) characterizing the springs and the displacement of the springs (Eqs. 3, 4).

$$F_{rc} = -E_{rc}RC \quad (3)$$

$$F_{\lambda} = -E_{\lambda}A \quad (4)$$

In rotational dynamics, if a rigid body is submitted to several forces, the resulting moment of all forces exerted on the rigid body is equal to the product of its angular acceleration and its moment of inertia. In our model, we have stated that the bar has no inertia. It follows that the resulting moment of all forces on the bar is null, and this is true whatever the rotation point considered.

Then, the resulting moment of all forces applied on the bar relative to the application point of F_{mus} is null (Eq. 5).

$$\beta R \frac{dV}{dt} + (\alpha + \beta - 1)(E_{\lambda}A) + (\alpha + \beta)(E_{rc}RC) = 0 \quad (5)$$

The derivative of V is consequently a linear combination of A and RC (Eq. 6) and, if the model is valid, in the true respiratory system the flow should be a linear combination of abdomen and rib cage cross sectional areas.

$$\frac{dV}{dt} = \frac{(1 - (\alpha + \beta))E_{\lambda}A}{\beta R} - \frac{(\alpha + \beta)E_{rc}RC}{\beta R}$$

which may be written

$$\frac{dV}{dt} = K_A A + K_{rc} RC \quad (6)$$

with

$$K_A = \frac{(1 - (\alpha + \beta))E_{\lambda}}{\beta R} \quad (7)$$

$$K_{rc} = -\frac{(\alpha + \beta)E_{rc}}{\beta R} \quad (8)$$

2.3 Validation with Experimental Data

Experimental data from recordings on eleven healthy volunteers (8 female, 3 male) were used to calculate the coefficients K_A and K_{rc} of Eq. 6. The healthy volunteers were between 19 and 55 years old (mean \pm SD): 28.5 ± 12.6 . The weight varied

between 46 and 87 kg (mean \pm SD: 61.6 \pm 10.6) and the height was between 154 and 185 cm (mean \pm SD: 168 \pm 10).

Airflow was recorded with a pneumotachograph (Fleisch head no. 1) placed on a face mask and a differential transducer (163PC01D36, Micro Switch). Mouth pressure was measured with a differential pressure transducer (142PC01D, Micro Switch). Leaks from around the mask were checked for before the recording was initiated using an infrared CO₂ analyser (Engstrom ElizalEliza MC), Rtb cage and abdominal signals were recorded by inductive plethysmography (Viasresp, RBF[®]).

Subjects were comfortably seated in a quiet room and were asked to relax and to breathe freely. The recording was performed with eyes open and lasted about 5 min for each of the five conditions: at rest and with four level of added loads. Data acquisition was started approximately 1 min after the addition of the resistance. Resistive loads were added throughout the entire breath and for each recording, the value of the resistance was calculated from the mouth pressure versus flow plot throughout the total recording. The mean value (\pm SD) for all resistances on the 11 subjects were at rest $R_0 = 0.75$ (± 0.03) for the apparatus resistance, $R_1 = 3.26$ (± 0.25), $R_2 = 5.27$ (± 0.34), $R_3 = 8.23$ (± 0.43) and $R_4 = 12.26$ (± 0.63) cm H₂O l⁻¹ s. The recordings were performed in a random order unknown to the subject and on two subjects (#4 and #10) only four recordings were performed (Calabrese et al. 2000).

K_A and K_{rc} of Eq. 6 were estimated breath-by-breath with a multiple linear regression using the airflow signal measured by pneumotachography, rib cage (RC) and abdominal (A) signals. Then the flow estimated by the model (dv^*/dt) (Eq. 6) and the determination coefficients R^2 were calculated breath-by-breath for the evaluation of the level of fit between experimental flow measured by pneumotachography and flow estimated by the model.

We have arbitrarily fixed at 0.70 the threshold above which we consider that a breath complies with the model ($R^2 \geq 0.70$). Figure 2 is an example of measured

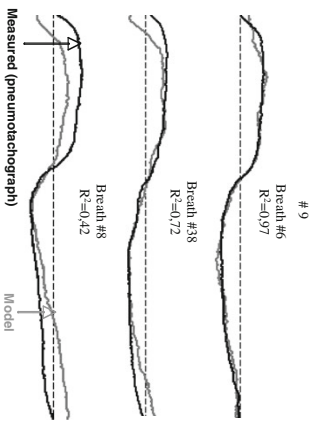


Fig. 2 Airflow measured by pneumotachography (*dotted line*) and airflow calculated with the model (*solid line*) for subject 9 at rest (R_0) for 3 breaths yielding different values of determination coefficient R^2

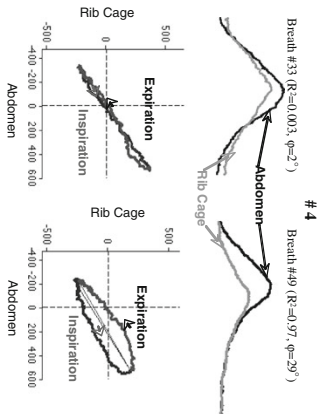


Fig. 3 Rib cage and abdomen signals recorded with RFP, and rib cage versus abdomen plots in arbitrary units. Two breaths are represented for subject 4 with the corresponding determination coefficient R^2 and phase difference ϕ

and reconstructed flows signals from five breaths with different R^2 of subject 9. Mean values of K_A and K_{rc} are calculated only on breaths with $R^2 \geq 0.70$.

Abdominal and rib cage signals from RFP on one hand and airflow from pneumotachography on the other hand are used to estimate K_A and K_{rc} values. However, if rib cage and abdomen signals are closely in phase, such parallel changes introduce indcision in the in the multiple linear regression calculation (badly conditioned matrix) and may decrease the determination coefficients R^2 . Phase differences were therefore calculated from rib cage versus abdomen plots (Lissajous curves) in order to estimate the amount of these parallel changes (Agostoni and Moggiotti 1966). The phase difference is expressed as angle ($^\circ$). Indeed, in Fig. 3 where are presented rib cage versus abdomen plots for two breaths from one recording along with the value of R^2 , one can see that a higher value of the phase difference (9°) is associated with a high value of R^2 . For breath #33, the phase difference is 2° and the fit as evaluated by R^2 is very poor ($R^2 = 0.003$), whereas for breath #49 a high phase difference (29°) is associated with a good fit ($R^2 = 0.97$).

3 Results

The results of the fit between the recorded flow signal and the model flow signal are gathered in Table 1 for all subjects and for all five conditions. For each recording two groups have been considered according to the value of the determination coefficients R^2 . For each resistance, the number of breaths in the group with $R^2 \geq 0.70$ followed by the number of breaths in the group with $R^2 < 0.70$ are given in the upper line. The mean value of phase difference ($^\circ$) for each group is given in the lower line.

Table 1 Number of breaths with $R^2 \geq 0.70$ (first number) and with $R^2 < 0.70$ (second number)

Subjects	#1	#2	#3	#4	#5	#6	#7	#8	#9	#10	#11										
R_0	n 31	44	13	63	1	67	47	15	27	28	27	5	76	16	49	60	3	0	41	1	75
φ	21	16	11	5	11	6	15	8	11	9	16	12	25	7	20	14	29	18	5	8	2
R_1	n 23	40	7	67	2	68	49	23	34	17	13	25	1	72	10	41	58	5	43	7	43
φ	17	10	12	8	22	6	15	9	19	13	18	15	42	12	18	13	34	25	14	9	14
R_2	n 5	49	10	56	1	52	55	12	39	13	20	11	2	68	5	41	60	3	3	36	57
φ	17	9	12	6	16	8	14	10	21	9	18	10	34	10	19	8	33	23	25	12	13
R_3	n 4	36	11	51	4	60	53	14	41	7	33	26	0	64	5	34	53	4	9	28	33
φ	19	10	12	6	20	8	20	12	19	10	22	16	8	19	8	38	29	33	21	13	8
R_4	n 4	36	12	50	4	57	5	13	16	5	68	8	25	33	13	18	14	34	3	3	3
φ	23	7	18	8	19	7	25	18	23	13	17	10	31	9	33	20	31	22	20	7	7

Above are the corresponding mean values (in italics) of the phase difference (φ) for all subjects and all resistances (R_0, R_1, R_2, R_3, R_4)
^a Missing recording

The number of breath with $R^2 \geq 0.70$ is higher than $R^2 < 0.70$ in subjects #4, #5 and #9.

The number of breath with $R^2 \geq 0.70$ increases with the load in subjects #5, #10 and #11 (up to R^2 only).

On the whole, $R^2 \geq 0.70$ for 1,193 breaths while $R^2 < 0.70$ for 1,778 breaths. One can see that for each condition and all subjects, the mean value of the phase difference is higher for the group of breath with $R^2 \geq 0.70$ than for the group of breath with $R^2 < 0.70$. Phase difference versus R^2 plots for each subject and all resistances show a significant positive correlation in all subjects.

Figure 4 is the plot of the mean values of K_A and K_{rc} calculated for each condition on those breaths with $R^2 \geq 0.70$. At a given condition, K_A and K_{rc} have opposite signs. K_A and K_{rc} increase or decrease (according to their sign) with increasing added load approaching zero at the highest added load.

In our model, K_A/K_{rc} ratio is mathematically independant of R (from Eqs. 7 to 8):

$$-K_A/K_{rc} = \frac{(1 - (\alpha + \beta))E_A}{(\alpha + \beta)E_{rc}} \tag{9}$$

We have calculated this ratio for each subject in all conditions, it appears that this ratio is roughly constant for subjects #2, 5, 10 and 11 (SD/mean < 17%). For subject # 1, 4, 6, 7 and 9, the variability is higher (24% < SD/mean < 40%). For

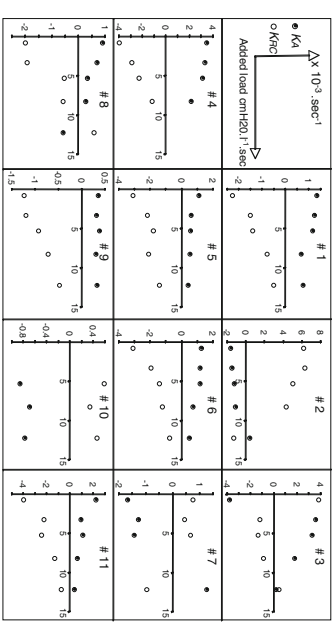


Fig. 4 Representation of K_A and K_{rc} (mean value on those breaths with $R^2 \geq 0.70$) for each added load condition and each subject

two subjects #3 and 8, the variability of K_A/K_{rc} ratio is very high (80 and 48% respectively).

4 Discussion

This study shows that 1,193 breaths on a total of 2,971 breaths (40%), recorded in eleven subjects in five conditions (rest and four level of resistive loadings), validate the model. Then, our simple model represents satisfactorily (i.e. with a determination coefficient $R^2 \geq 0.70$) the behavior of the chest wall motion in a significant number of breaths.

Starting from the lever system of Hillman and Fricucane (1987), we developed a simple dynamical model of the respiratory pump. This allowed to compare model simulation of airflow (obtained with abdominal and rib cage signals) with airflow measured by pneumotachography.

Many model of the respiratory system have been developed (Loring and Mead 1982; Macklem et al. 1979, 1983; Mead et al. 1985; Primano 1982; Ricci et al. 2002). Our model is realistic because it takes into account the two compartments considered passive, rib cage and abdomen, and the active respiratory muscles, elastic and viscous forces in relation to the respiratory muscle. The simplifications performed to minimize the number of parameters (i.e. parallel and vertical displacements, normalized horizontal distance between abdominal and rib cage elements) are minor. The geometric properties of the model (Eq. 1) are coherent with the Konno and Mead hypothesis which asserts that tidal volume is a linear combination of rib cage and abdomen cross sectional areas. The hypothesis of a system without inertia is a common assumption in respiratory mechanics.

The limits on the model are directly related to the hypothesis it includes: the geometric and mechanical properties of respiratory system are constant, at least over the breathing cycle. That mechanical properties remain stable over a respiratory cycle is a common assumption. That α and β remain constant during a respiratory cycle seems to be verified in a number of cycles where the model fits the data, but may be wrong for the others. The stability of α for a given subject is implicitly admitted as it is the condition of application of RIP technique. This leads to question about the stability of β : our results indicate that this parameter is stable for a number of cycles (those with $R^2 \geq 0.70$). The value of β depends upon the relative contributions of diaphragm, rib cage muscles and abdominal muscles to the act of breathing because their net action determines the relative motion of rib cage and abdomen. Because this net action can vary from breath to breath and from one condition to another, β may change from one breath to the other. Our results indicate, however, that β remains stable for some subjects (#2, 5, 10 and 11) presenting a low K_A/K_{rc} ratio variability.

Experimental data were obtained at rest and with the addition of four level loads throughout the entire breath. Adding ventilatory external loads has been used to simulate respiratory system disorders (Mille-Emlil and Zin 1986). Although, resistive loading is not entirely analogous to internal respiratory loading induced by airway diseases it has often been used as a tool to characterize the compensatory mechanisms of the ventilatory system (Altoise et al. 1979; Axen et al. 1983), the subject's tolerance to added loads (Freedman and Campbell 1970) and to study the sensations induced by these loads (Kelsen et al. 1981; Choman et al. 1990). For Mille-Emlil and Zin (1986) there are several reasons for studying loads: (1) elucidate basic physiology, (2) improve understanding and treatment of disturbances in patients with respiratory diseases and (3) assist in the design and use of breathing equipment for medical or other purposes. Another reason would be: explore respiratory muscles activity by non invasive techniques in conscious subjects (Gozal et al. 1995, 1996). Our study is clearly in line with the latter reason. The threshold of the determination coefficient R^2 (estimation of the level of fit between experimental flow measured by pneumotachography and flow estimated by the model) has been arbitrarily fixed at 0.70. This value is rather high but it can be seen in Fig. 2 that the fit appears satisfactory at this level of threshold.

The number of breath with $R^2 \geq 0.70$ for each recording is gathered in Table 1. This number varies amongst subjects and conditions. No trend was observed with increasing resistances. The accuracy of K_A and K_{rc} calculation may explain this variability in the number of breath with $R^2 \geq 0.70$. Indeed, the accuracy of coefficient estimation is related to the difference between abdominal and rib cage signals. This difference can be estimated from the Lissajous curves and expressed as the phase difference. Figure 3 and Table 1 show that high phase differences were often associated with high R^2 .

The variability in the number of breath with $R^2 \geq 0.70$ on one individual may have various origins. It can be explained in terms of fluctuations of the application point of the respiratory muscles force (F_{rms}) on the model's bar (Fig. 1). Indeed, when the position of the muscle force application point is at the bottom end of the dashpot, this results in parallel changes in RC and A signals, in other words a very

low phase difference, inducing indecision in the multiple linear regression calculation (badly conditioned matrix). On the other hand, elastances are greatly influenced by thoracic muscle tone which may vary in the course of the breath (Josenhans et al. 1975). This may impair the adequacy of the model which relies on the hypothesis that elastances are constant.

Figure 4 show that estimated K_A and K_{rc} have always opposite signs as it is imposed on theoretical values by Eq. 6. Furthermore, the coefficients increase or decrease (according to their sign) when the added load increases (except for subject #7 for both coefficients and for subject #9 for K_A). This is in agreement with our model hypotheses: Eqs. 7 and 8 indicate R is inversely proportional to K_A and K_{rc} , on the hypothesis of E_A and E_{rc} constant.

RIP is often used to obtain either a measure of tidal volume or the rib cage and abdomen signals indicating the contribution of the two compartments to ventilation. This remains valid during different respiratory conditions, as hypoventilation (Calabrese et al. 2007) and especially during loaded breathing (Carry et al. 1997; Eberhard et al. 2001).

RIP measurements and our model are complementary to understand chest wall motion. RIP is largely used to estimate thoracoabdominal asynchrony that is considered to be noninvasive indicators of airway obstruction (Hammer et al. 1992; Sackner et al. 1984; Cantineau et al. 1992). The hypothesis that thoracoabdominal asynchrony is related with airway obstruction, is in accordance with our model: if the resistance of respiratory system (R) increases, the viscous resistance force (F_R) of the dashpot applied on the bar is stronger involving rib cage and abdomen asynchrony (elastances E_A and E_{rc} supposed constant).

In conclusion, our model proved to be able to represent the behavior of the chest wall and thus may be useful to interpret the relative motion of rib cage and abdomen during quiet breathing. The model is simple in its conception and easy to use since three signals airflow (pneumotachography) and abdominal and rib cage signals (respiratory inductive plethysmography) are needed to calculate the model's parameters. The model could be a useful and complementary tool to experimental data to understand respiratory mechanics.

Acknowledgments We gratefully acknowledge the technical assistance of Angélique Broua.

References

- Aqostoni E, Mogroni P (1966) Deformation of the chest wall during breathing efforts. *J Appl Physiol* 21:1827–1832
- Calabrese P, Perantti H, Pham DT, Eberhard A, Bencherif G (2000) Cardiorespiratory interactions during resistive load breathing. *Am J Regul Integr Comp Physiol* 279:R2208–R2213
- Calabrese P, Beskege T, Eberhard A, Vove V, Bascioni P (2007) Respiratory inductance plethysmography is suitable for voluntary hypoventilation test. *Coff Proc IEEE Eng Med Biol Soc* 1:1055–1057
- Cantineau JP, Escourrou P, Sarrere R, Gauthier C, Goldman M (1992) Accuracy of respiratory inductive plethysmography during wakefulness and sleep in patients with obstructive sleep apnea. *Chest* 102:1145–1151

- Curry PY, Bacomnier P, Eberhard A, Cone P, Benchetrit G (1997) Evaluation of respiratory inductive plethysmography: accuracy for analysis of respiratory waveforms. *Chest* 111:1910–1915
- Eberhard A, Calabrese P, Bacomnier P, Benchetrit G (2001) Comparison between the respiratory inductance plethysmography signal derivative and the airflow signal. *Adv Exp Med Biol* 499:489–494
- Gilbert R, Auchincloss JH, Peppi D (1981) Relationship of rib cage and abdomen motion to diaphragm function during quiet breathing. *Chest* 80:607–612
- Goldman MD, Mead J (1973) Mechanical interaction between the diaphragm and rib cage. *J Appl Physiol* 35:197–204
- Hammer J, Newbe CJL, Deakkers TW (1992) Validation of the phase angle technique as an objective measure of upper airway obstruction. *Pediatr Pulmonol* 19:167–173
- Hillman DR, Finucane K (1987) A model of the respiratory pump. *J Appl Physiol* 63(3):951–961
- Josephs WT, Resecke TA, Schaller G (1975) Effective respiratory system elastance during positive-pressure breathing in supine man. *J Appl Physiol* 39:541–547
- Kono K, Mead J (1967) Measurement of the separate volume changes in rib cage and abdomen during breathing. *J Appl Physiol* 22:407–422
- Loring SH, Mead J (1982) Action of the diaphragm on the rib cage inferred from a force-balance analysis. *J Appl Physiol* 53:756–760
- Maackem PT, Roussois C, Derenne J, Delhez L (1979) The interaction between the diaphragm, intercostal/accessory muscles of inspiration and the rib cage. *Respir Physiol* 38:141–152
- Maackem PT, Maackem DM, De Troyer A (1983) A model of inspiratory muscles mechanics. *J Appl Physiol* 55:547–557
- Mead J, Smith JC, Loring SH (1985) Volume displacements of the chest wall and their mechanical significance. In: Roussois C, Maackem PT (eds) *The Thorax Part A*. Dekker, New York, pp 369–392
- Lung Biol Health Dis Ser
- Priniano PT (1982) Theoretical analysis of chest wall mechanics. *J Biomech* 15:919–931
- Rice SB, Cuzel P, Constantinou A, Similowski T (2002) Mechanical model of the inspiratory pump. *J Biomech* 35:139–145
- Sackner M, Gonzalez H, Rodriguez M, Beliso A, Sackner DR, Granvik S (1984) Rib cage and abdomen in normal subjects and in patients with chronic obstructive pulmonary disease. *Am Rev Respir Dis* 130:588–593
- Sharp JT, Goldberg NB, Druz WS, Damon J (1975) Relative contributions of rib cage and abdomen to breathing in normal subjects. *J Appl Physiol* 39:608–618
- Wade OL (1954) Movements of the thoracic cage and diaphragm in respiration. *J Physiol* 129:193–212
- Ward ME, Ward JW, Maackem PT (1992) Analysis of human chest wall motion using a two-compartment rib cage model. *J Appl Physiol* 72:1338–1347

II.5.2 Modèles non linéaires du générateur de rythme respiratoire

II.5.2.1 Modèle déterministe chaotique

En se basant sur l'hypothèse qu'en contrôlant la présence du chaos en modifiant un paramètre du système qui apporte des indications sur la nature chaotique du système, nous avons essayé de modifier, de manière expérimentale et en faisant des simulations, la dimension chaotique du système ventilatoire en modifiant les charges résistives chez des volontaires sains. Nous avons construit un modèle mathématique qui simule les interactions entre deux systèmes. Le premier, actif, est un générateur du rythme respiratoire représenté par un système déterministe chaotique. Le deuxième, passif, est le système respiratoire mécanique, représenté par un seul compartiment alvéolaire homogène d'élastance (E) relié aux voies aériennes rigides de résistance (R). Les données expérimentales utilisées ont été celles acquises lors d'addition de résistances au repos chez des volontaires sains. On observe avec les simulations la même tendance qu'avec les résultats expérimentaux.

Ces résultats supportent l'hypothèse de la nature chaotique du générateur de rythme respiratoire.

Thibault et al (2004) Effects of resistive loading on breathing variability - Non linear analysis and modelling approaches. Adv Exp Med and Biol

II.5.2.2 Oscillateur de Van Der Pol

Pour simuler les effets de la déglutition sur le rythme ventilatoire, nous avons utilisé un modèle du générateur de rythme respiratoire basé sur l'oscillateur de Van Der Pol modifié ([Pham Dinh et al, 1983](#)). Chez 4 sujets sains, les signaux respiratoires ont été enregistrés de façon non invasive pendant des périodes comportant des déglutitions. Les déglutitions observées peuvent être regroupées en trois catégories : celles qui débutent et finissent pendant une phase inspiratoire (rares), celles qui débutent et finissent pendant une phase expiratoire et enfin celles qui débutent en inspiration et finissent en expiration.

Le phénomène de la déglutition a été modélisé à partir des données physiologiques. Une déglutition se traduit, sur le plan mécanique, par une occlusion des voies

aériennes supérieures au niveau du larynx. Donc, pendant toute la déglutition, le volume pulmonaire reste constant, égal au niveau atteint en début de déglutition. Le fonctionnement du générateur de rythme respiratoire, de son côté, semble interrompu, arrêté momentanément pour reprendre, après la déglutition, dans un état semblable à celui observé au début de la déglutition. De plus, l'amplitude du cycle suivant une déglutition, semble être plus élevée que celle des cycles précédents.

Au niveau du modèle de l'oscillateur respiratoire central, les hypothèses suivantes ont été faites :

- au début de la déglutition, le point (x,y) représentant l'état de l'oscillateur dans le plan de phase est arrêté à l'endroit où il se trouve,
- ce point ne reste pas à cette position pendant toute la déglutition : il s'écarte de la position initiale (x,y) sur une trajectoire qui :
 - assure que le comportement de l'oscillateur après redémarrage (le point représentatif est la nouvelle condition initiale à la fin de la déglutition) sera « similaire » à ce qu'il aurait été sans déglutition, simplement décalé dans le temps. Le point doit donc rester sur un isochron. *L'isochron d'un point du cycle limite est l'ensemble des points du plan dont la trajectoire asymptotique est confondue avec celle du point du cycle limite* ([Pham Dinh et al, 1983](#)).
 - augmente l'amplitude du cycle suivant, le point s'éloigne donc, sur l'isochron, vers l'extérieur du cycle limite.

De plus, afin de définir le mouvement du point représentatif de l'état de l'oscillateur respiratoire pendant la déglutition, nous faisons l'hypothèse que la valeur absolue de la vitesse du point reste constante pendant la déglutition : le point se déplace donc sur l'isochron à une vitesse égale (en module) à celle sur le cycle limite au moment du début de la déglutition.

Les trois types de déglutition ont été simulés avec notre modèle, le résultat d'une simulation pour une déglutition en expiration est présenté sur la Figure 16.

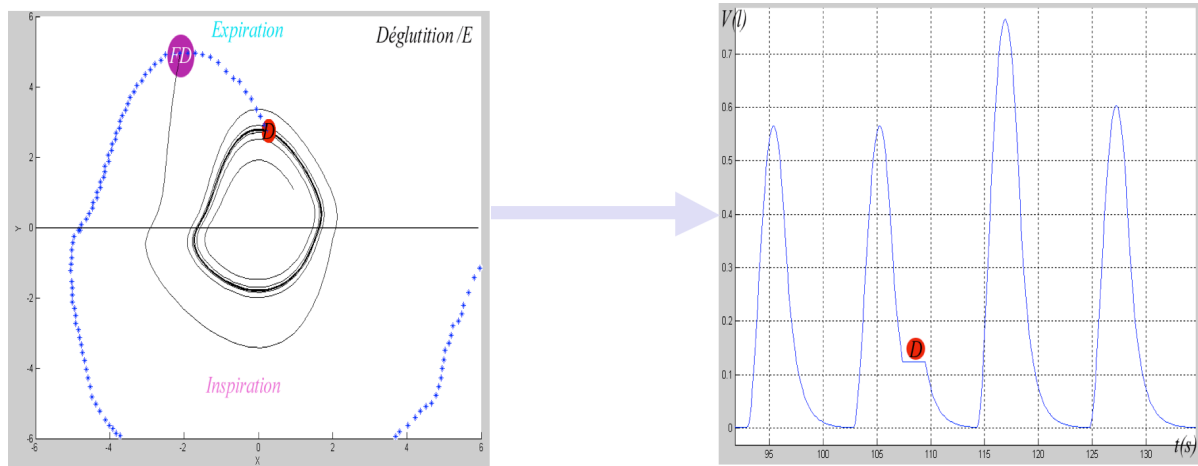


Figure 16 : Représentation des processus de simulation pour un type de déglutition en expiration (E). La figure de gauche représente la simulation de la déglutition au niveau du générateur de rythme respiratoire : le plus petit point (rouge, D) est le début de la déglutition, qui va se déplacer sur l'isochron du point d'arrêt (courbe en pointillée bleue) ; le plus gros point (violet, FD) représente la fin de la déglutition, à partir de ce point il y a un retour vers le cycle limite. La figure de droite représente les signaux de volume courant obtenus en sortie : pour le cycle avant la déglutition, pendant la déglutition (représentée par le point rouge, D) et les deux cycles suivants.

Les résultats des simulations de déglutition avec le modèle concordent avec ceux obtenus lors de déglutitions expérimentales, quelle que soit la phase du cycle respiratoire où survient cette déglutition.

Le modèle proposé a été validé qualitativement. Durant l'arrêt respiratoire induit par une déglutition, le générateur de rythme respiratoire se comporte comme un accumulateur de l'énergie qu'il ne peut dissiper pendant la durée de cet arrêt et qu'il restitue progressivement dès la reprise de son activité.

Ce travail a fait l'objet du coencadrement de deux masters 2 Ingénieries pour la Santé et le Médicament (Al Chama Feras et Mezioud Naïma) et de deux communications :

Al Chama et al. (2005) Effets de la déglutition sur le rythme respiratoire. Société Francophone de Biologie Théorique, Saint Flour

Baconnier et al (2006) How to simulate the effect of swallowing on the respiratory rhythm generator? Eur Respir J (European Respiratory Society Annual Congress Munich).

II.5.3 Modèle d'interaction cœur -respiration

Le modèle mathématique proposé intègre un modèle neuro-musculaire ventilatoire et un modèle cardiovasculaire. Le modèle neuro-musculaire ventilatoire est un modèle permettant de simuler la commande et l'activité des muscles respiratoires

ainsi que la mécanique du système thoraco-pulmonaire. Le modèle cardio-vasculaire minimaliste de Smith est constitué des deux ventricules et de compartiments supplémentaires pour les circulations systémique et pulmonaire. Ces deux modèles sont mis en interaction par l'intermédiaire de la pression pleurale (calculée par le modèle neuro-musculaire ventilatoire) et du volume de sang intra-thoracique (évalué par le modèle cardio-vasculaire). Les équations du modèle complet ont été programmées sous Berkeley-Madonna afin de simuler son comportement. Les simulations par le modèle sont en accord avec les données expérimentales ainsi que les données de la littérature.

Les résultats de ce travail suggèrent que le modèle proposé peut être utile dans l'interprétation des interactions cardio-pulmonaires.

Fontecave Jallon et al (2000) A model of mechanical interactions between heart and lungs. Philos Transact A Math Phys Eng Sci

II.5.4 Complexité

J'ai été responsable scientifique du projet "Interactions cardio-respiratoires: complexités nécessaires ou vestigiales ? Modèles et expériences" financé pendant 2 ans par le Programme Interdisciplinaire Complexité du Vivant & Action STIC-Santé (2004-2006).

L'objectif de l'étude était d'aborder la Complexité du vivant par la recherche des mécanismes des interactions cardio-respiratoires.

Un ralentissement cardiaque au cours d'une déglutition, quelle que soit la phase respiratoire, peut suggérer la persistance d'un mécanisme de ralentissement cardiaque en relation uniquement avec l'arrêt respiratoire comme chez les mammifères plongeurs. Sinon, il convient d'envisager une action spécifique de la déglutition sur les centres respiratoires. Pour apporter des éléments de réponse, nous avons comparé les variations de fréquence cardiaque chez l'homme sain au cours de différentes situations d'apnée : la déglutition, l'apnée volontaire dans l'air, l'apnée pendant l'immersion du visage dans l'eau (pour simuler la plongée). La Figure 17 est un exemple de signaux enregistrés au cours d'une déglutition. Le signal de fréquence cardiaque est calculé à partir du signal électrocardiographique.

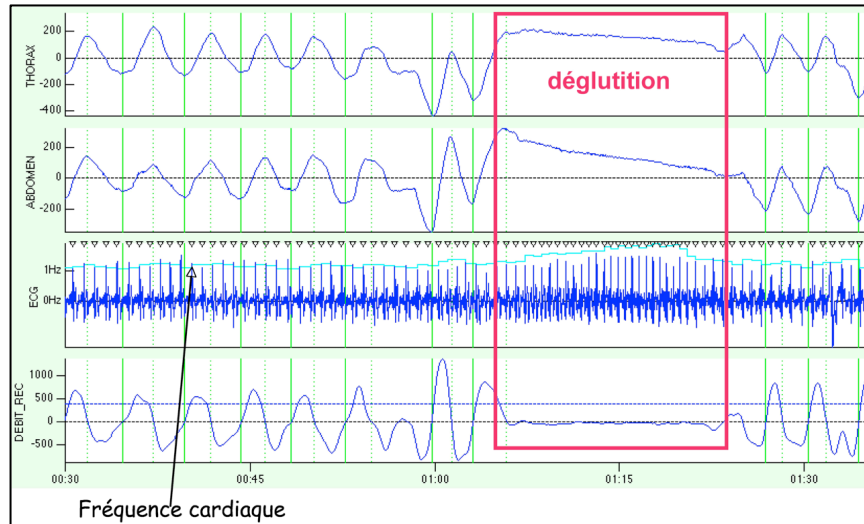


Figure 17 : Signaux enregistrés au cours d'une déglutition. Signaux thoracique (THORAX) et abdominal (ABDOMEN) mesurés par pléthysmographie respiratoire à variation d'inductance (PRI), ECG : électrocardiogramme (bleu foncé), fréquence cardiaque (bleu clair), DEBIT_REC : Débit reconstitué à partir des signaux thoracique et abdominal.

La moyenne, l'écart type et le coefficient de variation sont calculés sur la durée totale de l'événement (pendant) et sur une durée identique avant l'événement (avant) et sont représentés sur la Figure 18.

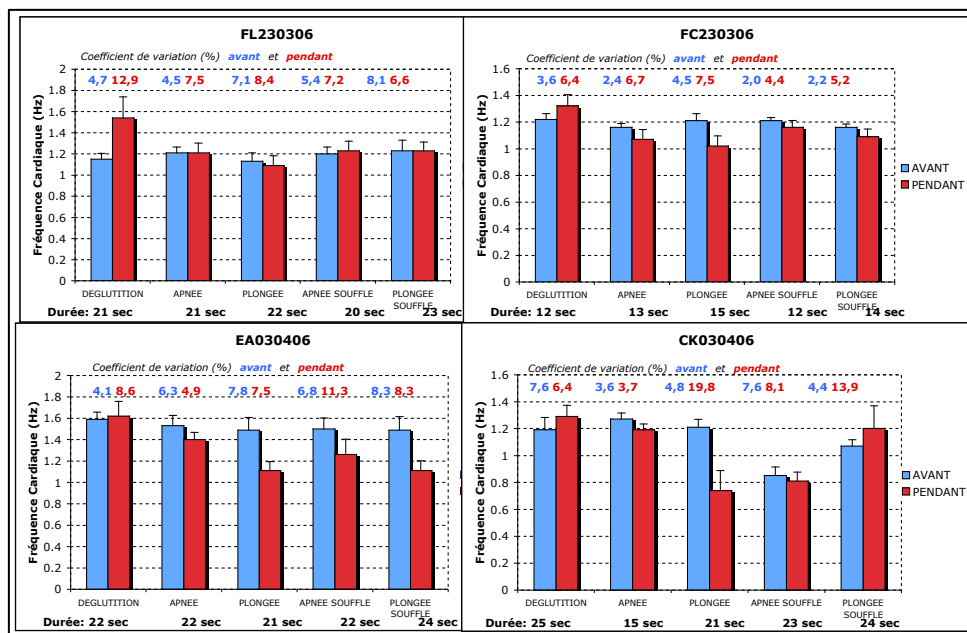


Figure 18 : Représentation de la valeur moyenne de la fréquence cardiaque, de l'écart type et du coefficient de variation avant et pendant chaque événement pour les 4 sujets.

DEGLUTITION: ingestion d'un grand verre d'eau (environ 200 ml) ; APNEE : apnée volontaire dans l'air
 PLONGEE : apnée "dans l'eau": le sujet plonge le visage dans de l'eau à température ambiante
 APNEE SOUFFLEE : apnée après une grande inspiration suivi d'un dégonflement progressif dans l'air
 PLONGEE SOUFFLEE : apnée après une grande inspiration suivi d'un dégonflement progressif dans l'eau à température ambiante.

Les durées des apnées sont imposées par la durée de la déglutition. Les durées sous l'axe des abscisses indiquent la durée sur laquelle les moyennes de la fréquence cardiaque sont calculées.

On observe chez tous les sujets une augmentation de la fréquence cardiaque pendant la déglutition, alors qu'elle diminue ou varie très peu pour tous les autres événements et chez tous les sujets (sauf apnée soufflée chez le sujet 4).

Le résultat attendu était un ralentissement du rythme cardiaque au cours de la déglutition suggérant la persistance d'un mécanisme de ralentissement cardiaque en relation uniquement avec l'arrêt respiratoire comme chez les mammifères plongeurs. Nos résultats montrent une augmentation de la fréquence cardiaque au cours de la déglutition ce qui suppose une action spécifique de la déglutition sur les centres respiratoires.

Ce travail a fait l'objet d'un rapport scientifique dans le cadre du projet "Interactions cardio-respiratoires: complexités nécessaires ou vestigiales ? Modèles et expériences" du Programme Interdisciplinaire Complexité du Vivant & Action STIC-Santé-2004-2005.

Les résultats du travail réalisé dans le cadre du projet " Interactions cardio-respiratoires : complexités nécessaires ou vestigiales ? Modèles et expériences." présentés dans II.5.2.2, pour la partie modèle et dans II.5.4, pour la partie expérimentale, constitueront une base de travail du projet ANR e-Swallhome sur la déglutition, présenté dans les perspectives.

II.6 TRAVAUX EN COURS ET PERSPECTIVES

II.6.1 Déglutition et respiration

Dans le paragraphe ci-dessus nous avons observé l'accélération de la fréquence cardiaque pendant la déglutition ce qui est contraire aux variations cardiaques obtenues au cours d'apnées. Ces résultats ont montré qu'il existait une coordination spécifique entre la déglutition et la respiration. Nous avons cherché à mieux comprendre les mécanismes à la base de cette coordination, d'autant plus qu'il existe des applications dans le cadre de dysfonctionnement de la déglutition consécutif à un Accident Vasculaire Cérébral (AVC). Ce travail a débuté dans le cadre du projet "Déglutition et Respiration : Modélisation et e-Santé à domicile" (e-SwallHome) financé par l'ANR Technologies pour la Santé et l'Autonomie (2014-2017). Ce projet multicentrique associe plusieurs laboratoires dont trois du site Grenoblois : TIMC-IMAG UMR 5525 CNRS-IPG-UJF, GIPSA-lab, UMR 5216 CNRS-IPG-UJF et AGIM, CNRS/UJF, FRE 3405 ainsi que Laboratoire Parole et Langage, CNRS UMR 7309 (Université Aix-Marseille), et plusieurs CHU français : de Montpellier, d'Aix Marseille, de Caen et deux sociétés Intrasense®, Montpellier et Bioclinome®, Grenoble.

Dans le cadre de ce projet ANR e-SwallHome, mon travail a consisté dans un premier temps à mettre au point un protocole permettant l'enregistrement d'événements de déglutition et de parole sur 15 volontaires sains. J'ai rédigé un document (**délivrable D3.1a**) qui décrit ce protocole en justifiant les choix de capteurs et le déroulement des séquences d'enregistrements par rapport à nos objectifs.

En complément des signaux ventilloires mesurés par PRI, un électroglottographe est utilisé pour mettre en évidence la déglutition ([Perlman and Grayhack, 1991](#); [Logemann, 1994](#); [Pédouroux et al, 2001](#)) et un microphone permet l'enregistrement du signal acoustique pour la phonation. Les capteurs de PRI, d'électroglottographie et le microphone sont présentés sur un sujet sur les photos de la Figure 19.

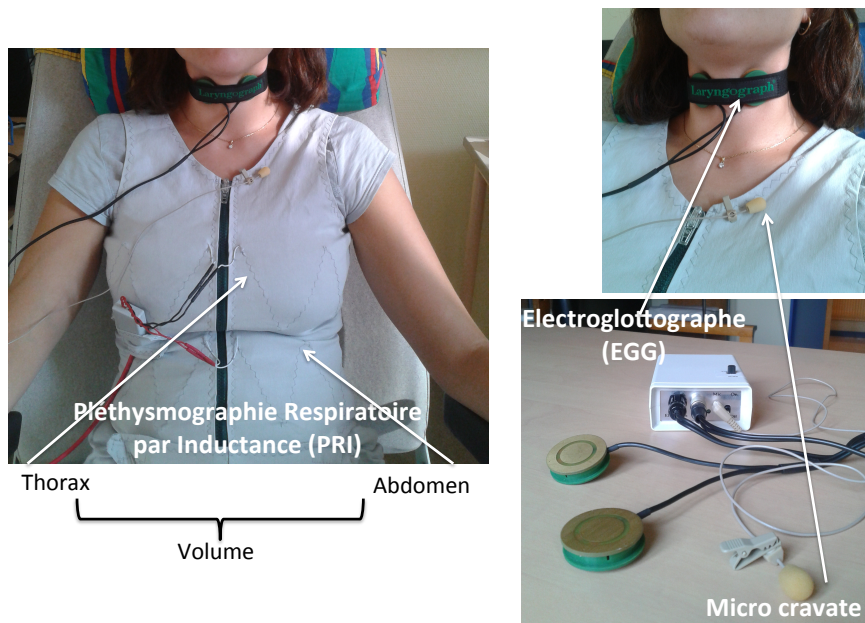


Figure 19 : Pléthysmographe respiratoire à variation d'inductance (ventilation), électroglottographe (variations d'impédance au niveau de la glotte) et microphone (signal acoustique) placés sur un sujet.

Les enregistrements sur volontaires sains ont été réalisés, et nous analysons actuellement le signal ventilatoire PRI pour la caractérisation des différentes phases de déglutition et de phonation. Un exemple d'enregistrement des différents signaux au cours d'évènements de déglutition et de parole est présenté sur la Figure 20.

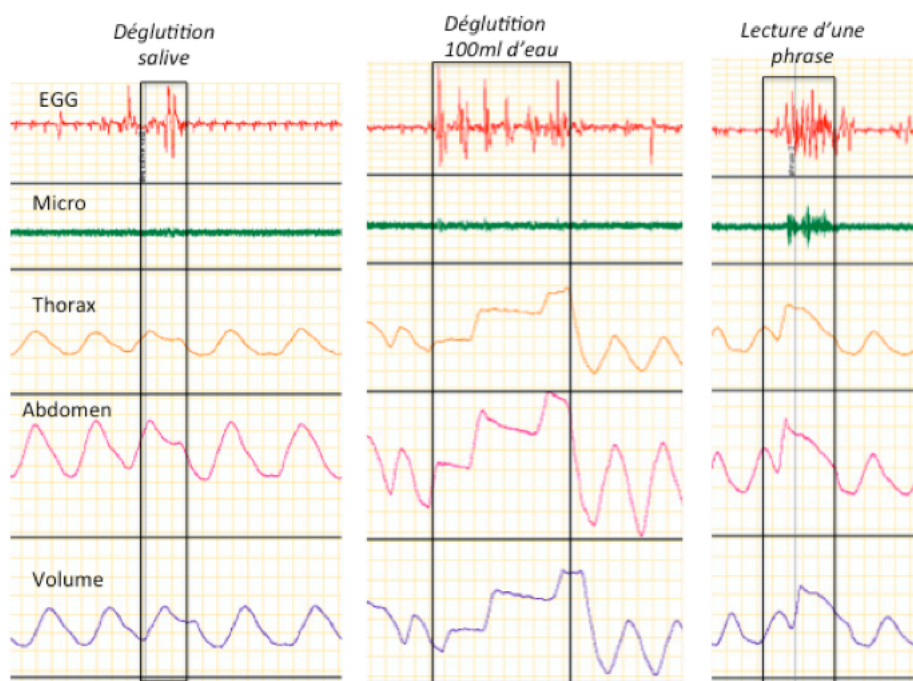


Figure 20 : Enregistrement sur un sujet sain des signaux électroglottographique (EGG), acoustique (micro) et de ventilation (thorax, abdomen et volume obtenus par pléthysmographie respiratoire à variation d'inductance) au cours d'évènements de déglutition et de parole.

Une partie de ce travail a fait l'objet de l'encadrement d'un master 1 Ingénieries pour la Santé et le Médicament en 2014 (pour la mise au point du protocole) et d'un projet ingénieur TIS5 en 2015 (pour l'enregistrement des volontaires sains et le développement d'un outil de traitement des données).

Une dernière phase du projet a pour objectif la mise au point d'un index d'évaluation de la déglutition. Ceci sera réalisé dans l'unité de "Neurologie vasculaire - Soins intensifs AVC" au CHU Grenoble Alpes à partir des déglutitions enregistrées chez les patients ayant eu un AVC à deux reprises : à 15 jours et à 6 mois de l'AVC. Ce travail a débuté en novembre 2016 avec l'inclusion d'un premier patient et sera poursuivi en 2017.

Par ailleurs, la méthode de simulation de la déglutition présentée §II.5.2.2 sera appliquée à ces enregistrements afin de comparer les résultats des sujets sains et pathologiques et de rechercher si le comportement du générateur de rythme respiratoire modélisé est modifié après un AVC.

II.6.2 Interactions phonation-ventilation

Cette thématique initiée par Nathalie Henrich-Bernardoni (**GIPSA-lab**) m'a intéressée parce que le contrôle de la ventilation joue un rôle déterminant dans la production des sons (parole et chant).

En effet, une coordination des mouvements ventilatoires, phonatoires et articulatoires est nécessaire pour la production de la voix humaine. De nombreuses techniques vocales dans la parole et dans le chant s'appuient sur cette coordination pour augmenter l'intensité vocale produite ou pour changer la qualité de la voix. La production de voix humaine est modélisée par la théorie source-filtre, qui a fait ses preuves dans le traitement de la parole normale mais qui montre ses limites quand on s'intéresse à la qualité vocale, aux aspects de forçage vocal, de dysphonie et au développement de troubles de la voix d'origine fonctionnelle. Dans cette approche théorique, les aspects phonatoires sont découplés des aspects articulatoires en première approximation. Les aspects respiratoires ne sont pris en compte que de façon très indirecte, le conduit vocal étant considéré acoustiquement fermé à la glotte pendant la phonation.

S'inscrivant dans une démarche pluridisciplinaire de physiologie, physique et phonétique, ce projet ambitionne de revisiter ce cadre théorique, en y incluant les effets liés aux interactions entre les trois niveaux respiratoire, phonatoire, et articulatoire. L'objectif de cette collaboration est d'aborder les mouvements ventilatoires, phonatoires et articulatoires au cours de différentes techniques de chant où l'aspect ventilatoire est essentiel à la réalisation de la technique, comme pour le Human Beatbox ou le chant diphonique. La description, l'exploration conduisant à une meilleure compréhension de cette coordination pourrait permettre de proposer des solutions de rééducation de la voix.

Dans ce cadre, nous avons eu l'opportunité d'enregistrer les mouvements respiratoires, phonatoires et articulatoires chez six chanteurs originaires de Mongolie au cours de différentes techniques de chant diphonique. Nous avons aussi enregistré un chanteur de Human Beatbox.

La première observation est que les interactions ventilation-chant sont visibles et parfois reproductibles sur le signal ventilatoire. Notre hypothèse est que, à l'instar de l'interaction ventilation –chant, l'interaction ventilation-parole pourrait être visible et reproductible sur un signal ventilatoire. Ceci pourrait être utilisé pour l'apprentissage de la parole et la réhabilitation de la phonation.

II.6.3 Le syndrome d'hyperventilation

En continuité de la thèse de Tudor Besleaga soutenue en 2011, une collaboration sera mise en place prochainement. Nous sommes actuellement en recherche d'un financement de thèse qui se ferait en cotutelle entre nos deux universités

En effet, nous souhaitons poursuivre notre collaboration avec Tudor Besleaga qui a été titularisé en 2014 au [département de Physiologie Humaine et Biophysique de l'Université de Médecine et Pharmacie "Nicolae Testemitanu" à Chisinau \(Moldavie\)](#). Ce département a une collaboration très étroite avec l'Institut de Neurologie et Neurochirurgie de Moldavie. Notre objectif serait d'explorer les dysfonctionnements de la fonction ventilatoire et de l'interaction cardio-respiratoire dans certaines pathologies neurologiques.

II.6.4 Asynchronisme thorax – abdomen : application

Une démarche de collaboration est initiée avec la Tunisie en continuité de la thèse d'Aïcha Laouani dont j'ai codirigé la thèse. Elle occupe actuellement un poste au [laboratoire de biophysique de la faculté de Médecine de Sousse \(Tunisie\)](#).

L'objectif de la collaboration serait l'étude de l'asynchronisme thorax –abdomen chez les enfants souffrant de pathologie obstructive chronique. Des enregistrements répétés ou en continue pourraient être réalisés afin d'évaluer les variations de l'obstruction au cours de la journée en fonction 1) de divers événements (prise de nourriture, sommeil, déplacements etc) et 2) de la thérapeutique.

Nous sommes actuellement en cours de recherche de financement.

II.6.5 Diagnostic médical à partir d'une analyse des gaz respiratoires

Je suis impliquée dans le projet intitulé " Fast and sensitive breath analysis for medical diagnostics" financé par l'ANR du programme grands défis sociétaux, vie santé et bien être PRCE : Projets de recherche collaborative-entreprises (2016-2018). Il implique le [Laboratoire de Physique Interdisciplinaire \(LIPhy\) de Grenoble](#), le [centre d'investigation clinique-innovation technologique \(CIC-IT\) de Grenoble](#) et notre équipe (PRETA, laboratoire TIMC-IMAG, porteur R Briot médecin urgentiste de l'équipe) ainsi que la société AP2E (SAS) à Aix en Provence. Ce projet translationnel comprend trois phases : 1) validation et certification de l'appareil de mesure rapide et précise de gaz, développé par le LIPhy (porteur du projet) pour la mesure de CO sur les poumons avant transplantation, 2) validation du CO comme indicateur de la qualité du greffon (poumon humain) et 3) identification et validation d'autres traceurs pouvant faire état de la qualité du greffon.

Ma participation dans ce projet de recherche se place au niveau de l'aide au développement d'un outil d'analyse et de traitement des données recueillies.

II.7 REFERENCES

- Agostoni E, Mognoni P (1966) Deformation of the chest wall during breathing efforts. *J Appl Physiol* 21 : 1827-1832
- Allen JL, Wolfson MR, Mc Dowell K, Shaffer TH (1990) Thoracoabdominal asynchrony in infants with airway obstruction. *Am Rev Respi Dis* 141 : 337-342
- Allen JL, Greenspan JS, Deoras KS, Keklikian E, Wolfson MR, et al. (1991) Interaction between chest wall motion and lung mechanics in normal infants and infants with bronchopulmonary dysplasia. *Pediatr Pulmonol* 11 : 37-43
- Anrep GV, Pascual W, Rossel R (1936) Respiratory variations of the heart rate, 1. The reflex mechanism of respiratory arrhythmia. *Proc Roy Soc London Ser B* 119-230
- Askelrod S, Gordon D, Ubel FA, Shannon DC, Barger AC, Cohen RJ (1981) Power spectrum analysis of heart rate fluctuation : a quantitative probe of beat to beat cardiovascular control. *Science* 213 : 220-222
- Askelrod S, Gordon D, Mahwed JB, Snidman NC, Shannon DC, Cohen RJ (1985) Hemodynamic regulation : Investigation by spectral analysis. *Am J Physiol* 249 : H867-H875
- Bachy JP, Eberhard A, Baconnier P and Benchetrit G (1986) A program for cycle-by-cycle analysis of biological rhythms. Application to respiratory rhythm. *Comp Methods Prog Biomed* 23 : 297-307
- Banzett RB, Mahan ST, Garner DM, Brughera A, Loring SH (1995) A simple and reliable method to calibrate respiratory magnetometers and respiration. *J Appl Physiol* 79 : 2169-2176
- Benchetrit G, Shea SA, Pham-Dinh T, Bodocco S, Baconnier P, Guz A (1989) Individuality of breathing patterns in adults assessed over the time. *Respir Physiol* 75 : 199-210
- Chien J, Ruan S, Huang YT, Yu C, Yang P (2013) Asynchronous thoraco-abdominal motion contributes to decreased 6-minute walk test in patients with COPD. *Respir Care* 58 : 320-326
- Davis GM, Cooper DM, Mitchell I (1993) The measurement of thoraco-abdominal asynchrony in infants with severe laryngotracheobronchitis. *Chest* 103 : 1842-1848
- Dejours P, Bechtel-Labrousse Y, Monzein P and Raynaud J (1961) Etude de la diversité des régimes ventilatoires chez l'Homme. *J Physiol (Paris)* 53 : 320-321
- Hammer J, Newth CJL, Deakers TW (1995) Validation of the phase angle technique as an objective measure of upper airway obstruction. *Pediatr Pulmonol* 19 : 167-173
- Hammer J, Newth CJL (2009) Assessment of thoraco-abdominal asynchrony. *Paediatr Respir Rev* 10 : 75-80
- Heymans C (1929) Über die physiologie und pharmakologie des herz-vagus-zentrums. *Ergebn Physiol* 28 : 244-311
- Hillman DR and Finucane K (1987) A model of the respiratory pump. *J Appl Physiol* 63 : 951-961
- Konno K, Mead J (1967) Measurement of the separate volume changes of rib cage and abdomen during breathing. *J Appl Physiol* 22 : 407-422

- Ludwig C (1847) Beitrage zur kennniss des einflusses des respirations-bewegungen auf den blutlauf im aortensysteime. Arch Anat Physiol 13 : 242-302
- Logemann JA (1994) Non-Imaging Techniques for the study of swallowing. Acta Otorhinolaryngol Belg 48 : 139-142
- Martinot-Lagarde P, Sartene R, Mathieu M, Durand G (1988) What does inductance plethysmography really measure ? J Appl Physiol 64 : 1749-1756
- Mayer OH, Clayton RG, Jawad AF, McDonough JM, Allen JL (2003) Respiratory inductance plethysmography in healthy 3- to 5-year-old children. Chest 124 : 1812-1819
- Morrow PE and Vosteen RE (1953) Pneumotachographic studies in man and dog incorporating a portable wireless transducer. J Appl Physiol 5 : 348-360
- Pédouroux P, Jacquot JM, Royer E, Finiels H (2001) Les troubles de la déglutition chez le sujet âgé. Procédés d'évaluation. Presse Med 30 : 1635-1644
- Perlman AL, Grayhack MA (1991) Use of EGG for measurement of temporal aspects of the swallow. Dysphagia 6 : 88-93
- Pham Dinh T, Demongeot J, Baconnier P, Benchetrit G (1983) Simulation of a Biological Oscillator: the Respiratory System. Journal of Theoretical Biology 20 : 113-132
- Pomfrett C, Barrie J, Healy T (1993) Respiratory sinus arrhythmia : an index of light anaesthesia. Br J Anaesth 71 : 212-217
- Proctor DF and Hardy JB (1949) Studies of respiratory air flow. 1. Significance of the normal pneumotachogram. Bull Johns Hopkins Hosp 85 : 253-280
- Reber A, Bobbia SA, Hammer J, Frei FJ (2001) Effect of airway opening manoeuvres on thoraco-abdominal asynchrony in anaesthetized children. Eur Resp J 17 : 1239-1243
- Ringel ER, Loring SH, McFadden ER Jr, Ingram RH Jr (1983) Chest wall configurational changes before and during acute obstructive episodes in asthma. Am Rev Respir Dis 128 : 607-610
- Seddon P (2015) Options for assessing and measuring chest wall motion. Paediatr Respir Rev 16 : 3-10
- Selbie RD, Fletcher M, Arestis N, White R, Duncan A, et al. (1997) Respiratory function parameters in infants using inductive plethysmography. Med Eng Phys 19 : 501-511
- Sharp JT, Goldberg NB, Druz WS, Fishman HC, Danon J (1977) Thoracoabdominal motion in chronic obstructive pulmonary disease. Am Rev Respir Dis 115 : 47-56
- Shea SA, Benchetrit G, Pham-Dinh T, Hamilton RD, Guz A (1989) The breathing patterns of identical twins. Respir Physiol 75 : 211-223
- Sivan Y, Deakers TW, Newth CJ (1990) Thoracoabdominal asynchrony in acute upper airway obstruction in small children. Am Rev Respir Dis 142 : 540-544
- Thornton JM, Guz A, Murphy K, Griffith AR, Pedersen DL, Kardos A, Leff A, Adams L, Casadei B, Paterson DJ (2001) Identification of higher brain centres that may encode the cardiorespiratory response to exercise in humans. J Physiol (Lond) 533 : 823-836
- Upton J, Brodie D, Beales D, Richardson J (2012) Correlation between perceived asthma control and thoraco-abdominal asynchrony in primary care patients diagnosed with asthma. J Asthma 49 : 822-829
- Wuyam B, Moosavi SH, Decety J, Adams L, Lansing RW, Guz A (1995) Imagination of dynamic exercise produced ventilatory responses which more apparent in competitive sportsmen. J Physiol (Lond) 482:713-724